THESE

présentée

A L'UNIVERSITE DE METZ

pour l'obtention du

DOCTORAT DE L'UNIVERSITE DE METZ

Spécialité : **CHIMIE PHYSIQUE**

par

Suzana Martinović

Laser Plasma Induced Ionization of Volatile Organic Compounds. Study of the Processes and Subsequent Ion/Molecule Reactions by Fourier Transform Ion Cyclotron Resonance Mass Spectrometry.

Soutenue le 10 juilliet 1997 devant la commission d'examen :

M. H.-E. Audier, Directeur de Recherche, Ecole Polytechnique - *Rapporteur*
M. P.-C. Maria, Maître de Conférences à l'Université de Nice - *Rapporteur*
M. J.-F. Muller, Professeur à l'Université de Metz - *Directeur de Thèse*
M. L. Klasinc, Professeur à l'Université de Zagreb - *co-Directeur de Thèse*
M. J.-C. Tabet, Professeur à l'Université de Paris VI - *Examinateur*
M. T. Cvitaš, Professeur à l'Université de Zagreb - *Examinateur*

Ce travail a été réalisé au Laboratoire de Spectrométrie de Masse et de Chimie Laser de l'Université de Metz et à l'Institut Ruder Boskovic de l'Université de Zagreb.

J'exprime au Professeur Jean-François Muller ma sincère gratitude pour m'avoir accueillie au sein de son laboratoire, pour la confiance qu'il m'a faite tout au long de ces travaux. Enfin, je voudrait le remercier de son implication dans ce sujet ô combien passionnant et de l'opportunité qu'il m'a offerte de mener à bien une collaboration internationale fructueuse.

Je voudrais remercier tout particulièrement le Professeur Leo Klasinc de l'Institut R. Boskovic de l'intêret qu'il a porté à mes recherches depuis le "Master of Sciences". Je le remercie également pour son ouverture d'esprit et pour sa contribution à la collaboration établie entre les deux laboratoires.

Je souhaite remercier le Gouvernement Français et le Ministère des Affaires Etrangères pour la bourse d'études qui m'a été accordée pendant un an et demi .

J'exprime tous mes remerciements à Monsieur Henri Audier Directeur de Recherche à L'Ecole Polytechnique et à M. Pierre-Charles Maria, Maître de Conférence à l'Université de Nice Sophia-Antipolis pour l'intérêt qu'ils ont porté à ce travail en acceptant d'en être les rapporteurs.

Je suis reconnaissante à Monsieur Jean Claude Tabet, Professeur à l'Université Paris VI d'avoir accepter de juger ce travail en participant à ce jury.

J'exprime tous mes remerciements au Docteur Christophe Masselon pour l'aide et le soutien qu'il m'a apportée notamment pendant la rédaction de ce mémoire.

Tous mes remerciements vont au Docteur Gabriel Krier du LSMCL, Ingénieur de Recherche pour son assistance technique sans égal au niveau des lasers et de la FTMS. Je voudrais également associer à ces remerciements M. Lionel Venex-Loset ingénieur d'étude.

Je ne saurais oublier le Professeur Eric Millon tant pour ses conseils que pour sa disponibilité dans les discussions scientifiques que nous avons eues.

Merci à Martine, notre adorable secrétaire, pour son aide administrative, sa gentillesse et sa disponibilité. Toujours présente pour mettre du baume au coeur quand on broie du noir.

Que tous mes collègues du LSMCL soient remerciés des cours de français pas toujours très orthoxes qu'ils m'ont prodiguée tout au long de mon séjour à Metz. Qu'ils soient également et au même titre que mes collègues du LKKAK de Zagreb, remerciés de la bonne humeur dont ils ont tous fait preuve et de l'aide tant morale que technique et scientifique qu'ils m'ont apportée aussi bien à Zagreb qu'à Metz.

Contents

General Introduction

The area of gas-phase ion chemistry has experienced rapid growth during the last two decades. Ion/molecule reactions are of major interest both from the standpoint of the fundamental chemistry involved and of practical analytical applications.

Many important environmental pollutants are volatile polyhalogenated organic molecules, from freons to pesticides. Among the various techniques for their determination, mass spectrometry remains one of the most sensitive. These molecules are quite labile and "soft" techniques are required for their ionization.

Studies of ion/molecule reactions ultimately led to the realization of Chemical Ionization - Mass Spectrometry. Chemical ionization (CI) has the advantage of being a "soft" ionization technique. A particularly useful approach has been the laser evaporation generation of metal ions in Fourier Transform Ion Cyclotron Resonance Mass Spectrometry (FT-ICR-MS or FTMS), an approach which permits chemical ionization while still maintaining the low pressure necessary for effective operation of the instrument. FTMS is a well adapted method in a gas phase reaction field, because it offers the advantages of ion trapping, excellent ion and neutral manipulation control, wide selection of ions to be studied, and wide range of possible experiments.

With the development of FTMS and the greater diversity and availability of lasers, a broad frontier of chemistry has opened. These two devices are ideally suited for coupling. The FTMS with its high sensitivity and the ability to acquire a complete, high-resolution mass spectrum from a single laser pulse makes it a method of choice for laser desorption (LD) mass spectrometry. Also, the ability of FTMS to store ions for long periods of time, along with the flux densities available in pulsed lasers, makes it reliable for the study of single and multiphoton/ion interactions.

Everyday work in mass spectrometry requires regular calibration of the instrument and of the obtained spectra. Internal calibration remains the most reliable method. Perfluorated molecules are commonly used calibrant molecules in Electron Ionization Mass Spectrometry (EI-MS). For the instrument devoted to LD experiments (few different lasers - frequent changing of wavelengths), fast and simple calibration remains to be a problem. It has to be underlined that the instrument in Metz has no other means of ionization apart of lasers.

In that context, we wanted to look at the possibility of applying some commonly used procedures in EI/MS to laser induced experiments. Namely, to use volatile perfluorotributylamine for a calibration of instrument and obtained spectra.

The aims of this Thesis are to determine the capabilities of different positive ions (produced by laser pulse) to ionize volatile polyhalogenated molecules and to define involved reaction mechanisms.

These molecules have high affinity to form negative ions, so complementary negative ionization should be used to accomplish the analysis. Negative chemical ionization can be induced by negative ions or by electrons emitted from the metal target. For unambiguous determination of products, an internal calibration process was searched.

This manuscript is presented in four chapters followed by appendices.

The first chapter describes briefly the mass spectrometry techniques applied in gas-phase ion-molecule reactions with basic principles of FTMS and laser desorption/ablation.

In the second chapter the experimental setup is described. Two FTMS instruments interfaced with different lasers and electron ionization possibilities were used. For the introduction of gas directly to the source cell the instrument has been adapted. Detailed experimental sequences and parameters are listed.

The third chapter deals with laser induced **positive ion** reactions with volatile organic molecules. It is devided into seven sections.

The first part is devoted to reactions of *acetophenone* with metal and silicon ions. As we only recently started to study ion/molecule reactions in gas phase in our laboratory, we wanted for a beginning, to start with a model molecule with already known behaviour towards some positive metallic ions. Compound had to be volatile and thus easily introductible in the spectrometer. Thus, we chosen acetophenone. We wanted at first, to ascertain already known mechanisms and second, to check it's reactivity towards other elemental ions. Reactivity of metal ions are correlated to their electronic configuration. After the establishment of experimental procedure and understanding of processes, we could apply this method to other compounds, in our case polyhalogenated molecules.

Second part discuss the study of reactions of *perfluorotributylamine* (PFTBA), molecule known in mass spectrometry as well as in medical experiments. 21 elemental positive ion (mostly first row transition metals, alkaline, earth-alkaline) reacted with PFTBA. Mechanisms of reaction are determined and compared to the analog of the tributylamine.

The control of PFTBA fragmentation is achieved by varying the kinetic energy of reagent ion. Positive metal ion ionization (reaction) is then applied to several other polyhalogenated molecules: dichlorodifluoromethane, halothane and endosulfane. The procedure of internal calibration with PFTBA is established.

In the fourth chapter, **Negative** Chemical Ionization (NCI) and its subsequent reactions are presented. NCI is applied to all above mentioned molecules. Three ionizing methods according to the ionizing projectiles were applied.

Electrons produced by laser irradiation of different metal samples and silicon wafer ionized neutral gas molecules by electron capture (Electron Capture Chemical Ionization). Electrons were produced in large irradiance band: from the high irradiance (10^9 W cm^{-2}) to low irradiance (photoelectrons).

When metal halide salts are irradiated by laser, production of halide ions occurs. They can be used for the Negative Ion Chemical Ionization (NICI) of studied molecules.

Dissociative electron capture can produce halide ions from the original gas molecule. Such ion can ionize other neutral molecules and the so-called "Self Negative Ion Chemical Ionization" (SNICI) occurs.

Finally, for a calibration in negative mode PFTBA was used.

Chapter I

Fourier Transform Ion Cyclotron Resonance Mass Spectrometry

1. Introduction

The area of gas-phase ion chemistry has experienced rapid growth during the last two decades.[1] Ion/molecule reactions are of major interest both from the standpoint of the fundamental chemistry involved and the practical analytical applications.

Studies of the reactions between ions and molecules in the gas phase can in principle provide a detailed and often quantitative insight into the intrisic reactivity of the ions and molecules involved in the absence of solvatation and counter ion effects. From these experiments, valuable hints can be derived on mechanisms operative in the condensed phase. The area of ion/molecule chemistry has benefited from the increased demand for more selective and efficient catalysts ; bringing together researchers with various backgrounds in organic, inorganic, and surface chemistry and catalysis. However, the understanding of reaction mechanisms is the key point in any area of chemistry, including the chemistry involved in numerous biological processes.

Some studies of the reactions of metal ions with organic molecules were directed toward the analytical applications. A particularly useful approach has been the generation of metal ions by laser evaporation in FTMS,[2] an approach which permits chemical ionization while still maintaining the low pressure necessary for effective operation of the instrument. Transition metal ions are known to undergo unusual and selective reactions with organic molecules. Localization of double bonds in olefins with Fe^+ ion reactions,[3a] work on pattern recognition methods for metal ion chemical ionization mass spectra;[3b,c] isomer discrimination of disubstituted benzene derivatives,[4] of C_5H_8 derivates[5] are just a few of possible applications.

2. Techniques for the study of ion/molecule reactions

At this time, virtually every mass spectrometric technique available today has been applied to the study of ion chemistry.[6]

The techniques can be classified into two large groups as shown in Figure I.1.: according to the type of mass spectrometer and according to the involved ionization technique. We can distinguish mass spectrometers with space resolved experimental sequences from mass spectrometers with time resolved sequences.

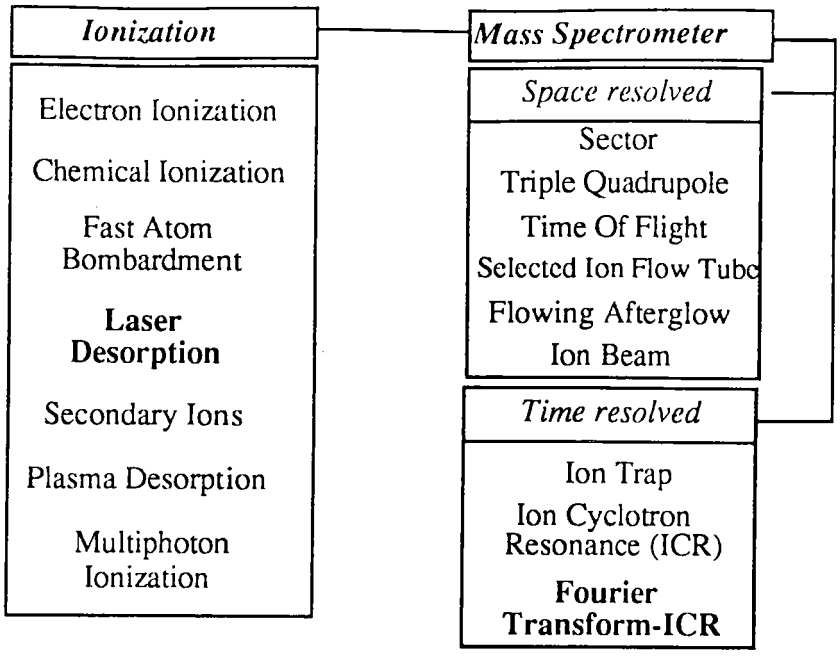

Figure I.1. Mass spectrometric techniques applied in ion/molecule reaction studies

The study of ion/molecule reactions became particularly feasible and appealing with the advent of Fourier transform mass spectrometers. The laser source lends itself particularly well to ICR spectrometry, because FTMS is inherently a pulsed technique and the use of a pulsed ionization source is straightforward.

2.1. *The FTMS*

Fourier Transform Mass Spectrometry[7] is a so called "tandem-in-time" method, which means that all ion manipulations take place within a single confined space (the trapping cell) but are separated in time (Figure I.2.). The ion trap (or cell) is in general of cubic or cylindrical shape. It is centered in an homogeneous magnetic field usually generated by a superconducting magnet (Figure I.3). Ions are either formed inside the cell or injected into it from an external ion source.

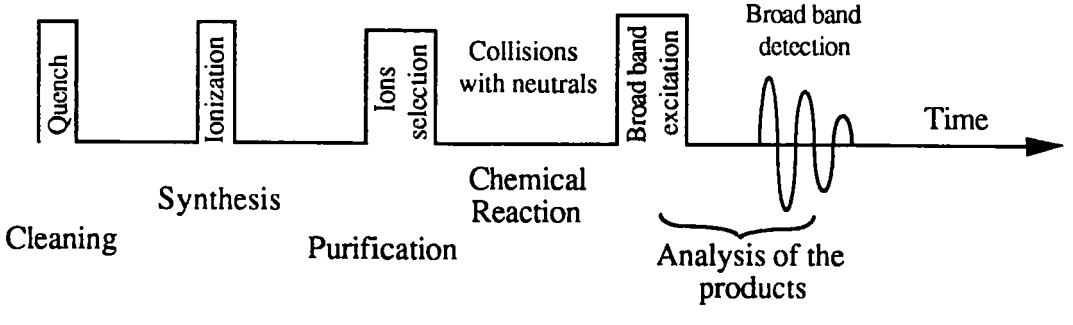

Figure I.2. Time resolved experiment sequence used in FTMS. Purification and reaction steps are optional.

An ion in a magnetic field will undergo a circular motion (so called cyclotron motion) in a plane perpendicular to the magnetic field at a frequency depending on its mass to charge ratio (m/z). The trapping in the z direction (parallel to the magnetic field) is achieved by the application of a DC voltage to a pair of opposite elecrtodes (called trapping plates) perpendicular to the magnetic field (Figure I.3.). Interactions of the ion with both electric and magnetic field allow its trapping, its manipulation and eventually its detection.

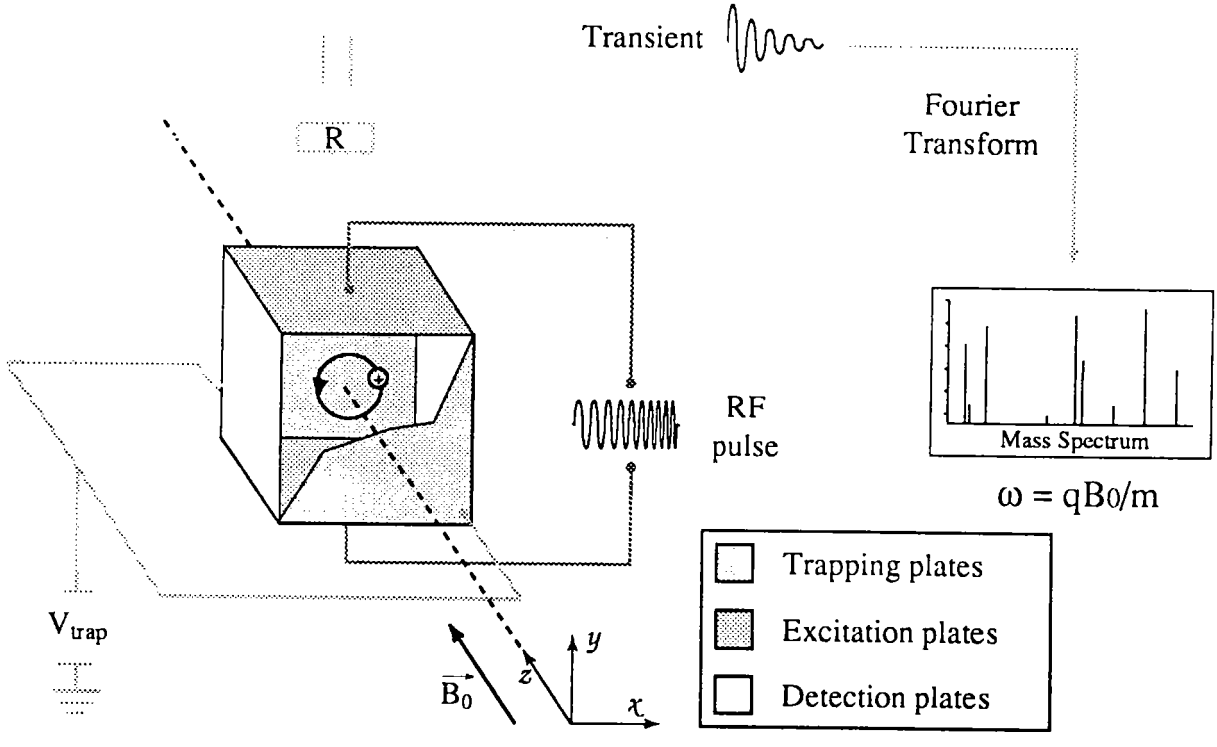

Figure I.3. FTMS general scheme

One necessary manipulation during an FTMS experiment is the excitation of the ion motion. It can be used to eject unwanted ions or to organize collisions between the ions and molecules, but its main purpose is to allow the detection of the ion packets. Practically, a radiofrequency pulse is applied on a pair of opposite electrodes (excitation plates). When the frequency of the pulse matches the ion cyclotron frequency (resonance excitation), the ion will absorb the energy of the excitation field and spiral out toward a larger orbit. Excitation can be performed by a radiofrequency chirp, a simple temporary voltage applied on the plates or by a computed waveform.

One of the unique features of FTMS is the non-destuctive process of ion detection. Instead of colliding with a conversion dynode or a microchanel plate, the ions are detected by the differential charge induced by their rotation on a pair of opposite electrodes (detection plates, see Fig I.3.).

After their formation or their introduction into the trapping cell, ions of same m/z ratio have the same frequency of motion but a random phase. The induced signal on the detection plates is zero (Figure I.4.).

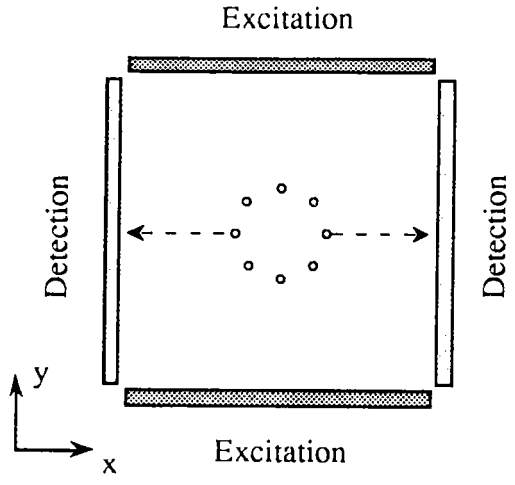

Figure I.4. Zero image current induced by an assembly of ions with random phase. The initial radius was increased for clarity.

Resonance excitation creates an alternative charge difference on excitation plates which displaces the ions off the axis of the cell (to approximately 50% of the cell's dimension) in a coherent ion packet. The rotation of this ion packet induces an image current on the detection plates. The frequency of this current equals the cyclotron frequency of the ions and its amplitude is proportional to the number of ions in the packet. (Figure I.5.).

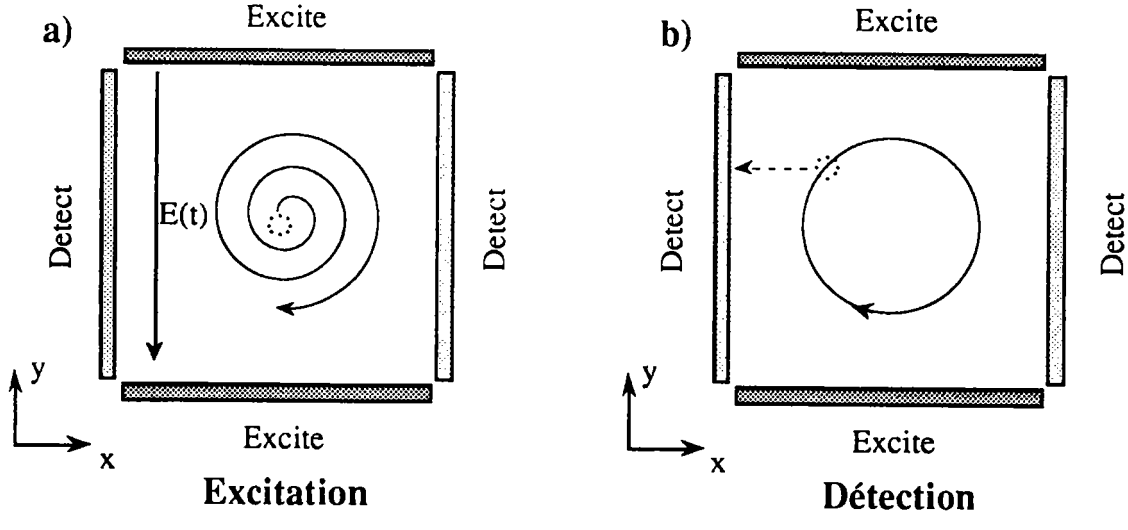

Figure I.5 . Principle of resonance excitation (a) and image current detection (b). The radiofrequency pulse (a) induces the gathering of the ions in a phase coherent packet and the increase of the cyclotron radius. Ions can then be detected through the charge they induce on the detection plates (b).

The global image current is the sum of the influences of all excited ion packets in the cell. It is collected as a transient current, converted into a voltage and digitized by a computer. The transient is then deconvoluted in its frequency components by Fourier transform. The resulting spectrum contains information about the frequencies and abundances of the detected ions.

The exceptional performances of FTMS are a result of the non-destructive detection method described by Comisarow and Marshall in 1974.[8] A detectable signal can be induced by as few as hundred ions and the detection is multichanel i.e. all ions are detected simultaneously by a single detector. Detection performances increase with the ions coherent motion duration and results totally unachievable by other techniques can be obtained if one manages to moderate dephasing processes. For example, Marshall et al.[9] have reported the detection of $^4He^+$ with a resolution greater than 200 000 000. Moreover, the method allows a remarkable precision in mass determinations (provided that a correct calibration law can be calculated) because frequencies can be measured with nine significant figures.

2.1.1. Lorentz force and cyclotron motion

A particle of charge q in a magnetic field $\mathbf{B_0}$ will undergo a circular motion with a fixed period depending on its initial velocity v. This effect is caused by the Lorentz force **F** :

$$\vec{F} = q\left(\vec{v} \times \vec{B}_0\right)$$

The angular acceleration is defined as :

$$\frac{d\vec{v}}{dt} = \frac{\left(v_{xy}\right)^2}{r} = r\omega^2 \quad \text{with} \quad v_{xy} = \sqrt{v_x^2 + v_y^2}$$

The magnetic field lies in the z direction, the Lorentz force in the xy plane. The equilibrium condition can be expressed as follows :

$$\frac{m \cdot v_{xy}^2}{r} = q \cdot v_{xy} \cdot B_0 \quad \text{with r the orbital radius}$$

The angular pulsation and the cyclotron frequency are then given by :

$$\omega_c = \frac{q \cdot B_0}{m} \quad \left(\text{rad} \cdot \text{s}^{-1}\right)$$

$$\nu_c = \frac{q \cdot B_0}{2\pi \cdot m} \ (Hz)$$

It is possible to calculate the equilibrium radius for a particle of mass m carrying a charge q (q=ze) and having a kinetic energy in the xy plane : $E_c = \frac{1}{2} m v_{xy}^2$

$$r = \frac{\sqrt{2m \cdot E_c}}{q \cdot B_0}$$

2.1.2. The electric trapping field

The application of a DC voltage on the trapping plates has the first effect to trap ions in the direction parallel to the magnetic field by creating a potential well (Figure I.6.)

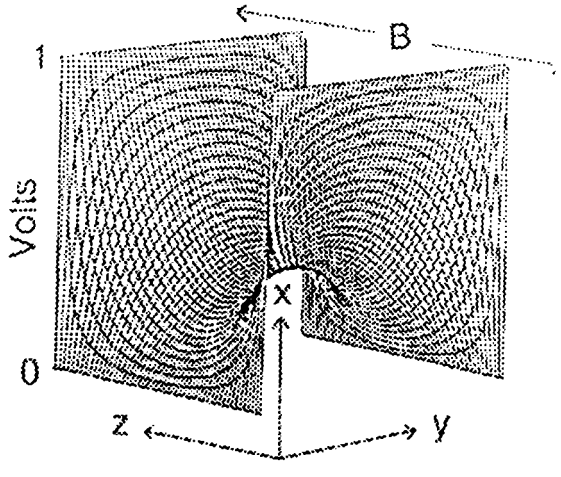

Figure I.6. Simion plot of the trapping field equipotentials between both trapping plates at a 1 V potential. Ions are confined in the xy plane by the magnetic force.

However, according to the Gauss law, the inward axial electric field must have a radial component directed outward, it happens to be a quadrupolar field. In other words, the field "flows" from the charged trapping plates to the earthed excitation and detection plates (Figure I.7.).

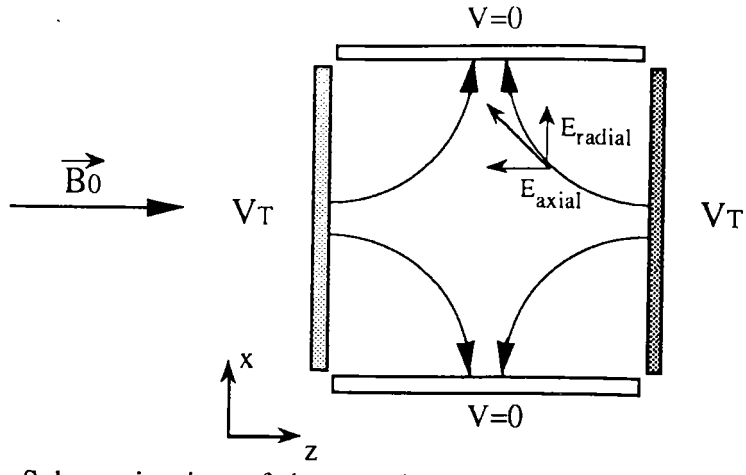

Figure I.7. Schematic view of the trapping electric field lines in a cubic cell

This effect complicates slightly the FTMS experiments. The radial electric field induces a force opposed to the Lorentz force (Figure I.8.). It has a non negligible effect on ions motion and on their capability to be detected.

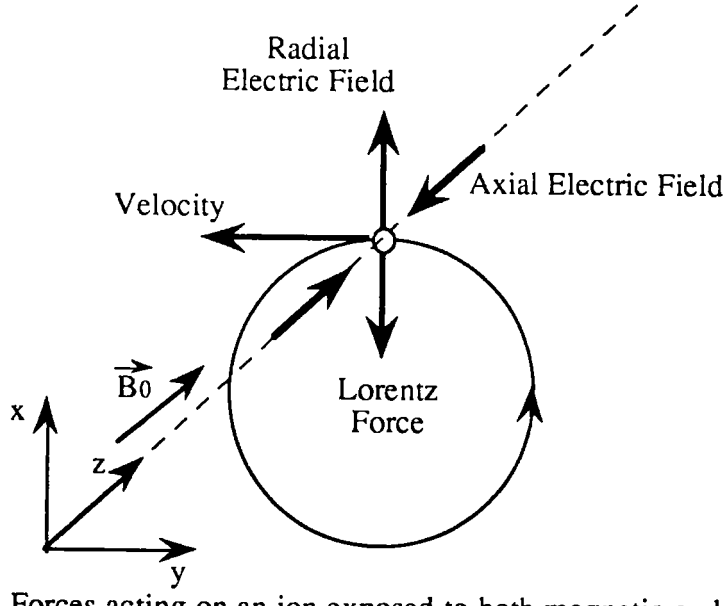

Figure I.8. Forces acting on an ion exposed to both magnetic and electric trapping fields.

The additional centrifugal force causes a shift of the cyclotron frequency. Moreover, the applied electric field induces two new modes of motion :

- the magnetron motion which is a slow precession of the ion cloud around an equipotential line of the electric field at a frequency ν_-.
- the trapping oscillations in the potential well at a frequency ν_z.

It is possible to calculate those frequencies starting from the general equation of the ion motion under the influence of the combined magnetic and electric fields. If the

electric field is assumed to be purely quadrupolar (which is nearly the case at the center of a cubic trap), the equilibrium condition can be expressed as follows :

$$\sum \vec{F} = q\left(\vec{E}_0 + \vec{v} \times \vec{B}_0\right) = m \cdot \frac{d\vec{v}}{dt}$$

Thus, in the radial plane (xy) :

$$m \cdot \omega^2 \cdot r = q \cdot B_0 \cdot \omega \cdot r - \frac{q \cdot E_0 \cdot r}{a}$$

Solving this equation leads to the reduced cyclotron and the magnetron angular frequency :

$$\omega\pm = \frac{q \cdot B_0 \pm \sqrt{q^2 \cdot B_0^2 - \frac{4m \cdot q \cdot E_0}{a}}}{2m}$$

The corresponding frequencies are :

$$\nu_\pm = \frac{q \cdot B_0 \pm \sqrt{q^2 \cdot B_0^2 - \frac{4m \cdot q \cdot E_0}{a}}}{4\pi m}$$

The electric trapping field creates a force along the cell axis which prevents ions to escape in the magnetic field direction. The axial component of the trapping field is given by :

$$E(z) = -\frac{dV(z)}{dz} = -\frac{4V_T}{a^2} \cdot z$$

The equation of motion on the z axis is thus :

$$q \cdot E(z) = -\frac{4V_T}{a^2} \cdot z \cdot q = m \cdot \frac{d\vec{v}_z}{dt}$$

The presence of both plates at the potential V_T induces an oscillation of ions along the cell's axis. This motion has the following frequencies :

$$\omega_z = \frac{2}{a}\sqrt{\frac{q \cdot V_T}{m}}$$

$$\nu_z = \frac{1}{\pi a}\sqrt{\frac{q \cdot V_T}{m}}$$

The combination of the three modes of motion, just described, generates a complicated trajectory of ions in the cell (Figure I.9.).

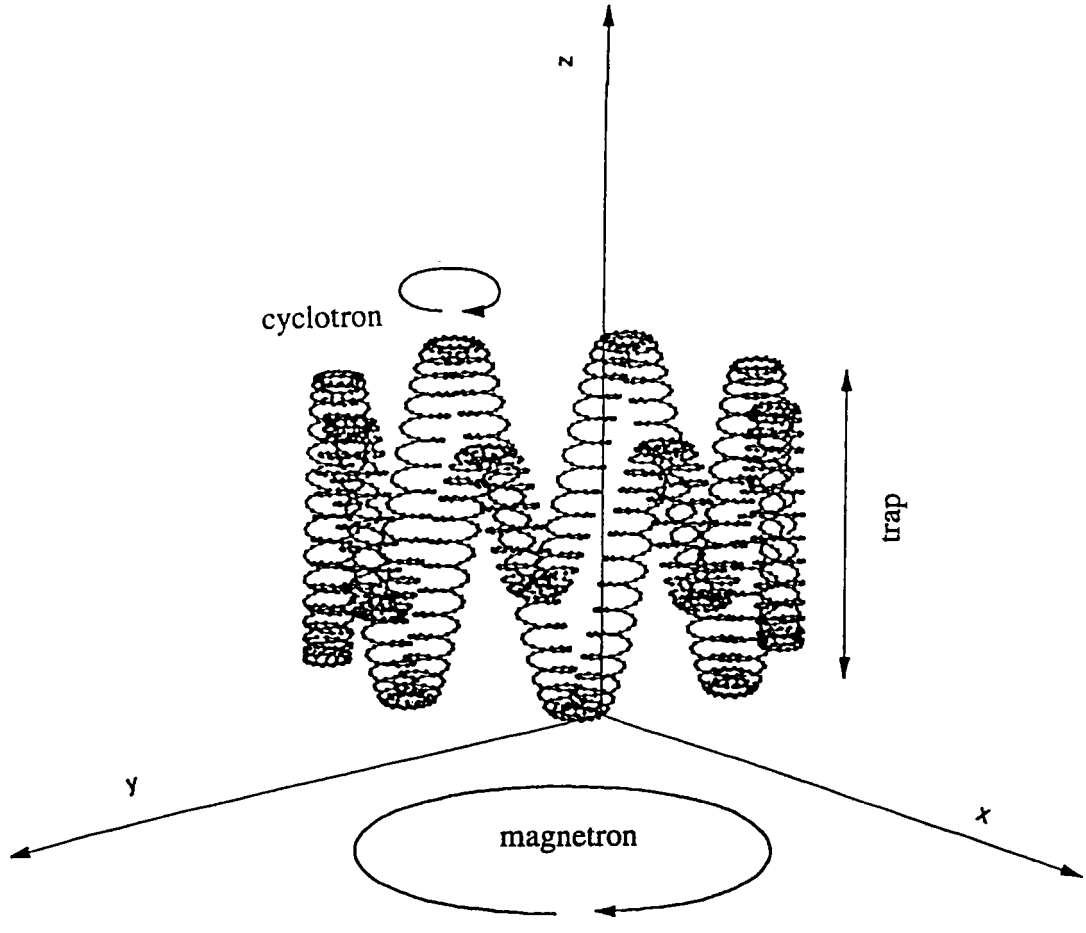

Figure I.9. Combination of the three natural motions of an ion in an FTMS cell. Cyclotron, magnetron and trapping oscillations.

2.1.3. Space charge effect and calibration laws

Up to now, we have assumed that the forces acting on the ion result only from its interactions with the electric and the magnetic fields. This is true as long as only one ion is trapped. When more ions are trapped together, coulombic interactions can become significant. For large ion populations these effects have a great impact on the obtained results and are called space charge effect (Figure I. 10.).

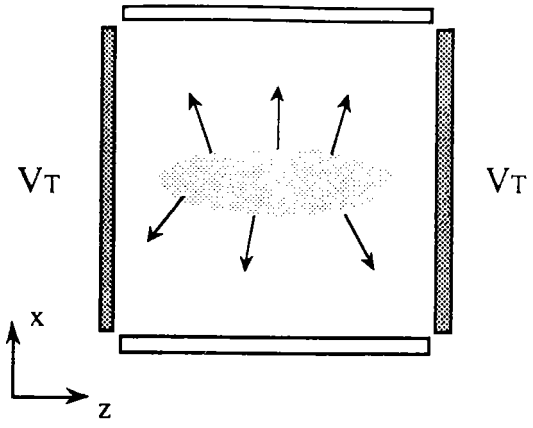

Figure I.10. Schematic view of the space charge effect.

Space charge effect can be aspproximated to an outward force depending on the number of ions trapped together. The first effect of space charge is the loss of mass precision. The equation of ions motion is perturbed by the additional outward force and the measured frequencies depend not only on the externally applied fields but on the charge density which can not be determined precisely. These effects can be partially compensated in the calibration law by introducing a global signal intensity term (see Table I.1.)

Table I.1. Calibration laws

Application	Calibration law
Zero electric field approximation (V_T=0)	$\nu_c = \frac{qB}{2\pi m}$
Pure quadrupolar field approximation	$\nu_+ = \frac{a}{m} + \frac{b}{m^2}$
Pure quadrupolar field approximation with space charge effect	$\nu_+ = \frac{a}{m} + \frac{b}{m^2} + \frac{c[I]}{m^2}$ *

* : [I] is the global intensity of all ions except those having the m/z value to be calculated.

The number of trapped ions can be regulated by using appropriate sequences but an information is lost : the initial relative amounts of ions formed. The space charge effect induces a decrease in the observed cyclotron frequencies, this effect is similar to the influence of an increase of the trapping potential. It has been suggested that a positive effect of the space charge would be created to attenuate the electric field inhomogeneities inside the cell.

2.2. Laser-matter interaction

Laser ablation/ionization has been subject of intensive research since its first applications at the beginning of the 70's. This can be explained by the following characteristics :

- possibility to ionize metals or insulator compounds,
- wide choice in the experimental parameters since various lasers are available,
- possibility to focus the beam on very small areas which opens the field of microanalysis.

Growing efforts have been made in order to understand the processes occurring during the laser-matter interaction. In fact, several parameters have to be taken into account. Some of them are listed in Table I.2.

Table I.2 Parameters important in the laser-solid interaction process.

Laser parameters	Target parameters
Irradiance	Thickness
Wavelength	Absorption coefficient
Pulse duration	Thermal conductivity
Incidence angle	Electrical conductivity
Repetition rate	Enthalpy of sublimation
	Surface state

The characteristics of laser ionization depends on the physical state of the analyte. In the gas phase, ionization processes are quite well known. In general, the ionization requires a relatively low energy. The general principles of electronic spectroscopy of atoms or molecules rule the process. In the solid phase, the processes leading to the ionization of the target are not so well known. Actually, the same laser beam has to transfer the material to the gas phase and ionize the atoms and molecules. Therefore, the mechanisms of laser ionization of solid materials are complicated.

2.2.1 Modeling of the laser ablation process

One of the oldest models of laser-matter interaction was proposed by Hercules in 1982.[10] During the impact of a laser beam at surface, numerous processes occur. The ablated depth as well as the relative contribution of the various processes ultimately depends on the wavelength and the irradiance of the incident beam for a

given material.

If we consider the laser vaporization/ionization of a material, four general mechanisms can be distinguished corresponding to four areas of the interaction surface:

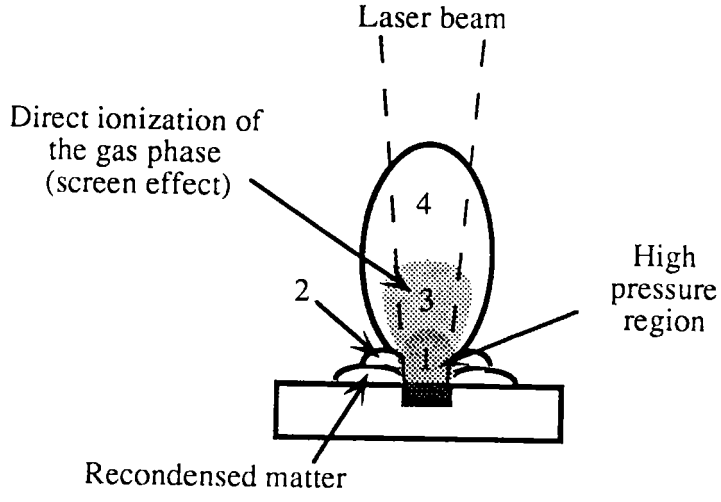

Figure I.11. Different zones in laser ablation process.

Area 1, where the laser beam strikes the surface, is characterized by a direct ionization of the solid, especially at high irradiance ($> 10^8$ W cm^{-2}). The temperature in this region can reach 3000 to 6000 K. Under these conditions, only atomic ions and few molecular fragments can be emitted.

Area 2, in the neighborhood of area 1 is a desorption region. It is characterised by a high temperature gradient due to the shockwave induced by the laser impact. High molecular weight ions as well as molecules are emitted from this region.

Area 3 corresponds to the ionization of the gaseous cloud above the surface by the dense photon beam (screen effect).

Area 4 is the region where ions are free from the mutual interactions.

The ablation depth per laser shot depends on the wavelength and the irradiance of the oncoming beam.

2.2.1.1. Wavelength effect

Depending on the wavelength, ablation processes can be very different. In the infrared, thermal mechanisms are favored, though in the ultraviolet, photochemical processes occur.

2.2.1.2. *Thermal effects*

The energy brought by the laser irradiation spreads through the material via thermal conduction. The IR photons are not energetic enough to achieve the ionization of the material, but they are very numerous and induce a heating of the surface by successive hits. The result is the melting and evaporation of the irradiated surface. One can consider in first approximation that the laser irradiation can be assimilated to as a heat source deposited on the surface of the material, it can be compared as well to the impact of a projectile on a target or an explosion of dynamite.

2.2.1.3. *Photochemical effects*

The absorption of UV photons by the material leads to transitions between the electronic states of the molecules (especially for polymers). The decomposition of the material is considered to be ablative ; three mechanisms can lead to this decomposition:

(i) first, the absorption of UV photons can promote the molecules to dissociative electronic states. This purely photochemical step is extremely short (less than 1 fs), it directly leads to the ablation of the substrate;

(ii) excited molecules (not yet ablated) relax by redistributing their energy excess as rotational or vibrational energy to the neighbouring molecules by collisions. This phenomenon results in a rapid and local heating of the sample. The subsequent absorption of several photons in the same area can lead to temperatures high enough to allow thermal decomposition of the molecules starting from the most fragile bonds (ion-covalent such as: hydrogen bonds, ionic interactions);

(iii) the absorption of the first UV photons induces a heating of the surface at the place of impact, which leads to an increase in the population of the vibrational excited states of the molecule. If these lifetime of vibrational-states is long enough for a second (or even third) photon absorption to take place, a photochemical dissociation of the molecules can be observed.

If the number of bonds broken during the process is high enough, there is a rapid increase in the local pressure leading to an explosive expansion of the material (supersonic beam).

2.2.1.4. Occurring processes vs. irradiance

Most of the ions (positive or negative), which bring information about the analysed material, are formed during the laser induced gaseous cloud expansion. The nature of this cloud depends on the irradiance. Moreover, it appears that the ion/neutral ratio is directly related to the irradiance used. Actually, for irradiances over 10^9 W cm^{-2}, this ratio can reach 0.1 to 0.01 while it is not over 10^{-5} for irradiances lower than 10^8 W cm^{-2} .[10]

Three different ablation/ionization processes can be distinguished with respect to the irradiance[11] :

- between 10^5 and 10^7 to 10^8 W cm^{-2}, laser desorption processes occur. They allow in many cases the detection of molecular or quasi-molecular ions.
- between 10^8 and 10^{10} W cm^{-2}, elemental ions are present together with ionized clusters depending on the studied material.
- above 10^{10} W cm^{-2} only elemental species are observed.

References

1. a) B. S. Freiser, *J. Mass.Spectrom.* **31** 703 (1996).
   b) K. Eller and H. Schwarz, *Chem. Rev.* **91** 1121 (1991).
   c) N. M. M. Nibbering, *Acc. Chem. Res.* **23** 279 (1990).
2. R.C. Burnier, T.C. Carlin, W.D. Reents, R.B. Cody, R.K. Lengel and B.S. Freiser, *J. Am. Chem. Soc.*, **101**, 7127 (1979).
3. a) D.A. Peake and M.L. Gross, *Anal. Chem.*, **57**, 115 (1985).
   b) R.A. Forbes, E.C. Tews, Y. Huang, B.S. Freiser and S.P. Perone, *Anal. Chem.* **59**, 1937 (1987).
   c) R.A. Forbes, E.C. Tews, B.S. Freiser, M.B. Wise and S.P. Perone, *Anal. Chem.* **58**, 684 (1986).
4. a) A. Bjarnason, J. W. Taylor, J.A. Kinsinger, R.B. Cody and D.A. Weil, *Anal. Chem.* **61**, 1889 (1989).
   b) J. Chamot-Rooke, J. Tortajada and J.-P. Morizur, *Eur. Mass. Spectrom.* **1**, 471 (1995).
5. J. Ni and A.G. Harrison, *Rapid Commun. Mass Spectrom.*, **10**, 220 (1996).
6. J.M. Farrar and W.H. Saunders, Jr., "Techniques for the Study of Ion-Molecule Reactions", Vol. XX, John Wiley & Sons, (1988).
7. A.G. Marshall and F. R. Verdun, "Fourier Transform in NMR, Optical, and Mass Spectrometry: A User's Handbook", Elsevier, Amsterdam (1990).
8. M.B. Comisarow and A.G. Marshall, *Chem. Phys. Lett.* **25**, 282 (1974).
9. A.G. Marshall and L. Schweikhard, *Int J. Mass Spectrom. Ion Processes.* **118/119,** 37 (1992).
10. D.M. Hercules, R.J. Day, K. Balasanmugam, T.A. Dang and C.P. Li, *Anal. Chem.*,**54**, 280A (1982).
11. A. Vertes, R. Gijbels and F. Adams, "Laser Ionization Mass Analysis", Vol. 124, John Wiley & Sons, (1993).

Chapter II
Experimental Part

In this chapter, materials and experimental set-up used in this work are presented. Two FTMS instruments have been used throughout this study, they will be both described herein. Experimental sequences and parameters will be discussed.

1. Instrumentation

The experiments have been performed on two FTMS instruments. Chemical ionization and ion/molecule reactions were performed on a Laser Microprobe FTMS 2000 instrument at the LSMCL (Laboratoire de Spectrométrie de masse et Chimie Laser) laboratory (University of Metz). This instrument is interfaced with different lasers. Electron ionization (EI) mass spectra were obtained on a FTMS 2001 instrument in LKKAK (Laboratorij za kemijsku kinetiku i atmosfersku kemiju) laboratory (Ruđer Bošković Institute, Zagreb) for comparison.

1.1. Laser Microprobe FTMS 2000

The FTMS laser microprobe at the LSMCL laboratory (University of Metz) is based on a commercial FTMS 2000 instrument (Nicolet, now Finnigan, Madison, WI, USA). It was originaly dedicated to electron or chemical ionisation. Several modifications were necessary to achieve the coupling with a laser ionisation source[1-8]. These modifications had to be done cautiously in order to allow the instrument to evolve with the FTMS technology. Devoted to laser induced experiments it has no possibility of standard electron ionization.

The mass analyzer is based on a double-cell (source cell and analyzer cell) enclosed in a ultra high vacuum chamber and centered in a very homogeneous magnetic field (Figure II.1).

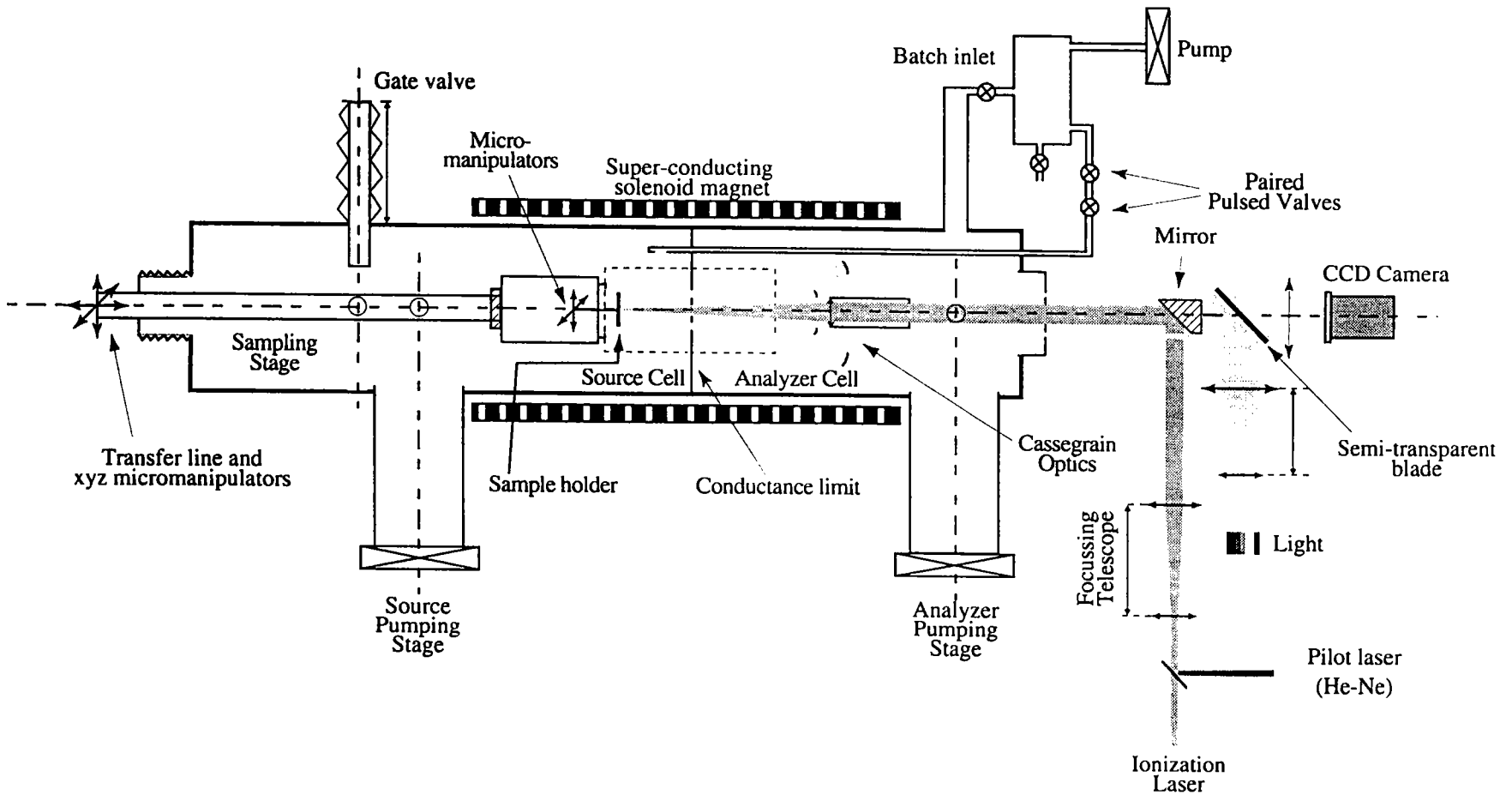

Figure II.1 Laser Microprobe Fourier Transform Mass Spectrometer FTMS 2000. General scheme.

1.1.1. The double-cell

It consists of two cubic cells made of amagnetic stainless steel plates with a honeycomb structure (see Figure II.2). Both cells share a common plate, the conductance limit, which is made of bulk metal and has a hole in its center to allow ions to cross from one cell to the other. This plate allows a differential pumping between the two cells. A part of the conductance limit is made of a quartz window covered with a very thin metallic grid. This allows the light to pass through the plate for visualization purposes. Each cell has its own trapping plate perpendicular to the magnetic field and two pairs of opposed electrodes for excitation and detection. The conductance limit plays the role of the second trapping plate for both cells. The analyzer cell's trapping plate is pierced to allow the laser beam to go through the cell. The source trapping plate is removable and has a hole in its center to permit the insertion of a sample holder. The cell dimensions are 5 cm x 5 cm x 5 cm. The double cell is fixed on metallic rods which support the cables necessary for the application of various electric potentials on the plates.

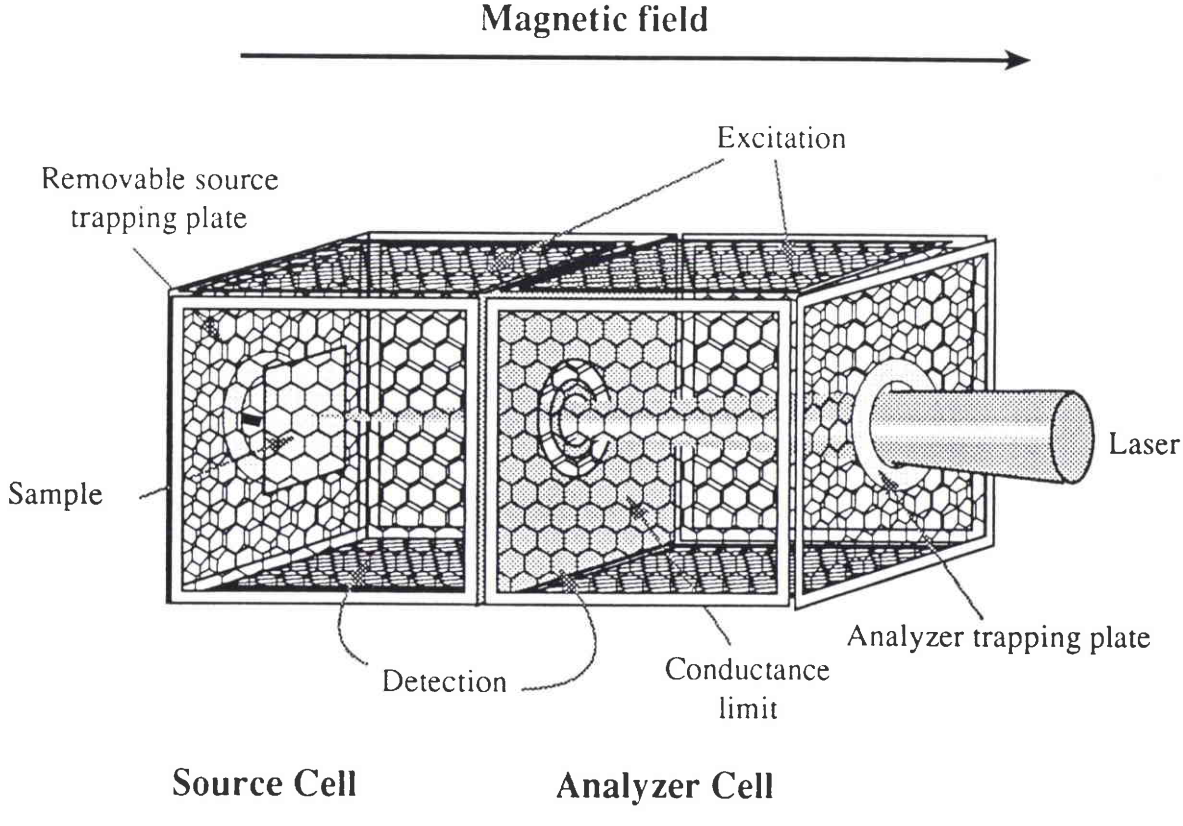

Figure II.2 : The double-cell (drawing taken from ref. 9).

1.1.2. The cryomagnet, the pumping and the electronics

The magnetic field is generated by a solenoïd superconductive magnet made of a niobium/titanium alloy coil. A two stage dewar, the first contaning liquid nitrogen and the second containing liquid helium allows the superconduction. The magnet provides a very homogeneous 3.04 T field on the axis of the chamber. Both cells are centered in the magnet's tore on the magnetic field axis.

FTMS performances are pressure dependant. In fact, collisions with a residual gas reduce the time of coherent motion of the ions and the signal gets lost (a loss of resolution). The different stages of the instrument are thus continuously pumped by high capacity pumps.

The sampling chamber, is pumped by a primary pump Alcatel (35 l h^{-1}) and a turbo-molecular pump (400 l s^{-1}). This system permits to reach a 10^{-6} Torr* pressure in few minutes.

The instrument's chamber is differentially pumped from the source and the analyzer side by two primary pumps (Alcatel 2012A, 16 l h^{-1}) and two diffusion pumps (650 l s^{-1}) When the gate valve (between sampling chambre and "instrument's chamber") is closed, the vacuum in the instrument is typically 10^{-9} Torr. When that valve is open, the pressure increases up to $5 \cdot 10^{-8}$ - 10^{-7} Torr in the source side but remains below $2 \cdot 10^{-8}$ Torr in the analyzer's side. Those pressures can temporarily increase when reactive gases are introduced into the chamber.

The instrument is equiped with various electronic systems for security and for the performance of experiment sequences. The programation of experiment sequences and the acquisition of data are based on a fast access of memory computer and various peripherals. Among them, the most important is the cell controller. It generates the various potentials which are applied to the cell plates. The cell controller is connected to the excitation plates via a power amplifier and collects the signal detected on the reception plates through a preamplifier. The main computer of the instrument is a SUN LX data station coupled to an Odyssey acquisition electronics.

---

* 1 Torr = 133.322 Pa

1.1.3. Sample introduction and manipulation

1.1.3.1 Solid samples (reagent ions)

The sample for laser desorption/ablation is attached on an amagnetic metal square sample holder (2 cm x 2cm) mounted on a sliding transfer line. The source trapping plate is part of the support and has to be removed from the chamber with the sample. The trapping voltage is applied on the plate and on the sample holder with a cable mounted in the transfer line.

This configuration with the sample holder inside the cell has been modified in the course of the present work because it was prejudicious to the high resolution capabilities of the instrument. Part of this work has thus been done with an external sample holder placed just outside the source cell. The sample support is equiped with a remote command x-y manipulation hardware.[7]

1.1.3.2. Liquid and gaseous samples (reactant molecules)

A glass tube filled with the liquid sample was mounted on the batch inlet and degased by repeated freeze-pump-thaw cycles. The gas phase of the sample was then introduced into the batch inlet container, up to a pressure of ca. 400 mTorr. There are two possibilities for the gas (evaporated liquid) samples introduction into the FTMS chamber. They can be introduced continuously through the batch inlet valve (Fig. II.1) in the analyzer side of the chamber. The second way is through the paired pulsed valves (General Valves, Fairfield, New Jersey). The opening of the first one (0.05 - 0.2 s) allows entering a gas into the volume between two valves. After the closure of the first one, the second one let the gas entering the chamber (time of the opening of the second valve 0.05 - 0.2 s). The exit of second pulse valve is connected to a home-made pipe to allow direct introduction of the gases into the source cell. We mounted this tube in order to perform ion/molecule reactions.

1.1.3.3. Cooling gas

For the laser produced reagent ions, argon has occasionnaly been used as cooling gas. The batch inlet container was filled with argon to a pressure of about 2 Torr. The gas was then introduced into the chamber by pulsed valves to a pressure of ca. 10^{-6} Torr in the source cell.

1.1.4. The laser ionisation interface

The key part of the laser ionization interface is a reversed Cassegrain optics[8] allowing the laser to be focussed on the target and the visualization of the sample These optics are mounted inside the spectrometer's chamber. The position of the focussing lenses can be changed with an external manipulator in order to provide ionization at various wavelength (from 190 to 360 nm)

Two lasers are coupled to the micorprobe. First, an excimer laser LPX 200 (Lambda Physic, Goettingen, Germany) and second, an Neodymium Yttrium Aluminium Garnet (Nd-YAG), Brilliant (Quantel, Les Ulis, France).

Table II.1. Characteristics of the laser beams delivered by the lasers coupled to the FTMS microprobe.

Wavelength / nm	Maximum output energy / μJ	Energy on the sample /μJ	Pulse duration / ns
193	200	82	23
248	200	140	34
266	63	188	4.3
355	63	188	4.3

The excimer laser allows the use of the 248 nm and 193 nm wavelength with krypton/fluorine and argon/fluorine mixtures respectively. The Nd-YAG laser is used in quadrupled mode (266 nm) and tripled mode (355 nm). The first and second harmonics of this laser (1064 and 532 nm respectively) can not be used with our configuration because the optics have been made for UV lasers (190 to 360 nm). The characteristics of the laser beams provided by our lasers are summarized in Table II.1.

The laser beam is brought to an adjustable telescope by means of two prisms. The adjustment of the telescope results in changes in the spot diameter on the sample, and therefore changes in the irradiance. Table II.2. shows the irradiances attainable with the different wavelengths currently used. The minimum value corresponds to the lowest output energy of the laser providing a reproducible beam. In fact, lower irradiances could be reached but fluctuations in the laser profile wouldn't allow a accurate determination of the irradiance on the sample.

The laser energy is measured in front of the entrance window of the chamber

with a photosensitive cell connected to a digital oscilloscope. The irradiance is then calculated with respect to the absorbance of the optics and the spot diameter for a given position of the telescope.

Table II.2. Accessible irradiance ranges.

Wavelength / nm	Maximum Irradiance / W cm^{-2}	Minimum Irradiance / W cm^{-2}
193	2.0 10^9	3.0 10^5
248	2.0 10^9	3.5 10^5
266	3.0 10^{10}	7.0 10^6
355	3.0 10^{10}	9.0 10^6

At the exit of the telescope, the beam is reflected by a mirror through a silica window towards the central lenses of the reverted Cassegrain optics in the spectrometer's chamber. It is then focussed on the sample through the holes in the analyzer's trapping plate and the conductance limit.

The external mirrors of the Cassegrain optics transmit the light of an external source to the sample and reflect the sample image to an external CCD camera. A lens allows the visualization ot the sample on a video monitor with a 300x magnification.

1.2. FTMS 2001

The FTMS at the LKKAK Laboratory in Zagreb, is a commercial FTMS 2001 instrument (Extrel, now Finnigan, Madison, WI, USA). It has many common features with the instrument in Metz: double cell, 3 T superconducting magnet, differential pumping (typically pressure in the source region : 10^{-8} Torr; pressure in the analyzer region : 10^{-9} Torr), batch inlets, pulsed valves.

The differences are as follow: The Nd-Yag laser has possibility to work on 1064, 532, 355 and 266 nm. The laser beam comes on the target sample at a 45° angle. Manipulation of the probe is posible in the z direction and the probe can be rotated (360°). Concerning the computer interface, the instrument is controlled by a 1280 Nicolet data station.

The most important difference for this work is that beside the laser interface the instrument allows electron ionization (Figure II.3.). EI mass spectra of all studied samples were acquired on that instrument.

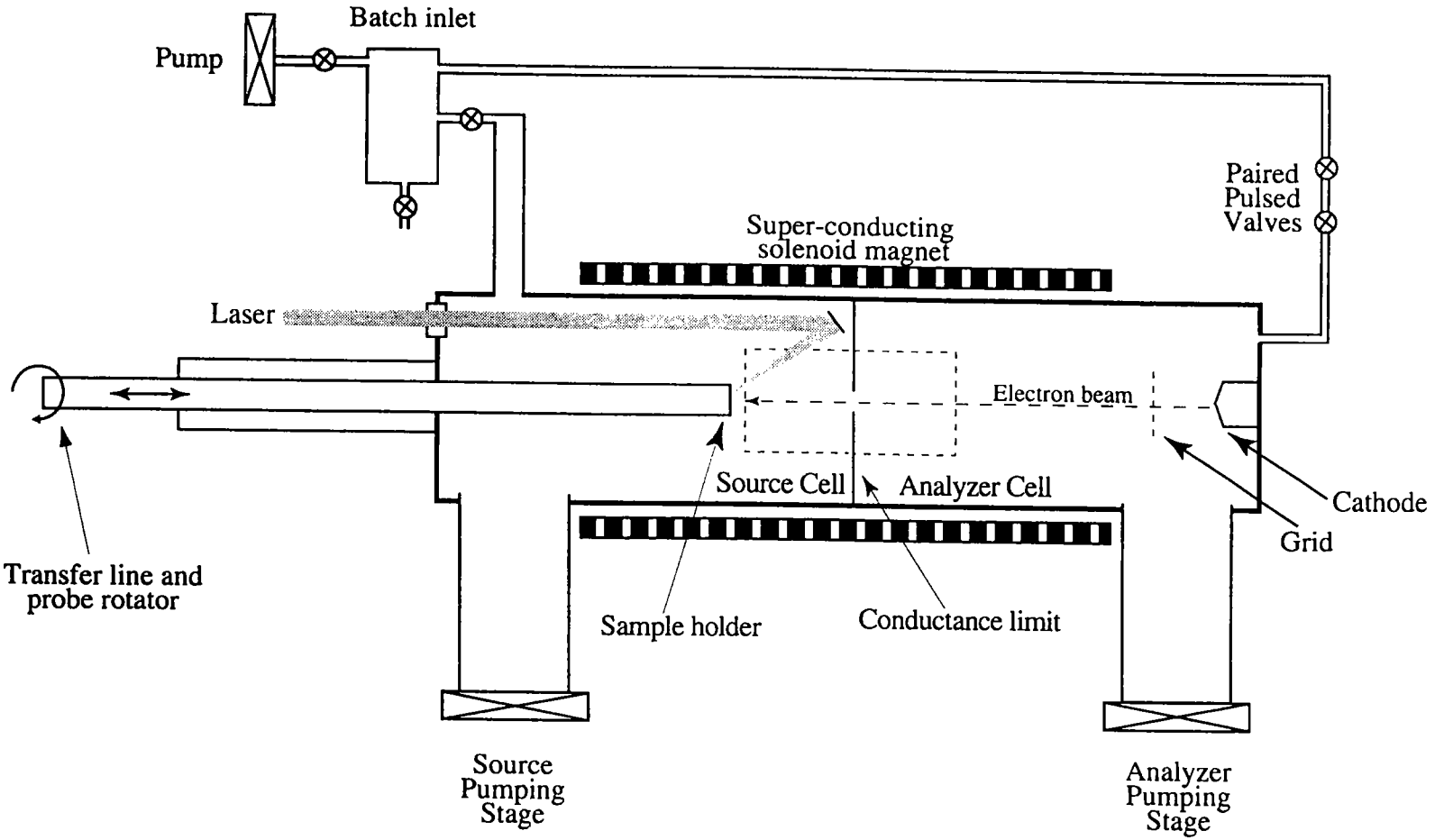

Figure II.3. The schematic pathways of the laser and electron beams in the FTMS 2001.

I.2.1. Electron Ionization FTMS Experiments

Typical parameters in the EI experiments are listed in Table II.3.

Table II.3. Typical experimental parameters for EI experiment sequence

	Parameter	Value
	Experimental type	STD
Pressure	Source	$6 \cdot 10^{-8}$ Torr
	Analyzer	$2 \cdot 10^{-9}$ Torr
	Quench duration	1 ms
Trapping	Trap Voltage	2.0 V
	Bias Voltage	5.0 V
	Conductance Limit	0 V
Ionization	Beam duration	4.0 ms
	Beam voltage	70 V
	Req. Current	4.0 µA
	Measured Current	3.7 µA
	Reaction delay	0.05 to 10 s
Excitation	Sweep rate	2500 Hz/µs
	Attenuation of excite RF	0 dB
	Low frequency	23298 Hz
	High frequency	2666.6 kHz
	Duration	1.07 µs
	Sweep Phase	0 deg
Detection	Receive side	Analyzer
	Receive time	82.23 ms
Digitization	Number of data points (Kbytes)	128
	Collected # Sweeps	300
	Detected Bandwidth	800 kHz
	Dwell Time	625 ns
	Mode (dir/het)	Direct
Transformation	Apodization	Blackman Harris 3 terms
	Zerofilling	2x

2. Chemicals

2.1. *Substances for reagent ion production*

Pure metal samples (Mg, Ca, Ti, V, Mn, Fe, Cr, Co, Cu, Zn, Al, Sn, Mo, Zr, and In) (purity higher than 99 %), silicon wafer and boron powder were used as a laser-pulse target for the production of reagent ions. Scandium is the only first row transition metal which has not been included in this studiy because it was not available to us. The only studied alloy was a stainless steel sample (Cr:Fe:Ni = 25%: 60%: 15%).

For alkali-metal ions formation the pellets of alkaline salt were shooted by the laser. Namely, Na^+ was produced from NaCl, K^+ from KCl, Li^+ from LiF and the earth-alkaline Ba^+ from $Ba(CO_3)_2$, From the halide salts, the corresponding halide ions were generated for negative ion chemical ionization.

2.2. *Volatile organic molecules*

a) Dichlorodifluoromethane, CF_2Cl_2: commercial Puff duster, ref. C829, Agar, Essex, England.

Large quantities of CF_2Cl_2 were manufactured each year (0.5 Mt/year) and in great part released to the atmosphere in the form of aerosol propellant or refrigerator coolant. In our case it was supstance of puff duster in spray. CF_2Cl_2 is a representative of the class of Freons. Photolysis of these halocarbons produces large quantities of chlorine which can react with O_3 to form O_2 and hence may cause a depletion of the ozone layer.

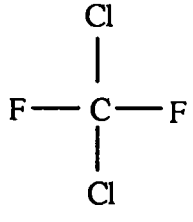

Figure II.4. Dichlorodifluoromethane

b) Halothane, (2-bromo-2-chloro-1,1,1-trifluoroethane) $BrCHClCF_3$, is a commonly used anesthetic. (99%, Aldrich, Saint-Quentin-Fallavier, France)

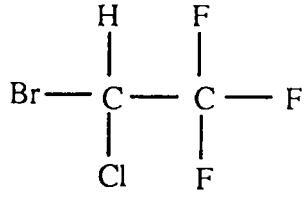

Figure II.5. Halothane

c) Endosulfane, ($C_9H_6Cl_6O_3S$) is a non-systemic insecticide and acaricide with contact and stomach action.[10]

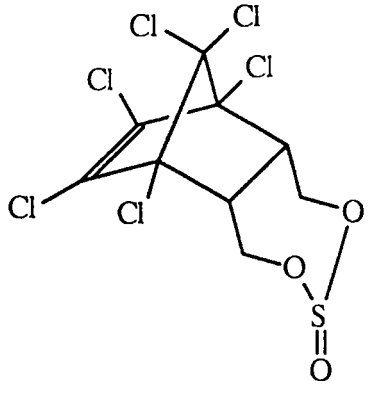

Figure II.6. Endosulfane

d) Perfluorotributylamine, $(C_4F_9)_3N$, (PFTBA) or heptacosafluorotributylamine (99%, Aldrich, Saint-Quentin-Fallavier, France) commonly used as an internal calibrant in electron ionization MS.

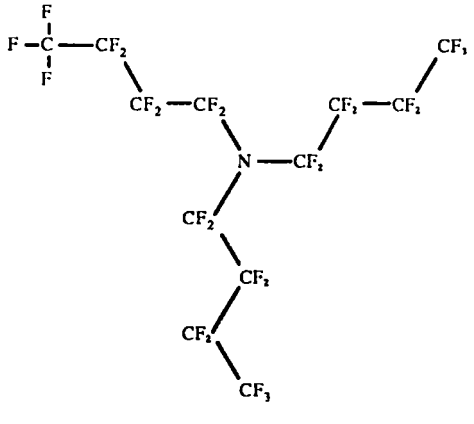

Figure II.7. PFTBA

e) Tributylamine, $(C_4H_9)_3N$, (99+%, Aldrich, Saint-Quentin-Fallavier, France) has a structure similar to PFTBA, the fluorine atoms being replaced by hydrogens.

f) Acetophenone, $C_6H_5COCH_3$, (99%, Aldrich, Saint-Quentin-Fallavier, France). It is a commonly encountered compond in many organic syntheses.

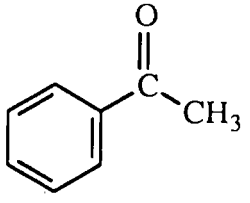

Figure II.8. Acetophenone

Some physical and chemical data about the studied compounds are listed in Table II.4.

Table II.4. Some characteristic of studied compounds (E_i = Ionization Energy, E_{pa} = Proton Affinity).

	Dichlorodi fluoromethane Cl_2CF_2	Halothane $BrCHClCF_3$	Endosulfane $C_9H_6Cl_6O_3S$	PFTBA $(C_4F_9)_3N$	TBA $(C_4H_9)_3N$	Aceto phenone C_8H_8O
M / g mol^{-1}	120	199	404	671	185	120
Physical state (at 25°C)	gas	liquid	solid	liquid	liquid	liquid
Vapor pressure [a] / kPa	651.0 (25°C)	39.9 (25°C)	0.0012 (80°C)[b]	0.073 (25°C)	0.010 (25°C)	0.049 (25°C)
E_i / eV [c]	11.75 ± 0.04	11.0	-	11.3	7.4	9.29 ± 0.03
$\Delta_f H$ (ion) /kJ mol^{-1}	656	363 (361)	-	-4466	492	810
E_{pa} [d] /kJ mol^{-1}	-	-	-	-	982	859

a, b, c, d data from references 10, 11, 12 and 13, respectively.

3. Experimental sequence

All chemical ionization and subsequent ion-molecule reaction experiments were performed on the FTMS 2000 laser microprobe in Metz. Typical experimental sequences are displayed in Figure II.9. and II.10. The first one displays the sequence with reagent gas introduction by pulsed valves, the reaction taking place in the source cell. The second one displays experiments obtained on the analyzer side when gaseous compounds are introduced directly through the batch inlet.

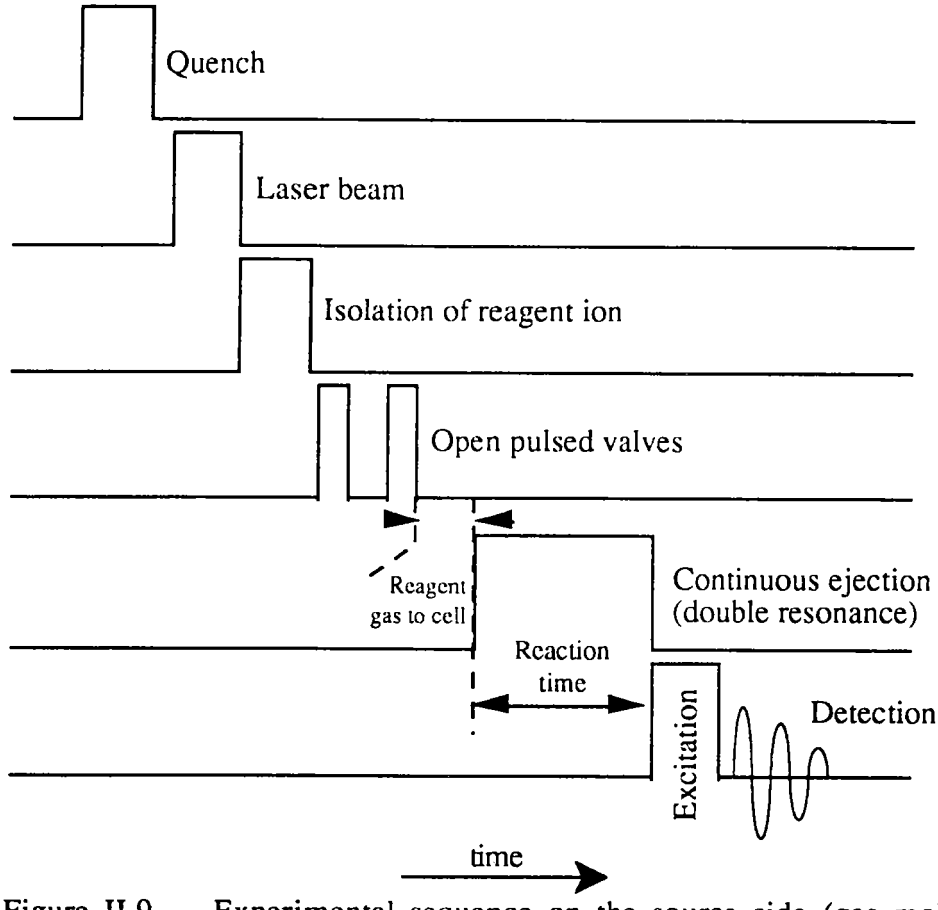

Figure II.9. Experimental sequence on the source side (gas molecules introduced through pulsed valves).

Quench

Every sequence begins or finishes with a quench. A large differential voltage applied on both trapping plates (± 10 V) is a quick non-selective way to remove all residual ions from the cell.

Laser beam / Ionization

All four available wavelengths 355, 266, 248 and 193 nm, have been used in this work, as the reaction products distributions and rates were not affected by the wavelength used for reagent ion formation. Irradiance used throughout this work was in the range 10^8 - 10^{10} W cm^{-2} (plasma ignition condition).

Isolation of reagent ions

In most cases a monoatomique positive ion was the only detected product of laser ablation/ ionization of the target sample. Thus, isolation of ion was not necessary. When some impurities were present (e.g. in the ablation of salt pellets) or when only one elemental isotope was desired, chirp (radio frequency sweep) or SWIFT ejection were performed to select the projectile ion. For an example of parameters used in such sequences see Table II.5.

Introduction of volatile compounds

The gas molecule were introduced directly in the source cell through a pulsed valve connected to a home-made pipe to a cell pressure of $8 \cdot 10^{-7}$ Torr. (Typical parameters are listed in Table II.5.)

Reaction time

A variable period in the range 0.001 to 30 s allowed ion/molecule reactions to occur.

Continuous ejection

To confirm some reaction pathways, ejection of certain ion (precursor) was undertaken. This was carried out by exciting continuously at the cyclotron frequency of the undesired ion. Ejection was applied through all reaction period.

Excitation

Product ions were then excited by a frequency chirp. Example parameters are in the Table II.5.

Detection

The image current was detected, amplified, digitized, apodized (Blackman-Harris 3 terms) and Fourier transformed to produce a mass spectrum.

Some experiments were performed in the analyzer cell. The experimental sequence is displayed in Figure II.10.

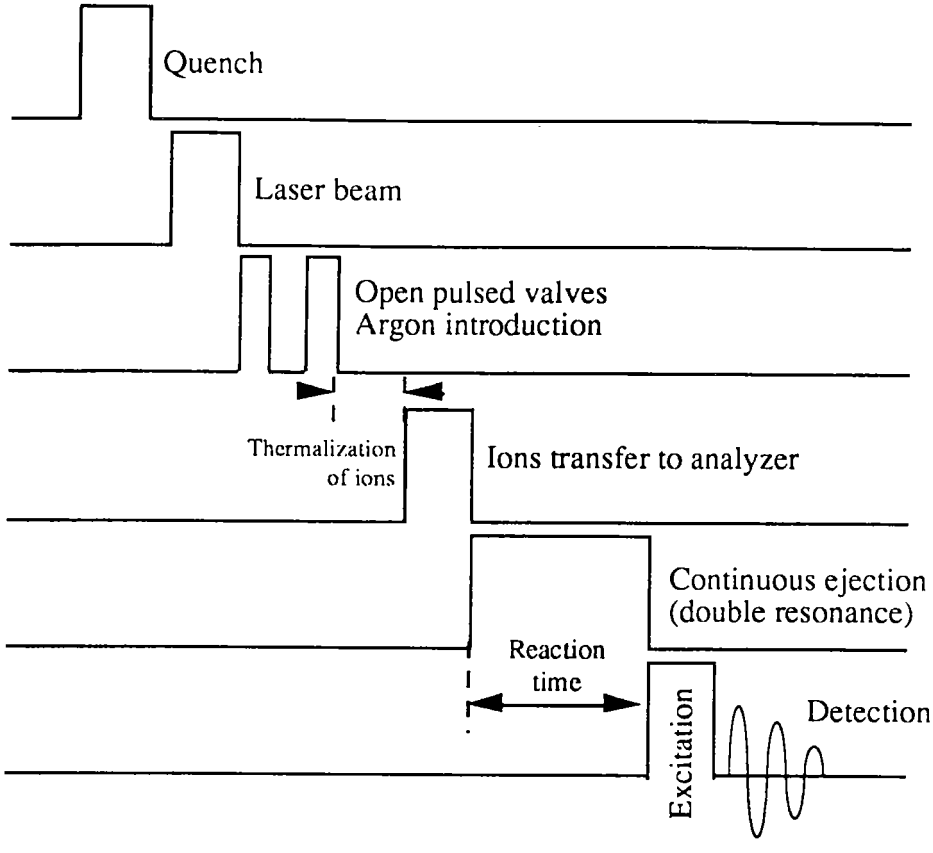

Figure. II. 10. Experimental sequence on the analyzer side.

Thermalization of reagent ions

Ions formed by laser desorption may exhibit a broad distribution of kinetic and internal energies. Same experiments have been performed with cooling of the primary ions in order to ensure that they are in their fundamental state. Produced ions (Al^+, In^+) were left to collide with argon gas which was introduced through pulsed valves in the source cell up to a pressure of ca. 6.10^{-7} Torr. However, in our experiments, the thermalization with argon gas did not change any reaction product or rate.

Ion transfer to analyzer cell

After cooling, the ions were allowed to transfer to the analyzer side. For that purpose the conductance limit was grounded during 0.01 s.

All experiment were carried out at the room temperature, typically around 25°C. Spectra representing ion/molecule reaction resulted from single sequence (no accumulation was performed).

Table II.5. Experimental parameters of the sequence used for the study of Mg^+ reaction with acetophenone. Experiments were conducted on the source cell, acetophenone introduced by pulsed valves.

	Parameter	Value
	Configuration	Internal sample
	Ionization laser	Nd-YAG : 266 nm
	Accumulation	No
	Trapping Potential	1.5 V
Reactive ion selection (Mg^+)	Sweep rate	500 Hz/µs
	Attenuation of excite RF	0 dB
	Lower frequeny	66701 Hz
	Higher frequency	1507.4 kHz
	Excitation period	2881 µs
	Batch inlet pressure	400 mTorr
	Pulsed valves opening period (each)	0.08 s
	Source pressure	~5 10^{-7} Torr
	Analyzer pressure	~2 10^{-8} Torr
	Reaction delay	0.05 to 10 s
Excitation	Sweep rate	2000 Hz/µs
	Attenuation of excite RF	0 dB
	Lower frequeny	23298 Hz
	Higher frequency	2666.6 kHz
	Excitation period	1323 µs
Detection	Acquisition frequency	2000 kHz
	Attenuation of detected signal	30 dB
	Number of data points	64 kbytes
	Detection duration	32.77 ms
	Apodization	Blackman Harris 3 terms
	Zerofilling	1

Table II.6. Additional parameters used in the analyzer side experiments.

	Parameter	Value
Thermalization	Batch inlet 1 pressure (Ar)	1.5 Torr
	Opening period (each)	0.08 s
	Source Pressure	~1 10^{-6} Torr
	Ion transfer time	0.001 s
	Batch inlet 2 pressure (PFTBA)	200 mTorr
	Analyzer Pressure	~7 10^{-8} Torr
	Reaction delay	0.05 to 10 s

References

1. Muller, J.F. ; Pelletier, M. ; Krier, G. ; Weil, D. and Campana, J. Proceedings of the 24th Conference of the Microbeam Analysis Society-Ashville, San Francisco Press, p.311., (1989)
2. Pelletier, M. ; Krier, G. ; Muller, J.F. ; Weil, D. and Campana, J. Proceedings of the 24th Conference of the Microbeam Analysis Society-Ashville, San Francisco Press, p.339.., (1989)
3. Muller, J.F. ; Tolitte, F.; Krier, G. ; Pelletier, M. ; Weil, D. and Johnston, M. "Advances in Mass Spectrometry" - Heyden and Sons Ltd - Ed Longevialle, vol 11, p. 1736. (1989)
4. Pelletier, M. ; Krier, G. ; Tolitte, F.; Muller, J.F. ; Weil, D. and Johnston, M. "Advances in Mass Spectrometry" - Heyden and Sons Ltd - Ed Longevialle, vol 11 p. 496. (1989)
5. Muller, J.F. ; Pelletier, M. ; Krier, G. ; Weil, D. and Campana, J. Pittsburg Conference, Atlanta, Proceedings, (1989)
6. Pelletier, M. ; Krier, G. ; Muller, J.F. ; Weil, D. and Campana, J. Proceedings of the 37th ASMS Conference on Mass Spectrometry - Miami, p. 1506 (1989)
7. Muller, J.F. ; Tolitte, F.; Krier, G. ; Berveiller, M. ; Eberhardt, A. and Dominiak, S. Patent n° 86-18244 published june 24 1988 as n°608 837
8. Muller, J.F. ; Tolitte, F.; Krier, G. and Pelletier, M. Patent n° 88-09438 Protection France, Suisse, Allemagne, Japon, Grande Bretagne
9. Masselon, C. Ph.D. Thesis, University of Metz, 1997.
10. CRC Handbook of Chemistry and Physics, ed.by. D. R. Lide, 73rd ed., CRC Press, Boca Raton, Florida, (1992-1993).
11. The pesticide manual, Ed. Worthing, British crop protection council, Croydon, (GB), 6th edition, (1979)
12. Lias S.G., J. Phys. Chem. Ref. Data, Vol **17**, (1988)
13. Lias S.G., Liebman, J.F. and Levin R.D., *J. Phys. Chem. Ref. Data*, Vol **13**, (1984)

Chapter III

Laser Produced Positive Ion Reactions With Volatile Organic Compounds

1. Ion reactivity and gas-phase reactions

Reactions between positive ions and molecules in the gas phase are eather exothermic or endothermic.

An attractive electrostatic interaction between a M^+ ion and an AB induced dipole, in the gas phase, can lead to the formation of a more stable (M^+····AB) complex than the starting reactants M^+ and AB. If the internal energy (E*) obtained during the formation of adduct composed of the positive (metal) ion and the neutral molecule, is sufficient to pass over the barrier of activation (E_a), the reaction is exothermic. Such reaction is presented in Figure III.1.1.

If the internal energy (E*) is not sufficient to reach the energy of activation, a reaction is endothermic (Figure III.1.b.) Such reaction can not be detected at least without bringing an extra kinetic energy.

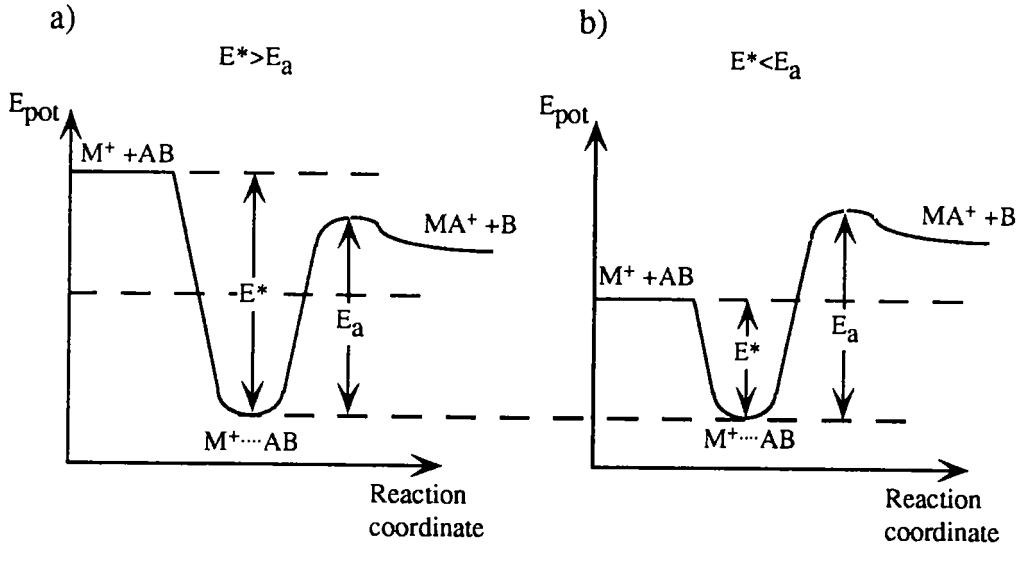

Figure III.1.1. The reaction profiles: a) exothermic and b) endothermic.

The energy of transition-state complexes is very difficult to estimate, herein calculations methods could help. The energy of the complex should on one hand, allow the breaking and formation of bonds (exchange energy) and and on other hand allow the change to reactive electronic configuration of the reagent ion (promotion energy).

In general, cationized molecules are more stable than radical molecular ions or protonated molecules. The fragmentation of the polar molecules resulting from cationization by alkali-metal ions (alkali-metal attachment) has a higher activation energy than splitting off functional groups after protonation. Cationization is,

therefore, potentially useful for the determination of molecular weights.[1]

Reactivity of the primary the ion can be defined in different ways. Babinec and Allison[2] referred reactivity of different metal ions according to the number of different decay products from the organometallic adduct. This corresponds to the number of different bonds in which a given metal ion is going to insert within an organic molecule.

Armentrout and Beauchamp[3] noted a correlation between bond energy $D°(M^+-CH_3)$ or $D°(M^+-H)$ and the "promotion energy" required to obtain a $3d^n4s^1$ configuration, $PE(s^1d^n)$, of the first-row transition-metal ion M^+ (also:called the first promotion energy).

The promotion energy (PE) is defined as the energy required to achieve a metal ion configuration leading to the formation of one (PE_1) or two (PE_2) σ-bonds. Reactivity is then controlled by the promotion energy and by the exchange energy lost upon bond formation.

Figure III.1.2. displays the correlation between the first promotion energy and $D°(M^+-CH_3)$ and $D°(M^+-H)$.

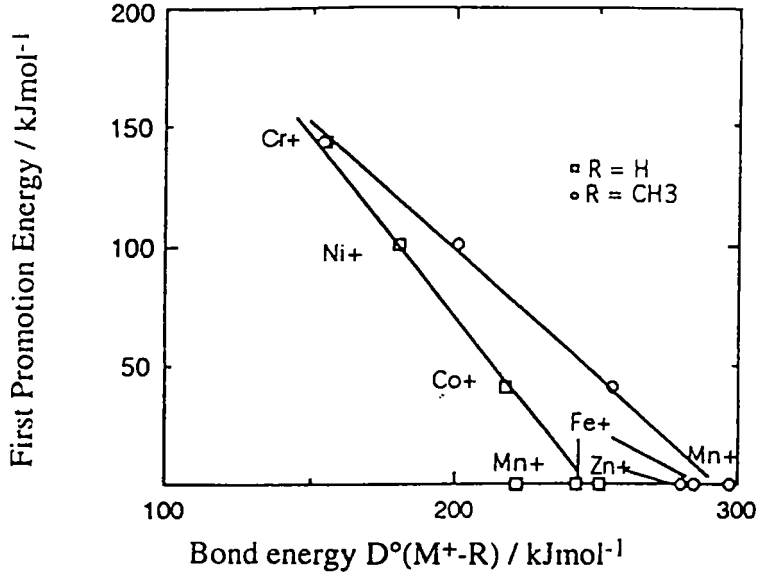

Figure III.1.2. The correlation between the first promotion energy and $D°(M^+-CH_3)$ and $D°(M^+-H)$ (taken from ref. 3).

These results showed that the insertion of a first row transition metal ions into one bond necessarily implies the formation of one σ bond. For the formation of one σ

bond one *s* or *p* electron is required. The promotion energies of different elemental ions used in this study are listed in Table III.1.1.

Table III.1. Electronic configurations, states, and promotion energies (eV) of studied simpleions. [4,5]

Metal	State	M^+ ground-state configuration	PE_1 / eV (ns^1 or p^1)	PE_2 / eV (ns^1p^1)	$PE_{2'}$ / eV (s^2)
Al	^1S	$3s^2$	4.6	4.6	-
Li	^1S	$1s^2$	59.02	61.28	-
Na	^1S	$2s^2$	32.8	-	-
K	^1S	$3s^2$	20.15	-	-
Mg	^2S	$2p^6\ 3s^1$	4.43	-	-
Ca	^2S	$3p^6\ 4s^1$	3.14	-	-
Ti	^4F	$3d^2\ 4s^1$	0	-	-
V	^5D	$3d^4$	0.36*	-	-
Cr	^6S	$3d^5$	1.52	<16.5*	6.4
Fe	^6D	$3d^6\ 4s^1$	0	6.8	2.8
Mn	^7S	$3d^5\ 4s^1$	0	10.3	6.7
Co	^3F	$3d^8$	0.5	9.9	4.9
Ni	^2D	$3d^9$	1.1	<18.15**	<18.15**
Cu	^1S	$3d^{10}$	2.8	13.4	8.5
Zn	^2S	$3d^{10}\ 4s^1$	0	12.8	7.61
B	^1S	$4s^2$	4.6	4.6	-
Si	^2P	$3p^1$	0	5.5	-
Sn	^2P	$5p^1$	0	-	-
In	^2P	$5s^2$	0	-	0
Zr	^3F	$4d^2\ 5s^1$	0	-	
Mo	^6S	$3d^5$	-	-	-

PE_1 promotion energy required to reach the lowest s^1 or p^1 configuration.
PE_2 promotion energy required to reach the lowest s^1p^1 configuration.
$PE_{2'}$ promotion energy required to reach the lowest s^2 configuration.
*Based on the Cr(III) limit, 133 060 cm^{-1};
**Based on the Ni(III) limit, 146 408 cm^{-1}

The observed correlation led to the proposal that the ground state of molecular species such as Co^+-CH_3 does *not* correlate with the ground-state fragments [$Co^+(3d^8)$-CH_3] but rather with [$Co^+(3d^74s^1)$-CH_3]. That is, for the first-row transition-metal ions, an s electronof the metal is required for the formation of first σ-

bond; and when considering the thermodynamics of this bond formation, one must be aware of the promotion energy required to achieve a $3d^n4s^1$ configuration. The results suggest that while $D°(Co^+(3d^n4s^1)\text{-}CH_3)$ and $D°(Fe^+(3d^n4s^1)\text{-}CH_3)$ are approximately equal,[3] the "observed" bond strengths (relative to the fragments in their ground states) differ due to the difference in promotion energies.

With respect to the first promotion energies, the first row transition metal ions are listed in the following order:

$$Fe^+ \sim Mn^+ \sim Zn^+ \sim Ti^+ < V^+ < Co^+ < Ni^+ \sim Cr^+ < Cu^+$$

The order of reactivity (reactivity = 1/PE) will be reverse.

These concepts explain the bond-strength trends, but these alone do not predict the reactivity trends since reactions which involve metal insertion require the formation of an intermediate in which two σ-bonds are formed to the transition-metal ion.

The first step of a gas-phase reaction between an organic compound and a transition-metal ion is usually the insertion of a metal atom into a bond. The insertion requires the formation of **two** bonds.[2] Presumably energy is required for the M^+ to achieve a configuration conductive to 2-bond formation.

The first-row transition-metal ions can be ordered in terms of the promotion energy required to achieve a configuration in which two electrons are not in d orbitals. This is apparently the configuration which is achieved as two σ-bonds are formed - the situation which exists when a metal ion is inserted into a single bond of an organic molecule. First-row transition-metal ions with high promotion energies are unreactive or insert only into a few type of bonds, while ions with low promotion energies appear to be more reactive, inserting into a wider variety of bonds. Thus, the order of reactivity is as follows:

$$Fe^+ > Co^+ > Ni^+ \sim Cr^+ > Mn^+ > Zn^+ > Cu^+$$

The insertion of metal ions into organic bonds showed to folow this order of reactivity.[2]

References

1. T. Fujii, M. Ogura, H. Jimba, *Anal. Chem.* **61**, 1026 (1989).

2. S.J. Babinec and J. Allison, *J. Am. Chem. Soc.* **106**, 7718 (1984).

3. P.B. Armentrout, L.F. Halle and J. Beauchamp, *J. Am. Chem. Soc.* **103**, 6501 (1981).

4. Moore, C.E. "Atomic Energy Levels"; U.S. Government Printing Office: Washington, DC, Vol. II, Circ. Natl. Bur. Stand. 467, (1952).

5. W.F. Meggers, C.H. Corliss and B.F. Scribner, Tables of Spectral-Line Intensies, National Bureau of Standards, Washington, Monograph 32 - Part II (1961).

III.2. Gas phase reactions of acetophenone metal and silicon positive ions

2.1. *Introduction*

Acetophenone is a widely used precursor in many organic synthesis. It was already studied in the gas phase, in reactions with some positive ions. In our laboratory, we only recently started to study ion/molecule reactions in the gas phase. As a starting point, we wanted to work with a model molecule of already known behaviour towards some positive metal ions. The compound had to be volatile and thus easily introducible into the mass spectrometer. Thus, we chosen acetophenone. We wanted first, to confirm already known mechanisms, and second to check its reactivity towards other elemental ions. After establishing the experimental procedure and gaining understanding of the involved processes, we could apply this method to other, in our case to polyhalogenated molecules.

In this chapter, we give a short overview of already known results on acetophenone-metal reactions. Metals which were not studied with acetophenone, were mostly studied with acetone, and these results are cited. After this, we display the results obtained in our studies of the acetophenone with 17 elements indicated in the periodic table given below. The mass spectra were interpreted and assigned and reaction mechanisms proposed. The results are presented in six sections according to the reaction mechanisms .

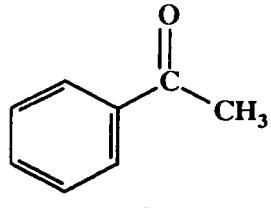

Acetophenone

IA																	0
	IIA											IIIB	IVB	VB	VIB	VIIB	
Na	Mg	IIIA	IVA	VA	VIA	VIIA	-----	VIII	-----	IB	IIB	Al	Si				
K	Ca		Ti	V	Cr	Mn	Fe	Co	Ni	Cu	Zn						
												In					
	Ba																

2.2. *Metal ions reactivity towards ketones (literature)*

Acetophenone is an aromatic ketone, widely used in organic synthesis[1]. The molecule readily vaporizes and can be easily introduced as a reactant gas for reaction with metal ions. Nevertheless, acetone, as the simplest ketone, has been studied most extensively.

In transition metal reactions with acetone, decarbonylation is afforded by Fe^+, Co^+ and Ni^+ ions[3-5]. Cr^+ is unreactive with acetone[6]. Mn^+ gives rise to $MnCH_3^+$ as has been reported in an ion-beam study[7]. Copper was initially reported to undergo dissociative attachment reactions with several small ketones other than acetone,[8] whereas later work reported the direct formation of condensation product with acetone[9]. The reactivity of acetone with Cr^+, Fe^+, Ni^+ and Cu^+ produced by resonant laser ablation results in the formation of single and bi-adduct ions, with some evidence of dissociative attachment reactions for Fe^+ and Ni^+ (metal carbonyl ions were observed)[10]. The oxygen affinity of Sc^+, Ti^+ and V^+ leads to abundant MO^+ ions formation in reactions with ketones, and moreover, MO^+ was found to be the exclusive product for Sc^+, Ti^+ and V^+ with acetone and some other ketones[3,11]. Zinc has the highest ionization potential of all transition elements and thus can easily induce charge transfer to organic molecules, as reported for reactions with alkanes[12] and alkenes[13].

Concerning the behaviour of the alkaline earth metals, comparisons of Mg^+ - acetone reactions with those of Al^+, Mn^+ and Cu^+, have shown that Mg^+ is a softer acid than Al^+, very similar in acidity to Mn^+ and Cu^+ ions[14].

For Al^+ and In^+, only adduct complexes were observed in reactions with ketones[3,15]. Reactions involving Si^+ ions have been investigated by selected-ion flow tube technique[16]. Reactions with oxygen containing molecules give rise mainly to the $SiOH^+$ product as it is the case for acetone[17]. We found no previous reports on the reactivity of Si^+ ion produced by laser ablation with organic molecules.

The acetophenone molecule was included in studies of aromatic compound reactions with Ni^+ ions[18] and Fe^+ ions[19] (fluoroacetophenone[20]), and Al^+ ions[21]. Cr^+ was found to be reactive with methylacetophenone and to induce dehydrogenation and elimination of CH_3 group[22].

The work reported here constitutes a systematic study of the reactivities of the alkaline earth metals (Mg, Ca and Ba), transition metals (Ti-Zn), group IIIA metals (Al

and In) and silicon ions produced by laser ablation, with the same organic molecule (acetophenone).

The comparison of gas-phase reactions among different groups and comparison with previous results is addressed. Fourier transform ion cyclotron resonance mass spectrometry[23] is ideally suited for this purpose, because abundant atomic ions may be produced by laser ablation/ionization and trapped for extended periods to produce various species, the time-evolution and reactivity of which can be monitored at high mass resolving power to facilitate the identification of products.

2.3. *Pathways for Gas-Phase Positive Ion Complexation and/or Reaction with Acetophenone*

Laser produced ions (M^+ = Na^+, Mg^+, Ca^+, Ba^+, Ti^+, V^+, Mn^+, Cr^+, Fe^+, Ni^+, Co^+, Cu^+, Zn^+, Al^+, In^+ and Si^+) were allowed to react with acetophenone, L, in the FTMS cell. A trial of thermalization of laser produced ions with argon gas, prior to acetophenone introduction, did not change any reaction product or rate. Nevertheless, we cannot completely exclude the possibility that some excited ions may be involved in the reactions. The products of primary, secondary and further reactions were detected with increasing reaction time. Therefrom, several types of reaction behavior can be distinguished:

i formation of ML_n^+ complexes,
ii decarbonylation of metal-ligand complexes, $[ML_n - CO]^+$,
iii dehydrogenation and dehydration, $[M(O)L_n - X]^+$, X= H_2, H_2O.
iv oxygen abstraction by silicon,
v charge transfer and/or electron ionization,
vi reactions involving water molecule.

Table III.2.1. summarizes the main products detected after reactions of cations with acetophenone. Among the first generation products, there are ML^+ complexes, products of their decarbonylation, ($[ML - CO]^+$), specific products of reaction with silicon ion, and products resulting from charge transfer and/or electron ionization followed by fragmentation. Secondary reaction products are adducts, decarbonylated adducts and protonated dimers of molecular ion. Higher order reaction results in adduct complexes. Dehydrogenation and dehydration processes products, which are observed for Ti^+ and V^+ reactions, are treated separately (see Table III.2.2.). Reactions involving water molecules are side reactions in the case of Ca^+, Ba^+ and Al^+.

Table III.2.1. Principal products of reactions of M^+ ions with acetiphenone (L), yields are given in %

M^+	Na^+	Mg^+	Ca^+	Ba^+	Mn^+	*Cr^+	*Fe^+	*Ni^+	Co^+	Cu^+	Zn^+	Al^+	In^+	Si^+
Primary Reaction														
ML^+	81	94	100	98	81	14	5	3	5	70	51	79	71	
$[ML-H]^+$														2
$[ML-CO]^+$							59	19	77					
$[L+H]^+$	8	2		2	8	->	2	<-	8	2		15	14	1
L^+		1				->	2	<-		1	47			2
$[L-CH_3]^+$	11	3			10	->	3	<-	5	26	2	6	9	2
$[L-O]^+$														60
$[L-OH]^+$									2					6
$[L-COCH_2]^+$													6	26
$[L-COCH_3]^+$					1				3	1				1
Secondary Reaction														
ML_2^+	80	100	100	100	96	18	10	6	13	98	40	66	80	
$[ML_2-CO]^+$							56	10	87					
$[L_2+H]^+$	20				4	->	1	<-	2	2	60	34	20	100
Tertiary Reaction														
ML_3^+		100	100	100	100							100		
Quaternary Reaction														
ML_4^+		100	100		100									

*Percentage of products are coadded as the reactive ions were produced simultaneously from a stainless steel sample.

2.3.1. Formation of ML_n^+ complexes

Almost all the studied ions (except Ti^+, V^+ and Si^+), associate with an intact ligand to form complexes according to the following equation:

$$M^+ + L \longrightarrow ML^+ \xrightarrow{(n-1)L} ML_n^+$$

n=2 : M = Na, Cr, Fe, Ni, Co, Cu, Zn, In
n=2-3 : M = Ba, Al
n=2-4 : M = Mg, Ca, Mn

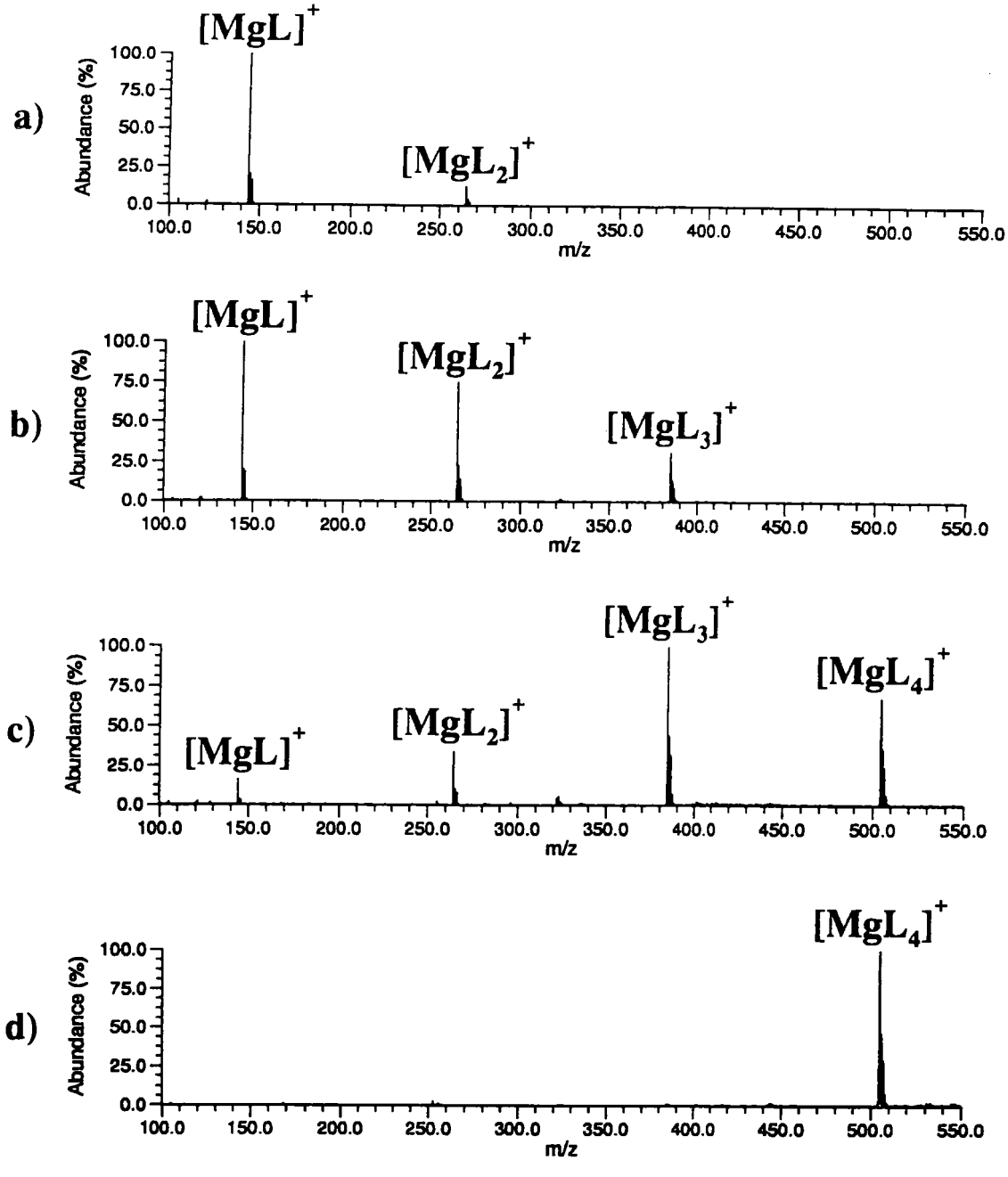

Figure III.2.1. FT-ICR mass spectra of the ionic products of the reaction of Mg^+ with acetophenone (L) at reaction time of: a) 1.0 s; b) 2.5 s, c) 5.0 s and d) 10 s .

Figure III.2.1. illustrates this type of behavior for the case where n = 2-4. Complexation of Mg^+ with an intact acetophenone molecule started at 0.1 s reaction time with the formation of MgL^+. As a function of reaction time, higher, successive complexes were produced and after 10.0 s, only MgL_4^+ was detected.

Mg^+ and Ca^+ (Figure in Appendix A) reactions lead to the formation of ML_n complexes (n=1-4), while in the case of Ba^+ (Figure in Appendix A), no formation of the complex with n=4 was observed, even with a reaction time of 20 s. Ba^+ was produced from a $Ba(CO_3)_2$ pellet and the production of neutral species seemed to be higher than in other reactions. The pressure conditions to obtain "resolved" spectra were more difficult to achieve. Thus it was difficult to monitor the Ba^+ ion reaction for a longer time. The variation of the relative abundances of products with the reaction period for alkaline earth metals is displayed in Figure III.2.2.

A comparison of the graphs shows that heavier ions have lower reaction rates. This result can be partially explained by the differences in cyclotron frequencies of the ions. Heavier ions having lower frequencies experience fewer collisions for a given period, namely: ν (Mg): 1948.3 kHz > ν (Ca): 1169.3 kHz > ν (Ba) 338.8 kHz. Mn^+ (Appendix A), heavier ion than Ca^+ and lighter than Ba^+, produces the same kind of successive complexes, n = 2-4, and agrees well with this explanation [ν (Mn): 850.5 kHz]. It yields complexes slightly slower than Ca^+ and faster than Ba^+.

Na^+, Cr^+, Cu^+ and Zn^+ ions (spectra in Appendix A) follow the tendency to form ML_2 complexes which become the main products at longer reaction times (a few seconds). Although Al^+ and In^+ form higher complexes, namely AlL_2, InL_2, and AlL_3 (Appendix A), the complexes containing one ligand molecule (ML^+) seem to be the most stable, even after a long reaction time ($t \geq 20$ s).

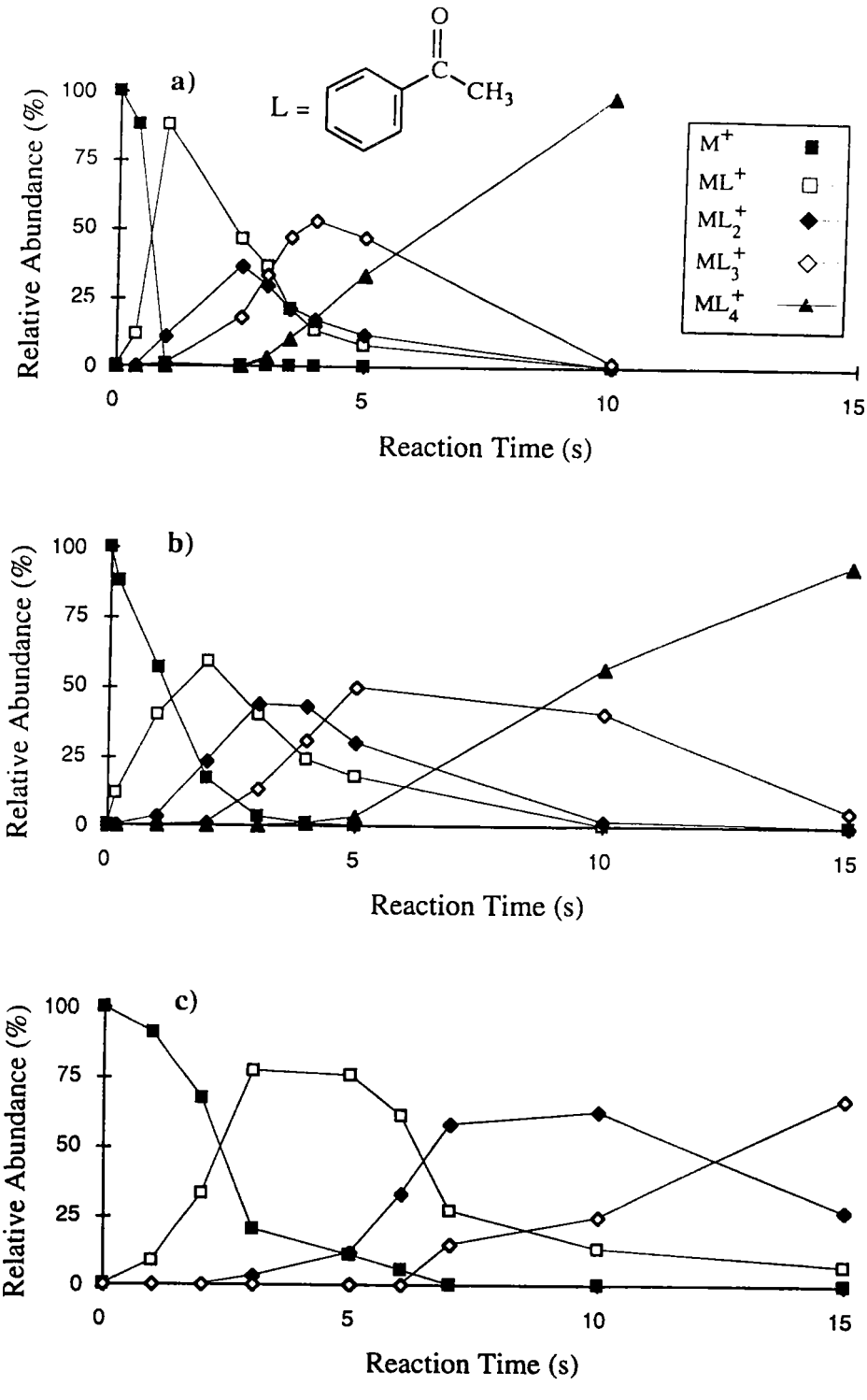

Figure III.2.2. Time-evolution of the relative abundances of the principal ionic species in the reaction of a) Mg^+, b) Ca^+ and c) Ba^+ with acetophenone (L).

2.3.2. Decarbonylation of metal-ligand complexes, $[ML_n - CO]^+$

Iron, cobalt and nickel ions induce the activation of a C-C bond in a ligand molecule. Our results are in agreement with those obtained for iron by Bjarnason et al.,[19] and for nickel ions by Stepnowski et al.[18] In the reaction of Fe^+, Co^+ and Ni^+ with acetophenone the elimination of carbonyl group [reaction (2)] is the dominant reaction. The mass spectra in Figure III.2.3. display the evolution of such products for Fe^+ and Ni^+ (ablated together with Cr^+ from stainless steel sample) reactions as a function of time.

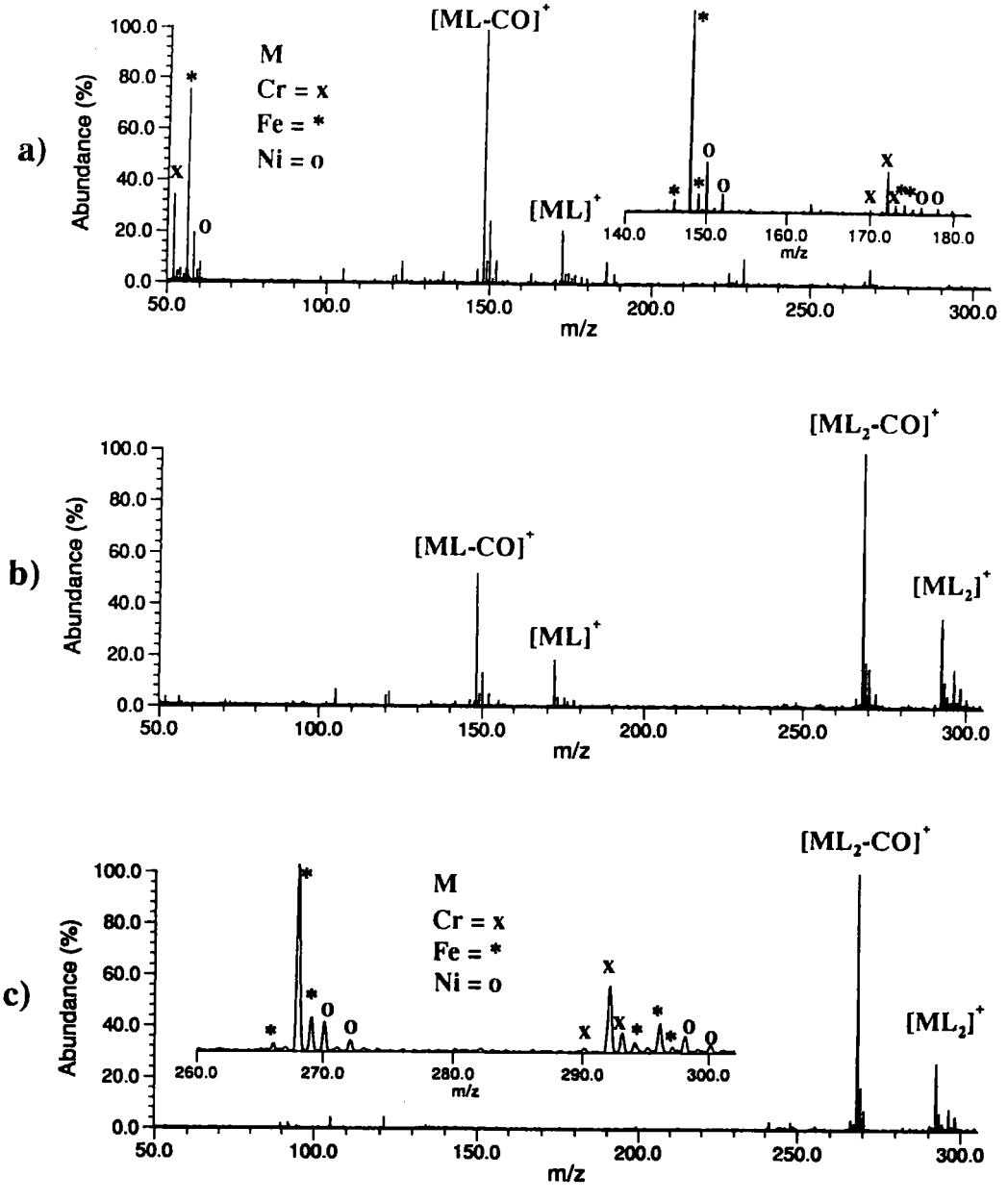

Figure III.2.3. FT/ICR mass spectra of the ionic products of the reaction of Cr^+, Fe^+ and Ni^+ (ablated from stainless steel sample) with acetophenone (L) at reaction times of a) 1.0 s, b) 3.0 s and c) 10 s. Note that the three ions form ML_n and only Fe^+ and Ni^+ induce decarbonylation. The insets show isotopic distribution of ions.

It was suggested that M^+ inserts into the C-CO bond, a methyl shift to the metal occurs, followed by the elimination of CO. A second ligand may add [reaction (3)] to $[ML\text{-}CO]^+$ without further fragmentation[19]. The formation of intact adducts occurs as well, [reaction (1)].

$$M^+ + L \rightarrow ML^+ \xrightarrow{L} ML_2^+$$
$$\downarrow -CO \qquad (2)$$
$$[ML - CO]^+ \xrightarrow{L} [ML_2 - CO]^+ \qquad (3)$$

M = Fe, Co, Ni

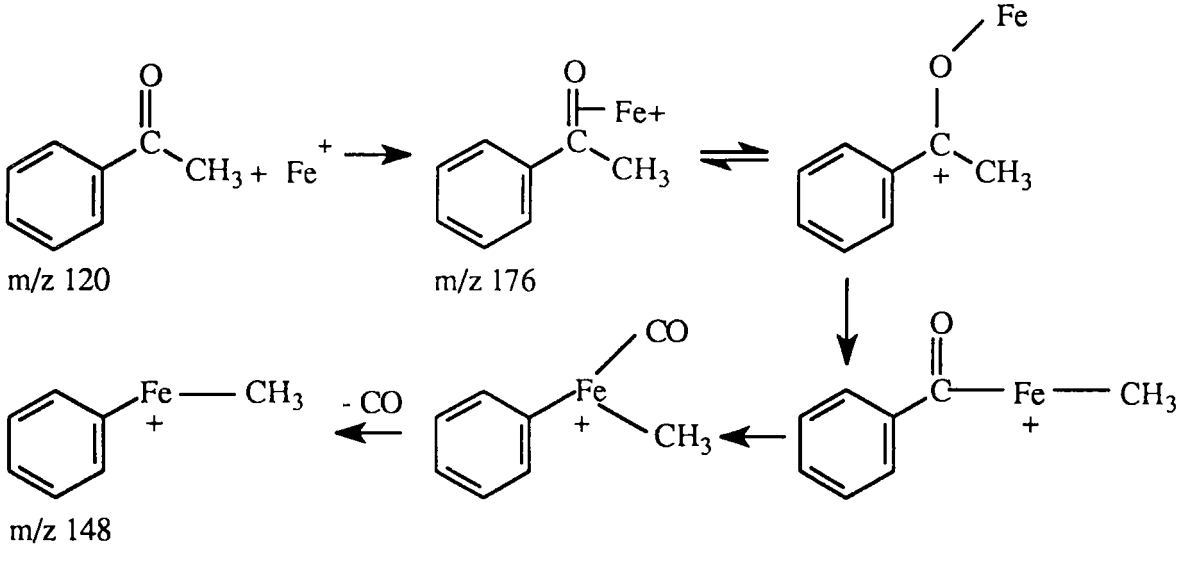

Figure.III.2.4. Mechanism of decarbonylation of acetophenone by iron (the same for Co^+ and Ni^+) ion.

The reactivities of metal ions are in correlation with their promotion energies and follow the order: $Fe^+ > Co^+ > Ni^+$, while Mn^+, Cr^+, Cu^+ and Zn^+ are unreactive. This reactivity order has been observed for other reaction systems [25-27]. It was interpreted in terms of promotion energy required to achieve a configuration with one[25] or two[26] non-d-electrons, leading to the formation of two σ-bonds. Namely, one electron in the valence s orbital, which is spin-decoupled from the remaining metal d electrons, $4s^1 3d^{n-1}$ and two *s* electrons: $3d^{n-2}4s^2$ or 1s and 1p : $3d^{n-2}4s^1 4p^1$.

2.3.3. Dehydrogenation and dehydration, $[M(O)L_n - X]^+$, X = H_2, H_2O

Transition metals with high oxygen affinities[28], such as titanium and vanadium cations were shown to form MO^+ in reactions with acetone[3, 29]. We have observed the same behavior with acetophenone. But, even in the absence of acetophenone

molecules, M^+ (M = Ti or V) ions form MO^+ and $[MO+H_2O]^+$ when trapped for a long period in the FTMS cell. This is presumably due to the presence of residual water molecules in the spectrometer. However, the presence of acetophenone leads to a dramatic increase of the intensities of these two characteristic ions.

After introduction of acetophenone, various complex cations were observed as shown in Figure III.2.5. and III.2.6. for Ti^+ and V^+, respectively.

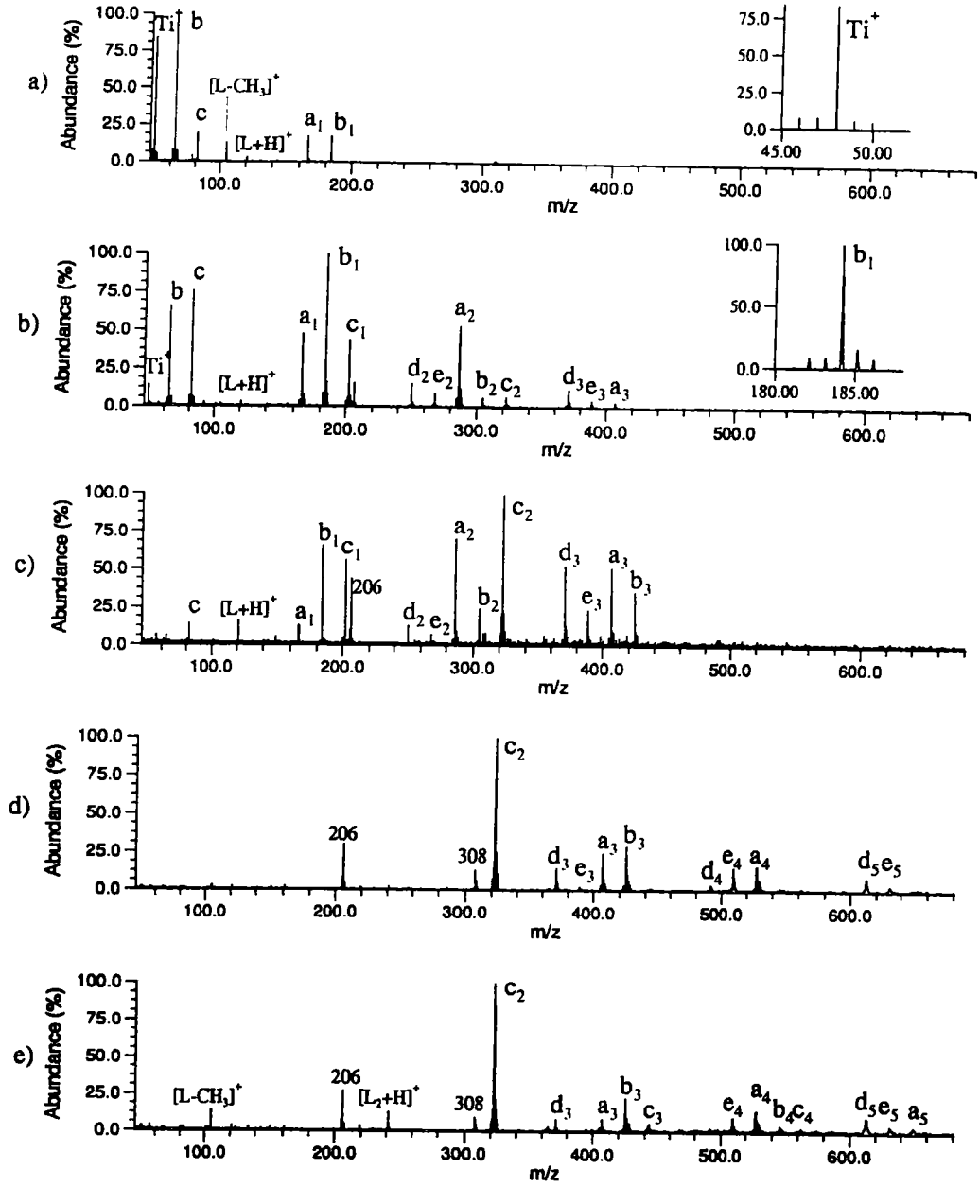

Figure III.2.5. FT-ICR mass spectra of the ionic products of the reaction of Ti^+ with acetophenone (L) at reaction time of a) 0.5 s, b) 1.0 s, c) 3.0 s, d) 5.0 s and e) 10 s. The assignment (a_n, b_n...) of products is given in Table III.2.2. The insets show isotopic distribution of Ti containing ions.

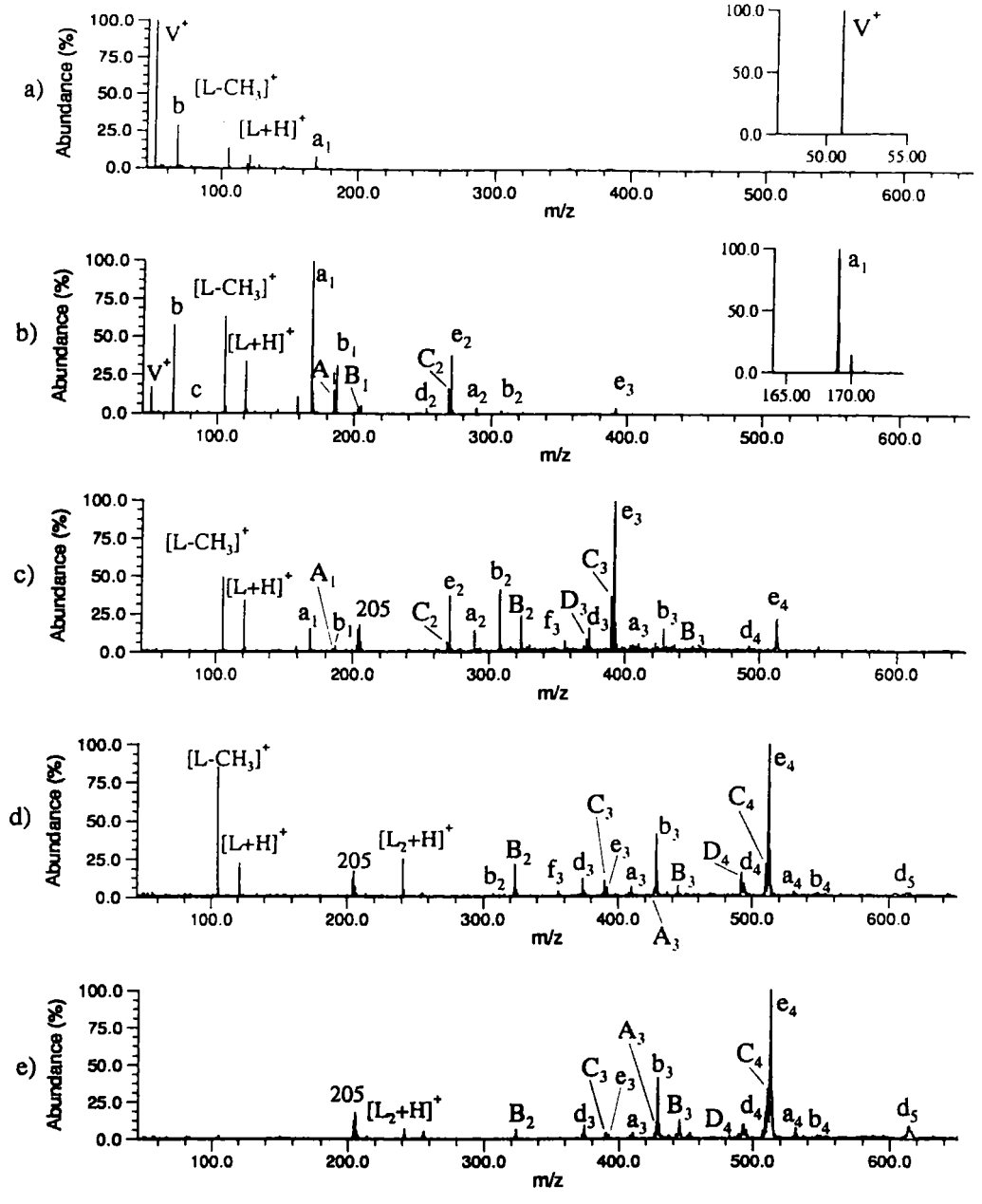

Figure.III.2.6. FT-ICR mass spectra of the ionic products of the reaction of V^+ with acetophenone (L) at reaction time of a) 0.2 s, b) 1.0 s, c) 3.0 s, d) 5.0 s and e) 10 s. The assignment (a_n, A_n...) of the products is given in the Table II.2.2. The insets show isotopic distribution of V containing ions.

Numerous reaction products involving up to 5 ligand molecules have been detected and their intensities monitored as a function of reaction time. Table III.2.2. summarizes the *m/z* values and relative abundances of the major products for Ti^+ and V^+ reaction with acetophenone. Two different assignments are sometimes given for a single ion (Assignment **I** and **II** in Table III.2.2.) because in some cases, two different pathways can give rise to the same ion as will be discussed below.

Table III.2.2. *m/z* values[a] and relative abundances (%) for the major products of reaction of M^+ (Ti and V) with acetophenone (L)

	Assignment I	Ti^+	V^+	Assignment II
b	MO^+	64	67	
c	$[MO+H_2O]^+$	82	85	
Primary Reaction Products				
a_1	$[MOL-H_2O]^+$	166 (32)	169 (64)	$[ML-H_2]^+$
A_1	$[MO_2L-H_2O]^+$	-	185 (11)	
b_1	MOL^+	184 (48)	187 (21)	
B_1	$[MO_2L]^+$	-	203 (4)	
c_1	$[MOL+H_2O]^+$	202 (20)	-	
Secondary Reaction Products				
d_2	$[MOL_2-3H_2O]^+$	250 (10)	253 (9)	$[ML_2-H_2-2H_2O]^+$
C_2	$[MO_2L_2-3H_2O]^+$	-	269 (23)	$[ML_2-2H_2-H_2O]^+$
e_2	$[MOL_2-2H_2O]^+$	268 (9)	271 (49)	$[ML_2-H_2-H_2O]^+$
a_2	$[MOL_2-H_2O]^+$	286 (60)	289 (9)	$[ML_2-H_2]^+$
b_2	MOL_2^+	304 (8)	307 (6)	
B_2	$[MO_2L_2]^+$	-	323 (4)	
c_2	$[MOL_2+H_2O]^+$	322 (13)	-	
Tertiary Reaction Products				
f_3	$[MOL_3-4H_2O]^+$	-	355 (4)	$[ML_3-H_2-3H_2O]^+$
D_3	$[MO_2L_3-4H_2O]^+$	-	371 (5)	$[ML_3-2H_2-2H_2O]^+$
d_3	$[MOL_3-3H_2O]^+$	370 (31)	373 (9)	$[ML_3-H_2-2H_2O]^+$
C_3	$[MO_2L_3-3H_2O]^+$	-	389 (16)	$[ML_3-2H_2-H_2O]^+$
e_3	$[MOL_3-2H_2O]^+$	388 (14)	391 (45)	$[ML_3-H_2-H_2O]^+$
a_3	$[MOL_3-H_2O]^+$	406 (31)	409 (4)	$[ML_3-H_2]^+$
A_3	$[MO_2L_3-H_2O]^+$	-	425 (1)	
b_3	MOL_3^+	424 (21)	427 (13)	
B_3	$[MO_2L_3]^+$	-	443 (3)	
c_3	$[MOL_3+H_2O]^+$	442 (3)	-	
Quaternary Reaction Products				
D_4	$[MO_2L_4-4H_2O]^+$	-	491 (6)	$[ML_4-2H_2-2H_2O]^+$
d_4	$[MOL_4-3H_2O]^+$	-	493 (5)	$[ML_4-H_2-2H_2O]^+$
C_4	$[MO_2L_4-3H_2O]^+$	-	509 (11)	$[ML_4-2H_2-H_2O]^+$
e_4	$[MOL_4-2H_2O]^+$	508 (32)	511 (68)	$[ML_4-H_2-H_2O]^+$
a_4	$[MOL_4-H_2O]^+$	526 (45)	529 (6)	$[ML_4-H_2]^+$
b_4	MOL_4^+	544 (14)	547 (4)	
c_4	$[MOL_4+H_2O]^+$	562 (9)	-	
Quinternary Reaction Products				
d_5	$[MOL_5-3H_2O]^+$	610 (55)	613 (100)	$[ML_5-H_2-2H_2O]^+$
e_5	$[MOL_5-2H_2O]^+$	628 (23)	-	$[ML_5-H_2-H_2O]^+$
a_5	$[MOL_5-H_2O]^+$	646 (22)	-	$[ML_5-H_2]^+$

[a] *m/z* values correspond to the most abundant isotope.

Most of the observed products can be explained in terms of complexation of MO^+ or $[MO+H_2O]^+$ ions with acetophenone and their subsequent fragmentation. For some products, however, one cannot rule out totally the formation and fragmentation of $[ML_n]^+$ complexes. It is worth noting that Ti^+ and V^+ can be distinguished through their particular behavior.

2.3.3.1. MO-complexes and dehydration

As stated above, Ti^+ and V^+ form MO^+ ions easily (**b**), in reactions with ketones. These ions are likely to react with neutral molecules to form MOL_n^+ complexes ($\mathbf{b_n}$). In fact, these ions have been detected and most of the observed products can be explained by dehydration of the MOL_n^+ complexes [reaction (4)]:

$$MO^+ + nL \rightarrow MOL_n^+ \rightarrow \left[MOL_n - xH_2O\right]^+ + xH_2O \qquad (4)$$

M = Ti, V; n = 1-5; x = 1-3.

This mechanism could be responsible for the formation of $\mathbf{a_n}$, $\mathbf{d_n}$, $\mathbf{e_n}$, $\mathbf{f_n}$ ions (see Table III.2.2, Assignment **I**). For ions $\mathbf{d_2}$, $[MOL_2 - 3H_2O]^+$, and $\mathbf{f_3}$, $[MOL_3 - 4H_2O]^+$, the loss of all oxygen atoms is achieved.

2.3.3.2. Dehydrogenation and dehydration

It has been reported that reaction of Ti^+ and V^+ with alkanes leads to the insertion of the metal ion into a C-H bond followed by a dehydrogenation of the complexes.[30] In our experiments, the $\mathbf{a_1}$ ion, m/z= 166 (for Ti) and 169 (for V), is the first complex ion being formed. i.e. before MOL^+ ion. Therefore, it is not completely satisfactory to assign the $\mathbf{a_1}$ ion as $[MOL-H_2O]^+$. Another possible explanation would be the formation of the ML^+ complex, immediately followed by dehydrogenation. Thus, $\mathbf{a_n}$ ions can also be assigned as $[ML_n - H_2]^+$ as noted in Table III.2.2., Assignment **II**.

The formation of other product ($\mathbf{d_n}$, $\mathbf{e_n}$, $\mathbf{f_n}$) can be explained by loss of xH_2O from these $[ML_n - H_2]^+$ ions (5):

$$M^+ + nL \rightarrow \left[ML_n - H_2\right]^+ \rightarrow \left[ML_n - H_2 - xH_2O\right]^+ \qquad (5)$$

M = Ti, V; n = 1-5; x = 1-4.

From our experiments it is impossible to favor one mechanism as responsible for the formation of the observed products. It is likely that both mechanisms take place, simultaneously. Both mechanisms (4) and (5), can be invoked for Ti^+ and V^+ reactions with acetophenone. For vanadium ion reactions, $\mathbf{e_n}$ ions seem to be the most stable after disappearance of $\mathbf{a_1}$. Moreover, for later reaction steps (n > 2), with longer reaction time (5s) ion $\mathbf{e_4}$ ($[VL_4 - H_2 - H_2O]^+$ or/and $[VOL_4 - 2H_2O]^+$), shows the highest intensity in the mass spectra. Ti^+ ion reactions yield $\mathbf{c_2}$ ion, as the most stable product. The existence of this ion cannot be explained by mechanisms (4) or (5) and it is not observed in V^+ reactions.

2.3.3.3. *Different reactions for Ti and V*

Ti^+ and V^+ show their specific behavior even if most of the products are formed for both cations. If we compare the summation spectrum from Ti^+ reactions (Figure III.2.7.a.) with that obtained by summing the V^+ reaction spectra (Figure III.2.7.b.) the differences can be clearly seen and are described below. Two additional pathways take place.

First, TiO^+ ions easily bind H_2O to form **c** ion $[MO + H_2O]^+$, which is hardly detectable in the case of vanadium. With increasing reaction time, this ion can react with acetophenone to form $\mathbf{c_n}$ complexes, where n= 1-4, according to the following equation:

$$(TiO + H_2O)^+ + nL \rightarrow [(TiO + H_2O)L_n]^+ \qquad (6)$$
$$n = 1\text{-}5$$

However, we cannot exclude the bonding of H_2O to $\mathbf{a_n}$ complexes to explain the $\mathbf{c_n}$ series. The formation of this series is very pronounced, and after a few seconds, $\mathbf{c_2}$ ions $[TiOL+H_2O]^+$ remain the major product ions even after the formation of higher order complexes (see Fig.III.2.6.). No $\mathbf{c_n}$ ions have ever been detected in the case of vanadium. The presence of $\mathbf{c_n}$ ions with Ti^+ and their absence with V^+ may be explained by the fact that TiO^+ has only one unpaired electron, which is not favorable for making two new bonds as required for activating another molecule. On the other hand, VO^+ has two unpaired electrons, making it more reactive.

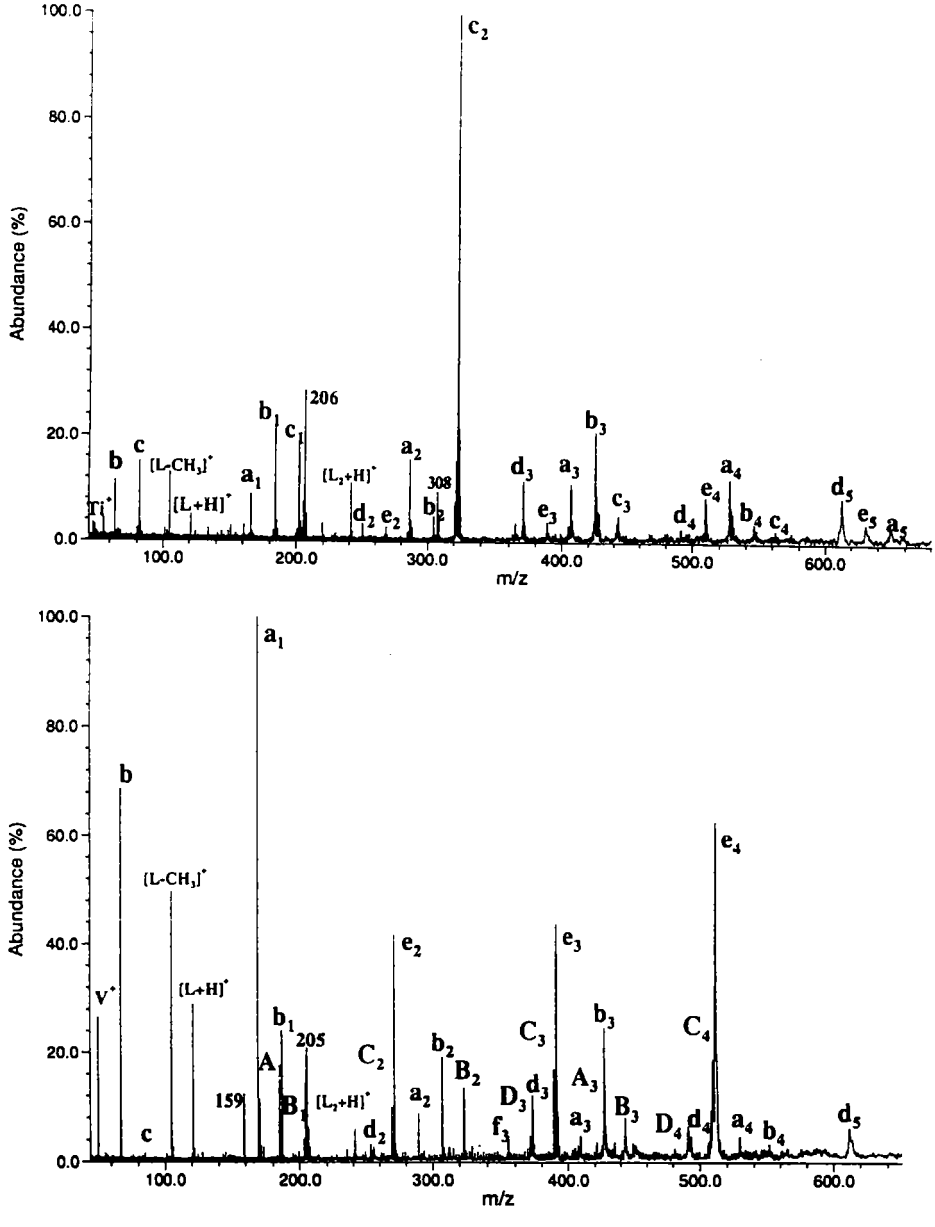

Figure III.2.7. Coadded spectra of a) the five spectra shown in Fig. III.2.5. for Ti^+ reactions, and b) the five spectra shown in Fig. III.2.6. for V^+ reactions with with acetophenone with different reaction times.

To monitor formation of titan complexes with acetophenone, especially those with water molecules, $\mathbf{c_n}$, we ejected Ti^+ ion, but only $^{48}Ti^+$ isotope. Evidence of titan (not becoming from oxide) containing complexes is obvious in formation of other isotope complexes. as shown in Figure III.2.8.

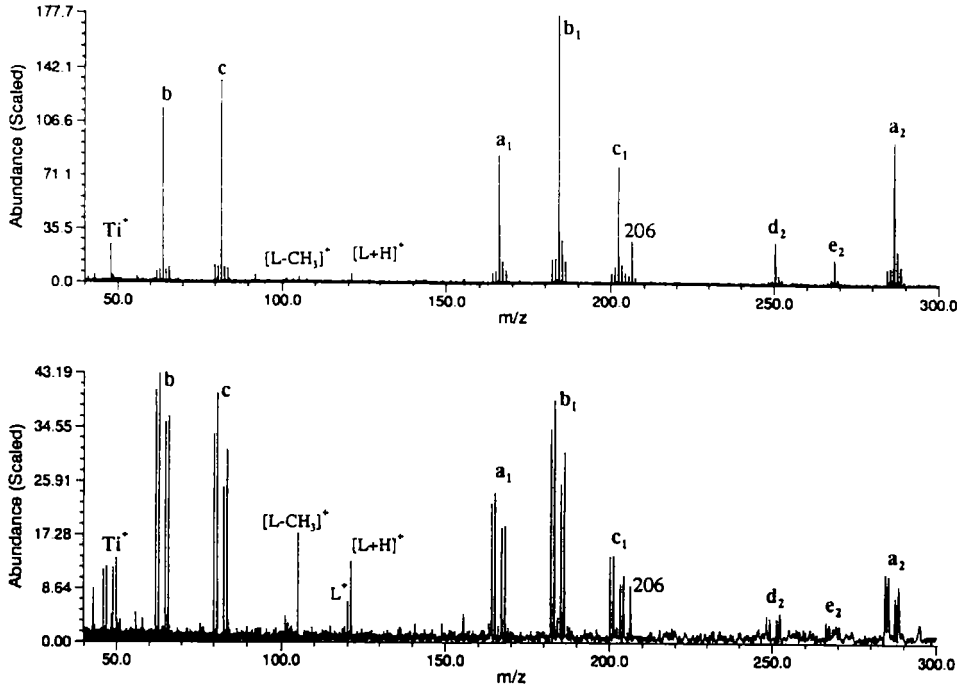

Figure. III.2.8. The ejection of $^{48}Ti^+$ results in formation of other Ti isotope complexes.

Second, reactions of V^+ with acetophenone give rise to four series ($\mathbf{A_n}$, $\mathbf{B_n}$, $\mathbf{C_n}$ and $\mathbf{D_n}$) of complex ions. They all contain one additional oxygen atom compared to the previously described ([VOL_n - xH_2O], n = 1-4; x = 0-3) series. Two mechanisms can be considered to explain this behaviour.

On one hand, a complexation of VO_2^+ by the ligand could be involved ($\mathbf{B_n}$ = $[VO_2L_n]^+$ series). However, "bare" VO_2^+ has never been detected. Dehydration of $\mathbf{B_n}$ complexes can yield in $\mathbf{A_n}$, $\mathbf{C_n}$ and $\mathbf{D_n}$ series i.e. in $[VO_2L_n - xH_2O]^+$ ions, as noted in Assignment **I**, Table III.2.2. and in following equation:

$$\left(VO_2^+\right) + nL \rightarrow VO_2L_n^+ \rightarrow \left[VO_2L_n - xH_2O\right]^+ + xH_2O \qquad (7).$$

n = 1-4, x = 1, 3, 4.

On the other hand, $\mathbf{C_n}$ and $\mathbf{D_n}$ series could result from dehydration and double dehydrogenation $[VL_n\text{-}2H_2\text{-}xH_2O]^+$ of the VL_n^+ complexes. ($[VL_n\text{-}2H_2\text{-}xH_2O]^+$). This mechanism can be related to equation (5) and Assignment **II** in Table II.2. 2.

In the mass spectra of Ti^+ reactions the peaks at *m/z* 206 and 308 do not correspond to Ti containing ions (as proved by the ejection experiment, Fig. III.2.8.) and are left unassigned. So are the peaks at *m/z* 159 and 205 in the V^+ reaction mass spectra.

2.3.4. Oxygen abstraction by silicon

The silicon ion, as the only non-metal ion studied her, shows specific reactions with acetophenone. The mass spectrum representing its behavior is given in Figure III.2.9.

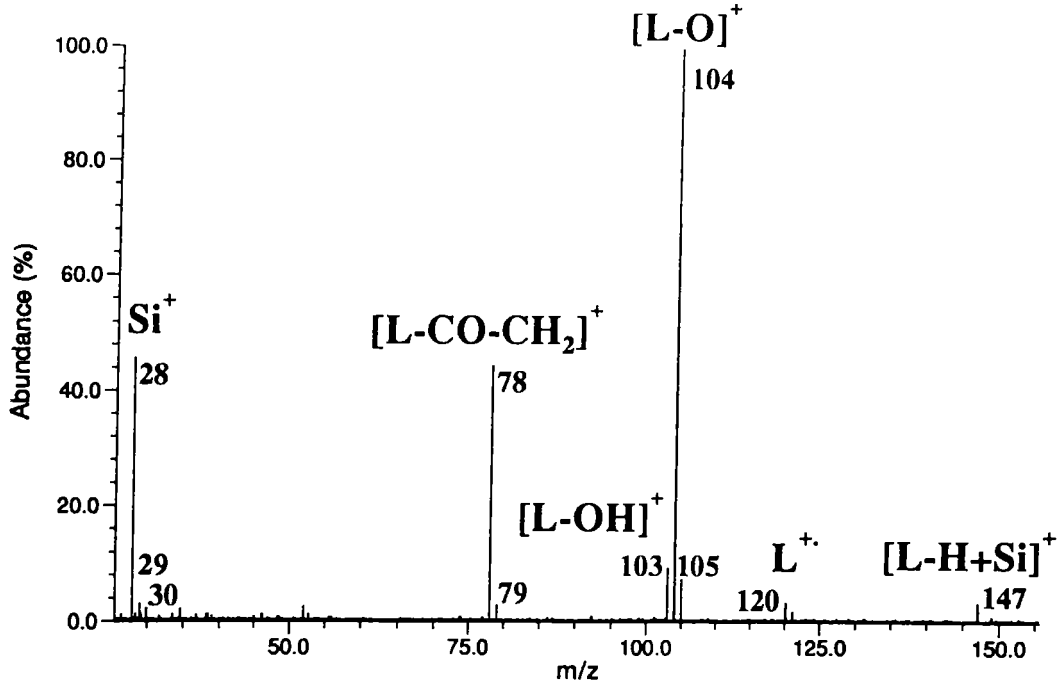

Figure III.2.9. FT-ICR mass spectrum of the ionic products of the reaction of Si^+ with acetophenone (L) at 0.1 s reaction time.

After a short reaction time (0.01 s) $[SiL-H]^+$, *m/z* 147, is detected with a low intensity (8a).

$$Si^+ + L \longrightarrow [SiL-H]^+ + H \qquad (8a)$$

$$\longrightarrow [L-O]^+ + SiO \qquad (8b)$$

$$\longrightarrow [L-OH]^+ + SiOH \qquad (8c)$$

$$\longrightarrow [L-COCH_2]^+ + SiOC_2H_2 \qquad (8d)$$

A major product in the reaction is represented by the peak *m/z* 104, assigned as styrene ion ($[L-O]^+$) which results from oxygen abstraction by silicon (8b). Abstraction of oxygen by silicon should be compared with the formation of titanium and vanadium oxides. On one hand, ionization energy (E_i) of TiO and VO are lower than the E_i of styrene (see Table III.2.3.) and hence the oxide will keep the charge according to the Stevenson-Audier rule. Both, TiO^+ and VO^+ were detected. On the other hand, styrene, having a lower E_i than SiO will keep the charge, as shown in

equation (8b) and thus $[L-O]^+$ will be formed

Table III.2.3. Ionization energies (E_i) of studied species and their oxides

M	E_i (M) /eV	E_i (MO) /eV
Ti	6.83	6.82[a]
V	6.75	7.23[a]
Si	8.15	11.43
C_8H_8O	9.29	-
C_8H_8	8.43	-

Values in table from reference 31
[a] taken from reference 28

A weak $[L-OH]^+$ ion signal, *m/z*103, was also detected. We can propose an elimination of SiOH (8c). No $SiOH^+$ has been detected in contradiction to the reported results concerning reactions of Si^+ with oxygen containing molecules[17]. Furthermore, we observed the formation of benzene ion, *m/z*78, (8d) which can be formed in the enol-form acetophenone reaction with Si^+.

2.3.5. Charge transfer and/or electron ionization

The molecular ion of acetophenone ($L^{+\cdot}$), its protonated molecules ($[L+H]^+$ and $[2L+H]^+$), and some fragments ($[L-COCH_3]^+$ and especially $[L-CH_3]^+$) are detected as byproducts of all studied reactions (except in the case of Ca^+ and Ba^+).

They are listed in Table III.2.1. It has to be underlined that the intensities of peaks corresponding to those ions are very low in comparison with peaks belonging to detected complexes. The exceptions are reactions with Si^+, V^+ and Zn^+.

At least two mechanisms could be invoked for the explanation of their formation.

The first mechanism is **charge transfer** followed by fragmentation (9), or selfprotonation (10).

$$L + M^+ \rightarrow L^{+\cdot} + M \rightarrow [L-X]^+ + X^{\cdot} + M \qquad (9)$$

$$X = CH_3,\ COCH_3$$

$$L^{+\cdot} + L \rightarrow [L+H]^+ + [L-H]^{\cdot} \qquad (10)$$

Wood et al.[21] have shown that the formation of ions from neutral molecules by charge transfer is not significant when the projectile ions are at their thermal ICR orbits (for the ICR time scale). The low abundances of such detected ions presumably

result from few ion/molecule encounters at low pressure. The newly formed ion may fragment if a considerable translational energy is imparted by the collision. When the projectile ions are resonantly excited, they gain kinetic energy and the ion/molecule encounter rate increases, as the authors observed for the Al^+/acetophenone reaction. We observed the same tendency. Thermalization of eventually produced, hot ions was applied for Al^+ and In^+ ions reaction by introducting argon gas. We observed no significant difference in the reactivity of the metal ions with or without the buffer gas present.

Recently, Lei and Amster[32] attributed charge transfer mechanisms to electronically excited states of studied Cu^+ and Fe^+ in reactions with amino acids, and not to their kinetic energy. Since the recombination energy of studied ions in their ground state is lower than the ionization energy of acetophenone, charge transfer is an endothermic process. Moreover, they stated that 100 collisions are adequate to relax the kinetic energy of the ions, but not enough to relax the internal energy. They found that thousands of thermalizing collisions are necessary to quench the charge-transfer reaction, and this quenching requires the application of quadrupolar excitation to prevent the loss of metal ions through collision-induced radial diffusion.

As expected, the charge transfer mechanism is especially pronounced in the case of Zn^+ ions because its recombination energy (9.39 eV) is higher than the ionization energy of acetophenone (9.29 eV). The formation of L^+ is in this case in competition with the formation of complexes which did not take place with any other ion studied.

According to our results we assume both the reactions of ground state metal ions to occur and the existence of some electronically excited ions.

A second possible mechanism is laser induced **electron ionization.** It is well known that a large number of electrons is produced during the laser/matter interaction at high irradiances ($> 10^8$ W cm^{-2}).

$$M \xrightarrow{\text{laser}} M^+ + e^- \qquad (11)$$

$$L + e^- \rightarrow L^{+\cdot} + 2e^- \qquad (12)$$

This was shown in some Time-Of-Flight mass spectrometry experiments[33]. Photoemitted electrons from the metal surfaces were used to ionize incoming molecules in the supersonic jet[33a] or, in another case, to ionize molecules already

desorbed by another laser[33b].

Our experiments show that molecular ($L^{+\cdot}$) and fragment ions ($[L\text{-}CH_3]^+$) detected even after a few seconds, give rise to a mass spectrum which is very similar to the one observed for electron ionization at ~10-15 eV. This effect is currently under investigation in our laboratory.

2.3.6. Reactions Involving Water Molecules

In some cases, namely for Ca^+, Ba^+ and Al^+ reactions, species containing hydroxyl group are formed. In the mass spectra of Ca^+ or Ba^+ reactions with acetophenone low intensity peaks (about 10% of the previous L_nM^+ peak) corresponding to $[L_nM+17]^+$, (n = 0-3 for Ca^+ and 0-1 for Ba^+) are present. These products result from OH incorporation and can be represented as $[L_n(M^{2+}OH^-)]^+$. As reported by Wu and Brodbelt[34] for the reaction of crown ethers with Mg^+, the alkaline earth metals bind hydroxide (OH^-) and attain a favored +2 oxidation state, so the net charge of the ion is +1. According to the mechanism they propose, a monopositive ion reacts with H_2O, donating its single 3s electron and causing homolytic cleavage of an O-H bond. Thus a hydrogen atom is released in the process, and the net product is $(M^{2+}\text{---}OH^-)^+$ as shown by relation (13). The reaction product is then effectively "solvated" by acetophenone molecules, resulting in $[L_n\text{---}(M^{2+}OH^-)]^+$, (14), with electrostatic bonds between oxygen atoms and the metal center.

$$Ca^+ + H_2O \rightarrow \left[Ca^+ \text{---} H_2O\right] \rightarrow \left[Ca^{2+}OH^-\right]^+ + H \qquad (13)$$

$$\downarrow nL$$

$$\left[L_nCa^{2+}OH^-\right]^+ \qquad (14)$$

In the Al^+ reaction spectra with 5 s and longer reaction times, minor peaks, corresponding to $[L_2Al]^+$, $[L_2Al+16]^+$ and $[L_2Al+34]^+$ are observed. This can be again compared to the results of Wu and Brodbelt,[34] who observed $[L'Al]^+$, $[L'Al+16]^+$ and $[L'Al+34]^+$ where L' was a polyether. In our case the product ions are assigned as $\{L_2[Al^{3+}(OH^-)_2]\text{-}H_2O\}^+$ and $\{L_2[Al^{3+}(OH^-)_2]\}^+$ respectively. The proposed reaction mechanism is as follows:

$$Al^+ + 2H_2O \rightarrow \left[H_2O\text{--}Al^+\text{--}H_2O\right] \xrightarrow{2L} \left[L_2Al^{3+}\left(OH^-\right)_2\right]^+ + H_2$$
$$\downarrow - H_2O$$
$$\left[L_2Al^{3+}\left(OH^-\right)_2 - H_2O\right]^+ \qquad (15)$$

Incorporation of OH groups is not observed for single ligand complexes.

It should be underlined that intensity of all mass peaks which correspond to the hydroxide incorporation are always very low.

2.4. Negative Ionization by Emitted Electrons

Working in negative-mode laser desorption of pure metals, we did not detect any particular anion. Nevertheless, emission of electrons from the metal occurs as mentioned above. After the introduction of acetophenone, anions assigned as $[L\text{-}H]^-$ are detected. The same result is obtained for all the pure elements studied. Negative chemical ionization by dissociative capture mechanism[35] is supposed, because the deprotonated molecular anion is detected. This result initiated a more detailed study of negative ionization of organic molecules induced by emitted electrons still under way in our laboratory.

2.5. Conclusions

The results presented here are in agreement with those previously observed for the reactions of Fe^+, Ni^+ and Al^+ with acetophenone. Additional reaction channels are observed and other transition metal ions (Ti-Zn), the alkaline earth metals (Mg, Ca and Ba), group IIIA metals (Al and In) and silicon ions reacted with the same molecule. A number of different reaction pathways could be identified: i) formation of ML_n^+ complexes (n = 2 for M = Na, Cr, Fe, Ni, Co, Cu, Zn, In; n=2-3 for M = Ba, Al; n =2-4 for M = Mg, Ca, Mn); ii) formation of $[M(O)L_n - X]^+$, where X is a ligand fragment, for Fe^+, Co^+ and Ni^+, X = CO; Ti^+ and V^+ bind oxygen atom and dehydrogenation and dehydration of complexes occur; iii) oxygen elimination by silicon; iv) charge transfer and/or electron ionization of ligand and its fragmentation. More detailed studies of mechanisms involved will be performed by CID*. Ionization and deprotonation of acetophenone molecule by electrons emitted from irradiated metals, initiated further studies in the negative mode.

---

* CID = Collision Induced Dissociation

REFERENCES

1. S.H. Pine, J.B. Hendrickson, D.J. Cram and G.S. Hammond, "Organic Chemistry" Fouth Edition, International Student Edition, McGraw-Hill Kogakusha, LTD, Tokyo, (1980).

3. R. C. Burnier, G. D. Byrd, T. J. Carlin, M. B. Wiese, R. B. Cody and B. S. Freiser, In *Ion Cyclotron Resonance Spectrometry II; Lecture Notes in Chemistry* Vol. 31; ed. by H. Hartmann and K.-P. Wanczek, p.98. Berlin, (1982).

4. L. F. Halle, W. E. Crowe, P. B. Armentrout and J. L. Beauchamp, *Organometallics*, **3** 1694 (1984).

5. R. C. Burnier, G. D. Byrd and B. S. Freiser, *J. Am. Chem. Soc.* **103** 4360 (1981).

6. H. Kang and J. L. Beauchamp, *J. Am. Chem. Soc.* **108** 5663 (1986).

7. L. S. Sunderlin and P. B. Armentrout, *J. Phys. Chem.* **94** 3589 (1990).

8. R. C. Burnier, G. D. Byrd and B. S. Freiser, *Anal. Chem.* **52** 1641 (1980).

9. P. I. Surrjasamita and B. S. Freiser, *J. Am. Soc. Mass Spectrom.* **4** 135 (1993).

10. C. G. Gill, A. W. Garrett, P. H. Hamberger and N. S. Nogar, *J. Am. Soc. Mass Spectrom.* 7 664 (1996).

11. M. A. Tolbert and J. L. Beauchamp, *J. Am. Chem. Soc.* **106** 8117 (1984).

12. R. Georgiadis and P. B. Armentrout, *J. Am. Chem. Soc.* **108** 2119 (1986).

13. D. A. Peake and M. L. Gross, *J. Am. Chem. Soc.* **109** 600 (1987).

14. L. Operti, E. T. Tews and B. S. Freiser, *J. Am. Chem. Soc.* **110** 3847(1988).

15. A. K. Chowdhury and C. L. Wilkins, *Int. J. Mass Spectrom. Ion Processes* **82** 163 (1988).

16. N. G. Adams and D. Smith, In *Techniques for the Study of Ion-Molecule Reaction,* ed. by J. M. Farrar and W. H. Saunders, Jr., John Wiley & Sons, New York (1988).

17. D. K. Bohme, *Int. J. Mass Spectrom. Ion Processes* **100** 719 (1987).

18. R. Stepnowski and J. Allison, *J. Am. Chem. Soc.* **111** 449 (1989).

19. A. Bjarnason and J. W. Taylor, *Organometallics* **9** 1493 (1990).

20. A. Bjarnason, J. W. Taylor, J. A. Kinsinger, R. B. Cody and D. A. Weil, *Anal. Chem.* **61** 1889 (1989).

21. D.T. Wood, A.G. Marshall and L. Schweikhard, *Rapid Commun. Mass Spectrom.* **8** 14 (1994).

22. J. Chamot-Rooke, F. Pennequin, J-P. Morizur, J. Tortajada, E. Rose and F. Rose-Munch, *J. Mass. Spectrom.* **31** 199 (1996).

23. A. G. Marshall, F. R. Verdun, *Fourier Transform in NMR, Optical and Mass Spectrometry. A User's Handbook*, Elsevier, Amsterdam, (1990).

24. a) J. F. Muller, M. Pelletier, G. Krier, D. Weil and J. Campana in *Microbeam A nalysis*, ed. P. E. Russell, p. 311. San Francisco Press, (1989).
b) M. Pelletier, G. Krier, J. F. Muller, D. Weil and M. Johnston, *Rapid Commun. Mass Spectrom.* **2** 146 (1988).

25. P. B. Armentrout, L. F. Halle and J. L. Beauchamp, *J. Am. Chem. Soc.* **103** 6501 (1981).

26. S. J. Babinec and J. Allison, *J. Am. Chem. Soc.* **106** 7718 (1984).

27. L. Z. Chen and J. M. Miller, *Rapid Comm. Mass Spectrom.* **6** 492 (1992).

28. E. R. Fisher, J. L. Elkind, D. E. Clemmer, R. Georgiadis, S. K. Loh, N. Aristov, L. S. Sunderlin and P. B. Armentrout, *J. Chem. Phys.* **93** 2676 (1990).

29. J. Allison and D. P. Ridge, *J. Am. Chem. Soc.* **100** 163 (1978).

30. a) M. A. Tolbert and J. L. Beauchamp, *J. Am. Chem. Soc.* **108** 7509 (1986).
b) K. Eller, W. Zummack and H. Schwarz, *J. Am. Chem. Soc.* **112** 621 (1990).

31. CRC Handbook of Chemistry and Physics, ed. D. R. Lide, 73rd ed., CRC Press, Boca Raton, Florida, (1992-1993).

32. Q. P. Lei and I. J. Amster, *J. Am. Soc. Mass Spectrom.* **7** 722 (1996).

33. a) F. Moritz, M. Dey, K. Zipperer, S. Prinke and J. Grotemeyer, *Org. Mass. Spectrom.* **28** 1467 (1993).
b) D. C. Schriemer and L. Li, *Anal. Chem.* **68** 250 (1996).
c) S. M. Colby and J. P. Reilly, *Int. J. Mass Spectrom. Ion Processes* **131** 125 (1994).

34. H.F. Wu and J.S. Brodbelt, *J. Am. Chem. Soc.* **116** 6418 (1994)

35. H. Budzikiewicz, *Mass Spectrom. Rev.* **5** 345 (1986).

III.3. Gas phase reactions of PFTBA with positive ions

3.1. *Introduction*

After establishing the experimental conditions and defining the processes in the (model) reactions between ions produced by laser ablation and acetophenone, they have been used for the ionization of polyhalogenated molecules. We started with perfluorobutylamine (PFTBA) molecule. In our case, PFTBA was chosen as the test compound for two main reasons: First, it can be representative for the behaviour of the class of polyhalogenated molecules and second, it is well known in mass spectrometry as a standard calibrant in electron ionization experiments.

Our experiments were directed toward the following objectives:

- To determine the capabilities of different positive ions to ionize PFTBA molecule and to define the involved reaction mechanisms.
- To apply ion (chemical) ionization to some other polyhalogenated molecules.
- To find a method to use the PFTBA for calibration (that remains an important and sometimes difficult point) in laser induced experiments. This requires high fragmentation of PFTBA.

This chapter begins with bibliographical data about PFTBA and about reactions of metal ions with amines in the gas phase Reactions of metal ions with polyhalogenated molecules are given after that . We present the results obtained in our studies of the reactivity of the perfluorotributylamine with 21 laser produced elemental ions (mainly transition-metal, alkaline, earth-alkaline). Originally, we started with aluminium and stainless steel (Al^+, Cr^+, Fe^+ and Ni^+ ions); materials commonly met in the laser desorption/ionization experiments. They can be present in the system as sample support or adhesive tape (e.g. Al-tape).

For a better understanding of the mechanisms involved in positive ion/PFTBA reactions, its hydrogenated analog tributylamine (TBA) was examined. In order to use PFTBA as a calibrant in LD experiments, internal ion impact ionization was chosen to increase the fragmentation of the molecular ion. Mass spectra with many well defined fragment ions could then be used in a calibration procedure analog to EI experiments. Ionization by laser-produced positive ions was further applied to several other polyhalogenated molecules. At last, to calibrate the mass spectra of those polyhalogenated compounds, highly fragmented PFTBA was used as an internal calibrant.

3.2. *Bibliographical overview*

3.2.1. Perfluorotributylamine

A search in the Current Contents database for perfluorotributylamine molecule provides at first, numerous references about its use in medical research.[1] The ^{19}F NMR spectroscopy uses perfluorocarbon aerosols for simultaneous analysis of lung structure and pulmonary oxygenation patterns *in vivo*.[1a,c,f] Perfluorocarbon emulsions (artificial blood[1g]) are used in different studies (e.g. liquid-liquid blood-gas exchange[1d]..). Beside this, perfluorotributylamine remains the molecule of choice in different mass spectroscopic studies.[2] Many new techniques which has to be certified are tested with PFTBA (e.g. high performance FTMS via single trap electrode[2a], a quadrupole mass filter quadrupole ion trap MS[2d]...)

PFTBA, $(C_4F_7)_3N$, is volatile and chemically inert. So that, its vapour can be introduced in a steady flow to a mass spectrometer, and then pumped out again rapidly without problems due to condensation, adsorption or decomposition. PFTBA molecule (M = 671 u) ionizes easily and gives numerous and well defined fragments with specific series in the positive and negative modes. Nevertheless, it was impossible to use it directly in laser desorption/ionization experiments because this ionization method deals with solid samples.

3.2.2. Metal ion reactivity towards amines

Metal ion reactions with amines have been mostly studied for the primary amines. Few data were found about the reactivity of metal ions towards tertiary amines and nothing at all about the perfluorinated ones.

At the end of 1984, Babinec and Allison[3,4] reported the chemistry of Cr^+, Mn^+, Fe^+, Co^+, Ni^+, Cu^+ and Zn^+ with n-propylamine. Fe^+ is the only first-row transition metal ion that inserts into the C-N bond of this amine. Fe^+ forms six products, of which the major one is due to insertion into the C_2H_5-CH_2NH_2 bond. Co^+ forms three products, and attack of the same C-C bond dominates. Ni^+ forms only one product, also due to attack at this C-C bond. Zn^+ and Mn^+ were unreactive. The Cu^+ and Cr^+ ions both induce hydrogen elimination. The correlation of ion reactivity with their electronic configuration is already presented in III.1.

Ethylamines were shown to be the most studied amines in the reaction with metallic positive ions.

Radecki and Allison[5] have studied reactivity of Co^+ towards mono-, di-, and triethylamine (TEA). Ions were produced by electron ionization in an ICR experiment. They reported that Co^+ abstracts a hydride unit from amines to form CoH whenever there is an α-hydrogen available but not when there is no α-hydrogen. This is explained as an attack of the metal ion at the α-hydrogen, association of the resulting metal hydride to the α-carbon, followed by elimination of the neutral metal hydride. Further, no insertion of Co^+ into C-N bond of primary and secondary amines was observed, while TEA does form products indicative of Co^+ insertion into the C-N bond. These authors further suggested the ability of Co^+ to insert into the C-N bonds of tertiary amines.

Karrass et al.[6] reported results contradictory to those in previously cited paper concerning monoethylamine reactions with Co^+. They noted the absence of oxidative addition of Fe^+ and Co^+ to the N-H bond, followed by β-hydrogen transfer and reductive elimination of H_2. Their labelling data prove that molecular hydrogen originates exclusively from the β and γ positions of the propyl chain.

The rates of hydride abstraction from mono-, di-, and trimethylamine (TMA) by Cu^+ and Ag^+ have been determined by Sigsworth et al.[7] in a flow reactor. Thermionic emission was used to produce metal ions. The formation of the metal hydride, according to the following equation:

$$Cu^+ + (CH_3)_3N \rightarrow H_2C = N(CH_3)_2^+ + CuH \quad (1)$$

was the only observed process in the reaction. It has been shown to be fast and exothermic. Relative to the other isomeric possibilities, the quaternary immonium structure given for $C_3H_8N^+$ product ions in eq.(1) was thought to be quite stable. Ground state Cu^+ has d^{10} configuration and is left with an empty s orbital with which it can bound; it is therefore conceivable that ligands could bond by donating two electrons to the empty orbital. Authors supposed the nitrogen lone pair of NR_3 to be the initial site for metal/ligand interaction.

The same amines were reported in reactions with laser-produced Ti^+, Ni^+ and Nb^+ ions.[8] Once again the early transition metal ions showed the preference for C-H activation. Ti^+ and V^+ gave rise to extensive dehydrogenation or losses of hydrogen molecules together with ethane while for Fe^+ - Ni^+ loss of CH_4 as well as C_2H_4 were observed. Cr^+ and Mn^+ formed adducts but unspecified amounts of single dehydrogenation were also present. Radical losses were often encountered and may point to the production of excited states in the laser ablation/pulsed molecular beam technique.

Mono-, di-, and trimethylamine (TMA) have been studied with the group 8-10 metal ions Fe^+, Co^+, Ni^+, Ru^+, and Rh^+. Hydride abstraction was observed in competition with dehydrogenation and demethanation.[9]

3.2.2. Metal ion reactivity towards polyhalogenated molecules

Small polyhalogenated molecules were subject of intensive studies. Most of them were directed toward their detection as environmental pollutants (freons). Metal-ion reactions with these compounds have not been thoroughly determined although there are many studies on reactivity of the alkyl halides.[10]

The reactions of singly charged atomic nickel ions with fluorinated hydrocarbons C_2F_4 and CF_4 were examined by using an ion beam apparatus.[11] It has been observed that the cross section of reaction of metal ion with C_2F_4 is strongly dependent on the relative kinetic energy of the reactants. Only endothermic processes were observed. Analysis of the thresholds for endothermic processes leading to the formation of nickel ion carbene species led to the bond dissociation energies $D°(Ni^+\text{-}CH_2) = 86 \pm 6$ kcal/mol and $D°(Ni^+\text{-}CF_2) = 47 \pm 7$ kcal/mol. In the reaction with C_2F_4 , products NiF^+, $NiCF_2^+$ and $NiC_2F_3^+$ were detected. Furthermore, NiF^+ and CF_3^+ were detected in reaction with CF_4.

Oxidation processes dominate the chemistry of Mg^+ with the CCl_4 and CH_2ClCH_2Cl.[12] Both yielded $MgCl_2$ neutral and a carbocation product. Similarly, $CFCl_3$ gives MgClF and CCl_2^+. These reactions refereed to be direct (in the one step). With $CHCl_3$, however, the oxidation clearly proceeds in a two-step process through a $MgCl^+$ intermediate. CH_3Cl, C_2HCl_3 and C_2Cl_4 were unreactive with Mg^+.

In the same work, Al^+ was found to be oxidized into $AlCl_2^+$ in the reaction with CH_2ClCH_2Cl. Chloride transfer follows, and neutral $AlCl_3$ and C_2H_4Cl were formed. Al^+ has been reported to react with CCl_2F_2 by fluoride transfer.

Ti^+ forms, among other products, TiF_2 from CF_2Cl_2 and $TiCl_2^+$ from di-, tri-, and tetrachlorethane. [13]

Transition - metal cationization of laser-desorbed perfluorinated polyethers was studied by means of FTMS by Cromwell et al.[14] Perfluorinated polyether (PFPE) films were desorbed by a laser pulse and then cationized by transition-metal ions desorbed/ionized by another laser. Two pulsed lasers were employed: a low irradiance laser for PFPE desorption and a high irradiance laser for metal ion formation.

Cationization was observed to occur in the gas phase above the sample surface only for a narrow range of ablation laser-pulse energies (0.25 - 0.32 mJ at 532 nm). All studied metal ions (Cu, Ni, Fe, Co, Ti, Mo, Ta, Ag, Mn, Al) except Au induced cationization of PFPE. No fragmentation of parent PFPEs was observed. This result supported the existence of an electrostatic bond between the metal ions and the parent polymers. It is difficult to draw any quantitative conclusions from these studies because the kinetic energies of the metal ions were not known and the complex-formation cross sections may depend on those energies. By comparing the cationized PFPE signal strength to the metal ion intensity, it appeared that the 4th row transition metals (Cr, Fe, Ni, Co, Cu, Zn) were the most efficient at cationizing the desorbed polymer.

RESULTS

3.3. *Ionization and Dissociation of PFTBA by Positive Ions*

In our experiments, 21 elemental monocharged ions, M^+, (see the periodic table below) were produced by pulsed laser ablation (irradiance 10^9 - 10^{10} W cm^{-2}) of solid samples.

IA																	0
	IIA											IIIB	IVB	VB	VIB	VIIB	
Li												B					
Na	Mg	IIIA	IVA	VA	VIA	VIIA	-----	VIII	-----	IB	IIB	Al	Si				
K	Ca		Ti	V	Cr	Mn	Fe	Co	Ni	Cu	Zn						
			Zr		Mo							In	Sn				

Ions were isolated and allowed to react with perfluorotributylamine $[CF_3(CF_2)_3]_3N$ (PFTBA = L) molecules. PFTBA was introduced into the FTMS chamber by pulsed valves or directly by a batch inlet system, to a pressure of about 10^{-7} Torr. There are no significant differences in the results obtained using both introduction methods.

On the contrary to acetophenone reactions, time does not seem to be an important parameter in the case of PFTBA. The increase of the reaction time, generally does not lead to the formation of new products. All products are formed during the first hundred milliseconds of the reaction. Their relative intensities increase within one second while those of projectile ion decrease.

Various reaction products have been detected depending on the projectile ion. No PFTBA molecular ion (*m/z* 671) was ever detected. The peak corresponding to this molecular ion was searched for extensively at different laser fluences, at different wavelengths, and of course with different projectile ions. Its non-detection is not surprising, since ionization of PFTBA molecule by a charge-transfer mechanism requires an energy higher than 11.3 eV. Not any of the studied ions has such a high recombination energy.

In almost all reactions, peaks corresponding to PFTBA fragments have been observed. Beside them, several metal-containing ions have been detected as well. To give an overview of the reaction products, we wanted to list all of them all in a common table. As for some reactions there is a long list of detected fragment ions (listed later in Table III.3.1), we selected all product ions that contain a metal atom, and some "high"-mass-fragment ions, that can be relevant for reaction mechanisms. They are gathered in Table III.3.1.

No clear periodic trend can be drawn out from those results. Thus, we can rather group the results according to plausible reaction pathways:

i) **common fragmentation ;**

ii) **formation of LM^+ complexes;**

iii) **abstraction of fluoride by metal;**

iv) **formation of $[L - F_2]^{+\cdot}$;**

v) **formation of LMF^+ complexes ;**

vi) **formation of $[LM - F]^+$;**

vii) **formation of $[L\text{-}C_4H_9 + M]^+$.**

Each of them will be displayed separately.

Table III.3.1. Selected product ions (metal containing ions and relevant fragmens) and their relative abundances from positive ion (M^+) - PFTBA (L) reactions

M	Li	Na	K	Mg	Ca	B	Al	Si	Ti	V	Cr	Mn	Fe	Co	Ni	Cu	Zn	Zr	Mo	In	Sn
$[L+MF]^+$	-	-	-	-	50	-	-	-	-	-	-	-	-	-	-	-	-	-	-	-	-
$[L+M]^+$	**100**	64	-	-	-	-	-	-	-	-	**100**	-	-	**100**	**100**	**100**	16	-	-	-	-
$[L+M-F]^+$	-	-	-	-	4	-	-	-	-	-	-	-	-	-	-	-	-	-	-	-	-
$[L-F]^+$ (m/z 652)	10	**100**	8	-	-	1	**100**	12	11	7	-	70	**100**	1	5	17	**100**	6	19	6	-
$[L+M-2F]^+$	7	-	-	-	-	-	-	-	-	-	-	-	-	3	1	8	-	-	-	-	-
$[L-2F]^+$ (m/z 633)	-	-	-	**100**	-	-	-	-	42	12	-	13	9	-	-	-	-	1	-	-	**100**
$[L-3F]^+$ (m/z 614)	2	-	10	-	-	9	14	8	7	10	-	23	1	1	-	2	9	5	9	4	-
$[L-4F]^+$ (m/z 595)	-	-	-	8	1	-	-	-	10	-	-	80	1	2	-	-	-	-	-	-	2
$[L-C_3F_7]^+$ (m/z 502)	5	97	5	13	4	12	9	10	-	30	-	96	-	1	-	-	-	9	-	**100**	-
$[L-C_4F_{11}]^+$ (m/z 414)	3	67	**100**	7	1	**100**	23	**100**	**100**	**100**	15	**100**	13	45	-	19	28	**100**	**100**	37	-
$[L+M-C_4F_9]^+$	-	-	-	3	**100**	-	-	-	-	-	-	-	-	31	-	-	-	-	-	-	-
$[M+F]^+$	-	-	-	3	34	-	-	18	-	7	-	-	-	-	-	-	-	-	-	-	-

Intensities are normalized to the most abundant selected peak (noted in bold).

3.3.1. Common Fragmentation

For almost all projectile ions (except Cr, Ca and Ni), product ions corresponding to PFTBA fragments have been observed. Ions Ti^+, V^+, Si^+ and B^+ induced the most intense fragmentation of PFTBA molecules. The resulting spectra are shown in Figure III.3.1.

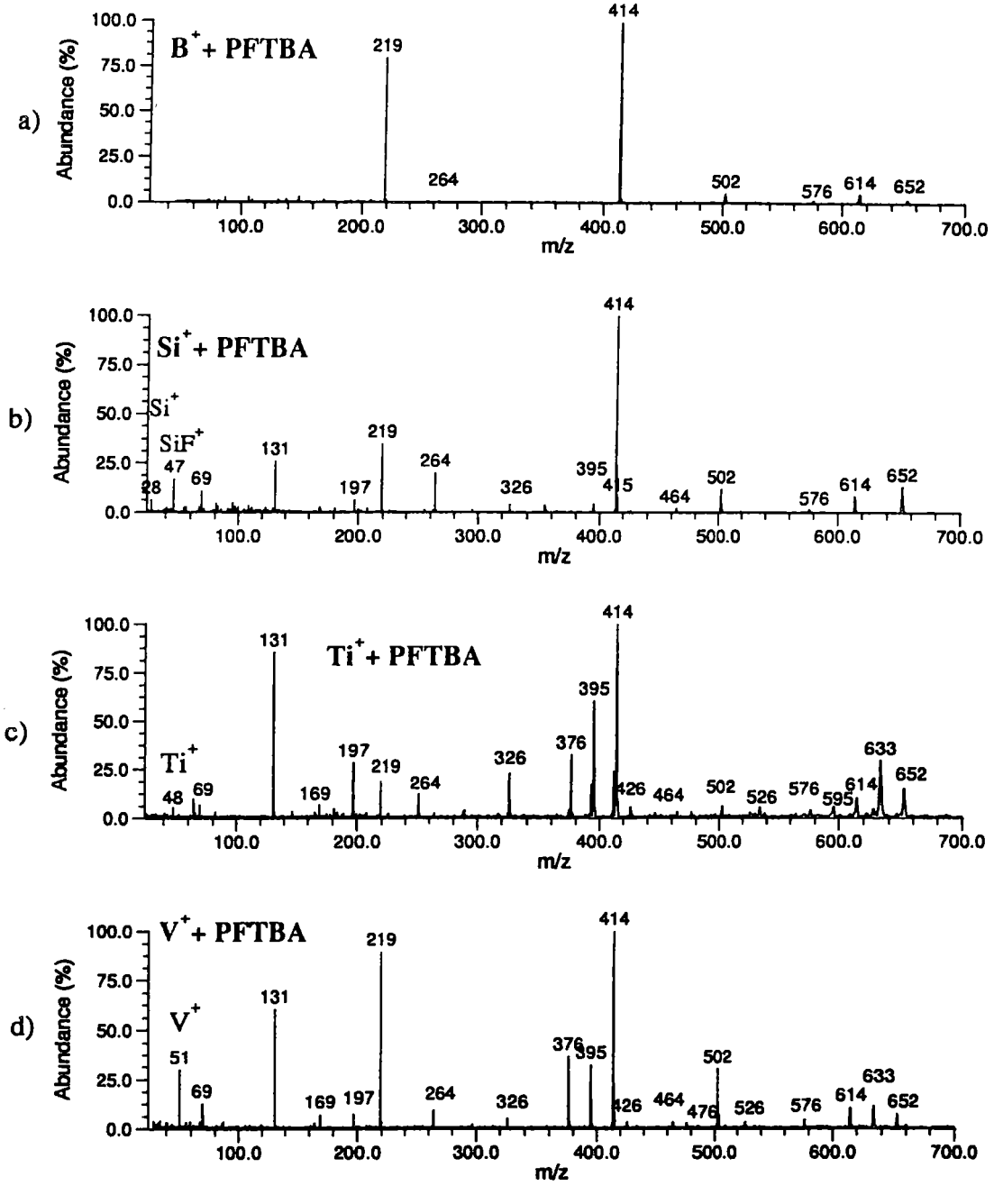

Figure III.3.1. Mass spectra of a) B^+, b) Si^+, c) Ti^+ and d) V^+ 1 s reactions with PFTBA. Ions are assigned in Table III.3.2.

Ion $[L\text{-}C_4F_9\text{-}F_2]^+$ *m/z* 414 is the main product in those reactions. Ti^+ and V^+ induce strong fragmentation with formation of many different ions. Most of them are characteristic for positive EI series of PFTBA fragments (see following title). Nevertheless, some of the observed ions (e.g. $[L\text{-}2F]^{+\cdot}$, *m/z* 633, and $[L\text{-}4F]^{+\cdot}$ *m/z* 595, have never been observed (up to our knowledge) in EI experiments. For four of the studied ions, (B^+, Si^+, Ti^+ and V^+), the ion $[L\text{-}F]^+$ ion product has been detected, which had not been observed either in classical EI mass spectra. All PFTBA fragment ions detected in our experiments are grouped in Table III.3.2. Spectra were calibrated using the fragments commonly found in EI spectra of PFTBA (marked with an asterisk*), other peaks were assigned according to this calibration. The relative mass error was typically less than 3 ppm. The ions marked in bold were the most frequently observed irrespective of the projectile ion.

Table III.3.2. Assignation of detected PFTBA fragment ions.

m/z	Assignation	*m/z*	Assignation
652	**$C_{12}F_{26}N^+$**	314	$C_6F_{12}N^+$
633	$C_{12}F_{25}N^{+\cdot}$	295	$C_6F_{11}N^{+\cdot}$
614	**$C_{12}F_{24}N^+$**	281	$C_6F_{11}^+$
602	$C_{11}F_{24}N^+$	269	$C_5F_{11}^+$
595	$C_{12}F_{23}N^{+\cdot}$	***264**	**$C_5F_{10}N^+$**
576	$C_{12}F_{22}N^+$	255	$C_7F_9^+$
557	$C_{12}F_{21}N^{+\cdot}$	250	$C_5F_{10}^{+\cdot}$
552	$C_{10}F_{22}N^+$	231	$C_5F_9^+$
545	$C_{11}F_{21}N^{+\cdot}$	226	$C_5F_8N^+$
533	$C_{10}F_{21}N^{+\cdot}$	***219**	**$C_4F_9^+$**
526	$C_{11}F_{20}N^+$	214	$C_4F_8N^+$
***502**	**$C_9F_{20}N^+$**	197	?
476	$C_{10}F_{18}N^+$	200	$C_4F_8^{+\cdot}$
469	$C_{11}F_{17}N^{+\cdot}$	181	$C_4F_7^+$
464	**$C_9F_{18}N^+$**	176	$C_4F_6N^+$
426	$C_9F_{16}N^+$	*169	$C_3F_7^+$
***414**	**$C_8F_{16}N^+$**	164	$C_3F_6N^+$
402	$C_7F_{16}N^+$	***131**	**$C_3F_5^+$**
395	$C_8F_{15}N^{+\cdot}$	119	$C_2F_5^+$
376	$C_8F_{14}N^+$	114	$C_2F_4N^+$
*364	$C_7F_{14}N^+$	100	$C_2F_4^{+\cdot}$
352	$C_6F_{14}N^+$	***69**	**CF_3^+**
326	$C_7F_{12}N^+$	50	$CF_2^{+\cdot}$

Different mechanisms are involved in the formation of the detected ions. Mechanisms induced by metal ion reaction (like fluoride abstraction) will be explained later. Some listed ions may be produced by direct fragmentation of the molecule, but some can result from rearrangements. It is worth noting that perhalogenated compounds resemble hydrocarbons in their mass-spectral behavior, including a high tendency for rearrangement.[15]

For K, B, Al, Si, Ti, V, Mn, Fe, Zr, Mo and In, ions marked in bold in the table, and some of their further fragments are the main yielded products. No complex ions containing those atoms were detected. The intensity distribution of the product ions is not the same for all regent ions as can be seen from Table III.3.1. Ion $[L-F]^+$, *m/z* 652, is the major product for the reactions involving K, Al, Fe and Zn. Ions Ti^+, Si^+, V^+, B^+, Zr^+ and Mo^+ mainly produce the $[L-C_4F_{11}]$, *m/z* 414, ion. In^+ mainly induce the formation of *m/z* 502, $[L-C_3F_7]^+$.

3.3.1.1. Comparison with EI spectra

The results displayed in the previous paragraph, where PFTBA was ionized and highly fragmented by Ti^+, Si^+, V^+, B^+, Zr^+ or Mo^+ ions (Fig. III.3.2.) can be compared with the standard Electron Ionization (EI) spectra of PFTBA. Spectra obtained by electron ionization were recorded on the FTMS 2001 instrument in Zagreb.

For the detection of the molecule ionized by EI, short delays between ionization and excitation/detection events are commonly used. A representative mass spectrum is in Fig. III.3.2.a. It was obtained at 20 eV electron energy and it does not differ a lot from a classical 70 eV EI spectrum recorded after a delay of 0.1 ms (Appendix B). The series of fragment ions is dominated by CF_3^+, *m/z* 69, and the highest-mass ion is $NC_{12}F_{24}^+$, *m/z* 614 detected with a low intensity.

But, if ions produced by EI are trapped for a longer delay before broad band excitation, higher mass ions can be detected. The spectrum obtained after 1 s delay is displayed in Figure III.3.2.b. The abundance of CF_3^+ (*m/z* 69) ion, decreases while, for higher mass fragments (e.g. *m/z* 264, 414, and 502), the intensities increase. Moreover, new high mass fragments are formed; in our case, ions with *m/z* higher than 614. Using a 1 s delay, even the $[L-F]^+$, *m/z* 652 ion has been produced. This ion, which has not been observed with short delays, has never been listed in any standard list of PFTBA fragments, not even in low abundance. [16] Thus, low mass ions, which are formed first, induce the formation of "high" mass fragments. Post chemical ionization (self CI) of neutral molecules by fragment ions occurred.

In the laser produced positive ion (Al^+, Fe^+)/PFTBA reactions, $[L-F]^+$ was detected already after 10 ms. It is much shorter than the time that low mass PFTBA fragments need to ionize (self-CI) neutral PFTBA and form $[L-F]^+$ (1s).

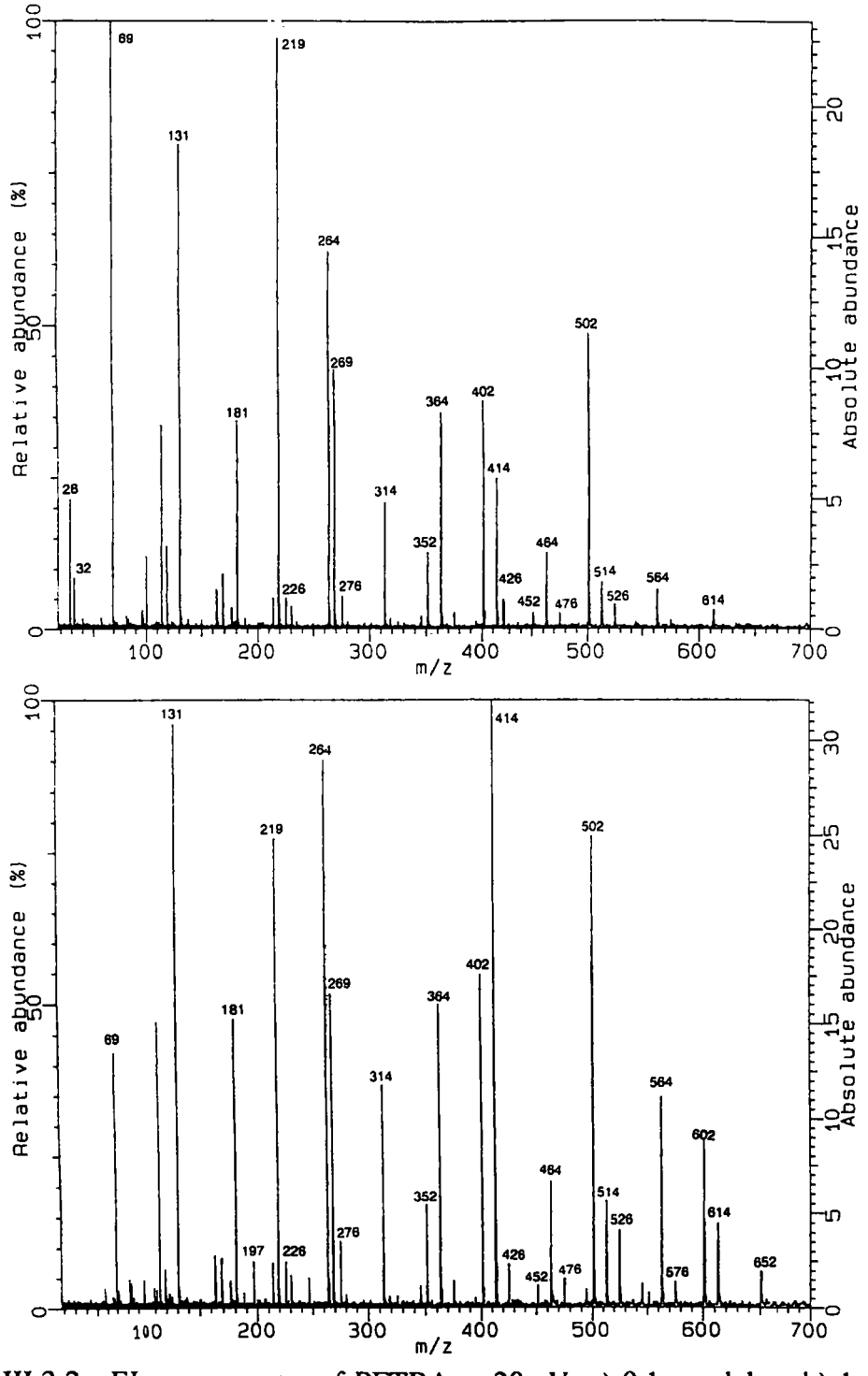

Figure III.3.2. EI mass spectra of PFTBA at 20 eV; a) 0.1 ms delay, b) 1 s delay .

Spectra obtained after ionization of PFTBA by ions produced by laser ablation in the case of Si, Ti, V, (Figure III.3.1.) resemble to one obtained after 1s reaction

delay after EI. Nevertheless, there are some peaks (m/z 633, 595, $[L-2nF]^+$, n = 0,1; that are not observed either in long delay - positive mode EI. That indicates special metal-ion/molecule interactions (more detailed, further in the text).

Thus, we can affirm that the ionization by laser-produced ions is much softer than EI even at very low electron beam potentials. Observed ion/molecule phenomena can be estimate to be driven below 5 eV.

3.3.2. Formation of LM^+ complexes

Li^+, Na^+, Cr^+, Co^+, Ni^+, Cu^+ and Zn^+ form adduct with PFTBA Ions $[M+L]^+$ are the most abundant ions for Li^+, Cr^+, Co^+, Ni^+ and Cu^+-reactions. The example of Cu^+ ion reaction is shown in Figure III.3.3.

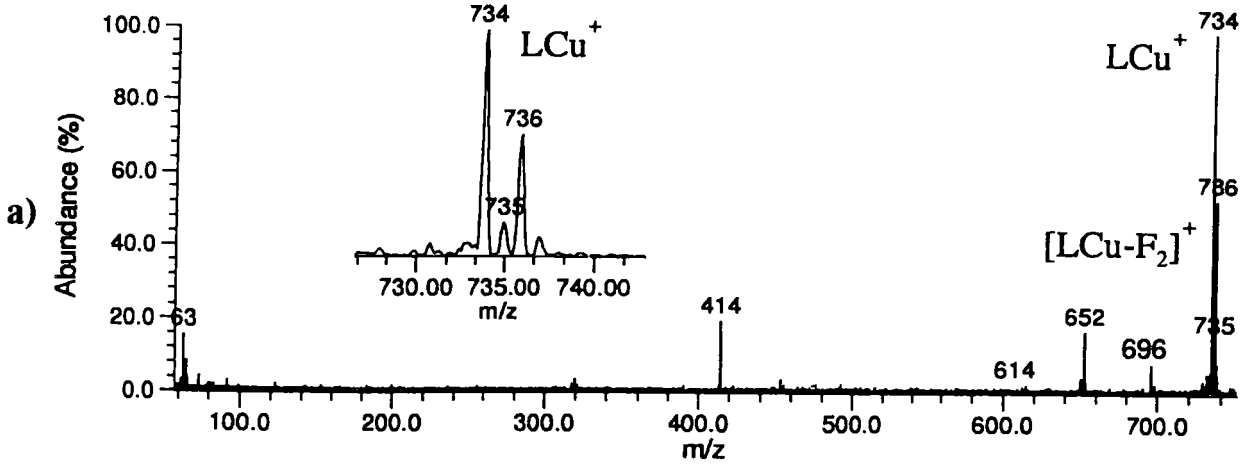

Figure III.3. 3. Mass spectrum Cu^+ + PFTBA

Ground state Cu^+ has a d^{10} configuration and is left with an empty s orbital with which it can bound; it is therefore conceivable that ligands could be bonded by donating two electrons to the empty orbital. Thus, one might expect the nitrogen lone pair of NR_3 to be the initial site for metal/ligand interaction.

The Cr^+ ($3d^5$), Co^+ ($3d^8$), Ni^+ ($3d^9$), and alkaline ions have also the possibility to accommodate two nitrogen lone pair electrons in a free s orbitale. So, it was not surprising to detect their adduct ions. Zn^+ with $d^{10}4s^1$ differs in electronic configuration and the formation of its adduct with PFTBA is accordingly less pronounced than the formation of the $[L-F]^+$ product ion (see Table III.3.1.).

3.3.2.1. Formation of $[LM-F_2]^+$ complexes

Elimination of F_2 from adduct complexes is observed for Li, Cr, Co, Ni, Cu and Zn. Ions $[LM - F_2]^+$ were observed, as shown in the case of copper (formation of *m/z* 734, see Figure III.3.3.) and in the case of nickel ions (formation of *m/z* 729, see Figure III.3.4.).

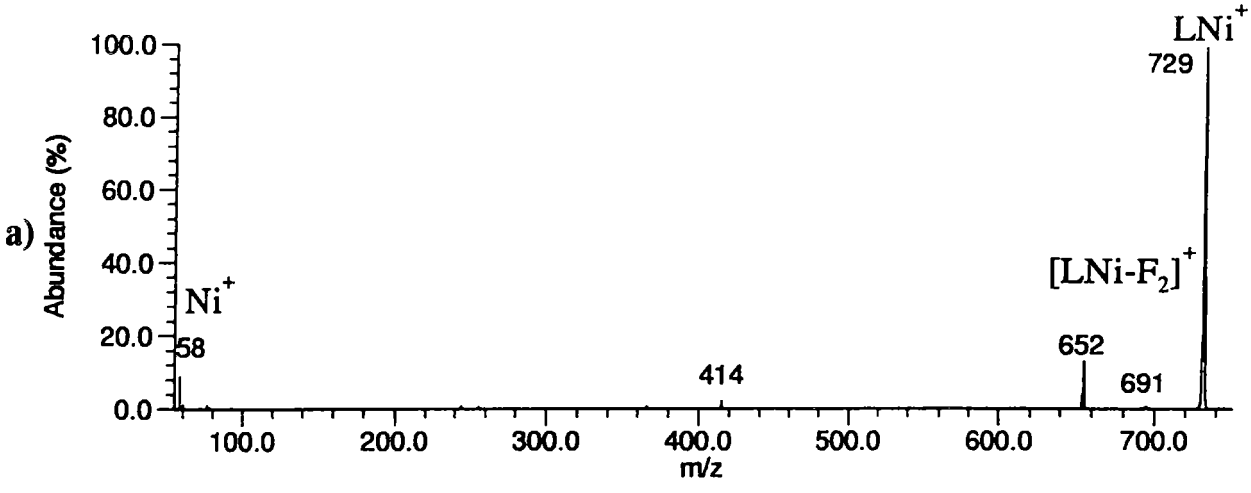

Figure III.3. 4. Mass spectrum Ni^+ + PFTBA

In the mass spectrum shown here, the main product is the adduct NiL^+. Its formation is followed by the elimination of F_2 leading to the $[LNi-F_2]^+$ ion, *m/z* 691. Such adduct formation was observed for alkali-metal ions, as expected, and for the following first row transition metal ions: Cr^+, Co^+, Ni^+, Cu^+ and Zn^+. Often in LD spectra $(L+M)^+$ ions, were M is alkali-metal atom, have been reported. Moreover, alkaline salts are added to allow adduct detection.

Subsequent elimination of F_2 from the complex occurred for Li, Cr, Co, Ni, Cu and Zn ions. In the case of Cu, this is in agreement with previously found dissociative attachment mechanism.[17]

3.3.3. Abstraction of fluoride by metal

The formation of $[L-F]^+$ ion has been observed for reactions with all the studied reagent ions. However, few of the projectiles (Mg, Sn and Cr) had to be resonantly excited in order to induce this fragmentation. $[L-F]^+$ is the main product for reaction of K^+, Al^+, Fe^+ and Zn^+ with PFTBA. The spectrum of Fe^+ - PFTBA is shown in Figure III.3.5.

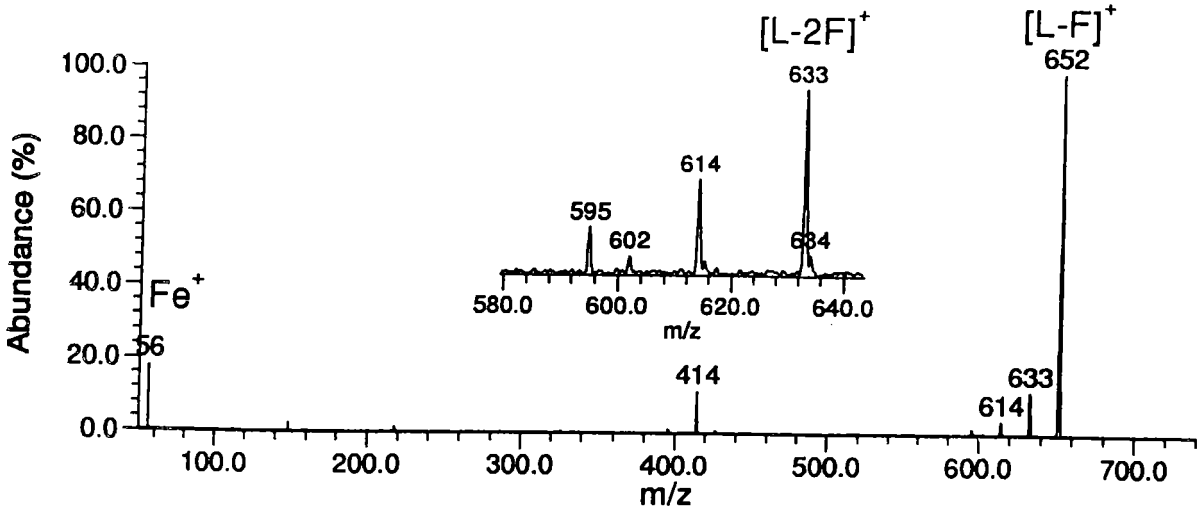

Figure III.3.5. Mass spectrum obtained after reaction of Fe^+ with PFTBA. Reaction time is 1s.

To explain the origin of the $[L-F]^+$ ion, we propose a mechanism of fluoride abstraction by the projectile ion:

$$M^+ + L \rightarrow [L-F]^+ + MF \quad (1)$$

Several primary (reagent) ion, with very different behavior towards PFTBA, led to the formation of the $[L-F]^+$ fragment. They are grouped in table III.3.3. according to their general reactivity.

Table III.3.3. Groups of metal ions that induce $[L-F]^+$ formation.

	Ions for which:	**M**
A	ML^+ was detected	Li, Na, Ni, Co, Cu, Zn,
B	No ML^+ was detected	Al, Fe, Mn, Ti, V, Si, B, Mo, Zr
C	ML^+ was detected (M^+ excited to form $[L-F]^+$)	Cr, Ca
D	No ML^+ was detected (M^+ excited to form $[L-F]^+$)	Mg, Sn
E	MF^+ detected	Ca, Si, (Mg, Sn)

We suppose that for the metal ions which form detectable ML^+ (group A in Table III.3.3.) the complexation occurs on the N atom (lone electron pair). From such

complexes, abstraction of fluoride (elimination of MF), analogous to hydride abstraction by Cu^+ reported by Sigsworth et Castelman[7] , can occur:

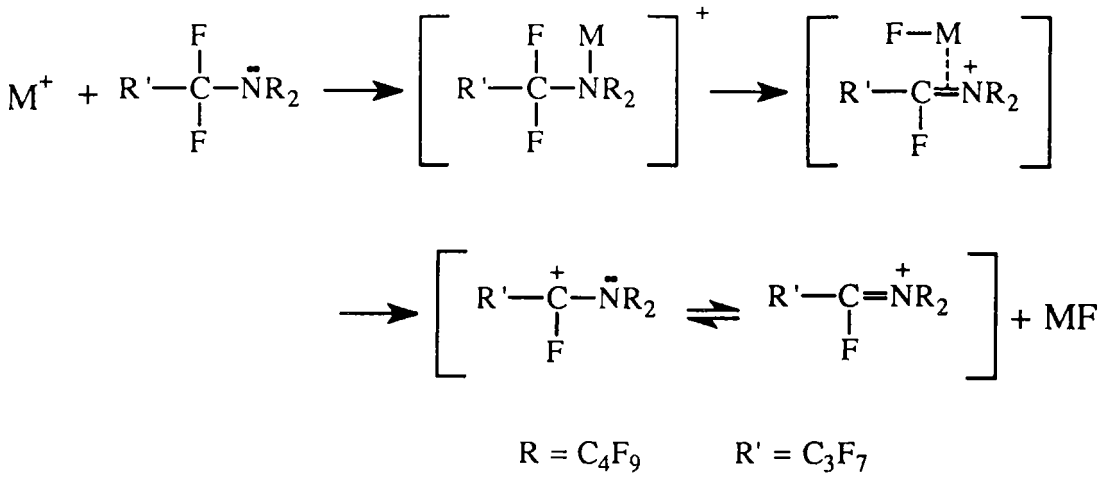

Figure III.3.6. Formation of $[L\text{-}F]^+$ (*m/z* 652) ion.

In order to support this mechanism, we isolated CuL^+ and tried to monitor their unimolecular decay. However, detectable CuL^+ ions seemed to be stable and gave no significant rise in fragment ions.

The formation of $[L\text{-}F]^+$ ion is the most strongly induced by metals for which ML^+ was not detected (group **B** in Table III.3.3.). These ions seem to be very reactive. Considering their $4s^1$ electronic configuration Ti^+, Fe^+, Mn^+ and Zn^+ are able to form one σ bond. Comparing the promotion energies for the formation of $4s^1$ configuration of first row transition metals, the order (of promotion energies, see Table III.1.1.) is as follows:

$$Fe^+ \sim Mn^+ \sim Zn^+ \sim Ti^+ < V^+ < Co^+ < Ni^+ \sim Cr^+ < Cu^+$$

The lower the promotion energy, the higher is the reactivity of the metal ion. For first row transition metal ions, the reactivity follows this order. Fe^+ and Zn^+ produced mainly $[L\text{-}F]^+$ (fluoride abstraction). However,the ions Mn^+, Ti^+ and V^+ produced in addition to $[L\text{-}F]^+$ a large number of fragment ions. While moving to the right side (Co^+, Ni^+, Cr^+ and Cu^+) more of adducts were detected. Thus, we cannot eliminate the possibility of M-F bond formation before the abstraction of fluoride.

For both proposed mechanisms (for group A: complexation on the lone electron pair of nitrogen; and for group B: attachment to F atom), the complex ML^+ should exist. It has been detected for group A ions only. For the reactions of B, C, and D

group ions, we can postulate the existence of a "short lived" transition state complex ion.

According to the Stevenson-Audier rule, MF has a lower ionization energy (E_i) than the [L-F] fragment if it takes a charge during the fragmentation of the transition complex.

Table III.3.4. Ionization energies (E_i) of studied elements and their fluorides.[18]

Metal	IE(M) / eV	IE(MF) / eV	IE(MF_2) / eV	IE(MF_3) / eV
Al	5.986	9.73 ± 0.1	8.1	15.45
Li	5.392	11.3	n.d.	n.d.
Na	5.139	n.d.	n.d.	n.d.
K	4.341	n.d.	n.d.	n.d.
Mg	7.646	7.68	(13.40)	n.d.
Ca	6.113	5.82-.7.0	n.d.	n.d.
Ti	6.82	n.d.	12.2± 0.5	n.d.
V	6.74	n.d.	n.d.	n.d.
Cr	6.766	n.d.	10.6± 0.3	12.5 ± 0.3
Fe	7.870	n.d.	11.3± 0.3	12.5 ± 0.3
Mn	7.435	8.3 ± 2	11.38 ± 0.2	12.57 ± 0.2
Co	7.86	n.d.	n.d.	n.d.
Ni	7.635	n.d.	n.d.	n.d.
Cu	7.726	10.15 ± 0.02	11.3-13.3	n.d.
Zn	9.394	n.d.	13.5	n.d.
B	8.298	11.12 ± 0.01	(9.4)	15.56 ± 0.03
Si	8.151	7.28	10.78 ± 0.05	(9.3)
Sn	7.344	7.04	(11.1)	n.d.
In	5.786	9.6 ± 0.5	n.d.	n.d.
Zr	6.634	n.d.	12.0± 0.15	n.d.
Mo	7.092	8.0 ± 0.3	9.0 ± 0.15	10.2 ± 0.5

n.d. = no data found

In the reactions of Ca^+, Si^+ ions, SiF^+ and CaF^+ are detected. Very few MgF^+, and SnF^+ (when Sn^+ ions were excited and then reacted with PFTBA) were also detected. From available data for ionization energies of MF (see Table III.3.4.) Ca, Sn, Si and Mg fluorides have the lowest IE (5.82-7.0; 7.04, 7.28 and 7.68 eV, respectively). From our results (and with respect to few data available), the ionization

energy of [L-F] can be estimated within the range from 7.69 to 8.0 eV. The upper limit of 8.0 eV is the E_i of molybdenum fluoride, and in Mo^+ reaction with PFTBA no MoF^+ was detected.

We can summarize, that the abstraction of fluoride from the PFTBA molecule (formation of $[L\text{-}F]^+$) is one of the dominate processes in positive ion/PFTBA reactions. At least two different mechanisms are involved: i) fluoride abstraction by the metal attached to the nitrogen lone electron pair and ii) fluoride abstraction through M-F bond formation. Moreover, for Fe^+ ion, the insertion in a C-F bond cannot be excluded, too.

3.3.4. Formation of $[L\text{-}F_2]^{+\cdot}$ ion

In the reactions of Mg^+ and Sn^+ ions with PFTBA, $[L\text{-}2F]^+$ ion (*m/z* 633) is mainly produced. Its negative analog is the main product in negative -laser induced-electron ionization of PFTBA (chapter IV). The spectrum resulting from Sn^+/PFTBA reaction is shown in Figure III3.7.a.(the Mg^+/PFTBA spectrum is given in Appendix B).

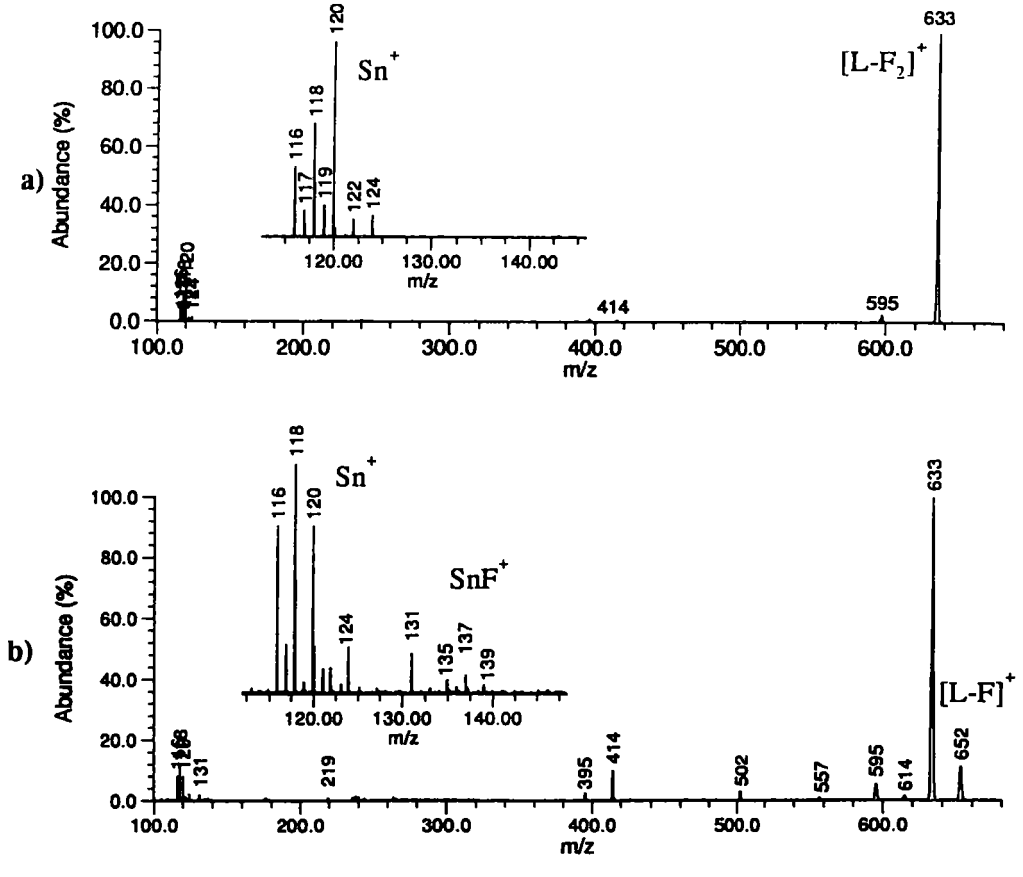

Figure. III.3.7. Mass spectra of Sn^+/PFTBA reaction: a) standard reaction, b) ^{120}Sn ion was excited prior to reaction with PFTBA (see III.5) and thus $[L\text{-}F]^+$ ion was formed. Insets show isotopic distribution of Sn^+ and formed SnF^+ ions.

Beside Mg^+ and Sn^+ ions, Ti^+, V^+, Mn^+ and Fe^+ produce $[L\text{-}F_2]^+$ ion as well, but in much lover abundance. The Fe^+ ion induces formation of $[L\text{-}F_2]^+$ions beside mainly produced $[L\text{-}F]^+$. Continuous ejection of $[L\text{-}F]^+$ in Fe^+ reaction, proved that $[L\text{-}F_2]^+$ is **not** its daughter ion. Formation of $[L\text{-}F_2]^+$ is flagrant process for Mg^+ and Sn^+ reactions with PFTBA. We suppose formation of MF_2 neutral product:

$$M^+ + L \rightarrow [L - F_2]^+ + MF_2 \qquad M = \mathbf{Mg}, \mathbf{Sn}, Ti, V, F \text{ and } Mn.$$

Oxidation process was already found to dominate the chemistry of Mg^+ with some organic chlorides. Upall et al. [12] reported formation of neutral Mg(II) products in the reactions with CCl_4 and CH_2ClCH_2Cl. Ti^+ formed TiF_2 in the reaction with CCl_2F_2.[13]

To explain formations of $[L\text{-}F_2]^+$ and $[L\text{-}F]^+$ ions for the certain ion reactions, we compared the enthalpies of formation of gaseous MF and MF_2.

Table III.3.5. Enthalpies of formation (Δ_fH) and the Gibbs energy of formation (Δ_fG) of metal fluorides.[19] (n.d = no data found)

	MF		MF_2		MF_3	
M	Δ_fH (kJ/mol)	Δ_fG (kJ/mol)	Δ_fH (kJ/mol)	Δ_fG (kJ/mol)	Δ_fH (kJ/mol)	Δ_fG (kJ/mol)
Li	-340.9	-361.7	n.d	n.d	n.d	n.d
K	-326.7	-344.8	n.d	n.d	n.d	n.d
Na	-290.4	-309.8	n.d	n.d	n.d	n.d
Ca	-272.3	-298.2	-784.5	-793.3	n.d	n.d
Al	-265.7	-291.2	-695.0	-704.8	-1209.3	-1192.7
Mg	-236.8	-262.8	-726.8	-733.0	n.d	n.d
In	-193.7	-216.7	-477.5	-486.8	-857.7	-842.2
B	-115.9	-143.7	-589.9	-601.4	-1136.6	-1119.9
Sn	-95.1	-121.6	-483.9	-492.3	n.d	n.d
Ti	-66.9	-98.3	-688.3	-694.9	-1188.7	-1175.7
Si	-20.1	-51.6	-587.9	-598.3	-1085.3	-1073.2
Cu	-12.5	-39.9	-266.9	-276.2	n.d	n.d
Ni	104.6	72.3	-335.6	-347.6	n.d	n.d
Zn	n.d	n.d	-494.5	-497.5	n.d	n.d
V	n.d	n.d	n.d	n.d	-1297.0	-1226.7
Co	n.d	n.d	-356.477	-369.947	n.d	n.d
Fe	n.d	n.d	-389.53	-400.055	-820.90	-812.8
Mn	n.d	n.d	-531.368	-542.599	n.d	n.d

The enthalpies are listed in the Table III.3.5. For the Cr, no data were disponible.

The enthalpies of MF and especially MF_2 formation are very negative and formation of those product is very exothermic. Nevertheless, the formation of all products and differences in ion reactivities cannot be completely explainable from this data.

Beside the basic ion $[L\text{-}F_2]^+$ ion, *m/z* 633, its daughter fragment $[L\text{-}2F_2]^+$ ion *m/z* 595, has also been observed. Its abundance is very weak and it appears *via* defluorination of the $[L\text{-}F_2]^+$ ion:

$$[L-F_2]^{+\cdot} \rightarrow [L-2F_2]^{+\cdot} + F_2.$$

Excited (cyclotron motion) Sn^+ ion produces some $[L\text{-}F]^+$ and SnF^+ ions. There is a competition between $[L\text{-}F]^+$ and SnF^+ to keep the charge (see the end of 3.3.2.)

3.3.5. Formation of LMF^+ complexes

For the calcium ion reactions with PFTBA, $[L+CaF]^+$ ions were detected. The corresponding mass spectrum is displayed in Figure. III.3.8.

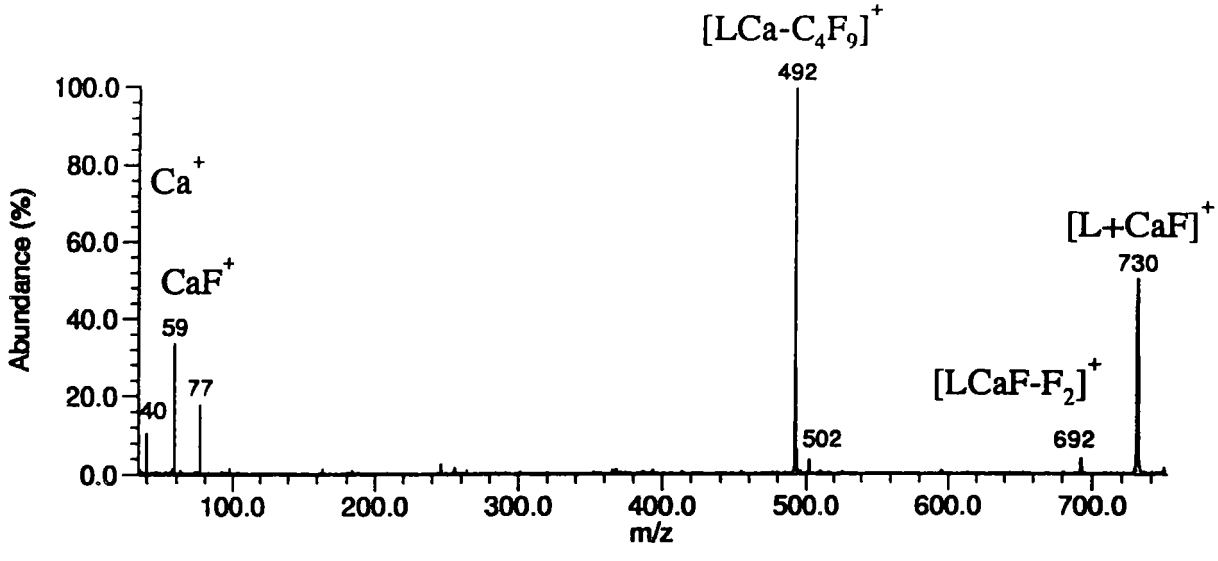

Figure III.3.8. Mass spectrum of Ca^+ reaction with PFTBA

Calcium ion has quite a particular reactivity with PFTBA. It was already mentioned in 3.3.2. that ions CaF^+ were detected. According to their low ionization energy, they keep the charge during the fragmentation of the unstable CaL^+ complex.

CaF^+ subsequently reacts with the neutral molecule to form the $CaFL^+$ complex:

$$CaF^+ + L \rightarrow CaFL^+$$

This mechanism was confirmed by continuous ejection of CaF^+: no adduct was observed.

3.3.5.1. Formation of [LM - F]+

Calcium is the only studied ion which in the reaction with PFTBA produced $[LM-F]^+$. The formation of this ion can be explained by elimination of F_2 from the $CaFL^+$ complex:

$$CaFL^+ \rightarrow [CaFL - F_2]^+ + F_2 .$$

3.3.6. Formation of $[L+M-C_4F_9]^+$

The remaining metal containing ion in the Ca^+ spectrum is $[L+M-C_4F_9]^+$. Such ions were detected only for Ca^+ and Co^+ reactions with PFTBA. The mass spectrum resulting from reaction of Co^+ with PFTBA is displayed in Figure III.3.9.

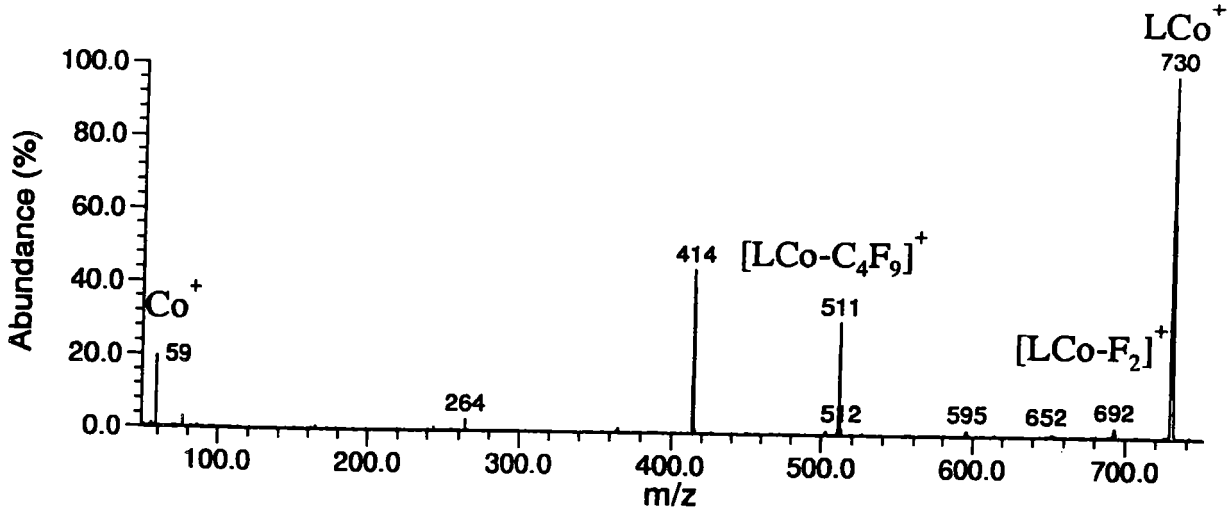

Figure III.3. 9. Mass spectrum Co^+ + PFTBA

The reaction leading to this product should involve metal insertion into a C-N bond. In a previous study of Co^+ reactions with amines,[5] the authors have found that

Co^+ does not insert in C-N bond of primary and secondary amines, but *does* insert into C-N bond of the tertiary (trietyl) amines. This mechanism can be involved in our case:

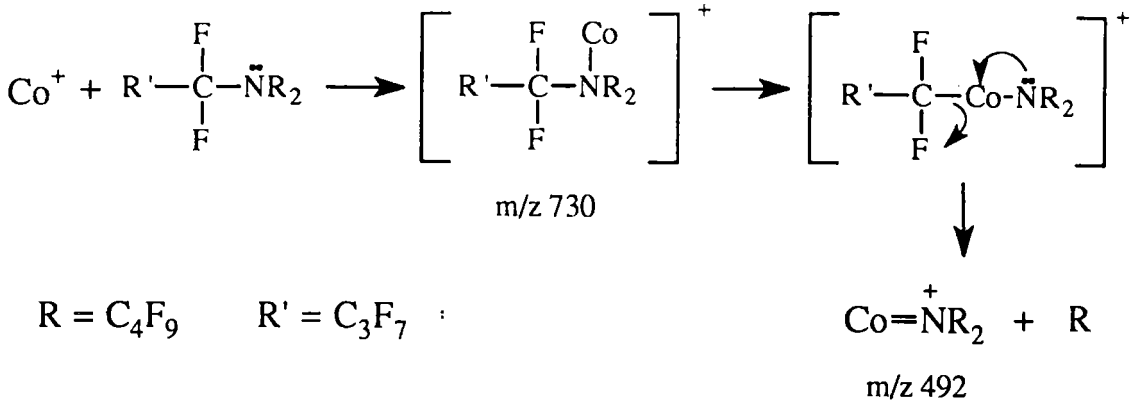

Figure III.3.10. Mechanism of insertion of a metal ion in the C-N bond.

3.3.7. Reactions of metal ions from an alloy

Stainless steel (Fe, Ni, Cr) was used as a laser target for the simultaneous production of Cr^+, Fe^+ and Ni^+. Those ions were left to react with PFTBA. The resulting spectrum is shown in Figure III.3.11.

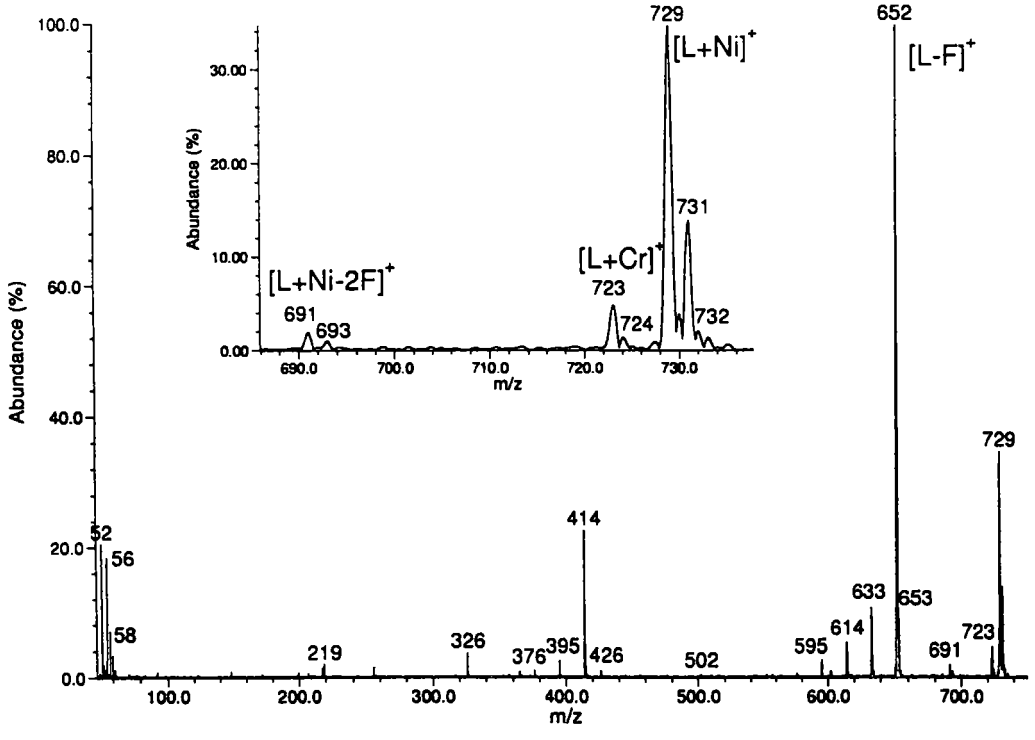

Figure III.3.11. Mass spectrum after reaction of stainless steel ions (Cr^+, Fe^+ and Ni^+) with PFTBA.

The metal ions kept their individual reactivity. Ni^+ and Cr^+ form mainly adduct ions, while Fe^+ induce formation of $[L\text{-}F]^+$ ion. In the alloy experiment, the initial quantities of ions were not the same and thus it is not surprising that the highest abundance ion is an Fe^+ induced product. But, it is interesting that even if we coadd the spectra obtained after their individual reactions, the resulting summing spectrum is very much alike the presented one. It means that for a same starting quantities of ions and neutral molecules, and the same given reaction time, Fe^+ will produce more of the detectable products than nickel and Cr^+. Abundance of Cr^+ products is lower than that of Ni^+ products. Those results (qualitatively) support the order of reactivity (Fe > Ni > Cr) established by Allison and Radecki [3] towards primary amines (III.1).

3.4. Conclusion

Studied positive reagent ions react differently with PFTBA. Some of observed mechanisms (adduct formation, fluoride abstraction...) can be explained with their promotion energies (concerning transition metal ions).

Ti^+, Si^+, V^+, B^+, Zr^+ or Mo^+ ions induced high fragmentation of PFTBA. We cannot exclude that produced ions were kinetically excited.

Earth -alkaline metal ions (Mg^+ and Ca^+) did not form the same type of product, as it was the case in the reactions with acetophenone. Sn^+ is found to react as Mg^+, while for the reactions of Co^+ with PFTBA the same type of ions was observed as for Ca^+ ions. Enthalpies of formation of $[L\text{-}F]^+$ and $[L\text{-}F_2]^+$ are negative for most of ions and thus reactions are exothermic.

There is still need for a better understanding of involved mechanisms in positive ion- PFTBA reactions.

References are on the page 103, after chapter III.7.

III.4. Reactions with Tributylamine (TBA). Comparison with PFTBA

For a better understanding of PFTBA reactions with different elemental positive ions, comparative reactions with its hydrogenated analog, tributylamine (TBA, $[CH_3(CH_2)_3]_3N$) have been studied.

Preliminary results have been obtained. In these experiments, the following elements were tested: Al, V, Ti, Mg, and Sn. The resulting ions are grouped in Table III.4.1.

Table III.4.1. Approximated relative intensities of products of Al, Ti, Mg, and Sn (M) ions with TBA (L).

	Al^+	Mg^+	Sn^+	*Ti^+
Short reaction time products				
LM^+	90	100	20	15
$[L+H]^+$	20	5	5	50
L^+	-	95	-	5
$[L-H]^+$	100	80	100	80
Long reaction time products				
LM^+	-	-	-	-
$[L+H]^+$	100	100	100	100
L^+	-	-	5	-
$[L-H]^+$	30	35	100	20

*For the Ti^+ reaction ion *m/z* 171 that contain Ti is the basic detected product.

In this case, and unlike what was observed in PFTBA reactions, the reaction time plays an important role. At short reaction time adduct ions are detected. With longer reaction time the formation of $[L+H]^+$ becomes dominant. The molecule has a high proton affinity (982 $kJmol^{-1}$).

3.4.1. Charge transfer

TBA has lower ionization energy (7.4 eV) than most of the ions studied in PFTBA experiments. Thus, charge transfer is expected to be primary ionization mechanism for the ionization of the molecule. This was indeed observed in Mg^+ -TBA reaction (E_i(Mg) = 7.5 eV) as can be seen on the spectrum from Figure III. 4.1. However, other ions studied in the reactions with TBA have lower E_i than TBA (see Table III.3.4.

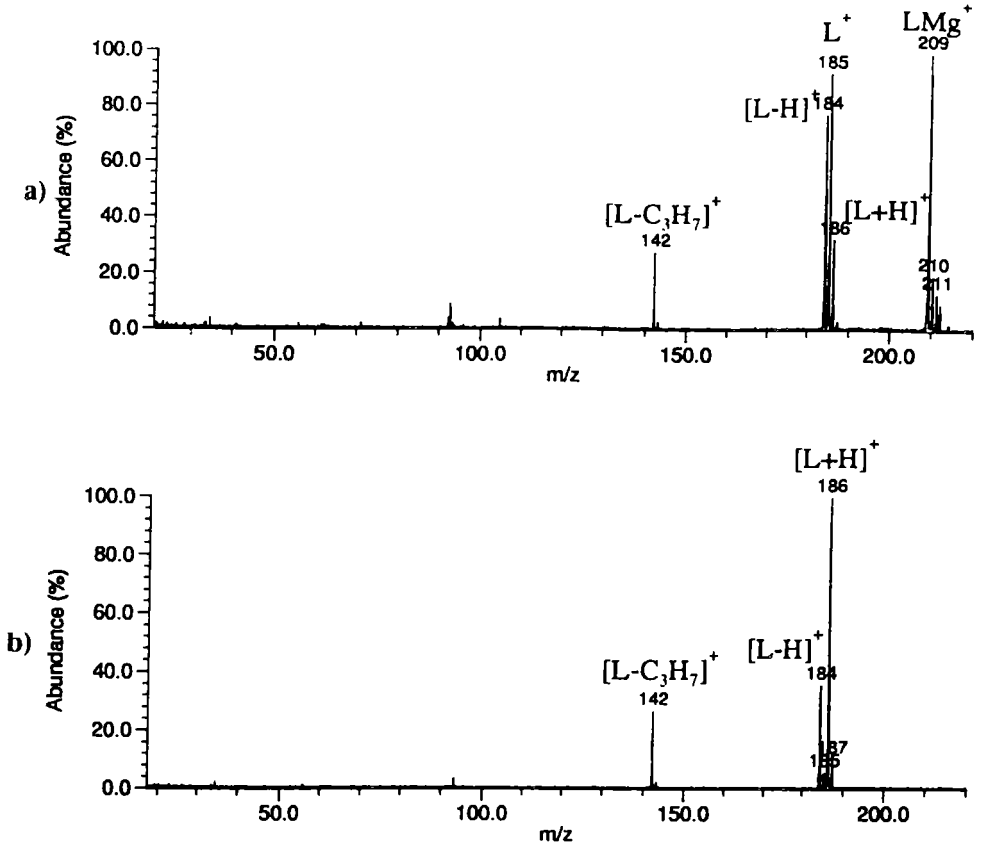

Figure III.4.1. Mass spectra after reaction of Mg^+ with TBA: a) delay 0.2 s; b) 10 s.

The molecular ion is the main product. Besides, an adduct ion LMg^+ is detected. With longer reaction time, formation of protoneted species $[L+H]^+$ is favored.

3.4.2 Hydride abstraction

Hydride abstraction from TBA by all studied ions has been observed. In the case of Al^+, peak that corresponds to he $[L-H]^+$ ion appears in the spectrum after 10 ms. At a reaction time longer than 1 s, $[L+H]^+$ ion always becomes dominant. Ion LM^+ disappears. The process is obvious from the mass spectra in Figure III.4.2.

3.4.3. Other reactions

Cationization by metal ion (formation of adducts) occurs immediately, as one of the first processes, at the same time as $[L-H]^+$ formation.

Protonation of TBA molecule becomes the main process with longer reaction time.

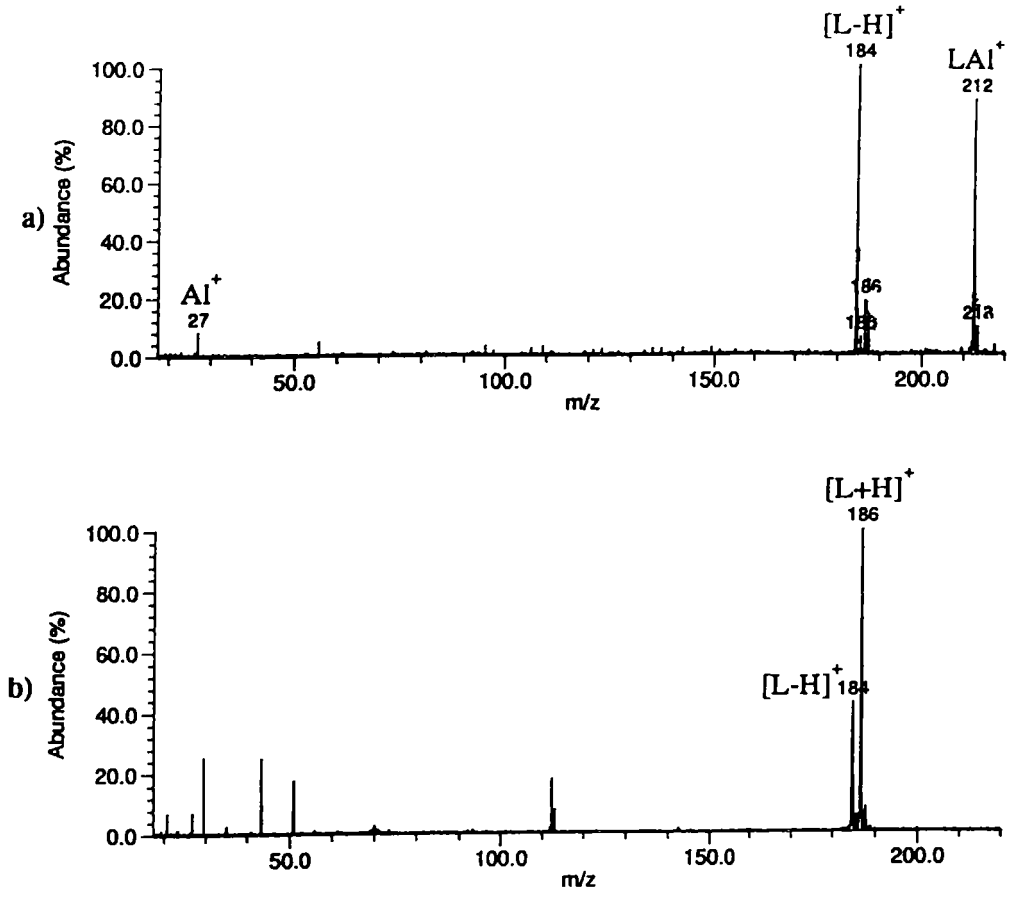

Figure.III.4.2. Mass spectra of Al^+-TBA reactions: a) reaction delay 0.2 s, and b) 10s delay .

3.4.4. Conclusion

Reactions of PFTBA cannot simply be compared with TBA reactions. Even if amino aspect of molecule should play certain role in involved mechanisms, there is big difference between H and F. Reactions of TBA should been done with some more representative ions.

III.5. Internal Ion Impact Ionization

In chapter III.3. we have shown that different levels of PFTBA molecule fragmentation were observed for different projectile ions. It would be desirable to have a possibility to control the fragmentation of the molecule. A classical method to fragment ions is collision-induced dissociation (CID). To perform CID in FT-ICRMS, it is advisable to isolate a parent ion from other ions in the trap. Once selected, the parent ion may then be excited to a larger ICR orbit to speed it up and increase its likelihood for dissociation. The total radial (xy) kinetic or translational energy, T(J), of an ion is given by equation (1)[20-22]

$$T = \frac{m}{2}\omega^2 r^2 = \frac{q^2 B^2}{2m} r^2 \qquad (1)$$

in which m is mass of the ion, ω is the cyclotron frequency, r is the radius, q is the ion's electrostatic charge and B is the magnetic field strength. From eqn (1), a singly charged ion of m = 1000 u in a 3.0 T magnetic field at a radius of 1cm has 43 eV of translational energy. However, only a small fraction of this energy is available in the center-of-mass frame, E (c.m.)[23]

$$E(\text{c.m.}) = T\frac{m_t}{m_p + m_t} \qquad (2)$$

in which m_t is the mass of the target collision CID gas and m_p is the mass of the excited parent ion. Thus, for CID of a singly charged ion of 1000 u with argon gas, the center-of-mass frame energy is only 1.7 eV. Such a low center-of-mass frame energy is too low to produce extensive fragmentation. Thus, as a consequence of equat. (1) and (2), collision-induced dissociation is limited in conventional FTMS because only relatively low laboratory-frame and center-of-mass frame energy can be accessed by heavy singly charged ions (> 500 u), compared to sector instruments.[24] Another disadvantage is the increase of pressure with introduction of collision gas. This can be especially inconvenient for a possible calibration experiments, where sample should be in the chamber at the same time as the calibrant (PFTBA).

Schweikhard et al.[25] proposed a method for accessing very high translational and center-of-mass frame energy by means of excitation of the cyclotron motion of high cyclotron frequency (low mass-to-charge ratio) ions in the presence of neutral species. They proposed that the low mass-to-charge ratio ions formed by any standard ionization technique (EI, CI, LD) could act as projectile to ionize the neutral species while depositing considerable energy leading to dissociation. They called this technique "Internal Ion Impact Ionization" (IIII) (Figure III.5.1).

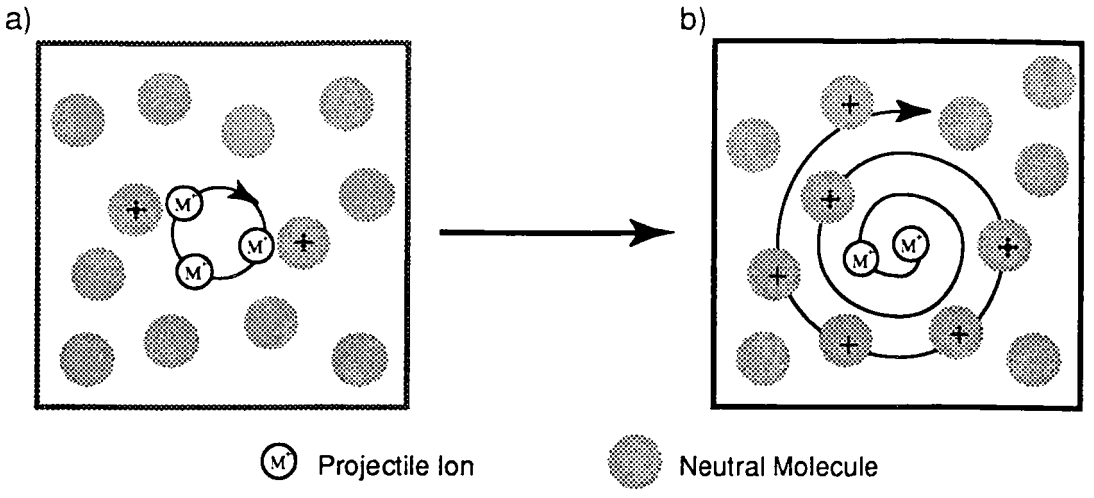

Figure III.5.1. Pictorial representation of internal ion impact ionization process. a) Projectile ions (M^+) formed by LD are in their ICR orbits, b) the cyclotron motion of the projectile ions is excited, ionizing neutrals in the trap. (adapted from ref. 24)

According to eq.(1), an Al^+ projectile ion (27 u) excited to a cyclotron orbit of 1.0 cm in a 3.0 T magnetic field has a translation energy of ~ 1600 eV. The kinetic energy in the center-of-mass frame in a collision between Al^+ and a neutral species (671 u) is ~ 1540 eV, because the projectile ion has a low mass and the target neutral high mass. Projectile ions with excited cyclotron motion, thus, serve for an ionization and subsequent dissociation of neutral molecules in FTMS. The technique is similar to the original ICR technique of pulsed ion double resonance[26] later extended to FT-ICR-MS[27,28], in which ions are excited in presence of neutrals to induce endothermic ion-molecule reactions.

In our case, similar experiments were performed with all projectile ions which have not produced significant fragmentation of PFTBA molecule. Those are Al, Mg, Ca, Cr, Mn, Fe, Co, Cu, Zn and Sn ion. The results of the excitation of Al^+ ions and subsequent ionization and fragmentation of PFTBA molecules are shown in Figure III.5.2. The spectra resulting from other ions are given in **Appendix B**. The fragment ion with lowest mass-to-charge ratio detected in Al^+ - PFTBA reaction (without Al^+ excitation) is around *m/z* 250 (Figure III.5.2.a). The main product is $[L-F]^+$ ion. There are some low intensity fragment ions as well.

In next experiment, isolated Al^+ projectiles were excited at their cyclotron frequency (1.731 MHz) with an RF amplitude of 110 Vpp, for 8 ms. The delay period after excitation was 1 s. Excited aluminum ions passing through clouds of heavy neutrals or ions induce their ionization and significant fragmentation. The resulting spectrum is shown in Figure III.5.2.b.

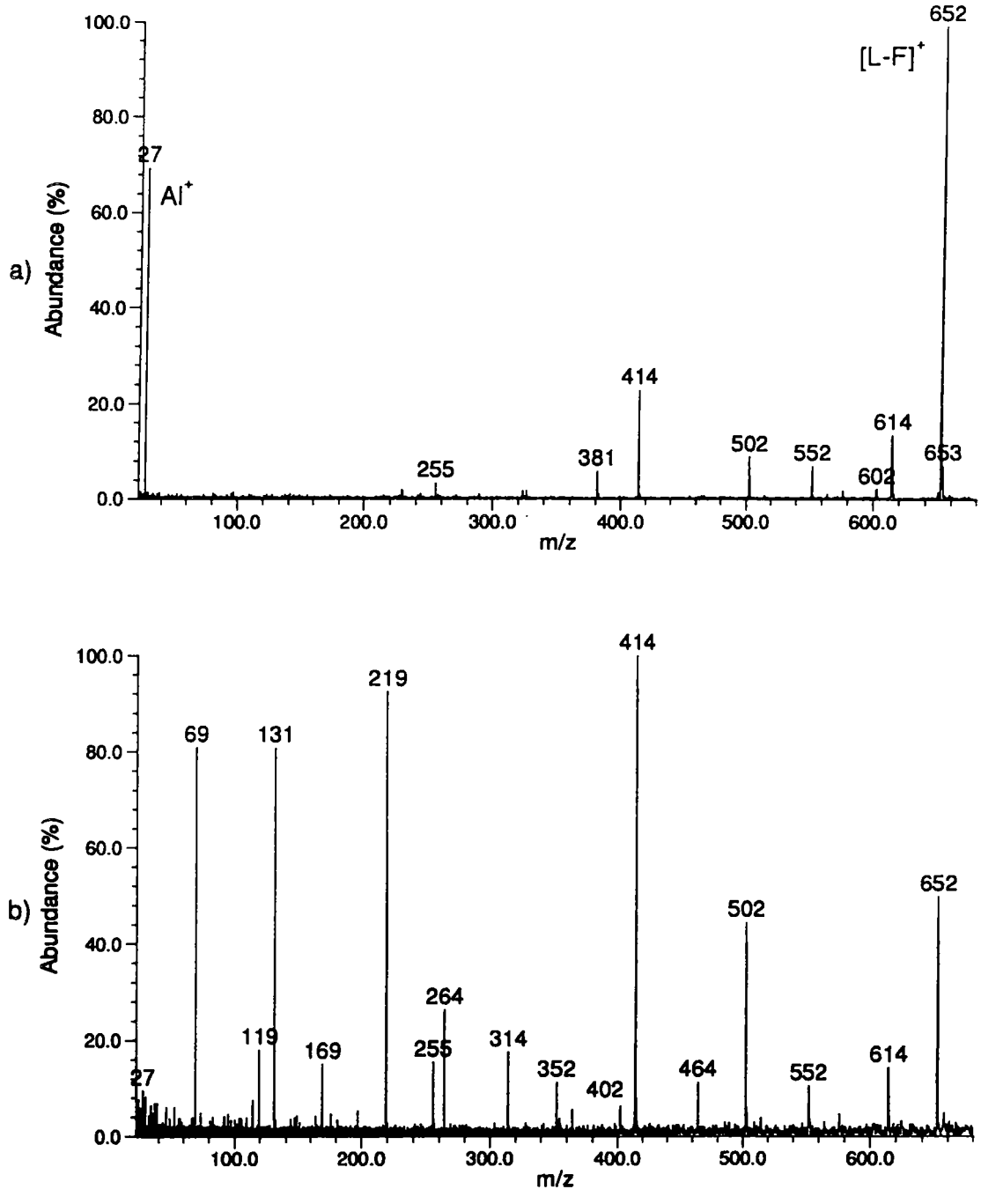

Figure III.5.2. Positive ion FT-ICR mass spectra of the products of the Al^+ reaction with PFTBA (L), a) without prior Al^+ excitation, b) with excitation of cyclotron motion of the projectile Al^+ ions. Delay before broadband excitation was 1.0 s in both cases. Assignation of fragment ions is given in Table III.3.1.

Even better example of control of the fragmentation rate of PFTBA can be seen from Ca^+ experiment shown in Figure III.5.3. The ions resulting from the reaction of Ca^+ ions with PFTBA without prior excitation of Ca^+ cyclotron motion are mainly

metal containing ions and almost no PFTBA fragment is detected (Figure III.5.3.a.).

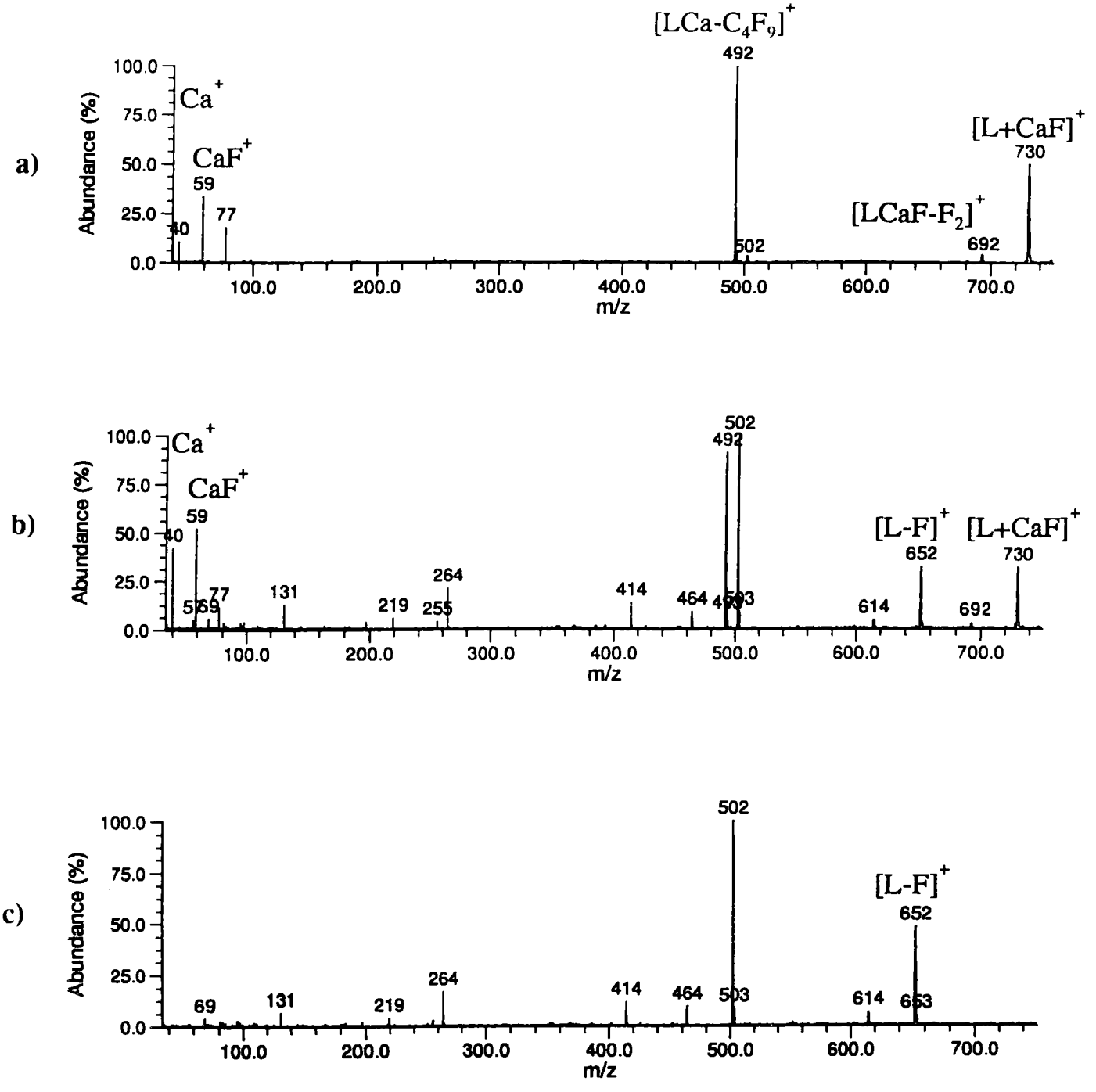

Figure III.5.3. Mass spectra of Ca^+-PFTBA 1 s reaction products, a) no excitation of Ca^+, b) "soft" excitation of Ca^+ and c) "hard" excitation of Ca^+ ions.

If the cyclotron motion of Ca^+ ions were excited prior to reaction with PFTBA. (1.16932 MHz) with an RF amplitude of 0.1 Vpp, for 100 ms, product ions shown in Fig b were detected. The metal-atom containing ions are still present, and the PFTBA fragment ions appeared as well. When the ions are excited "strongly" (RF amplitude of 110 Vpp, for 8 ms), only PFTBA fragments were detected. We can see that by tuning

the conditions of excitation of the projectile ion, a stronger fragmentation was induced.

In the cited work,[24] N_2 was ionized by EI in a cloud of PFTBA. Surprisingly few low mass PFTBA fragments beside the N_2^+ ion were detected. After the isolation of N_2^+ projectile ion and the excitation at its cyclotron motion, more PFTBA fragment ions were produced as shown in Figure III.5.4. copied from the cited reference.

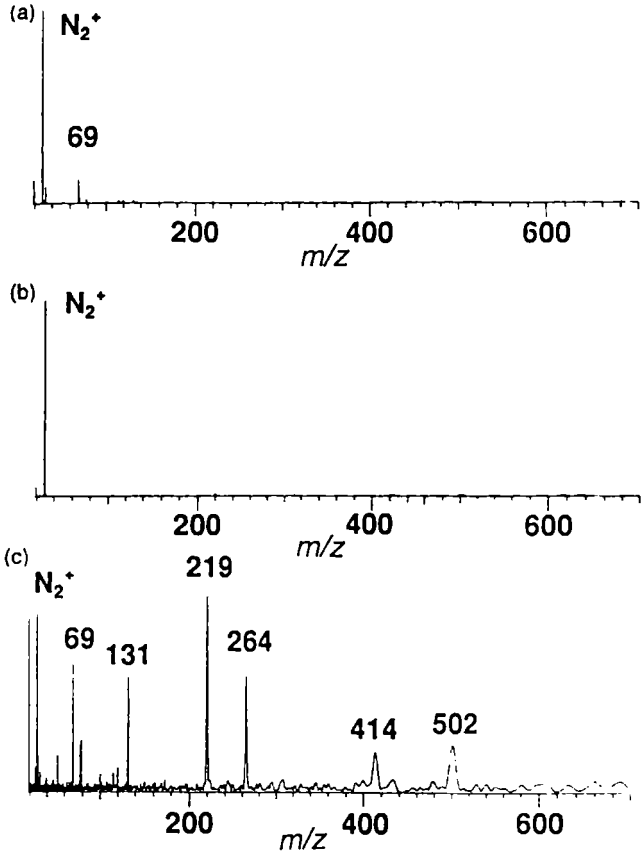

Figure III.5.4. (a) EI of PFTBA and air in source trap at 5 10^8 Torr. (b) all ions below 1.55 MHz are ejected from the trap by double-resonance, leaving N_2^+ ions. (c) Excitation of cyclotron motion of the projectile ions thorough a cloud of PFTBA ionizes PFTBA by the IIII process (from ref. 24)

Comparing these results with ours, we can conclude that ionization and fragmentation of neutral molecule can be well controlled in the case of projectile ions produced by laser ablation. Without changing pressure conditions a molecule can be "softly" ionized or very "hardly" ionized and fragmented. Mass spectra containing known adduct ions (ML^+, up to *m/z* 740) and well defined PFTBA fragment ions as well as some metal ions provide a mass range (*m/z* ~ 20-740) for calibration even broader than PFTBA in EI experiments(*m/z* 69-502).

III.6. Application of Positive Ion CI to some other polyhalogenated compounds

From the studies of PFTBA reactions with primary positive ions, we learned that the molecule can be ionized in different ways depending on the reagent ion. Different processes, from cationization to strong fragmentation were observed. In the case of PFTBA, information from detected ions kept specificity of the molecule. Thus, we wanted to enlarge our study by applying the (chemical) ionization by laser-plasma generated positive ions to some other polygalogenated molecules, namely: halothane, dichlorodifluoromethane and endosulfane. The molecules differ in their size, their physical state, but all are sufficiently volatile in our experimental conditions (ultra high "vacuum").

Table III.6.1. Studied compounds and some experimental conditions

Molecule	λ / nm	Projectile ion	Vapor pressure/kPa
Cl_2CF_2	355	Al, Na, Cu	651.0 (25°C)
$BrCHClCF_3$	355	Al, Na	39.9 (25°C)
$C_9H_6SO_3Cl_6$	355, 248	Al	0.0012 (80°C)

6.1. Positive ion CI of Dichlorodifluoromethane

Sodium chloride, metal aluminum and copper samples were irradiated by 355 nm laser beam (E = 10^8 W cm^{-2}) for the production of projectile ions. They were isolated and dichlorodifluoromethane (Cl_2CF_2, Mw = 120 u) was introduced in the chamber. The mass spectrum obtained after Al^+ ionization (reaction) of dichlorodifluoromethane is shown in Figure III.6.1.

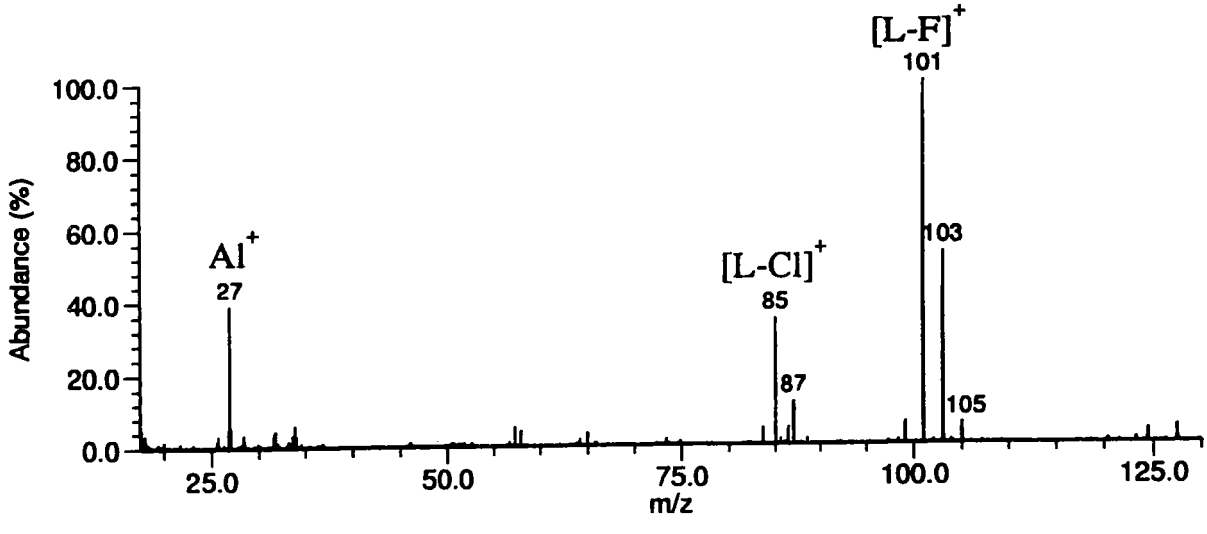

Figure III.6.1. Mass spectrum of CCl_2F_2 ionized in reaction with Al^+.

The ions detected in reactions with the three selected reagent ions are listed in Table III.6.2.

Table III.6.2. Relative intensities of detected products in ionization of dichlorodifluoromethane (in %)

M	L^+ *m/z* 120	$[L-F]^+$ *m/z* 101	$[L-Cl]^+$ *m/z* 85
Al	-	100	50
Cu	-	50	100
Na	-	5	100

As it can be seen from the table, no molecular ion was ever detected. The observed fluoride transfer in the case of Al^+:

$$Al^+ + Cl_2CF_2 \rightarrow Cl_2CF^+ + AlF$$

is in agreement with expectations based on the relative fluoride affinities. Bond strengths and enthalpies of formation MX are listed in Table III.6.3. They can be compared with dichlorodifluoromethane bond strengths (Table III.6.4.).

Table III.6.3. Enthalpies of formation and bond strength of MX (M = Al, Na, Cu; X = F, Cl)[18]

	AlCl	AlF	NaCl	NaF	CuCl	CuF
Δ_fH/ kJ mol^{-1} (298.15K)	-51.5	-265.7	-181.4	-290.5	91.2	-12.6
D°(M-X) /kJ mol^{-1} (298.15K)	448	663.7	412.7	519	382.9	413 ± 13

Table III.6.4 Bond strengths in Cl_2CF_2 [17b]

Bond	**$D°_{298}$ / kJmol^{-1}**
F-$CFCl_2$	460 ± 25
Cl-$CClF_2$	318 ± 8

The same tendency was expected for Cu and Na as well but formation of CuCl and NaCl domin ated over NaF and CuF formation. Nevertheless, aluminum has the highest affinity towards F.

6.2. *Positive ion CI of Halothane*

Aluminum and NaCl were used as targets for a formation of Al^+ and Na^+ projectile ions (λ = 355 nm, E = 10^8 W cm^{-2}). After the introduction of halothane ($BrCHClCF_3$, Mw = 198 u) molecules, and their reaction, the positive ions were detected. Representative spectra are presented in Figure III.6.2.

In the case of Al^+, molecular ion of halothane is the main product. When Na^+ was used as reagent ion, L^+ was also detected but in lower abundance. The main product was $[L-Br]^+$.

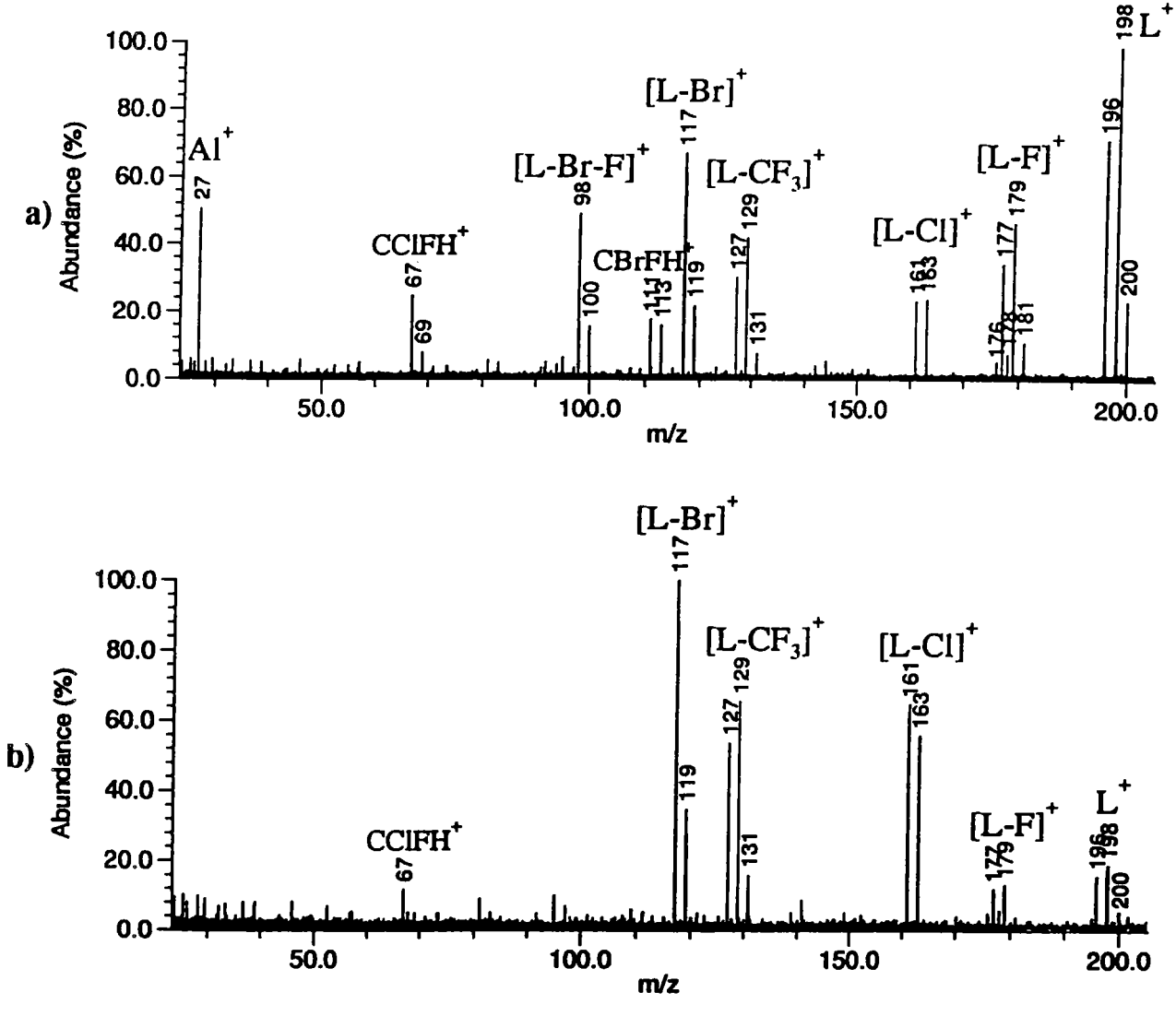

Figure III.6.2. Mass spectra of halothane ionized by a) Al^+ and b) Na^+.

There can not be simple charge transfer from Al^+ and Na^+ to halothane

molecule since their ionization potentials are much lower than halothane E_i (Table III.6.5).

Table III.6.5. Ionization energies (E_i) of halothane and reagent elements[18b]

	$BrCHClCF_3$	Al	Na
E_i /eV	11	5.986	5.139

Br-C is the weakest bond in halothane (274.9 ± 6.3 $kJmol^{-1}$)CRC and is easily broken. Br^- and $[L-Br]^+$ are the most abundant detected fragments in negative and positive mode, respectively. Comparing the relative intensities of detected $[L-F]^+$ and $[L-Cl]^+$ ions in dichlorodifluoromethane and halothane spectra, we observe that Al^+ induces more of $[L-F]^+$ formation, while Na^+ induces more of $[L-Cl]^+$. Bond strengths of diatomic molecules are listed in table III.6.6.

Table III.6.6. Bond strengths in diatomic molecules.[18b]

Bond	$D°_{298}$ / $kJmol^{-1}$
C-C	607 ± 21
C-Cl	397 ± 29
C-Br	280 ± 21
C-F	552
C-H	338.32

6.3. Positive ion CI of Endosulfane

Endosulfane powder sample was deposited on a part of the solid sample probe. After the introduction of the probe inside the spectrometer, endosulfane evaporated continuously. The pressure in the chamber was $3 \cdot 10^{-8}$ Torr. Endosulfane was then available in the gas phase for reaction with the laser-produced ions. On another part of the sample holder, an aluminum sample was mounted. Aluminum was irradiated by 355 nm laser beam (E = 10^8 W cm^{-2}) to form projectile ions. The spectrum detected after 1s reaction time is shown in Figure III.6.3.a.

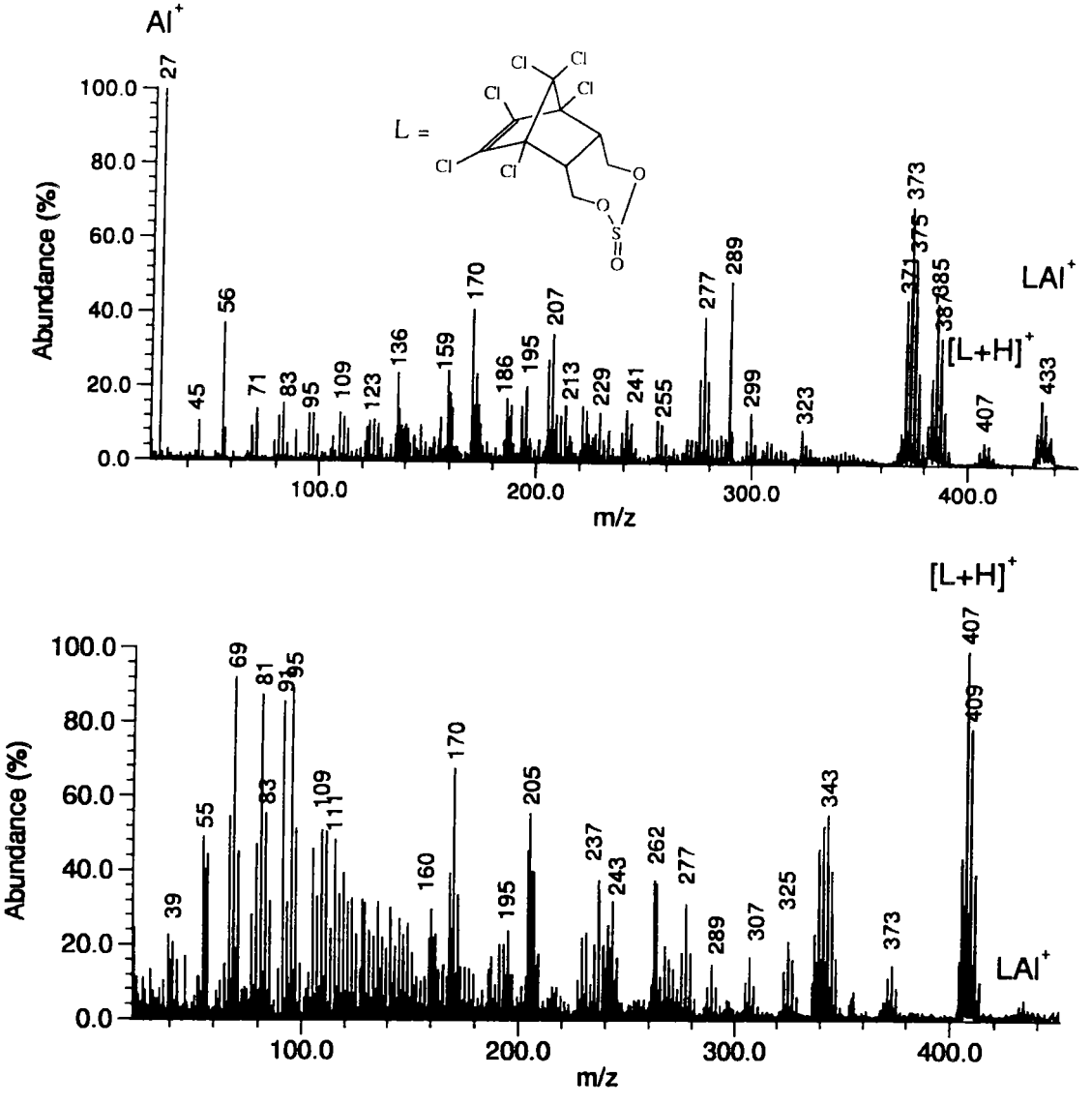

Figure III.6.3. Spectra obtained after Al^+ reaction with endosulfane: a) in a standard reaction; b) in reaction with excited Al^+ ion.

From the spectra we can see that "standard" reaction produce more important quantity of adduct ions, while reaction with excited ions yielded more molecular (protonated) ions.

Table III.6.7. Assignation of some detected positive ions in mass spectrum of endosulfane (L).

m/z	Assignation	Elemental composition
431-449	$[L+Al]^+$	$[C_9H_6SO_3Cl_6Al]^+$
405-413	$[L+H]^+$	$[C_9H_7SO_3Cl_6]^+$
404-412	$\mathbf{L^+}$	$\mathbf{[C_9H_6SO_3Cl_6]^+}$
369-377	$[L-Cl]^+$	$[C_9H_6SO_3Cl_5]^+$
305-311	$[L-Cl-SO_2]^+$	$[C_9H_4OCl_5]^+$

The ions were assignated after the calibration with PFTBA as internal calibrant, which is explained below.

6.4. Conclusion

Volatile organic polyhalogenated samples (either solid, liquid or gaseous) were ionized by positive ions produced by laser ablation. Halothane and endosulfane yielded molecular ion, while dichlorodifluoromethane reacted by halide transfer mechanism.

III.7. Calibration with PFTBA as internal calibrant

For precise assignation of detected organic molecular and fragment ions an internal calibration procedure is recommended. We searched for a calibrant adapted to halogenated molecules that can be used in laser induced experiments.

PFTBA molecule (as already well known calibrant in EI MS) with its well defined fragments could be used in internal calibration of halogenated molecules. We have shown in III.5. that PFTBA molecule could be ionized and highly fragmented by internal ion impact ionization with Al^+ ion produced by laser ablation (Figure III.5.2.). This method has been further applied for internal calibration of endosulfane sample.

Simultaneous ionization of studied molecule and PFTBA molecule should be achieved. It was important to introduce adequate amount of PFTBA molecule in the chamber: sufficiently to produce PFTBA signals, and not to much to allow ionization of endosulfane. Endosulfane sample was evaporating from the solid sample in the chamber and PFTBA was introduced by the batch inlet to a pressure of $5 \cdot 10^{-8}$ Torr. The laser pulse was directed to an aluminum target, the cyclotron motion of Al^+ ion was excited and during a delay of 100 ms both molecules were ionized and fragmented. The spectrum resulting from this experimental sequence is shown in Figure III.7.1.

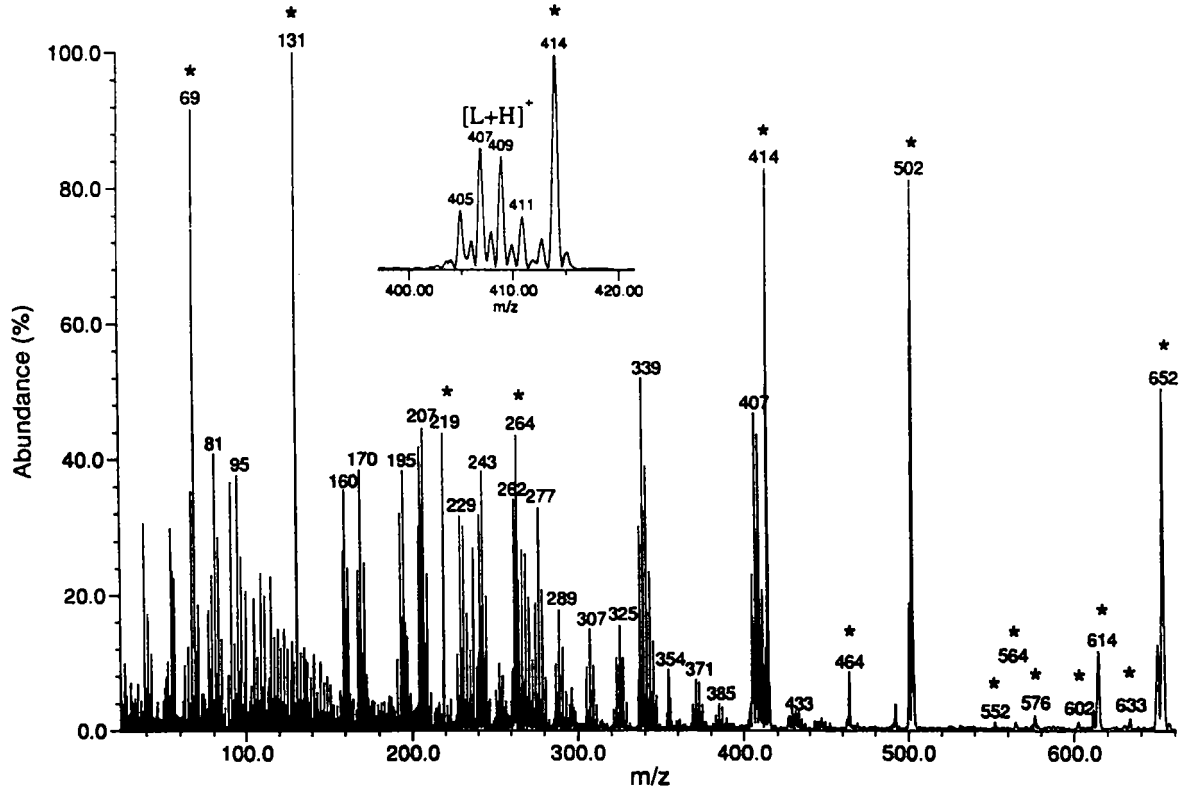

Figure III.7.1. Mass spectrum of positive ions of endosulfane with PFTBA as internal calibrant. PFTBA fragment ions are marked with *.

Series of well known PFTBA fragments and ions have allowed the calibration through the mass range of endosulfane sample. Calibration accuracy of 10 mu (ca. 4 ppm) has been achieved. Assignation of detected peaks is already given in the Table III.6.6. Calibrated spectrum has allowed the assignation of endosulfane signals.

Those results show that PFTBA is an adequate calibrant for polyhalogenated molecules ionized by laser produced metal ions

8. Conclusions

We have shown that PFTBA can be ionized by laser-produced positive ions. There are different products and mechanisms in the ion-PFTBA reactions. PFTBA can be cationized by Li^+,Cr^+, Co^+, Ni^+, Cu^+, Na^+ and Zn^+ ions. Subsequent elimination of F_2 from the formed complex can be observed. Al^+, Fe^+, Zn^+ mainly abstract fluoride from the molecule. Mg^+ and Sn^+ ions induce elimination of F_2 from the molecule. Strong fragmentation has been achieved by B, Si, Ti, V, and some less strong with In, Zr and Mo ions. For Co^+, an insertion in a C-N bond is supposed according to detected products. Ca^+ reacts in specific way with PFTBA. Abstraction of fluoride produced CaF^+ which subsequently reacts with neutral molecule and $CaFL^+$ complexes are detected.

Bracketing of ionization energies of detected and non detected MF^+ ions has allowed us to estimate the ionization energy of $[(C_4F_9)_2N{=}CFC_3F_7]$ in the range between 7.69 and 8.0 eV.

Reactions of PFTBA cannot be simply compared with TBA reactions. Even if the similarity of the functional group (i.e. amine) should play a common role in the involved mechanisms, there is large difference between H and F.

Excitation of cyclotron motion of projectile ions induces high fragmentation of PFTBA molecule. The control of experimental parameters allows the control of the fragmentation. Mass spectra containing well known adduct ions (until m/z 740) and well defined PFTBA fragment ions as well as some metal ions give a mass range (*m/z* 20 - 740) appropriate for calibration even broader than spectra of PFTBA in EI experiments(m/z 69-502). Such obtained series of ions are useful for usual instrument calibration.

Other polyhalogenated molecules: dichlorodifluoromethane, halothane and endosulfane were ionized by (chemical) laser produced positive ions. The main detected products are listed in Table III.8.1.

Table III.8.1 Detected molecular and quasi-molecular ions

Molecule	**Detected positive ions**			
PFTBA $(C_4F_9)_3N$	ML^+			$[L-F]^+$
TBA $(C_4H_9)_3N$	ML_n^+	$[L+H]^+$	L^+	
Dichlorodifluoromethane				$[L-F]^+$
Cl_2CF_2				$[L-Cl]^+$
Halothane			L^+	$[L-Br]^+$
$BrCHClCF_3$				
Endosulfane	ML^+	$[L+H]^+$	L^+	
$C_9H_6SO_3Cl_6$				

Defined ionization and fragmentation of the PFTBA molecule was successfully used for an internal calibration procedure of endosulfane mass spectra. It opens possible application to other polyhalogenated molecules.

References

1. a) R.G. Pratt, J. Zheng, B.K. Stewart, Y. Shiferaw, A.J. McGoron, R.C. Samaratunga and S.R. Thomas, *Magn. Reson. Med.*, **27**, 307 (1997).

   b) G. Bekyarova, T. Yankova and B. Galunska, *Artif. Cell Blood Sub.*, **24**, 629 (1996).

   c) S.R. Thomas, R.G. Pratt, R.W. Millard, R.C. Samaratunga, Y. Shiferaw, A.J. McGoron and K.K. Tan, *Magn. Reson. Imaging*, **14**, 103 (1996).

   d) H. Mizuno, J. Isobe, S. Matsunobe, T. Nakamura, Y. Shimizu and S. Hitomi, *Int. J. Artif. Organs*, **17**, 609 (1994).

   e) T. Kojima, N. Sawada, M. Oyamada, H. Chiba, H. Isomura, M. Mori, *J. Cell Sci.*, **107**, 3579 (1994).

   f) S.R. Thomas, R.W. Millard, R.G. Pratt, Y. Shiferaw and R.C. Samaratunga, *Artif. Cell Blood Sub.*, **22**, 1029 (1994).

   g) S. Kashimoto, T. Nakamura, A. Nonaka, M. Kume, T. Oguchi and T. Kumazawa, *Brit. J. Anaesth.*, **73**, 380 (1994).

2. a) V.H. Vartanian and D.A. Laude, *J. Am. Soc. Mass Spectrom.*, **6**, 812 (1995).

   b) K.R. Mohan, M.G. Bartlett, K.L. Busch, A.E. Shoen and N. Gore, *J. Am. Soc. Mass Spectrom.*, **5**, 576 (1994).

   c) F.A. Londry, G.J. Wells and R.E. March, *Hyperfine Interact.*, **81**, 179 (1993).

   d) K.R. Jonscher, J.R. Yates, *Anal.Chem.*, **68**, 659 (1996).

   e) G. O'Connor, L. Ebdon, E.H. Evans, H. Ding, L.K. Olson and J.A. Caruso, *J. Anal. Atom. Spectrom.*, **11**, 1151 (1996).

   f) T-C.L. Wang; T.L. Ricca and A.G. Marshall, *Anal. Chem.*, **58**, 2935 (1986).

   g) D.A. Laude Jr. and S.C. Beu, *Anal. Chem.*, **61**, 2422 (1989).

   h) P. Caravatti and M. Allemann, *Org. Mass Spectrom.*, **26**, 514 (1991).

   i) P.B. Grosshans, R. Chen, P.A. Limbach and A.G. Marshall, *Int J. Mass Spectrom. Ion Processes*, **139**, 169 (1994).

3. S.J. Babinec and J. Allison, *J. Am. Chem. Soc.*, **106**, 7718 (1984).

4. J. Allison, *Prog. Inorg. Chem.*, **34**, 627 (1986).

5. B.D. Radecki and J. Allison, *J. Am. Chem. Soc.*, **106**, 946 (1984).

6. S. Karrass, T. Prüsse, K. Eller and H. Schwarz, *J. Am. Chem. Soc.*, **111**, 9018 (1989).

7. S.W. Sigsworth and A.W. Castleman, *J. Am. Chem. Soc.*, **111**, 3566 (1989).

8. H. Sato, M. Kawasaki, K. Kasantani, T. Oka, *Nippon Kagaku Kaishi*, 1240 (1989).

9. M.A. Tolbert, J.L. Beuchamp, *J. Phys.Chem.*, **90**, 5015 (1986).

10. K. Eller and H. Schwarz, *Chem. Rev*, **91**, 1121 (1991).

11. L.F. Halle, P.B. Armentrout and J.L. Beauchamp, *Organometallics*, **2**, 1829 (1983).

12. J.S.Uppal and R.H. Stanley, *J. Am. Chem. Soc.*, **104,** 1229 (1982).

13. J.S.Uppal and R.H. Stanley, *J. Am. Chem. Soc.*, **102,** 4144 (1980).

14. E.F. Cromwell, K. Reihs, M.S. de Vries, S. Ghaderi, H.R. Wendt and H.E. Hunziker, *J. Phys. Chem.*, **97**, 4720 (1993).

15. F.W. McLafferty and F. Turecek, "Interpretation of Mass Spectra", University Science Books, Mill Valley, California, 4th ed. (1993).

16. J.R. Chapman, "Pratical Organic Mass Spectrometry-A Guide for Chemical and Biochemical Analysis" John Wiley & Sons, Chichester, 2nd ed.(1993).

17. R.C. Burnier, G.D. Byrd, T.J. Carlin, M.B. Wiese, R.B. Codym and B.S. Freiser, in "Ion Cyclotron Resonance Spectrometry II", Ed, by H. Hartmann and K.P. Wanczek, Springer-Verlag Berlin, pp. 98-118 (1982).

18. a) S.G. Lias , J.E. Bartmes, J.F. Liebman, J.L. Holmes, R.D. Levin and W.G. Mallard, *J. Phys. Chem. Ref. Data* , 17, Suppl. 1., (1988).

b) CRC Handbook of Chemistry and Physics, Ed. by D.R. Lide, 73rd ed., CRC Press, Boca Raton , Florida (1992-1993).

19. I. Barin, F. Sauert, E. Schultze-Rhonhof and W. S. Sheng, "Thermochemical Data of pure Substances", VCH, 2nd ed.(1993).

20. A.G. Marshall and F. R. Verdun, "Fourier Transform in NMR, Optical, and Mass Spectrometry: A User's Handbook, Elsevier, Amsterdam (1990)

21. P.B. Grosshans, P.J. Shields and A.G. Marshall, *J. Am. Chem. Soc.*, **112,** 1275 (1990).

22. L. Schweikhard, G.M. Alber and A.G. Marshall, *Physica Scripta,* **46,** 598 (1992).

23. K.L. Busch, G.L. Glish and S. McLuckey, "Mass Spectrometry/ Mass Spectrometry: Techniques and Applications of Tandem Mass Spectrometry", VCH, Deerfield, FL (1988).

24. T.D. Wood, A.G. Marshall and L. Schweikhard, *Rapid Comm. Mass Spectrom.*, **8,** 14 (1994).

25. L. Schweikhard, G.M. Alber and A.G. Marshall, *J. Am. Soc. Mass spectrom.* **4,** 177 (1993).

26. M.B. Comisarow, V. Grassi and G. Parisod, Chem. Phys. Lett, **57,** 413 (1978).

27. M. Bensimon and R. Houriet, *Int. J. Mass Spectrom. Ion Processes*, **72,** 93 (1986).

28. R.A. Forbes, L.M. Lech and B.S. Freiser, *Int. J. Mass Spectrom. Ion Processes*, **77,** 107 (1987).

Chapter IV

Laser-Induced Negative Chemical Ionization of Polyhalogenated Organic Compounds

1. Introduction

This chapter is devoted to the Negative Chemical Ionization (NCI) induced by laser desorption/ablation products.

We shall distinguish between "Negative" **Electron** Chemical Ionization (NECI) and Negative **Ion** Chemical Ionization (NICI) depending on the ionization source. NECI applies low energy electrons and Electron Capture Chemical Ionization (ECCI) takes place. There are several mechanisms involved in this ionization method. NICI involves negative ions to ionize substrate molecules. In our case those projectile ions are produced by laser desorption/ionization. Moreover, ECCI can induce dissociation of fragment halide ions from the substrate molecule. Such ions can be used to ionize remaining neutral molecules. This method will be referred to as "Self NICI".

Our objective was to ionize and detect volatile polyhalogenated molecules by means of laser desorption/ablation. Those molecules have a high propensity to form negative ions. In order to enable an unambiguous determination of products, an internal calibration process was searched. Results from positive and negative chemical ionization could give complementary information about the molecules.

FT-ICR- mass spectrometer is well adapted for the analysis of negative ions. It is easy to switch from positive to negative mode function, it requires only the change in trap voltage. Working at quite low pressure allows high sensitivity in the detection of negative ions.

In this chapter, a short bibliographic review of Negative Chemical Ionization is given. Mechanisms of negative ion formation and methods for projectile ions production are explained for both "negative"-electron and negative-ion chemical ionization. Laser induced production of electrons and negative ions *versus* standard chemical ionization sources is described. Chemical ionization of polyhalogenated organic molecules is briefly reviewed.

After this, our results are presented with respect to ionizing methods (electron capture chemical ionization, negative ion chemical ionization and self negative chemical ionization) applied to polyhalogenated molecules.

2. Negative Chemical Ionization

The ability to form negative ions is useful in any analytical technique since the negative molecular ion may have a greater stability than the corresponding positively charged ion and may provide complementary structural information through different fragmentation processes. During an ionization process, such as electron ionization, negatively as well as positively charged ions are formed. But, it was not before chemical ionization (CI) ion sources and quadrupole instruments, which allowed an easy switch from positive to negative ionization, appeared on the market that negative ion (NI) mass spectrometry became recognized as a useful addition to the MS resources.[1]

In contrast to the case of ionization under conventional electron ionization conditions, low energy electrons are readily captured by many organic compounds without inducing extensive fragmentation. A resurgence of interest in negative ions began with the development of a simple and convenient means of generating a large population of electrons with near thermal energy in the ion source. This was achieved by Hunt et al.[2] following earlier work by Von Ardenne et al.[3] and Dougherty and Weisenberger[4] by the simple expedient of using the reagent gas in a conventional chemical ionization source as a moderator for the initially energetic electrons. Negatively charged reagent gas ions may also be generated in a chemical ionization source, providing a further extension to the experimental control of analytical information available under CI conditions.

Negative ion formation is not limited to CI operation since most of the recent ionization techniques (laser desorption, for example)[5] also operate readily in this mode. The analysis of labile molecules is common with techniques such as fast atom bombardment[6] and thermospray ionization,[7] where ion/molecule reactions are involved in the formation of analyte-related ions in the negative ion mode just as in the positive ion mode.[8]

A CI source permits interaction of electrons with inert gas molecules so that the electrons are readily thermalized. In addition, negative plasma ions can be produced in CI sources which react specifically with substrate molecules.

Thus, under CI conditions, negative ions from the sample molecule may be produced by :

- the interaction of **electrons** with neutral molecule, or

- the reaction of **other ions** with neutral molecules.

Different mechanisms are involved in negative ion formation, either in electron induced, or in ion induced negative chemical ionization as shown in Figure IV.1.

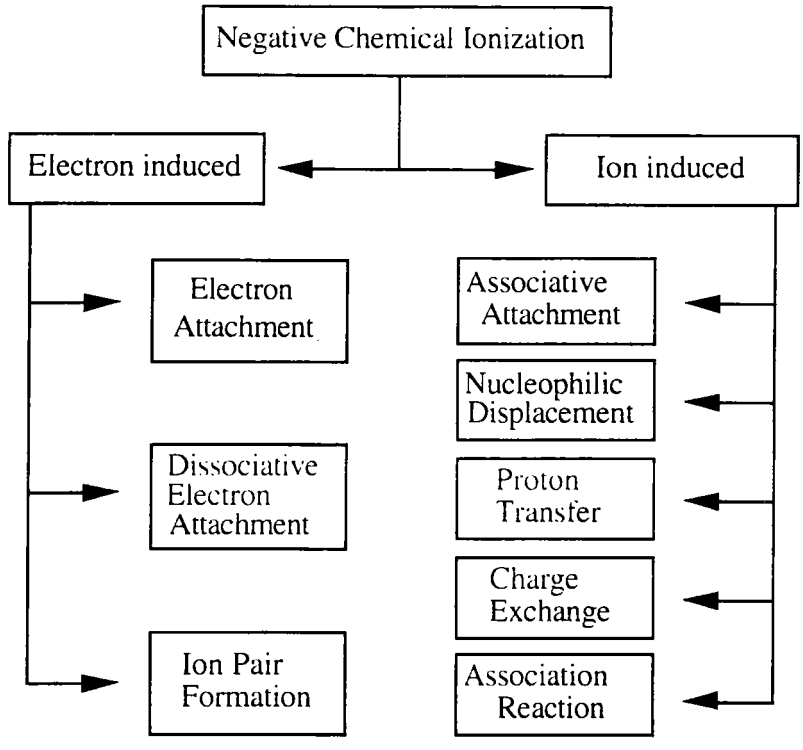

Figure IV.1. Mechanisms of negative ion formation by NCI methods.

The mechanisms will be described further in the text. In both cases, different methods for production of interacting electrons and ions can be used. We will talk about "standard" chemical ionization sources and laser induced electron/ion formation.

2.1. Negative ions produced by the interaction of electrons with neutral molecules

Electron Capture Chemical Ionization (ECCI) is a "soft" ionization technique which takes advantage of the interactions between thermal (low energy) electrons and electrophilic molecules.

2.1.1. Modes of electron-induced negative ion formation

Depending of the energy of the electron and the nature of the molecule, one of three basically different processes can occur. For molecule AB these processes are

conventionally classified as follows :[9]

(i) Electron attacment:

$$AB + e^- \rightarrow AB^{-\cdot}$$

(ii) Dissociative electron attachment:

$$AB + e^- \rightarrow A^- + B^{\cdot}$$
$$\rightarrow A^{\cdot} + B^-$$

(iii) Ion pair formation:

$$AB + e^- \rightarrow A^- + B^+ + e^-$$
$$\rightarrow A^+ + B^- + e^-$$

Processes (ii) and (iii) may involve the breaking of one or more bonds.

(i) Resonance electron attachment produces a molecular negative ion ($AB^{-\cdot}$) and occurs at electron energies near 0 eV.[10,11] Electron attachment does not necessarily lead to the formation of stable molecular or high mass fragment ions for all kinds of compounds.[12] However, most persistent organic environmental contaminants are highly aromatic and/or halogenated, and these factors facilitate the electron attachment process.

Upon capturing an electron, a long-lived complex is formed, which may exist for 10^{-6} s or more before reverting to the neutral molecule and a free electron (autodetachment). Ions with long lifetimes tend to be generated from molecules with positive electron affinities (often conjugated systems bearing electron-attracting substituents) and from large molecules where the excess energy imparted by the electron can be distributed among many internal degrees of freedom. During its lifetime, the molecule-electron complex can undergo collisional stabilization (if there is sufficient gas density) and give a stable molecular anion detectable by mass spectrometry. When this process proceeds with high efficiency, it is ideally suited for the quantitation of organic molecules.[13]

For electron attachment, two cases arise depending on whether the electron affinity of AB is < 0 (Figure 2a) or > 0 (Figure 2b).[14] Electron affinity (EA) is defined

as the energy of the ground state neutral species and an electron at infinite distance minus the energy of the ground state of the negative ion. When the EA is <0, a Franck-Condon transition leads to an unstable molecular anion AB^{-*} which may disappear by autodetachment :

$$AB^{-*} \rightarrow AB + e^{-}$$

or, if above the dissociation limit, may dissociate to $A\cdot + B^{-}$. Autodetachment, in this situation, is usually very rapid and occurs within a vibrational period leaving little possibility for collisional stabilization of AB^{-*} unless the pressure is very high. Stabilization by radiation emission is also possible but not probable.

(ii) Resonance attachment of electrons may also lead to dissociation (unimolecular decomposition). Dissociative electron-attachment reactions are observed for electrons with energies between 0-15 eV.[15,16] However, the optimum electron energy (the energy at which the cross-section for the reaction is maximum) varies from compound to compound.[14-16] The process will occur (Fig 2c) if the capture of an electron leads, by a vertical Franck-Condon transition, to a repulsive state of AB^{-} which dissociates to form $A\cdot$ and B^{-}, with a possible excess of kinetic energy.[17,18]

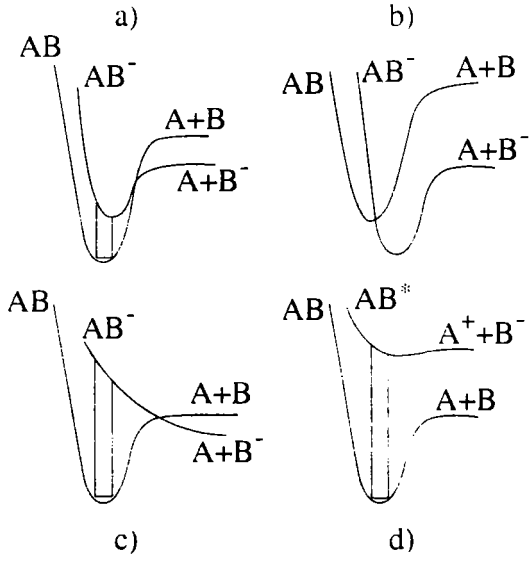

Figure IV.2. Potential energy curves for negative ion formation (adapted from 14).

(iii) In ion pair formation, Figure 2d, the electron provides the energy necessary to form an excited molecule which dissociates (or predissociates) to give a positive and a negative ion. The thresholds for such processes usually lie above 10-15

eV electron energy, and the cross section increases approximately linearly with the excess energy to an energy roughly three times the threshold energy. Negative ion formation by ion-pair formation does not appear to be particularly important under CI conditions.[14]

The relative rates of these competing processes depend on the energy distribution of the electrons (Table IV.1.), and the energy distribution depends in turn on the reagent gas, on its temperature, and on its pressure, as well as on the potentials in the ion source and on the energy of the primary electrons.

Table IV.1. Electron energy ranges in electron capture chemical ionization.[9]

Modes of negative ion formation	**Energy / eV**
Resonance electron attachment	0
Dissociative electron attachment	0-15 (up to ca. 5 eV[1])
Ion pair formation	> 10

Different authors give different respective energies for these processes.

2.1.2. Production of (low energy) electrons for NCI

Ideally, one requires a beam of monoenergetic electrons with near thermal energies for the formation of negative ions by electron capture.

2.1.2.1. Standard CI techniques for electron formation

High energy electrons emitted from the filament of an electron-ionization ion source can be thermalized by a buffer gas at a pressure of about 1 Torr. The thermalization occurs by inelastic collisions and by ionization processes. Different gases have been used for the enhancement gas in EC-MS, but methane is the most common. Bombardment of methane with 100 eV electrons (from the filament of an EI-MS instrument) produces positive ion in high abundance:

$$CH_4 + e^- \rightarrow CH_4^{+\cdot} + 2e^- \rightarrow CH_3^+ + H + 2e^-$$

For each positive ion that is produced, a low energy secondary electron is also generated. In addition, the ionization of methane removes about 30 eV from the

primary electron. The energy of the electron is further reduced by collisions with other neutral methane molecules. Therefore, operation of a mass spectrometer under high-pressure conditions with methane produces a population of electrons having an energy distribution close to thermal values. In fact, Hunt and Crow found that about 50% of these electrons have energies close to zero.[19]

The ideal buffer gas should just produce thermal electrons with a well defined energy distribution close to zero energy. Moreover, it should not interfere with the ionization process nor react with the substrate molecules.[1] None of the reagent gases suggested in the literature come close to this ideal, and, therefore, the appearance of the NCI spectrum of a given compound in extreme cases can change with the gas used as well as with experimental parameters. For any buffer gas, however, ion source pressure has been found to affect sensitivity and relative ion abundances.[20]

The manner in which the ion-source pressure affects abundances is somewhat complex. Increasing the pressure increases the degree of electron thermalization and lowers the mean electron energy, thus producing a more suitable energy distribution for resonance electron attachment. Increasing the buffer gas pressure also increases the stabilization of excited molecular anions by collisions. This stability ultimately results in extending the lifetimes of the negative ions with respect to autodetachment. Stabilization of the molecular ions may also suppress other electron-molecule reactions such as dissociative electron capture. However, when the ion-source pressure becomes too high, the transmission of ions out of the source is reduced.

The rate constants for electron capture depend on:

(a) the electron affinity of the substrate molecule,
(b) the activation energy for the anion formation,
(c) the collision cross-section,
(d) the decomposition (autodetachment) rate of the anion formed.

The most important factor here is the collision cross-section. For organic compounds it varies over a range of six orders of magnitude. At most favorable circumstances (polyhalogenated compounds) the rate constants for electron capture may reach values several times 10^{-7} cm^3 s^{-1}.[14] This selective ionization favors the formation of stable negative ions from most halogenated environmental contaminants, such as polychlorinated biphenyls and chlorinated pesticides.

2.1.2.2. *Laser induced generation of electrons*

It is well known from experimental[21] and theoretical studies[22] that two limiting cases of laser ionization exist; they can be distinguished by the amount of energy which is deposited per unit area on the target by a single laser pulse. The processes generated by a low power flux laser pulse are usually classified as laser desorption while the high power density limit is referred to as laser plasma ionization. (Light power flux is measured in units W/cm^2 and used as a synonym of light intensity and named irradiance).[23]

When photons with an energy higher than the work function (the energy required for an electron to escape a solid surface) of metal hit it, a swarm of electrons instantaneously leaves the surface according to the photoelectric effect.[24] In general there are three different ways electrons can be ejected from the target:

i - photon-induced electron emission (photoelectric effect);
ii - electron emission due to a high target temperature. (- plasma ignition)
iii - field emission

i) The photoelectric effect is due to the absorption of photons by e. g., the surface of a metal.[25] The energy of the impinging photon is used to emit an electron out of the metal. The excess energy, i. e. the difference between the photon energy hν and the work function W_a of the target, is transformed into the kinetic energy of the electron corresponding to the following equation:

$$h\nu = W_a + \frac{1}{2} mv^2$$

This equation shows that if the applied wavelength is short enough and thus the applied energy exceeds the work function of the target, the electron kinetic energy spreads over a wide range between 0 eV and the value $h\nu - W_a$. The electron work functions of target substances that were studied in this work are listed in Table IV.2.

However, for MS investigations in general the kinetic energy distribution of the electrons should be as narrow as possible in order to define the internal energy of the molecular ion as exactly as possible. Therefore, the wavelength of the photons should be adjusted in such a way that the photon energy equals the work function of the target. Then, electrons are emitted with nearly no kinetic energy and, after acceleration in an electric field, their kinetic energy distribution is rather sharp.

Table IV.2. Electron work functions (Wa), ionization energies (E_i) and electron affinities (E_{ea}) of target substances. (values from ref.26)

Element	Wa / eV	E_i / eV	E_{ea} / eV
Mg	3.66	7.646	not stable
Ca	2.87	6.113	0.0184
Al	4.28	5.986	0.441
Ti	4.33	6.82	0.079
V	4.3	6.74	0.525
Cr	4.5	6.766	0.666
Mn	4.1	7.435	not stable
Fe	4.5	7.870	0.151
Co	5.0	7.86	0.662
Ni	5.5	7.635	1.156
Cu	4.65	7.726	1.235
Zn	4.33	9.394	not stable
In	4.12	5.786	0.3
Si	4.85	8.151	1.385
Sn	4.42	7.344	1.112
Pb	4.25	7.416	0.364
Zr	4.05	6.84	0.426
Mo	4.6	7.099	0.746

ii) - Electron emission due to a high target temperature

Increasing the laser irradiance on the target eventually leads to saturation effects. The number of electrons no longer suffices to absorb all the photons hitting the target. Hence the excess photons are absorbed by the target, now heating the target itself. Raising the temperature of the target eventually leads to the thermal emission of electrons according to the Boltzmann factor k_bT. Eventually, even the atoms from metal target may be desorbed. Thermal emission process leads to electrons with a broad kinetic energy spread according to the Maxwell velocity distribution. This distribution is even broader than that of photon-emitted electrons. Thermal electrons are emitted over a longer period of time than photoelectrons. The time scheme for laser induced generation of electrons is shown in Figure. IV.3.

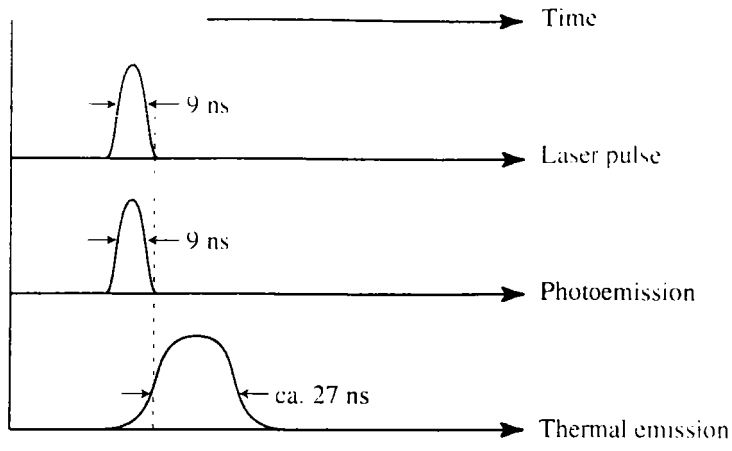

Figure IV.3. Time scheme for laser-induced generation of electrons (According to 24)

iii) - Field emission

The work function of a sample is strongly influenced by electromagnetic fields. Thus, applying electric field to the metal, the work function can be lowered leading to an increased probability for electron emission due to tunneling effects. Comparatively low voltages are sufficient to lead to field emission if there are sharp edges or tips producing high electric field strengths. Field emission being a continuous process, thus producing ions not at fixed short time but continuously, results in a decrease in mass resolution.

Some applications of positive mode ionization by electrons emitted by metal surfaces irradiated by laser beam, have been shown in Time Of Flight mass spectrometry[24,27,28]. Photoemmited electrons from the metal surfaces were used to ionize incoming molecules in a supersonic jet[24] or, in other case, to ionize molecules already desorbed by another laser[28]. It was shown that plasma electrons induce competitive ionization of ablated tetraphenylporphirin in positive and negative mode.[29]

2.2. *Negative ions produced by the reaction of neutral molecule with other ions*

Negative ion chemical ionization (NICI) can be defined as a reaction between some negative ion and the neutral molecule (atom) under study to produce a negatively charged species derived from the neutral.

2.2.1. Modes of ion-induced negative ion formation

These reactions can conveniently be grouped into five major categories:[14]

(i) Associative Detachment Reactions

Negative ions may disappear from system by associative detachment reaction :

$$X^- + AB \rightarrow ABX + e^-$$

where AB is a neutral species. Such reactions have been studied primarily in simple systems. The prevalence of associative detachment reactions in more complex systems applicable to chemical ionization has not been studied. However, it is a complication which should be borne in mind since it can lead to a decrease in sensitivity.

(ii) Displacement and Elimination Reactions (or Nucleophilic displacement)[8]

The displacement reaction:

$$X^- + AB \rightarrow AX + B^-$$

is the gas-phase equivalent of the S_N2 reaction so extensively studied in solution. Displacement reactions generally are observed if they are exothermic and if there is no easy proton transfer process from AB to X^-.

(iii) Proton Transfer Reactions

$$M + X^- \rightarrow (M - H)^- + HX$$

The tendency for an anion X^- to accept a proton from a particular analyte molecule may be assessed from a knowledge of proton affinity values for the anions. The proton affinity of the anion X^- is the negative of the reaction enthalpy:

$$XH \rightarrow X^- + H^+ \qquad E_{pa}(X)^- = \Delta_r H$$

Thus, the observation of the reaction

$$X^- + HY \rightarrow HX + Y^-$$

implies that $PA(X^-) > PA(Y^-)$, i.e. the reaction is exothermic.

Table IV.3. Proton affinities (PA) of halide ions and electron affinities (EA) of the corresponding atoms .[14]

Anion (X^-)	PA (X^-)/kJ mol^{-1}	EA(X)./kJ mol^{-1}
F^-	1554	328
Cl^-	1395	349
Br^-	1354	324

Analyte anions produced by proton transfer have very little excess internal energy. As can be seen from the last equation, no new bonds are involved in the formation of the analyte anion so that most of the excess energy resides in the neutral derived from the reagent gas ion. As a result, negative ion proton transfer spectra generally contain abundant quasi-molecular ions but very few fragment ions.

Anions with lower proton affinity such as Cl^- are of a limited value for the production of analyte anions by proton transfer, although they will form hydrogen-bonded complexes with more acidic molecules. These same hydrogen-bonded intermediates may alternatively react by elimination of a small neutral molecule such as HF, HCl, or H_2O.[30]

(iv) Charge Exchange Reactions

The charge exchange reaction:

$$A^- + B \rightarrow B^- + A$$

will be exothermic provided that the EA of B is greater than the EA of A. Negative ion charge exchange reactions will occur if the electron affinity of molecule B is greater than that of molecule A.

Charge exchange also provides a mechanism for the loss of analyte ions.[31] For example, fluorine radicals, formed when freon reagent gas is used as a source of

chloride ions, have such a high electron affinity that they readily remove analyte ions, resulting in a reduced sensitivity for electron capturing materials:

$$M^- + F \cdot \rightarrow M + F^-$$

(v) Association Reactions
(Nucleophilic addition)[8]

$$M + X^- \rightarrow MX^-$$

Stable addition complexes may be formed by nucleophilic attack with anions of low proton affinity, such Cl^- and $O_2^{-\bullet}$, which cannot usually react by proton transfer. The chloride anion formed by electron bombardment of dichlorodifluoromethane (Freon 12)[32] forms stable hydrogen-bonded complexes which account for the majority of the ionization in the spectra of a number of acids, amides, aromatic amines, and phenols.[33] The chloride anion also forms stable $(M+Cl)^-$ complexes with a range of other compound types and has been used in the analysis of polychlorinated aliphatic compounds.[34]

2.2.2. Production of reactive negative ions for NICI

2.2.2.1. "Classical" Chemical ionization reagents

There are many specific reagent gases that yield negative ions which can be reagent for ionization of substrate molecule. Usually they are formed by electron ionization. H^- from H_2; $O^{-\bullet}$, $O_2^{-\bullet}$, $O_3^{-\bullet}$ from O_2; O^-, NO^- from N_2O; NH_2^- from NH_3 and many others.[1]

Halide ions are yielded from many reagent gases as well. CHF_3, CF_4, NF_3, and occasionally SF_6 or SO_2F_2 give rise to F^- ion. It has been used comparatively rarely as a reagent ion. Typical reactions involved are formation of $[M+F]^-$, $[M-H]^-$, and S_N. It is not a strong Brønsted base and is not capable of abstracting a proton from alkanols, amines, alkanes, alkenes, or most nitriles.

The Cl^- ion is readily formed under CI conditions by dissociative electron capture by CH_2Cl_2, CCl_2F_2, CCl_4, $CCl_2F\text{-}CClF_2$, $CHCl_3$. (In the case of CCl_2F_2 reagent gas at 20 Pa and 200°C there is 99% of Cl^- produced and 1% of F^- reactive anions[1]). The main application of Cl^- as a reagent gas ion has been in analytical

problems (molecular weight determination) as, e.g., in the identification of compounds in environmental, biological, or industrial materials. The Cl^- is a weak Brønsted base and will abstract a proton only from very acidic compounds. In the absence of such acidic hydrogens, $[M+Cl]^-$ attachment ions frequently are formed. Compounds which can form strong H-bridges give rise to abundant $[M+Cl]^-$ ions. Hydrocarbons, tertiary amines and nitriles give no $[M+Cl]^-$. Thus, Cl^- may be used as a selective reagent ion for a trace analysis of compounds in matrices which are not ionized by Cl^-.

The Br^- ion, which can be prepared by dissociative electron capture by $CBrF_3$, $CHBr_3$, $CH_2Br\text{-}CH_2Br$, is an even weaker base than Cl^- and reacts with substrates containing a modestly acidic hydrogen by formation of $[M+Br]^-$.[36]

2.2.2.2. Laser desorption /ionization produced ions for CI

Laser ablation is much more used for the production of the positive reagent ions than for negative reagents. Byrd, using the LD/I method, produced copper anions from copper[36]. However, he concluded that the quantity of Cu^- was insufficient for ion-molecule reactions to be studied. In contrast, gold anions were formed in high abundance in the work of Weil et al. and their reactions with alcohols were studied.[37] Neverthless, electron impact ionization remains the method the most used for the formation of negative reagent ions.[38]

Laser ablation/ionization of alkali-metal halide salt produces halide anions that can further ionize substrate molecules.[39] There is a minimum energy required for the formation of X^- ions, which depends on the crystal lattice of the salt. As the laser fluences increases, ions and electrons are emitted and a laser-induced plasma is eventually created. In general, the ignition of the surface plasma marks the transitions from desorption to the ablation regime and occurs over a wide range of materials, pulse lengths and wavelengths near an intensity threshold of ca. $2 \times 10^8 - 10^9$ Wcm^{-2}.[41]

2.3. Negative Chemical Ionization of Halogenated Organic Molecules

The high electron affinity of polyhalogenated organic compounds makes NCI a very sensitive method for qualitative and quantitative analyses of different pesticides, freons, and similar compounds in biological and environmental samples. The majority of publications deals with work-up procedures, suitable standards, standardization of MS procedure, reproducibility and detection limits.[42]

The major fragmentation pathway of alkyl and aryl halides at both 70 and near 0 eV is the formation of X^-; a result expected because of the high electron affinity of the halogen atoms (Table IV.3.). The energetic of formation of F^- and $[M-F]^-$ ions from fluoroakanes have been studied.[43] Parent negative ions are detected at formation energies of 0-1 eV for a number of species including perfluorocyclobutane,[44] perfluorocyclobutene,[45] perfluorobenzene,[45,46] and perfluorotoluene. Alkyl[47] and aryl[45,48] chlorides produce Cl^- and $[M-Cl]^-$ ions at both 70 and near 0 eV.

Dispert and Lacmann[49] were the first who detected the molecular ion of CF_2Cl_2 molecule but in a small amount of stable parent ions. A potassium atom beam in the energy range 1-30 eV have been used to induce electron transfer in collisions with halogenated methane molecules CF_4, CF_2Cl_2, $CHCl_3$ and CCl_4. They defined electron affinity of 0.4 ± 0.3 eV for CF_2Cl_2. The difference between the appearance potentials of the parent ion and Cl^- is equivalent to the dissociation energy of $CF_2Cl^-Cl^-$ and amounts to only 0.1-0.4 eV. This small bond energy of CF_2Cl_2 is reflected in the small relative ion yield of only 0.1%. It is known from thermochemical data that the fluorine atom is much more strongly bound to the central C-atom than chlorine. Therefore, the abundance of F- is only about 4% of that of Cl^-.

Hasemi et al. have studied electron capture induced processes in CF_3Cl, CF_4, C_2F_4, and CF_3Cl/H_2O.[50] The reaction of negative ions with halomethanes is the subject of several studies in Nibbering's group.[51]

Methane/NICI has been used for the analysis of halogenated hydrocarbons[52], chlorophenols,[53] chlorinated dibenzofurans[54] and iso-butane for polychlorodibenzo-p-dioxins.[55]

ECCI gave rise to molecular ion of endosulfane molecule,[56] and many other polyhalogenated organic environmental contaminants (polychlorinated biphenyls, polychlorinated dibenzo-p-dioxins and dibenzofurans; polychlorinated naphthalenes, terphenyls and diphenyl ethers; polychlorinated benzenes, phenols, anisoles, and styrenes...)[13,57]

Cromwell et al. detected negative ion fragments of perfluorinated polyether (PFPE) films in two laser pulse experiment.[59] PFPE were desorbed by a laser pulse. Second puls (a high fluence) served for the formation of transition-metal ions in positive mode experiment. In negative mode, secondary reactions can result from electron attachment to a neutral fragment or dissociation of a negatively charged fragment.

3. Results and discussion

Laser ablation/desorption of pure metals or metal salts was used for the formation of electrons or negative ions. Those negative species served as projectiles for the ionization of various halogenated molecules. The procedure applied for the study of negative ions is summarized in Figure IV.4.

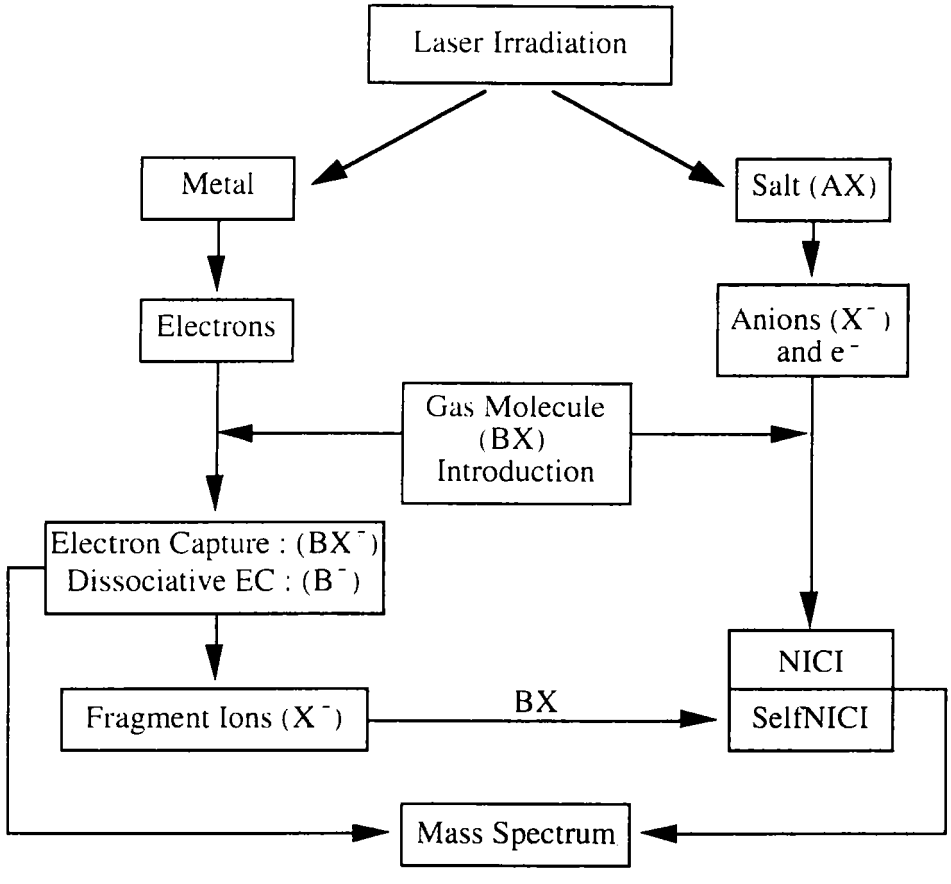

Figure IV.4. Negative Chemical Ionization (NCI) methods used in experiments.

Depending on the nature of ionizing projectiles three different ionizing methods can be distinguished:

1) *Electron Capture Chemical Ionization (ECCI);*
2) *Negative Ion Chemical Ionization (NICI) and*
3) *"Self Negative Ion Chemical Ionization" (SNICI).*

Electron Capture Ionization (EC) uses electrons produced from the irradiated (metal) surface. The molecules are ionized by electron/molecule interactions. The main mechanisms of ion formation are resonance electron capture and dissociative electron capture (Figure IV.5.a).

In Negative Ion Chemical Ionization (NICI) experiments, halogen ions formed from metal halide salt were used as ionizing projectiles (Fig. IV.5.b). In some cases, a fragment ion (X^-) produced by dissociative electron capture of the studied molecule was used as projectile ion. The substrate molecule was consequently ionized by one of its own fragments. This method is referred to as "Self Negative Ion Chemical Ionization" (SNICI) (Fig. IV.5.c).

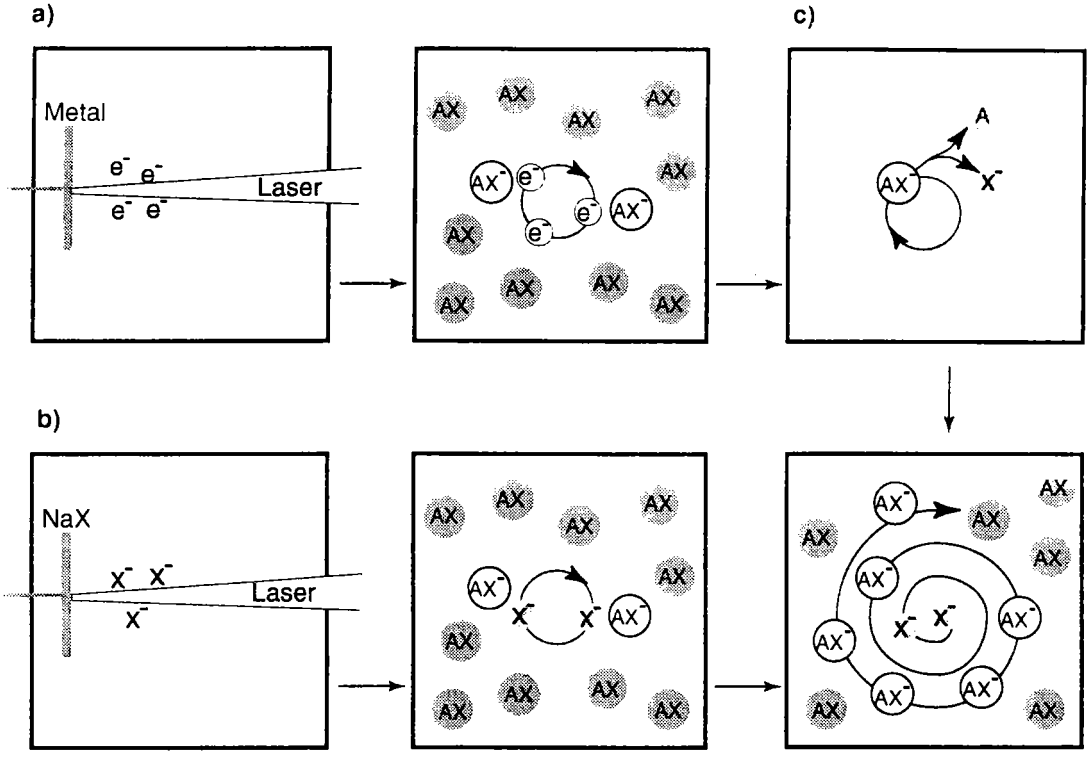

Figure IV.5. Pictorial presentation of negative ionization of neutral molecules. Experimental events: a) ECCI b) NICI c) SNICI

In our experiments, different metals and salt targets were irradiated by a laser beam to produce the ionizing projectiles for halogenated organic molecules (See Table IV.4.). Dichlorodifluoromethane (Cl_2CF_2, gas), halothane ($BrCHClCF_3$, liquid), perfluorotributylamine ($(C_4F_9)_3N$, liquid), and endosulfan ($C_9H_6SO_3Cl_6$, solid) have been studied. Four different wavelengths were used in our experiments (Table IV.4.). All four in PFTBA studies, and mainly 355 nm for the study of other molecules. Molecules were introduced into the FTMS chamber and ionized by the appropriate methods. For ECCI experiments, aluminum was chosen as laser target. It has been extensively studied in positive ion mode experiments. Thus, it would be the most appropriate to have the possibility to easily turnswitch positive to negative ion analysis without changing a lot the experimental conditions.

Table IV.4. Some conditions used in negative mode experiments.

Molecule	λ / nm	ECCI - laser target	NICI - laser target
PFTBA	355, 266, 248, 193	Mg, Ca, Ti, V, Mn, Co, Cr, Fe, Ni, Cu, Zn, Al, Zr, Mo, Sn, Si	NaCl, KCl, LiF
Cl_2CF_2	355	Al	NaCl
$BrCHClCF_3$	355	Al	NaCl
$C_9H_6SO_3Cl_6$	355, 266, 248	Al	-

The three methods show to be complementary to each others in the analysis of samples. Resulting molecular (L^-), and/or fragment ions were detected and assigned. Mechanisms of ion formation are proposed. To be able to unambiguously define the elemental composition of the detected species, we were searching for an appropriate calibrant molecule that can be used even with unknown samples. PFTBA was again the molecule of choice. An example of negative ion internal calibration is given for endosulfane.

3.1. Electron Capture Chemical Ionization (ECCI)

It is known that a large number of electrons is produced during the laser-matter interaction at high irradiance (>10^8 W cm^{-2}).

$$\text{Metal} \xrightarrow{\text{laser}} \text{Metal}^+ + e^-$$

In positive mode, it is possible to monitor the influence of irradiation on the production of positive ions by their detection. In negative mode, on the contrary, no ions produced from the irradiated surface were detected at any studied irradiance and wavelength.

3.1.1. ECCI of Perfluorotributylamine

In our experiments, laser desorption/ablation of any studied pure sample (metals: Mg, Ca, Ti, V, Mn, Co, Cr, Fe, Ni, Cu, Zn, Al, Zr, Mo, Sn and silicon wafer) did not produce any detectable negative ions (all signal was at noise level) at any used wavelength (λ = 193, 248, 266 and 355 nm). So, we suppose that the electrons produced during the laser/surface interaction were the species responsible for negative

ionization. PFTBA molecule ($(C_4F_9)_3N$, Mw = 671 u), was ionized by electrons emitted from each of the above mentioned elements. PFTBA was introduced in the chamber after the laser shot on the metal surface, ionized, and its fragment ions were detected. Characteristic series of negative ions is shown in the spectrum in the Figure IV.6. for the case of an aluminum target.

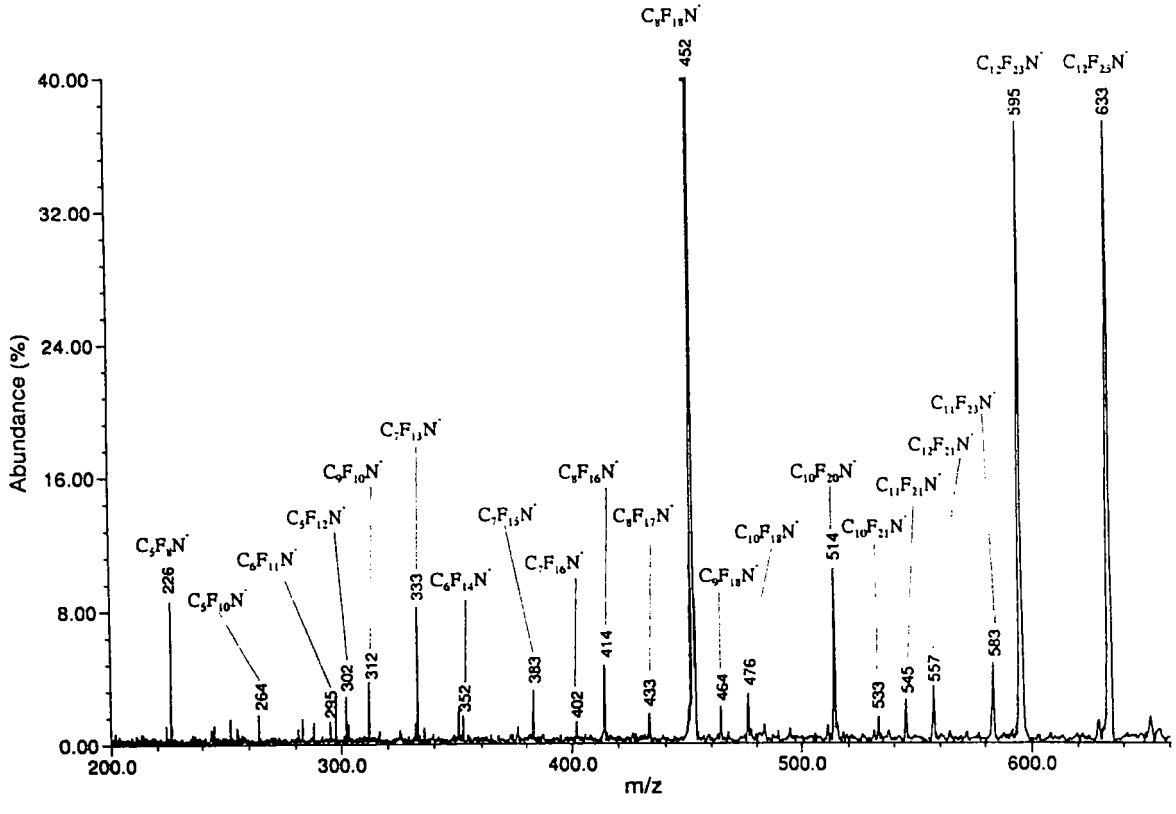

Figure IV.6. Negative ion mass spectrum obtained after laser-induced electron ionization of PFTBA (laser irradiance 10^8 W cm^{-2}). The metal target was aluminum.

No molecular ion has ever been detected. When formed by resonant electron capture, its lifetime must be less than ca. 10 μs[60] which is much shorter than the time scale of the FTMS experiment (several ms).

$$N(C_4F_9)_3 + e^- \rightarrow ([N(C_4F_9)_3]^- \cdot *) \qquad m/z\ 671$$

The basic detected peak corresponds to the $[M-2F]^-$ ion, *m/z* 633. The ion, *m/z* 452, $[M-C_4F_9]^-$ is the second most stable product .The formation of negative ions under the employed conditions is probably due to the dissociative electron capture

process:

$$([N(C_4F_9)_3]^- \cdot *) \rightarrow N(C_4F_9)_2C_4F_7^- \cdot + F_2 \qquad m/z\ 633$$

$$\rightarrow N(C_4F_9)_2^- \cdot + C_4F_9 \qquad m/z\ 452$$

The ion at *m/z* 595, $[L\text{-}2F_2]^-$, should result partially from the unimolecular decay of the molecular ion, and partially from the $[L\text{-}F_2]^-$ ion as shown by continuous ejection of $[L\text{-}F_2]^-$, *m/z* 633:

$$[L-F_2]^- \cdot \rightarrow [L-2F_2]^- \cdot + F_2$$

Ion $[M\text{-}C_4F_9]^-$, *m/z* 452, is the product of a direct unimolecular decay.

Electrons produced from the other pure elements ionized PFTBA molecule in very similar way and corresponding mass spectra are displayed in **Appendix C**. Ions detected in all metal electron-PFTBA ionization are assigned in Table IV.5.

Table IV.5. Negative ions detected after the electron ionization of PFTBA.

m/z	Assignation	*m/z*	Assignation
633	$C_{12}F_{25}N^-$	**312**	$\mathbf{C_9F_{10}N^-}$
595	$C_{12}F_{23}N^-$	302	$C_5F_{12}N^-$
583	$\mathbf{C_{11}F_{23}N^-}$	295	$C_6F_{11}N^-$
564	$C_{11}F_{22}N^-$	**283**	$\mathbf{C_5F_{11}N^-}$
557	$C_{12}F_{21}N^-$	276	$C_6F_{10}N^-$
526	$C_{11}F_{20}N^-$	264	$C_5F_{10}N^-$
514	$\mathbf{C_{10}F_{20}N^-}$	255	$C_7F_9^-$
476	$C_{10}F_{18}N^-$	231	$C_5F_9^-$
464	$C_9F_{18}N^-$	226	$C_5F_8N^-$
452	$\mathbf{C_8F_{18}N^-}$	219	$C_4F_9^-$
433	$\mathbf{C_8F_{17}N^-}$	214	$C_4F_8N^-$
414	$C_8F_{16}N^-$	**183**	$\mathbf{C_3F_7N^-}$
383	$\mathbf{C_7F_{15}N^-}$	169	$C_3F_7^-$
364	$C_7F_{14}N^-$	164	$C_3F_6N^-$
352	$C_6F_{14}N^-$	119	$C_2F_5^-$
333	$\mathbf{C_6F_{13}N^-}$	114	$C_2F_4N^-$
314	$C_6F_{12}N^-$	69	CF_3^-

Ions marked in bold were never detected in positive ion mode experiments.

Negative electron ionization of PFTBA molecules occurred throughout the range of irradiance < 10^{-7} W cm^{-2} to 10^{9} W cm^{-2}. The detected spectra do not vary a lot with changing the delay before broadband excitation. All detected ions were produced already after few tens of miliseconds.

3.1.1.1. Comparison to standard EI spectra of PFTBA

Standard Electron Ionization (EI) of PFTBA molecules was performed on the FTMS 2001 mass spectrometer. Spectra with different electron-beam potential were acquired. There is no significant difference among low and high potential electron ionization mass spectra. When the ionization potential was decreased, ions were detected only after longer delays. For example, at 5 eV, 1 s was necessary to detect PFTBA ions. Figure IV.7. displays the negative ion EI spectrum of PFTBA at 5 eV.

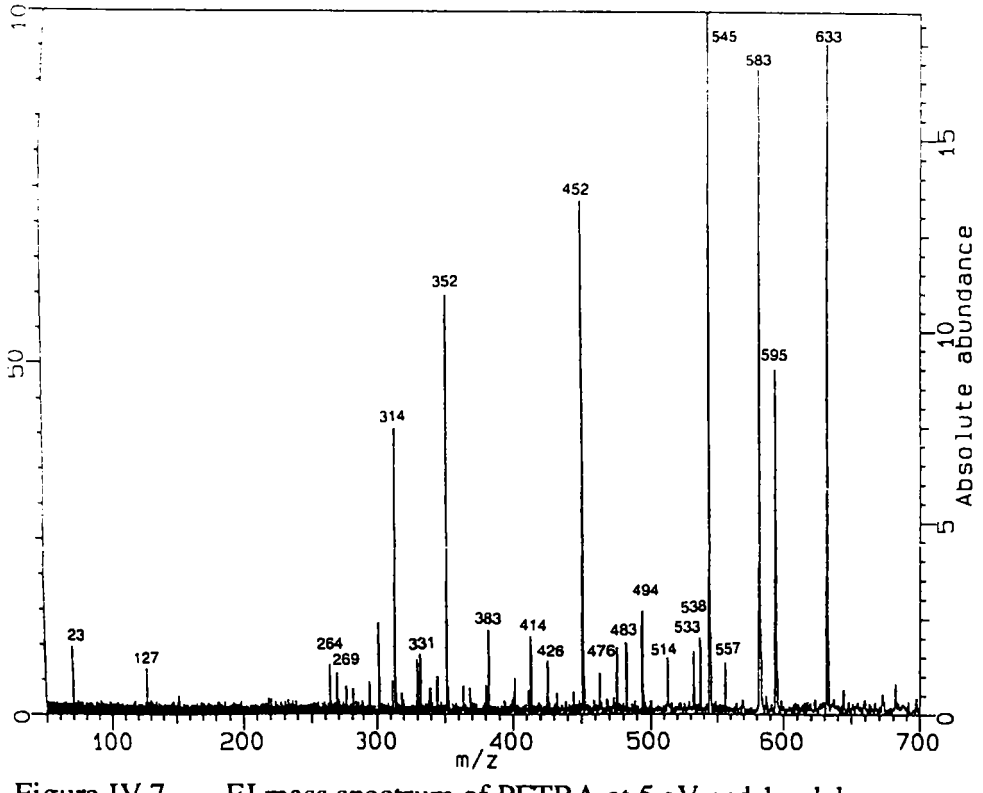

Figure IV.7. EI mass spectrum of PFTBA at 5 eV and 1 s delay.

Actually, there is no difference in the ions detected at 5 and 70 eV. The difference is in the absolute abundances of all ions that decrease with the voltage. Relative abundances remain the same.

Negative ion spectra obtained by standard EI ressemble to those obtained by laser induced electron capture ionization. In the laser experiment, remarkably high

quantities of *m/z* 633 and 452 ions,are detected, while the main products in EI spectra are ions *m/z* 545, 582.

It seems that "metal"-electrons have lower energy than those from EI and thus induce less fragmentation.

3.1.2. ECCI of Halothane

The electrons were produced by laser ablation of an aluminum target (λ = 355 nm, E =10^8 W cm^{-2}). Halothane ($BrCHClCF_3$, Mw = 198 u) sample was introduced to the chamber and ionized. Product of dissociative electron capture is observed :

$$e^- + BrCHClCF_3 \rightarrow Br^- + CHClCF_3$$

Bond strength of Br-C bond is the lowest in the molecule (274.9 ±6.3 kJ mol^{-1})[26] and thus Br^- is easily formed and thus mostly detected. In positive mode, the corresponding $[M-Br]^+$ ion was the most stable fragment detected.

3.1.3. ECCI of Dichlorodifluoromethane

Dichlorodifluoromethane (Cl_2CF_2, Mw = 120 u) was introduced in the chamber and ionized by electrons produced from laser ablation of aluminum target. Chlorine ions were mainly detected. In this case again, dissocciative electron capture occurs:

$$e^- + Cl_2CF_2 \rightarrow Cl^- + ClCF_2.$$

Table IV. 6. Bond strengths[26] in Cl_2CF_2

Bond	$D°_{298}$ / kJ mol^{-1}
F-$CFCl_2$	460 ± 25
Cl-$CClF_2$	318 ± 8

Comparison of the bond strengths in the molecule suggests the dissociation of Cl^- ion as the result of breaking the weakest bond in the molecule.

3.1.4. ECCI of Endosulfane

Electron capture ionization is competitive with Cl^- self chemical ionization of endosulfane. Thus, they are treated in parallel in part 3.3. of the present chapter IV.

3.2. *Negative Ion Chemical Ionization (NICI)*

Laser desorption/ablation of metal-halide salts produces large amount of halide ions. Such formed ions can be isolated and trapped in the FTMS cell. They are excellent ionizing reagents for negative ion chemical ionization.

3.2.1. NICI of PFTBA

Cl^- and F^- ions were produced by laser ablation of NaCl, KCl, $CaCl_2$ and LiF at 355 nm wavelength ($E = 10^9$ W cm^{-2}). Such formed ions were isolated and used for chemical ionization of gaseous molecules.

In the case of PFTBA molecule, the detected fragments were mainly the same as those obtained by electron chemical ionization. The main ion is still $[L-2F]^-$, *m/z* 633. If X^- (X = Cl, F) ions were left for longer time (few hundreds of ms) with PFTBA, the ions $[L-2F+X]^-$ were detected. F^- ions need somewhat shorter time than Cl^-. $[L-2F+F]^-$, *m/z* 652, were produced even after 0.2-0.4 s, Figure IV.8. The quantity of detected $[L-2F+Cl]^-$ ion depended on the time delay. $[L-2F+Cl]^-$ ion became the main product after 10 seconds.

The mass spectrum displayed in Figure IV.8.b. shows the formation of $[L-2F+X]^-$ ions. In this spectrum, both chlorine isotopes were isolated and left to react with PFTBA, thus the resulting ion has the isotopic distribution of two chlorine atoms, *m/z* 688, 670.

$$N(C_4F_9)_3 + X^- \longrightarrow [N(C_4F_9)_2 C_4F_7 + X]^- + F_2 \qquad X = F,\ Cl$$

At high irradiance ($E > 10^8$ W cm^{-2}) laser beam, electron are emitted from the metal-halide salt as well as halide ions. At short time delay they ionize PFTBA as in the case of ECCI. At longer reaction time, Cl^- and F^- "attack" the neutral molecules and halide attachment with subsequent F_2 elimination occurs.

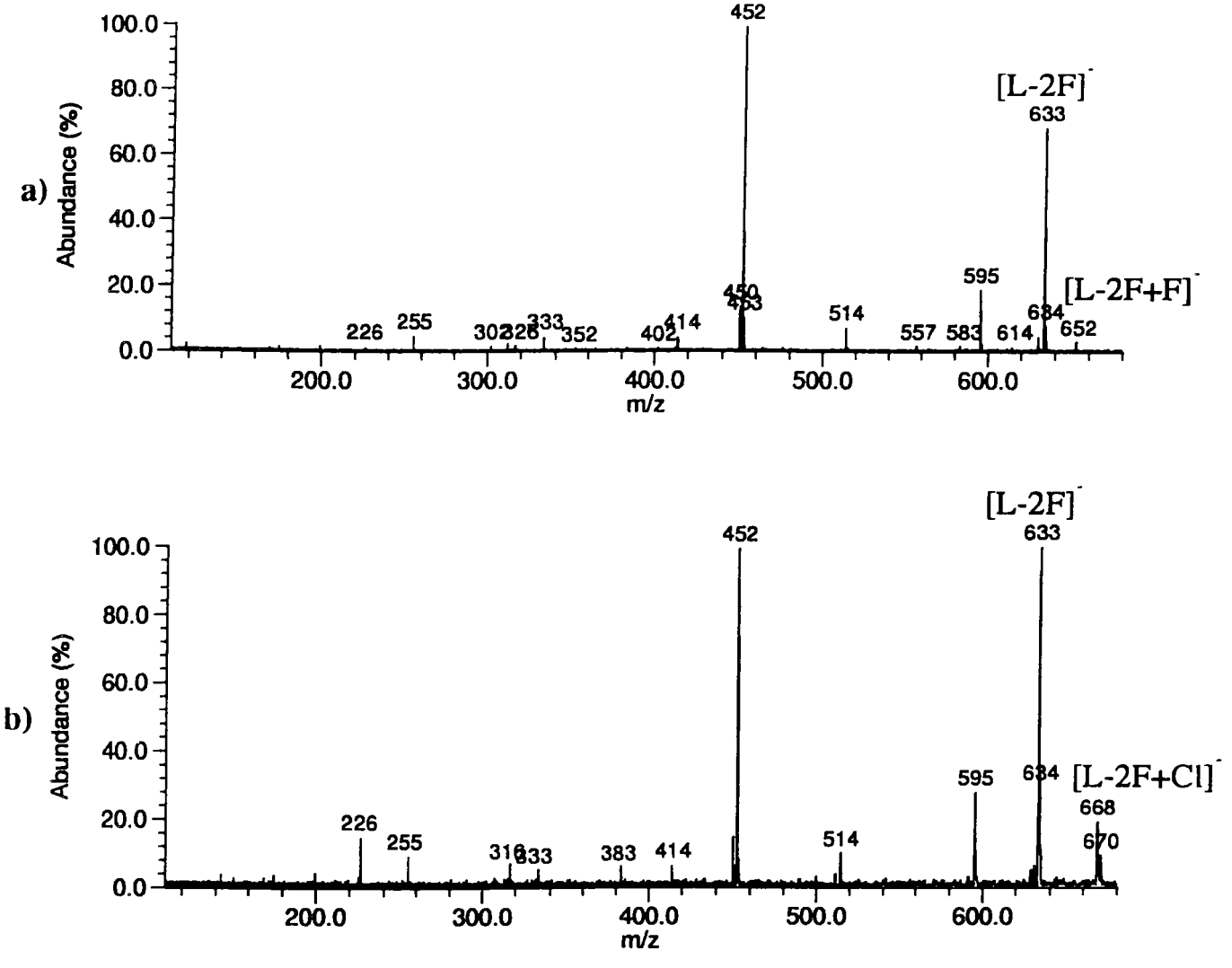

Figure IV.8. CI mass spectra of PFTBA with a) F^- reagent ion and b) Cl^- reagent ion.

3.2.2. Comparison of NICI and Positive Ion CI of PFTBA

All PFTBA detected fragment ions obtained by CI of PFTBA are summarized in Tables IV.7. and IV.8. There are some common filiations in positive and negative modes (outgreyed in the tables). Actually, we can not certify their structural similarities. Ions marked with an asterisk (*) are major products in the case of Mg^+ and Sn^+ reactions but are present only in low abundance in the case of Fe^+, Mn^+, Ti^+ and V^+.

Table IV.7. Negative PFTBA fragment ions (by ECCI)

	x=0	x=1	x=2	x=3	x=4	x=5	x=6	x=7	x=8	x=9	x=10
$NC_{12}F_{27-x}$	-	-	**633**	-	**595**	-	557	-	-	-	-
$NC_{11}F_{25-x}$	-	-	583	564	545	526	-	-	-	-	-
$NC_{10}F_{23-x}$	-	-	533	**514**	-	476	-	-	-	-	-
NC_9F_{21-x}	-	-	-	464	-	-	-	-	-	-	312
NC_8F_{19-x}	-	**452**	433	414	-	-	-	-	-	-	-
NC_7F_{17-x}	-	402	383	364	-	-	-	-	-	-	-
NC_6F_{15-x}	-	352	333	314	295	276	-	-	-	-	-
NC_5F_{13-x}	-	302	283	264	-	226	-	-	-	-	-
NC_4F_{11-x}	-	-	-	214	-	-	-	-	-	-	-
NC_3F_{9-x}	-	-	-	164	-	-	-	-	-	-	-
NC_2F_{7-x}	-	-	-	114	-	-	-	-	-	-	-

Table IV.8. Positive PFTBA fragment ions (by positive ion CI)

	x=0	x=1	x=2	x=3	x=4	x=5	x=6	x=7	x=8	x=9	x=10
$NC_{12}F_{27-x}$	-	**652**	633*	**614**	595*	576	557	-	-	-	-
$NC_{11}F_{25-x}$	-	602	-	-	545	526	-	-	469	-	-
$NC_{10}F_{23-x}$	-	552	533	-	-	476	-	-	-	-	-
NC_9F_{21-x}	-	**502**	-	464	-	426	-	-	-	-	-
NC_8F_{19-x}	-	-	-	**414**	395	376	-	-	-	-	-
NC_7F_{17-x}	-	402	-	364	-	326	-	-	-	-	-
NC_6F_{15-x}	-	352	-	314	295	-	-	-	-	-	-
NC_5F_{13-x}	-	-	-	264	-	226	-	-	-	-	-
NC_4F_{11-x}	-	-	-	214	-	176	-	-	-	-	-
NC_3F_{9-x}	-	-	-	164	-	-	-	-	-	-	-
NC_2F_{7-x}	-	-	-	114	-	-	-	-	-	-	-

3.2.3. NICI of Halothane

Chloride ions were produced by laser ablation of sodium chloride at 355 nm. Cl^- ions ionized halothane molecules but, as in the case of electron capture, Br^- gave the most intense peak. After some longer delay (all spectra were acquired at more than 1s reaction delay) $[L-H]^-$ and surprisingly $[L+F]^-$ are also detected:

$$Cl^- + BrCHClCF_3 \rightarrow Br^- + HCClCF_3 + \frac{1}{2}Cl_2$$

$$Br^- + BrCHClCF_3 \rightarrow BrCClCF_3^- + HBr$$

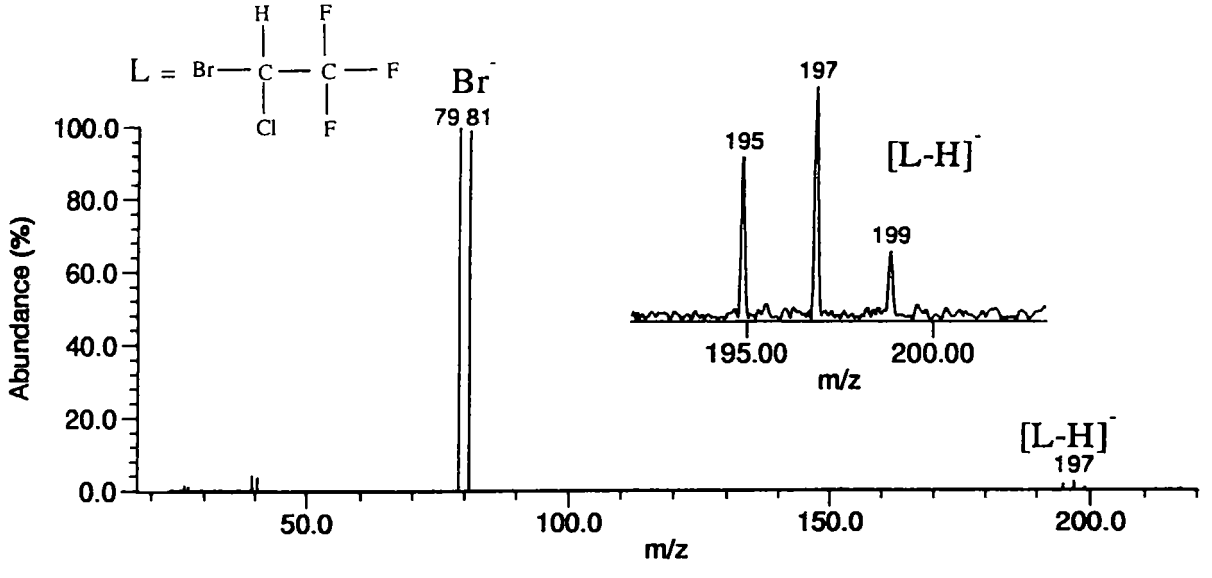

Figure IV.9. Negative ion mass spectrum of halothane ionized by Cl^- from NaCl target.

3.2.4. NICI of Dichlorodifluoromethane

To produce Cl^- reagent ions, sodium chloride target was irradiated by 355 nm laser beam. Dichlorodifluoromethane was introduced in the chamber by pulsed valves. Chlorine ion collided with molecules and few reaction occurred. Mass spectrum representing this reaction is shown in Figure IV.10. The reaction time was 1 s.

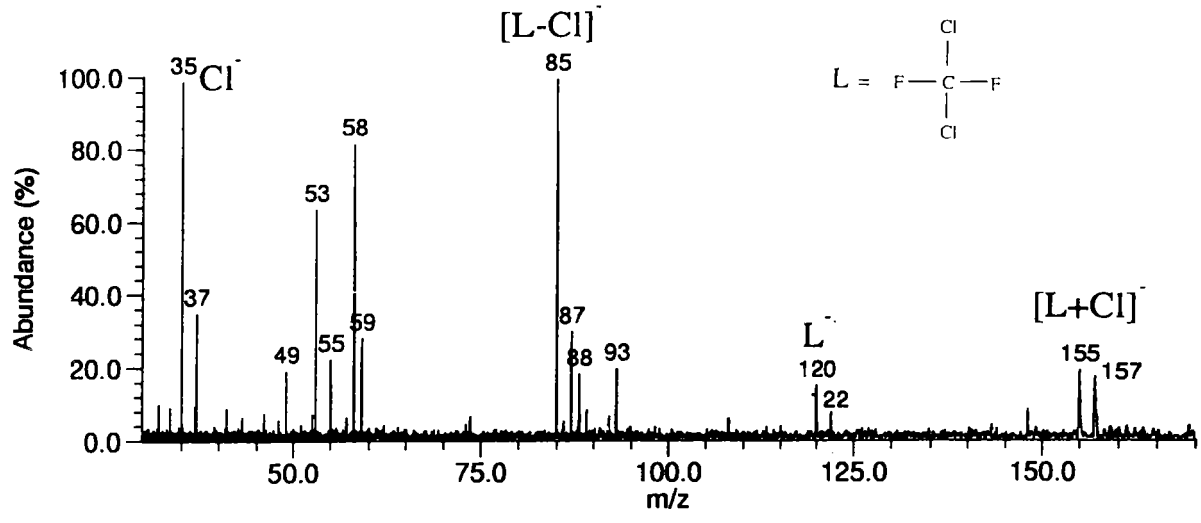

Figure IV.10. Negative ion mass spectrum of Cl_2CF_2 ionized by Cl^- from the NaCl target.

The charge-exchange reactions produce molecular ions (*m/z* 120). Few fragment ions were detected as well, namely $[L\text{-}Cl]^-$ (*m/z* 85) and Cl^-.

$$Cl^- + Cl_2CF_2 \rightarrow [Cl_2CF_2 + Cl]^-$$

$$\rightarrow Cl_2CF_2^- + \frac{1}{2}Cl_2$$

On the other hand, association reactions produce $[L+Cl]^-$ ions (*m/z* 155,157,159).

3.3. "Self negative ion chemical ionization" (SNICI)

If electrons produced by laser irradiation of metal sample have relatively high kinetic energy, dissociative electron attachment, as presented in IV.2.1.1. can occur. Dissociation of negative halogen ion showed to be favored. The produced negative halogen ion , X^-, can be used to ionize the neutral molecule remaining in the cell. X^- can be left for a long time in his "natural" motion or it can be resonantly excited and thus produces more collisions with neutral molecules. As the ionizing projectile comes from the neutral molecule that is the analyte itself, we called this method Self-Negative Ion Chemical Ionization (SNICI). SNICI with no excitation of ions and SNICI with excitation of X^- ions have to be dinstinguished.

3.3.1. Self-NICI of Dichlorodifluoromethane

As shown in 3.1.3. the electrons emitted from irradiated aluminum target induced dissociation of Cl^-:

$$e^- + Cl_2CF_2 \rightarrow Cl^- + ClCF_2.$$

Such formed chlorine ions were excited at their cyclotron frequency for 8 ms prior to reaction with dichlorodifluoromethane. Reaction time of one second allowed the association reaction with neutral molecules :

$$Cl^- + Cl_2CF_2 \rightarrow [Cl_2CF_2 + Cl]^-$$

Spectrum on Figure IV.11. presents self-chemical ionization of dichlorodifluoromethane .

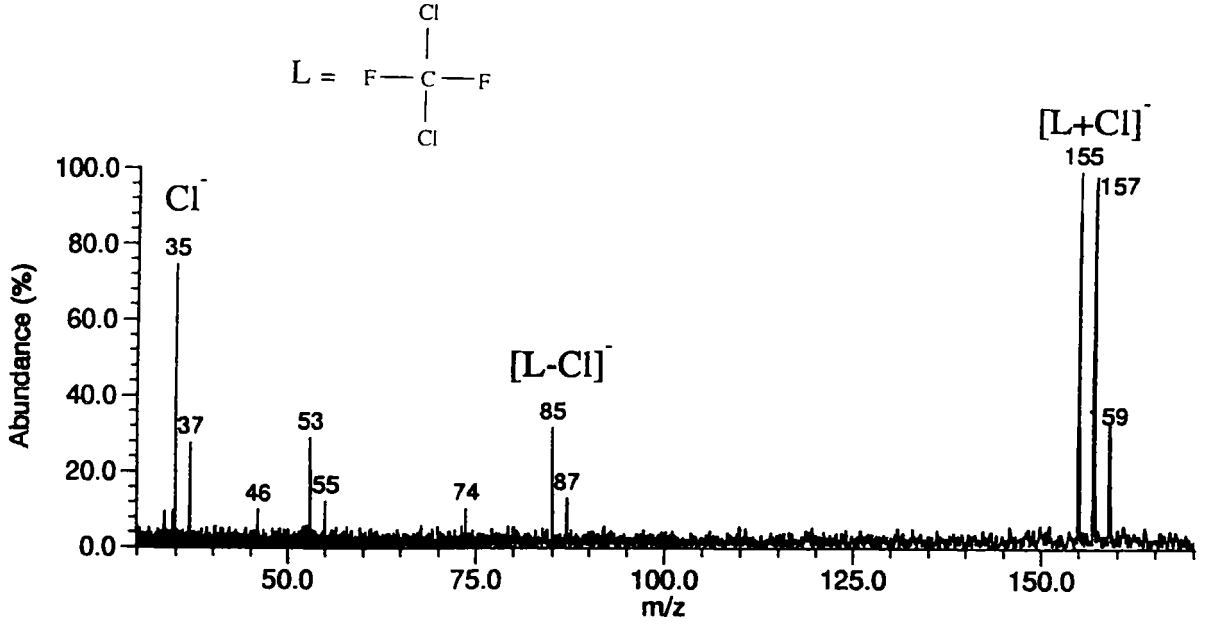

Figure IV.11. Negative ion mass spectrum of dichlorodifluoromethane by selfchemical ionization .

3.3.2. ECCI and Self-NICI of Endosulfane

Endosulfane powder sample was evaporated in the FTMS chamber from the

sample holder (p= 3 x 10^{-8} Torr). Aluminum target was mounted on another part of sample holder. Laser ablation of aluminum produced electrons that ionized evaporated endosulfane molecules.

Several parameters may influence the endosulfane detection. Laser wavelength did not change obtained spectra. Changing irradiance from 10^9 to 10^6 Wcm^{-2} did not change Cl^- as the main product. The time delay between laser shot and excitation of ions was very important. In Figure IV.12. mass spectra with different delays are displayed.

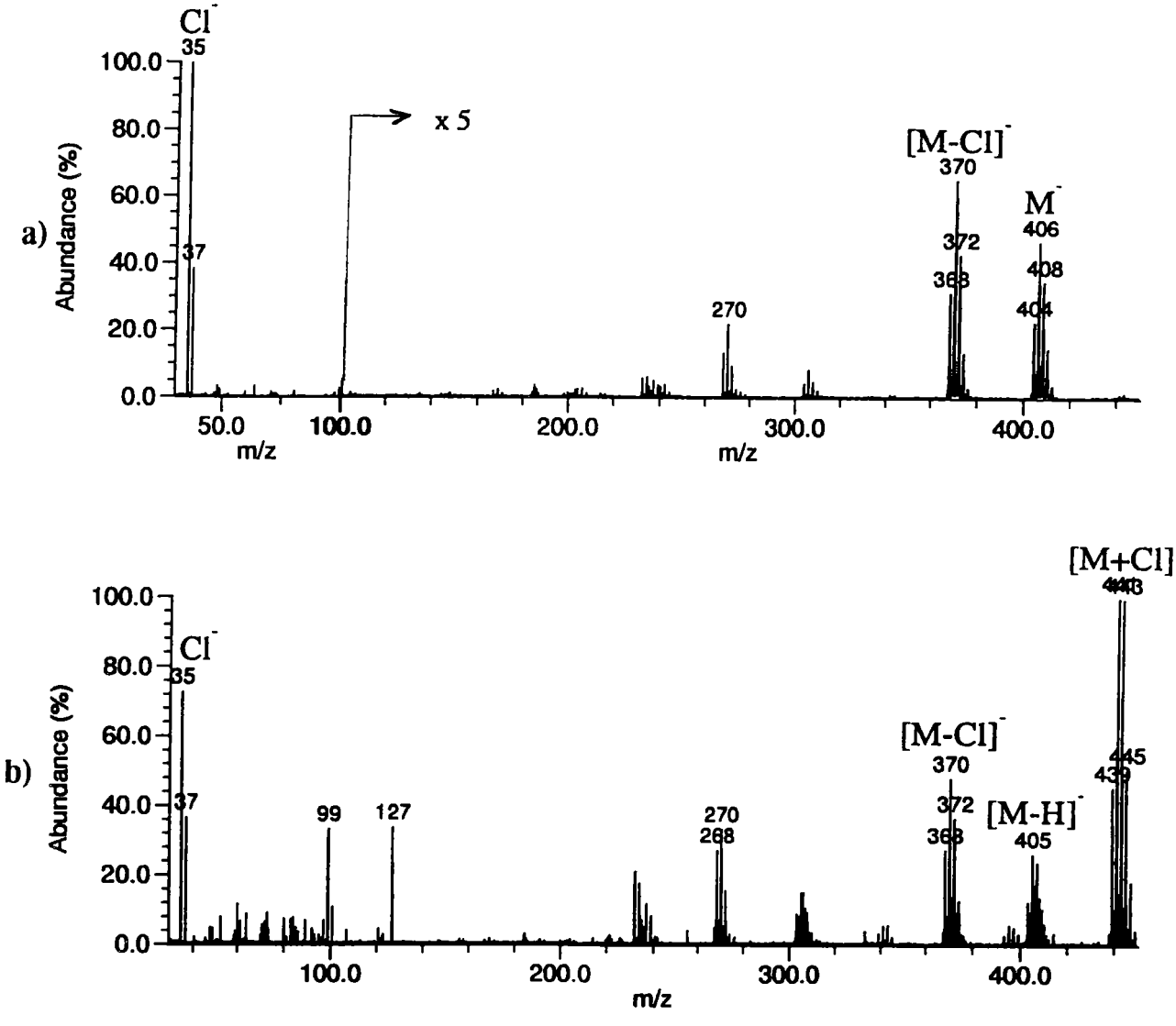

Figure IV.12. Mass spectra of endosulfane at a) 5ms and b) 1s delay.

At short delay (< 50 ms) ions Cl^-, L^-, $[L\text{-}HCl]^-$, $[L\text{-}HCl\text{-}SO_2]^-$, $[L\text{-}2HCl\text{-}SO_2]^-$ are detected as shown in Figure IV.12 a. Cl^- is the main product. There is

clearly pronounced (almost) single isotopic distribution of L^- .

With a longer "reaction" time (≥ 50 ms), $[L-H]^-$ and $[L+Cl]^-$ ions appears (Figure IV.12.b). Almost each ion begins to have parallel deprotonated distribution. It is specially pronounced for L^- ion. With a longer delay, $[L-H]^-$ ion became more important than L^- ion as shown in graph in Figure IV.13.

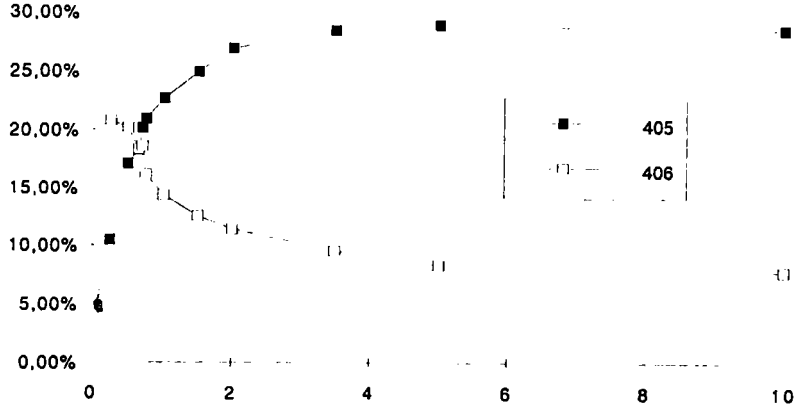

Figure IV.13. Time evolution of $L^{-\cdot}$ (406) and $[L-H]^-$ (405) ions of endosulfane.

Thus, we can distinguish two modes of ionization of endosulfane: electron capture and selfchemical ionization by Cl^- ions.

ECCI

Electron capture occurs through electron attachment mechanism immediately after the laser shot:

$$e^- + L \rightarrow L^-,$$

and through dissociative electron attachment, where Cl^- is the main dissociation ion product:

$$e^- + L \rightarrow Cl^- + [L-Cl]$$

and

$$e^- + L \rightarrow [L-HCl]^- + HCl$$

Monitoring of the time evolution of $[L-Cl]^-$ and $[L-H-Cl]^-$ in comparison with L^- and $[L-H]^-$ ions (Figure IV.14.), shows that $[L-Cl]^-$ and $L-HCl]^-$ are not fragments from L^- and $[L-H]^-$ ions. They are products of dissociative reactions competitive to

electron attachment.

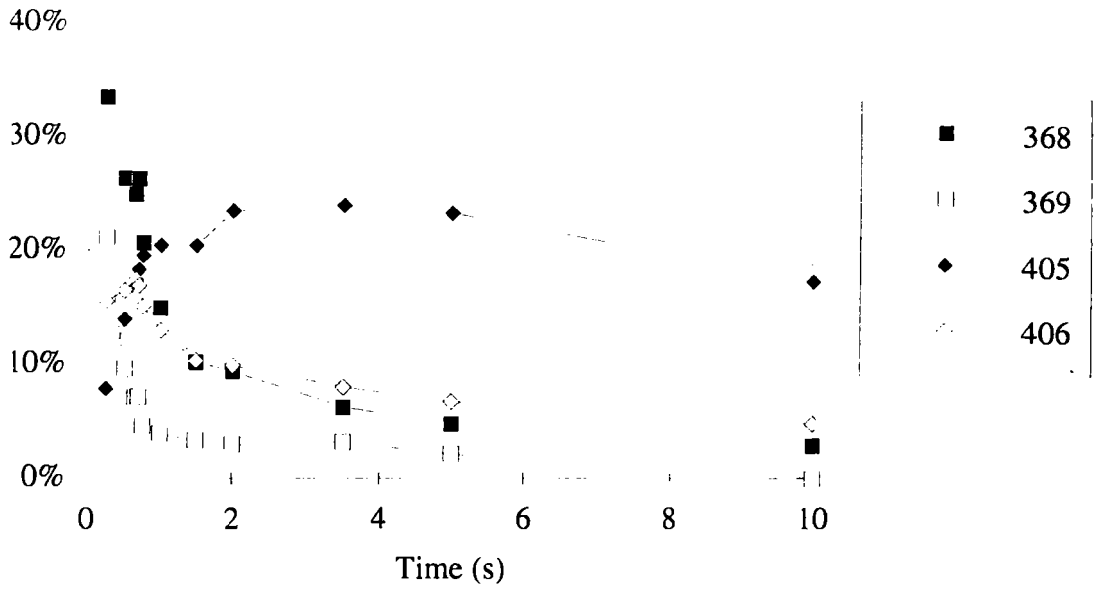

Figure IV.14. Time evolution of $[L-Cl]^-$ (369) and $[L-HCl]^-$ (368) in comparison with L^- (406) and $[L-H]^-$ (405) ions.

Self-NICI

Dissociated Cl^- ion served as ionizing species for remaining substrate molecules. The selfchemical ionization (association reaction) by Cl^- ions occurred:

$$Cl^- + L \rightarrow [L + Cl]^-$$

At the same time, proton transfer gave rise to $[L-H]^-$ ion:

$$Cl^- + L \rightarrow [L - H]^- + HCl$$

$[L+Cl]^-$ ion appears at about 50 ms delay, and at about 200 ms becomes the main product apart from Cl^-. A spectrum with 1 s delay is shown in Figure IV.15. There is parallel formation of $[L-H+Cl]^-$ ions, followed by yield of ions at *m/z* 395.

To prove the implication of Cl^- ionin the production of $[L+Cl]^-$ and $[L-H]^-$ ions, Cl^- was ejected from the cell and long delay (1s) was allowed before excitation. When comparing the spectra in the Figure IV.15. a) and b) obtained with the same delay, it is obvious that without Cl^-, the formation of $[L-H]^-$ ions is almost negligible.

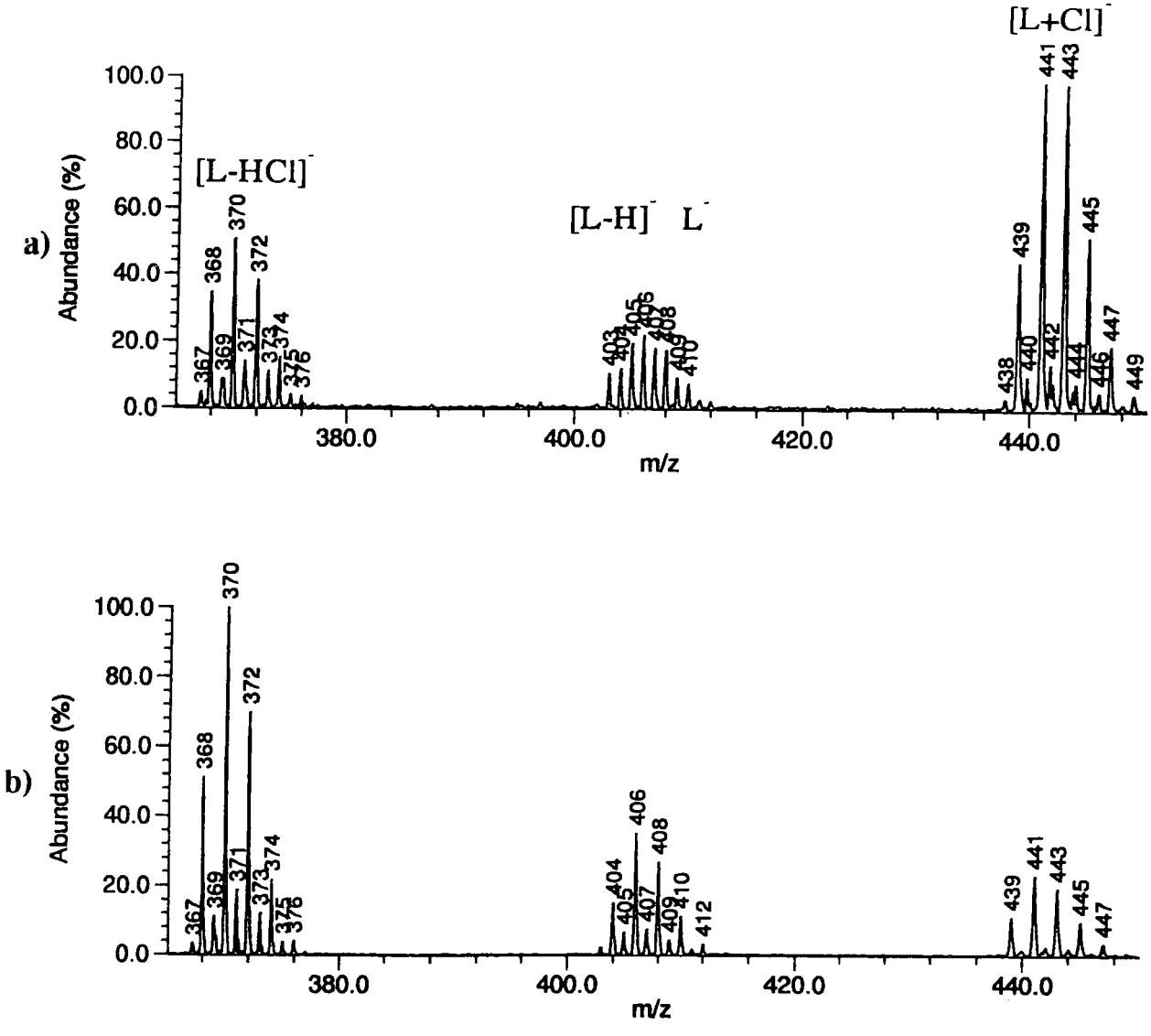

Figure IV.15. Mass spectra obtained a) without ejection of Cl^- ; b) with ejection of Cl^-. Delay before excitation was 1s.

Ejection of Cl^- has no influence on the formation of L^- ion that was formed by electron attachment. On the contrary, ions $[L-H]^-$ and $[L+Cl]^-$ are products of Cl^- reaction with L, and Cl^- ejection influence strongly the formation of those ions. Lower mass fragments seem to be yielded by fragmentation of two main units (H)Cl and $(H)SO_2$ as assigned in Table IV.6.

3.4 Internal calibration with PFTBA molecule

For the assignation of detected organic molecular and fragment ions internal calibration is recommended. We searched for a calibrant adapted for negative mode

ionization and thus with similar electron affinities as studied halogenated molecules.

PFTBA molecule (as already well known calibrant in EI MS) with its well defined fragments was tested in internal calibration of halogenated molecules. Here we present the sample calibration of endosulfane.

Endosulfane sample was evaporating from the sample holder in the chamber ($p=10^{-8}$ Torr). PFTBA molecules were introducing by batch inlet (p = 250 mTorr, PSource = $5 \cdot 10^{-8}$). Laser pulse was directed to aluminum target and simultanious ionization of PFTBA and endosulfane molecules occurred. Series of PFTBA fragments (*) and Cl^- ions allowed calibration through the mass range of the endosulfane sample. Figure IV.16. displays the mass spectrum with the detected endosulfane and PFTBA ions. Calibration table with PFTBA peaks and chloride peaks gives confidence level of 3 Hz and an average absolute error of 7 ppm. The assignation of detected peaks is given in the Table IV.9.

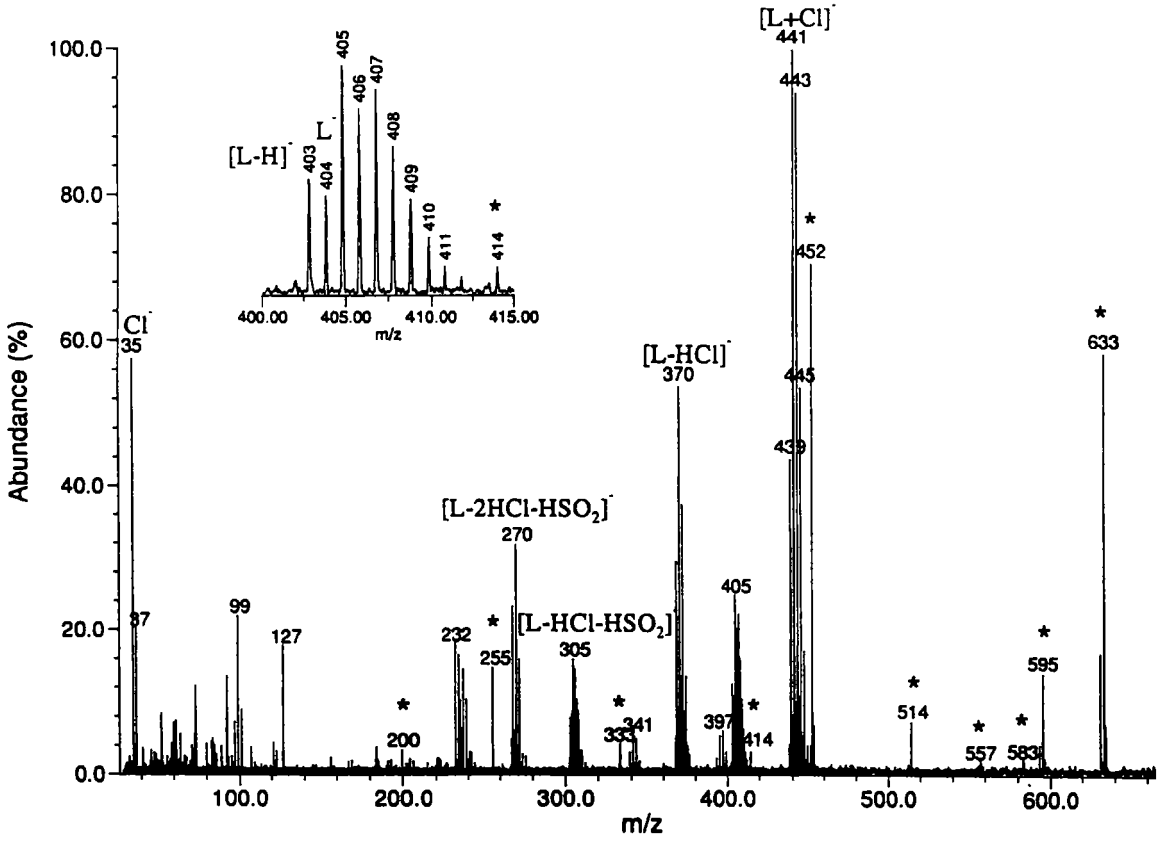

Figure IV.16. Mass spectrum of endosulfane with PFTBA* as a internal calibrant.

Table IV.9. Assignation of detected negative ions in mass spectrum of endosulfane (L).

m/z	Assignation	Elemental composition
439-449	$[L+Cl]^-$	$[C_9H_6SO_3Cl_7]^-$
438-448	$[L+Cl-H]^-$	$[C_9H_5SO_3Cl_7]^-$
404-412	L^-	**$[C_9H_6SO_3Cl_6]^-$**
403-411	$[L-H]^-$	$[C_9H_5SO_3Cl_6]^-$
369-377	$[L-Cl]^-$	$[C_9H_6SO_3Cl_5]^-$
368-376	$[L-HCl]^-$	$[C_9H_5SO_3Cl_5]^-$
339-347	$[L-SO_2H]^-$	$[C_9H_5OCl_6]^-$
304-310	$[L-HCl-SO_2]^-$	$[C_9H_5OCl_5]^-$
303-309	$[L-HCl-HSO_2]^-$	$[C_9H_4OCl_5]^-$
268-274	$[L-2HCl-SO_2]^-$	$[C_9H_4OCl_4]^-$
267-273	$[L-2HCl-HSO_2]^-$	$[C_9H_3OCl_5]^-$
235-241	$[L-2HCl-C_4H_4SO_3]^-$	$[C_5Cl_5]^-$
99-101		SO_2Cl

4. Conclusion

In negative chemical ionization experiments, three methods were employed depending on the ionizing projectiles.

Electrons produced by laser irradiation of different metal samples and silicon wafer ionized neutral gas molecules by electron capture. In our case resonance electron capture or dissociative electron capture products were detected. Electrons were produced in a large irradiance band: from high irradiance (10^9 Wcm^{-2}) to low irradiance (photoelectrons).

When metal halide salts were irradiated by laser, production of halogenid negative ions and electrons occurred. They were used for the ion chemical ionization (NICI) of the studied molecules.

Dissociative electron attachment can produce halide ions from the original gas molecule. Such ion can ionize other neutral molecules and so-called "Self Negative Ion Chemical Ionization" (Self-NICI) occurred.

In this chapter we showed that those methods are well adapted for ionization of halogenated organic compounds (positive electron affinities). The main products of all three modes of ionization are summarized in table IV.10.

Table IV.10. The basic detected product by different used methods of studied molecules

Molecule	**(Dissociative) ECCI**	**NICI**	**Self-NICI**
Cl_2CF_2	Cl^-	L^-, $[L+Cl]^-$	$[L+Cl]^-$
$BrCHClCF_3$	Br^-, $[L-H]^-$	Br^-, $[L-H]^-$, $[L+F]^-$	
$C_9H_6SO_3Cl_6$	L^-, Cl^-		$[L-H]^-$, $[L+Cl]^-$
PFTBA	$[L-2F]^-$	$[L-2F+X]^-$	

Molecular or quasi-molecular ions and corresponding fragments were detected for all molecules. Used methods are complementary. Moreover, they are complementary with positive mode chemical ionization (ion-molecule reactions).

PFTBA molecule was shown to be a reliable internal calibrant for polyhalogenated compounds. The PFTBA fragments in the range of *m/z* 633-200, together with halide ion (*m/z* 35 in the case of Cl^-), allow the calibration of the acquired spectra in a broad mass range.

References

1 H. Budzikiewicz, *Mass Spectrom. Rev.*, **5,** 345 (1986).

2. D.F. Hunt, G.C. Stafford Jr, F.W. Crow and J.W. Russell, *Anal. Chem.*, **48,** 2098 (1976).

3. M. Von Ardenne, K. Steinfelder and R. Tuemmler, *Electronen-anlagerungs-Massenspektrographie Organicher Substanzen*, Springler-Verlag, New York, (1971)

4. R.C.Dougherty and C.R. Weisenberger, *J. Am. Chem. Soc.*, **90,** 6570 (1968).

5. a) S. Martinovic, Lj. Pasa-Tolic, D. Srzic, N. Kezele, N. Plavsic, and L. Klasinc, *Rapid Commun. Mass Spectrom.*, **10,** 51 (1996).

   b) D. Srzic, Lj. Pasa-Tolic, S. Martinovic, N. Plavsic, and L. Klasinc, *Rapid Commun. Mass Spectrom.*, **8**, 56 (1994).

7. M. Gregoti, P. Castelnovo, J. Mass Spectrom. **31**, 994, (1996).

8. J.R. Chapman "Practical Organic Mass Spectrometry-A Guide for Chemical and Biochemical Analysis" John Wiley & Sons, Chichester, 2nd ed. (1993).

9. J.H. Bowie, *Mass Spectrom. Rev.*, **3,** 161 (1984).

10. B.M. Smirnov, Negative Ions; McGraw-Hill; New York, (1982).

11. L.G. Christophorou, *Environ. Health. Perspec.*, **36,** 3 (1980).

12. D.F. Hunt and F.W. Crow, *Anal. Chem.*, **50,** 1781 (1978).

13. V.S. Ong and R.A. Hites, *Mass Spectrom. Rev.*, **13,** 259 (1994).

14. A.G. Harrison "Chemical Ionization Mass Spectrometry" CRC Press, Boca Raton, Fl. 2nd ed. (1992).

15. H. Budzikiewicz, *Angew. Chem. Int. Ed. Engl.*, **20,** 624 (1981).

16. J.G. Dillard, *Chem. Rev.*, **73,** 589 (1973).

17. L.G. Christophorou, R.N. Compton, G.S. Hurst, G.S. Reinhardt, *J. Chem. Phys.*, **45,** 536 (1996).

18. P.J. Chantry and G.J. Schulz, *Phys. Rev.*, **156,** 134 (1967).

19. D.F. Hunt and F.W. Crow, *Proceedings of the 9th Materials Research Symposium*, April 1978, NBS Special Publication 519, National Bureau of Standards, Washington, D.C. pp.601-607 (1979).

20. a) E.A. Stemmler and R.A. Hites, *Biomed. Mass Spectrom.*, **15,** 659 (1988).

    b) J.A. Laramee, B.C. Arbogast, M.L. Deinzer, *Anal. Chem.*, **58,** 2907 (1986).

21. G.J.Q. Van der Peyl, W.J. Van der Zande, P.G. Kistemaker, *Int. J. Mass Spectrom. Ion Processes*, **62**, 51 (1984)

22. A. Vertes, P. Juhasz, M. De Wolf and R. Gijbels, *Scaning Microsc.*, **2,** 1853 (1988)

23 A. Vertes, M. De Wolf, P. Juhasz and R. Gijbels, *Anal. Chem.*, **61,** 1029 (1989)

24. F. Moritz, M. Dey, K. Zipperer, S. Prinke and J. Grotemeyer, *Org. Mass. Spectrom.*, **28,** 1467 (1993).

25. L. Bergman and C. Schäfer, Lehrbuch der Experimentalphysik, Vol. III, 7th ed., pp. 700-711. Walter de Gruyter, Berlin (1978).

26. CRC Handbook of Chemistry and Physics, Ed.by. D. R. Lide, 73rd ed., CRC Press, Boca Raton, Florida, (1992-1993).

27. S. M. Colby and J. P. Reilly, *Int. J. Mass Spectrom. Ion Processes,* **131,** 125 (1994).

28. D. C. Schriemer and L. Li, *Anal. Chem.*, **68,** 250 (1996).

29. J. Ha, J.D. Hogan, and D.A. Laude, Jr., *J. Am. Soc. Mass Spectrom.*, **4,** 159 (1993)

30. K.R. Jennings, in Specialist Periodical Report, Mass spectrometry, Vol 4. (Ed. R.A.W. Johnstone), p.203, Chemical Society, London.

31. R.C. Dougherty, *Anal. Chem.*, **53**, 625A (1981).

32. A.L. Ganguly, N.F. Cappuccino, H. Fujiwara, and A.K. Bose, *J.Chem.Soc. Chem. Commun.*, **?**, 148 (1979).

33. H.P. Tannenbaum, J.D. Roberts, and R.C. Dougherty, *Anal. Chem.*, **47**, 49 (1975).

34. a) R.C. Dougherty, M.J. Whitaker, L.M. Smith, D.L. Stalling, and D.W. Kuehl, *Environ. Health. Perspect.*, **36,** 103 (1980)

b) R.C. Dougherty, *Biomed. Mass Spectrom.*, **8,** 283 (1981)

c) D.W. Kuehl, M.J. Whitaker, and R.C. Dougherty, *Anal. Chem.*, **52,** 935 (1980).

35. G.W. Caldwell, J.A. Masucci and M.G. Ikonomou, *Org. Mass Spectrom.*, **24**, 8 (1989)

36. G.D. Byrd, Ph.D. Thesis, Purdue University, (1982).

37. D.A. Weil, and C.L. Wilkins, *J. Am. Chem. Soc.*, **107**, 7316 (1985).

38. a) B.S. Freiser, *J.Mass Spectrom.*, **31**, 703 (1996).

b) J.W. Larson and T.B. McMahon, *J. Phys. Chem.*, **88,** 1083 (1984).

c) L. Sallans, K.R. Lane and B.S. Freiser, *J. Am. Chem. Soc.*, **111,** 865 (1989).

d) L. Sallans, K.R. Lane, R.R. Squires and B.S. Freiser, *J. Am. Chem. Soc.*, **107**, 4379 (1985).

39. A. McIntosh, T. Donovan, and J. Brodbelt, *Anal. Chem.*, **64**, 2079 (1992).

40. J.F. Muller, Mémoires et Etudes Scientifiques Revue de Métallurgie - Septembre 1982, p. 482.

41. R.F. Haglund, and N. Itoh in "Laser Ablation, Principles and Applications", Ed. J.C. Miller, Springler-Verlag, Berlin, pp.26-28, (1994).

42. a) T. Cairns, L. Fishbein, R.K. Mitchum, *Biochem. Mass Spectrom.*, **7,** 484 (1980)

b) N.H. Mahle, and L.A. Standoff, *Biochem. Mass Spectrom.*, **9,** 45 (1982)

c) W.F. Miles, N.P. Gurprasad, and G.P. Malis, *Anal. Chem.*, **57,** 1133 (1985).

d) P.P. Schmid, M.D.J. Müller, *J. Asocc. Off. Anal. Chem.*, **68,** 427 (1985).

43 a) P.W. Harland and J.C.J Thynne, *Int. J. Mass Spectrom. Ion Phys.*, **10,** 11 (1972).

b) P.W. Harland and J.C.J Thynne, *J. Chem. Phys.*, **74,** 52 (1970).

c) T.Su and L.J. Kevan, *J. Chem. Phys.*, **77,** 148 (1973).

d) A.A. Christodoulides, L.G. Christophorou, R.Y. Pai and C.M.J. Tung, *J. Chem. Phys.*, **701**, 156 (1979).

44. D. Lifshitz, and R. Grajower, *Int. J. Mass Spectrom. Ion Phys.*, **10,** 25 (1972).

45 W.T. Naff, C.D. Cooper, and R.N. Compton, *J. Chem. Phys.*, **49,** 2784 (1968).

46. K.S. Grant, and L.G. Christophorou, *J. Chem. Phys.*, **65,** 2784 (1976).

47. Z. Luczynski, and H. Wincel, *Int. Radiat. Phys. Chem.*, **7,** 705 (1975).

48 L.G. Christophorou, R.N. Compton, G.S. Hurst, P.W. Reinhardt, *J. Chem. Phys.*, **45,** 536 (1966).

49. H. Dispert, and K. Lacmann, *Int. J. Mass Spectrom. Ion Phys.*, **28,** 49 (1978).

50. R. Hashemi, A. Kühn and E. Illenberger, *Int. J. Mass Spectrom. Ion Processes*, **100,** 753 (1990).

51. a) P.O. Staneke, G. Groothuis, S. Ingemann and N.M.M. Nibbering, *J. Phys. Organic Chemistry*, **7,** 471 (1996).

b) P.O. Staneke, G. Groothuis, S. Ingemann and N.M.M. Nibbering, *Int. J. Mass Spectrom. Ion Processes*, **150,** 99 (1995).

c) P.O. Staneke, G. Groothuis, S. Ingemann and N.M.M. Nibbering, *Int. J. Mass Spectrom. Ion Processes*, **142,** 83 (1995).

d) M. Born, S. Ingemann and N.M.M. Nibberring, *J. Am. Chem. Soc.*, **116,** 7210 (1994).

52. F.W Crow, A Bjorseth, K.T Knapp and R. Bennett, *Anal. Chem.* **53,** 619 (1981).

53. a) M.Deinzer, D. Griffin and T. Miller, *Biomed. Mass Spectrom.*, **6,** 301 (1979).

b) K.L. Busch, A. Norström, C.-A. Nilsson, M.M. Bursey and J.R. Hass, *Environ. Hlth. Persp.*, **36,** 125 (1980).

54. C. Rappe, H.R. Buser, D.L. Stalling, L.M. Smith and R.C. Dougherty, *Nature*, **292,** 524 (1981).

55. R.C. Dougherty, M.J. Whitaker, L.M. Smith, D.L. Stalling and D.W. Kuehl, *Environ. Hlth. Persp*, **36,** 103 (1980).

56. R. A. Hites, *Int. J. Mass Spectrom. Ion Processes*, **118/119,** 369 (1992).

57. a) *Analytical News*, pp.8-9, Spring 1996.

b) F.L. Lépine, S. Milot and O.A. Mamer, *J. Am. Soc. Mass Spectrom.*, **7,** 66 (1996).

c) R. J. Letcher and R.J. Norstrom, *J. Mass Spectrometry*, **32,** 232 (1997).

d) R. Théberge and M. Bertrand, *J. Am. Soc. Mass Spectrom.*, **7,** 1109 (1996).

e) J.G. Dillard, *Biochemical Applications of Mass Spectrometry* **Chap 28** 927-945 (1980).

f) M.A. Dearth and R.A. Hites, *J. Am. Soc. Mass Spectrom.*, **1**, 99 (1990).

g) J.A. Laramée, C.A. Kocher and M.L. Deinzer, *Anal. Chem.*, **64**, 2316 (1992).

58. P. Kebarle and S. Chowdhury, *Chem. Reviews*, **87**, 513 (1987).

59. E.F. Cromwell, K. Reihs, M.S. de Vries, S. Ghaderi, H.R. Wendt and H.E. Hunziker, *J. Phys. Chem.*, **97**, 4720 (1993).

60. a) S. Catinella, P. Traldi, X. Jiang, F.A. Londry, R.J.S. Morrison, R.E. March, S. Grégoire, J-C. Mathurin and J-C Tabet, *Rapid Comm. Mass Spectrom.*, **9**, 1302 (1995).

b) J-C. Mathurin, S. Grégoire, A. Brunot, J-C Tabet, R.E. March, S. Catinella and P. Traldi, Accepted for publication in *Int J. Mass Spectrom. Ion Processes.*

Overall Conclusion

Laser induced plasma products were successfully used for the chemical ionization of volatile polyhalogenated organic molecules. Positive and negative mode ionization were studied by Fourier transform ion cyclotron resonance mass spectrometry.

We can conclude that the applied chemical ionization methods are complementary and give adequate information about the studied compounds.

Detected ions concerning molecular, quasi-molecular related adduct ions of all the studied compounds are briefly summarized in the following table:

Compound	**Positive Ions**				**Negative Ions**		
Acetophenone $C_6H_5COCH_3$	ML_n^+	$[L+H]^+$	L^+				$[L-H]^-$
PFTBA $(C_4F_9)_3N$	ML^+			$[L-F]^+$	$[L-F_2+X]^-$, $[L-F_2]^-$		
TBA $(C_4H_9)_3N$	ML_n^+	$[L+H]^+$	L^+		not detected		
Dichlorodifluoromethane Cl_2CF_2				$[L-F]^+$ $[L-Cl]^+$	$[L+Cl]^-$	L^-	
Halothane $BrCHClCF_3$			L^+	$[L-Br]^+$	$[L+F]^-$		$[L-H]^-$
Endosulfane $C_9H_6SO_3Cl_6$	ML^+	$[L+H]^+$	L^+		$[L+Cl]^-$	L^-	$[L-H]^-$

(M = metal; L^+ or L^- = molecular ion)

Positive chemical ionization occurs *via* ion/molecule reactions. To establish the experimental procedure and understand involved mechanisms, a model system was first studied. For that purpose the acetophenone molecule was chosen, because its behavior towards some positive metallic ions was already known. Laser produced elemental positive ions were allowed to react with acetophenone. Ions from different groups of elements (M^+ = Na^+, Mg^+, Ca^+, Ba^+, Ti^+, V^+, Cr^+, Mn^+, Fe^+, Co^+, Ni^+, Cu^+, Zn^+, Al^+, In^+ and Si^+) were studied as projectile (reagent) ions. The presented results are in agreement with those previously reported in the literature for the reactions of Fe^+, Ni^+ and Al^+ with acetophenone. Several additional reaction pathways have been deduced from our experiments:

i) the formation of ML_n^+ complexes (n = 2 for M = Na, Cr, Fe, Ni, Co, Cu, Zn, In; n = 2-3 for M = Ba, Al; n = 2-4 for M = Mg, Ca, Mn);

ii) besides, Fe^+, Co^+ and Ni^+ involve decarbonylation of formed complex with ligand;

iii) Ti^+ and V^+ bind oxygen atom; dehydrogenation and dehydration of complexes is observed.

iv) products of oxygen abstraction by Si^+ are detected.

The reactivities of metal positive ions towards acetophenone molecule are correlated with their electronic configuration, and they are in agreement with their promotion energies.

After establishing experimental conditions and defining the processes in the (model) reactions between ions produced by laser ablation and acetophenone, we applied them for ionization of polyhalogenated molecules.

Laser produced ions (mainly transition metal-, alkaline-, earth-alkaline-), (M^+ = Li^+, Na^+, K^+, Mg^+, Ca^+, B^+, Ti^+, V^+, Mn^+, Cr^+, Fe^+, Ni^+, Co^+, Cu^+, Zn^+, Al^+, In^+, Sn^+, Zr^+ ,Mo^+ and Si^+) were isolated and reacted with perfluorotributylamine (PFTBA, L). Various reaction products have been detected depending on the reagent (projectile) ions. Several types of reaction behavior can be distinguished from the obtained results:

i) common fragmentation; for all studied M^+ except Mg^+, Ca^+, Cr^+, and Sn^+;

ii) the formation of LM^+ complexes for Li^+, Na^+, Ni^+, Co^+, Cu^+, and Zn^+;

iii) the formation of $[LM - 2F]^+$ for Na^+, Ni^+, Co^+, Cu^+ and Zn^+;

iv) the abstraction of fluoride by metal for all studied M^+ except Mg^+, Ca^+, Cr^+, and Sn^+;

v) the abstraction of F_2 by metal for Mg^+, Sn^+, Ti^+, V^+, and Mn^+;

vi) the formation of LMF^+ and $[LM - F]^+$ complexes for Ca^+;

vii) the formation of $[L\text{-}C_4H_9+M]^+$ for Ca^+ and Co^+.

Molecular ion (L^+) was not detected. Reactivities of the transition metal ions were correlated to their electronic configuration and promotion energy. Nevertheless, there are several observed reactions that still need mechanistic explanation.

Reactions of the perfluorinated amine (PFTBA) were compared to several analog reactions of the hydrogenated one (TBA). Mechanisms of reactions of TBA and PFTBA are not the same. Apart of amine characteristics, perhalogenation plays an important role in the behavior of the molecules. PFTBA has high electron affinity while TBA has very high proton affinity. Nitrogen lone pair should be more available

in TBA than in PFTBA, where fluorine withdraws the electrons.

Positive ion ionization was applied to other polyhalogenated molecules: dichlorodifluoromethane, halothane and endosulfane were ionized by laser produced positive ions. Molecular ion or products of halogen abstraction were mainly detected as presented in the "conclusion" Table.

Excitation of cyclotron motion of laser produced positive reagent ions has been performed in order to induce high fragmentation of PFTBA molecule. The control of experimental parameters allows the control of the fragmentation. Mass spectra containing well known metal adduct ions (up to *m/z* 740), well defined PFTBA fragment ions (*m/z* 69-652) as well as some metal ions, give the large mass range (~ *m/z* 20-740) for the calibration. This is even broader than PFTBA fragments range in EI experiments (*m/z* 69-502). Such obtained series of ion is useful for both regular instrument and spectral calibration.

To accomplish analysis of polyhalogenated molecules, negative chemical ionization has been performed. Those molecules have high electron affinity and thus easily form negative ions. Again, PFTBA, dichlorodifluoromethane, halothane and endosulfane were under investigation.

We employed three ionizing methods according to the reagent species.

Electrons produced by laser irradiation of different pure metal samples and silicon wafer ionized neutral gas molecules by electron capture. In our case, resonance electron capture or dissociative electron capture products were detected. Electrons were produced in a large irradiance range: from the high irradiance (10^9 Wcm^{-2}) to low irradiance (photoelectrons).

When metal halide salts were irradiated by laser, halide ions were formed. They were used for the ion chemical ionization (NICI) of studied molecules.

Dissociative electron capture can produce halide ions from the original gas molecule. Such ions can react with other neutral molecules and so-called "Self Negative Ion Chemical Ionization" (SelfNICI) occurred.

We showed that those methods are well adapted for ionization of polyhalogenated organic compounds (positive electron affinities). Molecular or quasi-molecular ions and corresponding fragments were detected for all molecules. Not any of methods can be considered as universal. They are complementary. Moreover, they are complementary with positive mode chemical ionization (ion/molecule reaction).

PFTBA showed to be a well adapted internal calibrant for laser induced chemical ionization of halogenated molecules in positive and negative mode. In positive mode, internal ion impact "fragmentation" allows the possibility to control the fragmentation of molecule and thus the range of the calibration *m/z* range. In negative mode the PFTBA fragments are in the range of *m/z* 633-200, and together with halide ion (*m/z* 33 in the case of Cl^-), allow calibration of molecules in that range of masses (*m/z* 633-33). Molecules with high electron affinity alike PFTBA could be similary ionized and thus, calibrated. We showed the calibration of endosulfane positive and negative spectra with PFTBA as internal calibrant.

Briefly, from the analytical point of view, laser induced positive and negative chemical ionization of (polyhalogenated) volatile organic molecules was proved successful. This ionization method could be further applied in other mass spectrometric techniques.

Even in a broader *m/z* range than in an EI experiment, PFTBA can be used as an internal calibrant in positive and negative mode for the calibration of the instrument as well as the acquired spectra.

From the mechanistic point of view, reaction pathways already known from the literature have been confirmed, and many newly proposed.

Nevertheless, some more work is needed in order to fully understand some of the observed reactions. For example, mechanisms of Si^+/acetophenone reactions will be better established by use of deuterated reagent; more detailed studies of mechanisms involved in Ti^+ and V^+ reactions will be performed by continuos ejection of different complex precursors... Reactions with some other perhalogenated molecules can help in better understanding of PFTBA involved mechanisms.

A better control of experimental condition for photoemission of electrons from the metal induced by laser pulse should allow insight into electron attachment reactions.

With this work we actually just entered in the rich world of gas phase reactions and we have lot of things to learn.

* * *

Prošireni sažetak

IONIZACIJA HLAPLJIVIH ORGANSKIH SPOJEVA PROIZVODIMA LASERSKE PLAZME. STUDIJ MEHANIZAMA ION/MOLEKULNIH REAKCIJA SPEKTROMETRIJOM MASA UZ FOURIEROVU TRANSFORMACIJU.

Prošireni sažetak

Područje ion-molekulnih reakcija u plinskoj fazi iskusilo je izuzetan napredak tokom dva zadnja desetljeća. To područje je od velikog interesa sa stajališta bazične kao i sa stajališta primjenjene kemije (sinteza metalnih i inih komplekasa s organskim molekulama).

Fourier transformirana spektrometrija masa (Fourier transform ion cyclotron resonance mass spectrometry, FTMS) je jako dobro prilagođena izučavanju reakcija u plinskoj fazi. Njene prednosti su: mogućnost pohranjivanja iona na duže vrijeme (više desetaka sekundi), kontrola manipuliranjem ionima i neutralnim specijama, mogućnost selekcije pojedinih iona i stoga široke mogućnosti izvođenja raznih eksperimenata.

Razvojem FT-spektrometrije masa i široke primjene različitih lasera, otvorene su nove granice kemije u plinskoj fazi. FTMS i laseri su izvrsno prilagođeni za međusobno sučeljavanje. FTMS sa svojom visokom osjetljivošću i mogućnosti polučavanja visoko-razlučenog spektra masa iz jednog jedinog laserskog pulsa, svrstava se u tehniku izbora za lasersku desorpcijsku spektrometriju masa.

Mnoga značajna ekološka zagađivala su polihalogeni organski spojevi, od freona do raznih pesticida. Važno ih je detektirati vrlo osjetljivim metodama jer su i vrlo male količine značajne za zagađivanje okoline. Spektrometrija masa u najširem smislu ima značajnu ulogu u njihovom određivanju. Ti su spojevi dosta labilni i stoga za njihovu ionizaciju trebaju biti primjenjene takozvane blage ionizacijske tehnike. Te molekule imaju izraženi elektronski afinitet i stoga su često lakše detektirane u obliku negativnog iona.

U ovom radu predstavljeni su rezultati proučavanja reakcija u plinskoj fazi između nabijenih čestica (pozitivnih i negativnih iona te elektrona) s organskim lako hlapljivim spojevima. Laseri različitih valnih duljina (355, 266, 248 i 193 nm) su korišteni za desorpciju/ablaciju krutog uzorka i ionizaciju atoma. Kao meta za laserski udar upotrebljavani su čisti metali, soli metalnih halogenida i silicij. Na taj način su proizvedeni pozitivni i negativni ioni te elektroni. Formirani kationi su bili izolirani u ćeliji FTMS-a i zatim pušteni da reagiraju s raznim organskim molekulama. Reakcije

su praćene u funkciji različitih vremena reakcije, valne duljine, jačine laserskog zračenja....) Snimljeni spektri su interpretirani i određeni su mase i elementarni sastavi asignirani. Reaktivnosti pojedinih metala su korelirane s njihovom elektronskom konfiguracijom i predlozeni su reakcijski mehanizmi.

U prvom pogalavlju su predstavljene reakcije u plinskoj fazi u sirokom smislu. Dan je pregled literature koji obuhvaća razne tehnike korištene u izučavanju reakcija u plinskoj fazi s naglaskom na FTMS tehnici i interakciji laser-tvar.

U drugom poglavlju, predstavljeni su instrumenti i metode korišteni u ovom radu. Opisana su dva FTMS instrumenta (FTMS 2000 u Metzu i FTMS 2001u Zagrebu). Prvi je sučeljen s NdYag (valne duljine: 355 and 266 nm) i excimer (248 i 193 nm) laserom, dok drugi pored Nd-Yag lasera ima mogućnost elektronske ionizacije. Nakon laserske desorpcije i formiranja iona, organske molekule su uvođene u ćeliju spektrometra. U tu svrhu na instrumentu FTMS 2000 nadograđena je cijev za uvod uzorka neposredno u ćeliju izvora iona ("source"). Organski spojevi su uvođene kroz pulsne ventile nadovezane na cijev ili kroz tzv. "batch inlet". Objašnjeni su osnovni principi rada instrumenta. Opisani su parametri korišteni u pripremi uzoraka i izvođenju eksperimenata.

Reakcije **pozitivnih iona** formiranih laserskom desorpcijom s organskim molekulama su tema trećeg poglavlja. Ono započinje pregledom literaturnih navoda.

Zatim su izloženi rezultati vlastitih istraživanja. Acetofenon ($C_6H_5COCH_3$, L) je poslužio kao modelna molekula za reakcije s metalnim i silicijevim ionima. Kako je ovo bilo prvo istraživanje reakcija u plinskoj fazi u našem laboratoriju, odlučili smo započeti istraživanje spojem za koji već od prije postoje utvrđeni mehanizmi reakcija s ionima željeza, nikla i aluminija. Mehanizmi utvrđeni u tim reakcijama su potvrđeni te eksperimentalni uvjeti primjenjeni u izučavanju reakcija s preostalim ionima (M^+ = Na^+, Mg^+, Ca^+, Ba^+, Ti^+, V^+, Mn^+, Cr^+, Fe^+, Ni^+, Co^+, Cu^+, Zn^+, Al^+, In^+ i Si^+) elementarnih iona. Utvrđeni su sljedeći mehanizmi;

i) *formiranje* ML_n^+ *compleksa* (n = 2 :M = Na, Cr, Fe, Ni, Co, Cu, Zn, In; n = 2-3 :M = Ba, Al; n = 2-4 :M = Mg, Ca, Mn)

ii) *dekarbonilacija metal-ligand compleksa,* $[ML_n - CO]^+$, (za M= Fe, Ni, Co)

iii) *dehidrogenacija i dehidratacija,* $[M(O)L_n - X]^+$, X= H, H_2O (M=Ti, V);

iv) *abstrakcija kisika silicijevim ionom* (M=Si)

v) *reakcije izmjene naboja* (M=Zn).

Uočena je velika reaktivnost prijelaznih metala. Željezo je najreaktivnije u reakciji dekarbonilacije, a zatim kobalt pa nikl, što je u skladu s njihovim promocijskim energijama potrebnim za stvaranje dviju σ veza.

Eksperimentalni uvjeti utvrđeni za ove reakcije su zatim primjenjeni u izučavanju polihalogeniranih organskih spojeva. Molekule perfluorotributilamina ($(C_4F_7)_3N$, L) su reagirale s 21 različitim elementarnim kationom (M^+ = Li^+, Na^+, K^+, Mg^+, Ca^+, B^+, Ti^+, V^+, Mn^+, Cr^+ Fe^+, Ni^+, Co^+, Cu^+, Zn^+, Al^+, In^+, Sn^+ i Si^+). Različiti rakcijski prozvodi su detektirani ovisno o raekcijskom ionu. Uglavnom, možemo razlikovati nekoliko glavnih mehanizama:

i) *formiranje LMF^+ iona*, za M = Li i Ca;
ii) *formiranje LM^+iona* za M = Li, Na, Cr, Co, Ni, Cu i Zn;
iii) *abstrakcija fluora*, *$[L - F]^+$* za sve izučavane ione;
iv) *formiranje $[LM - F]^+$* za M = Ca;
v) *$[L\text{-}C_4H_9+M]^+$* za Ca i Co;

i nekoliko sporednih. Molekulni ion (L^+) nije detektiran. Reakcijski produkti i mehanizmi su uspređivani s vodikovim analogom (tributilaminom).

Nekoliko drugih polihalogenih molekula (dikloro-difluorometan (Cl_2CF_2), halotan ($BrCHClCF_3$) i endosulfan ($C_9H_6SO_3Cl_6$)) je zatim uspješno ionizirano reakcijama s metalnim pozitivnim ionima. Rezultati su sumirani u sljedećoj tablici:

Tablica : Detektirani pozitivni molekulni(L) and kvazi-molekulni ioni

Molekula	**Detektirani pozitivni ioni**			
PFTBA $(C_4F_9)_3N$	ML^+			$[L\text{-}F]^+$
TBA $(C_4H_9)_3N$	ML_n^+	$[L+H]^+$	L^+	
Diklorodifluorometan Cl_2CF_2				$[L\text{-}F]^+$ $[L\text{-}Cl]^+$
Halotan $BrCHClCF_3$			L^+	$[L\text{-}Br]^+$
Endosulfan $C_9H_6SO_3Cl_6$	ML^+	$[L+H]^+$	L^+	

Četvrto poglavlje je posvećeno **negativnoj kemijskoj ionizaciji** gore spomenutih polihalogenih (ekološki značajnih) spojeva. NaCl, KCl, LiF su bili mete laserske ablacije u svrhu stvaranja Cl^- i F^- iona. Laserskom ablacijom metala su proizvedeni elektroni. u našem slučaju, obzirom na ionizacijsko sredstvo (ion, elektron..) , razlikujemo tri vrste negativne ionizacije.

i) Negativna kemijska ionizacija "hvatanjem" elektrona (Electron Capture Chemical Ionization (ECCI); Elektroni emitirani iz metala imaju znatno manju kinetičku energiju od istih emitiranih s katode. Spektri snimljeni nakon ionizacije elektronima proizvedenom laserskom desorpcijom su uspoređivani s onima proizvedenim standardnom elektronskom ionizacijom.

ii) Kemijska ionizacija negativnim ionom (Negative Ion Chemical Ionization (NICI); Cl^- i F^- ioni su prizvedeni desorpcijom soli metalnih klorida i florida i zatim reagirali s molekulama.

iii) Samo-kemijska ionizacija negativnim ionom ("Self Negative Ion Chemical Ionization" (SNICI); Često se kao proizvod ECCI ionizacije disocira puno halogenih negativnih iona. Isti mogu poslužiti za ionizaciju preostalih molekula. Ioni mogu biti ubrzani i tako prouzrokovati veći broj sudara s molekulom, ili naprosto biti ostavljeni da duže vrijeme (nekoliko s) reagiraju s molekulama.

Komplementarnost svih triju eksperimentalnih metoda i laki prijelaz s jedne na drugu metodu, dovodi do uspješne ionizacije i detekcije polihalogenih organskih spojeva. Rezultati su ukratko sumirani u sljedećoj tablici:

Spoj	**(Disociativni) ECCI**	**NICI**	**SNICI**
Cl_2CF_2	Cl^-	L^-, $[L+Cl]^-$	$[L+Cl]^-$
$BrCHClCF_3$	Br^-	Br^-, $[L-H]^-$, $[L+F]^-$	$[L-H]^-$, $[L+F]^-$
$C_9H_6SO_3Cl_6$	L^-, Cl^-		$[L-H]^-$, $[L+Cl]^-$
PFTBA	$[L-2F]^-$	$[L-2F+X]^-$	

Možemo zaključiti da lako hlapljivi organski spojevi mogu biti vrlo uspješno ionizirani ion-molekulnim reakcijama polučenim ionima ili elektronima formiranim laserskom desorpcijom/ablacijom, kako u pozitivnom, tako i u negativnom postupku. Reaktivnost pojedinih metala je velika i stoga ionizirani produkti mogu podlijeći značajnim reakcijama i tako biti promjenjeni.

Résumé étendu

Ionisation induite par plasma laser de composés organiques volatils. Etude des processus et des réactions ion/molécule consécutives par spectrométrie de masse de résonance cyclotronique à transformée de Fourier

Introduction

Le domaine de la chimie des ions en phase gazeuse a connu une expansion rapide durant les deux dernières décennies. Les réactions ion/molécule sont en effet intéressantes tant du point de vue fondamental qu'au niveau de leurs applications analytiques.

De nombreux polluants de l'environnement sont des composés organiques volatils polyhalogénés. Parmis les techniques qui permettent leur détection, la spectrométrie de masse joue un rôle majeur. Ces composés étant relativement fragiles, des méthodes d'ionisation dites "douces" sont nécessaires.

L'étude des réactions ion/molécule a conduit à la mise au point de l'ionisation chimique (CI). Cette méthode présente en effet l'avantage d'être "douce". Une approche particulièrement intéressante d'ionisation chimique a été la génération d'ions primaires par ablation/ionisation laser dans le cas d'analyses par spectrométrie de masse par résonance cyclotronique à transformée de Fourier (FT-ICR-MS ou FTMS). Cette approche permet l'ionisation chimique tout en maintenant le vide nécessaire au bon fonctionnement de l'instrument.

La FTMS est une technique particulièrement bien adaptée à l'étude des réactions ion/molécule en phase gazeuse. Elle offre en effet la possibilité de piéger les ions pendant de longues périodes et de contrôler précisément les manipulations des ions et des neutres. De plus, une grande variéte d'ions peuvent être étudiés dans des conditions expérimentales diverses.

Avec le développement de la FTMS et la diversité des sources laser disponibles, un large champ d'investigation de la chimie s'est ouvert. Le couplage de ces deux appareils est en effet particulièrement intéressant. La FTMS, grâce à sa sensibilité élevée et sa capacité de produire un spectre à haute résolution à partir d'un seul tir laser, est la méthode de choix pour la désorption laser couplée à la spectrométrie de masse.

Tout travail en spectrométrie de masse requiert l'étalonnage périodique de l'appareil et des spectres obtenus. La méthode de l'étalon interne demeure la plus fiable. Pour des instruments consacrés uniquement à l'ionisation laser, il n'existe pas de méthode d'étalonnage simple et universelle. Les molécules polyhalogénées sont des étalons fréquement rencontrés en spectrométrie de masse couplée à l'ionisation par faisceau d'électrons (EIMS).

Dans ce contexte, nous avons étudié la possibilité d'appliquer une procédure courament utilisée en EIMS aux expériences de désorption laser FTMS : l'utilisation de la perfluorotributylamine pour l'étalonnage de l'instrument et des spectres obtenus.

Les objectifs de ce travail de thèse sont de déterminer les capacités de différents ions positifs (formés par ablation laser) à ioniser les composés volatils polyhalogénés et de définir les mécanismes réactionnels impliqués.

Ces molécules polyhalogénées ayant la particularité de former facilement des ions négatifs, l'ionisation en mode négatif a donc été employée en complément. L'ionisation chimique négative peut-être induite par des ions négatifs ou par des électrons émis par le métal irradié par le laser. Pour une détermination précise des produits formés, une méthode d'étalonnage en ions négatifs a également été mise au point.

Ce manuscript se compose de quatre chapitres suivis d'appendices. Le premier chapitre résume les applications de la spectrométrie de masse à l'étude des réactions en phase gazeuse. Les principes de la FTMS et de l'ablation/ionisation laser y sont également décrits.

Partie expérimentale

Dans le second chapitre, notre dispositif expérimental est détaillé. Deux spectromètres de masse à transformée de Fourier couplés à différents lasers et à une source d'ionisation par faisceau d'électrons ont été utilisés au cours de cette étude. La microsonde laser FTMS du laboratoire LSMCL a été adaptée pour permettre l'introduction d'un gaz réactif directement dans la cellule source. Une séquence expérimentale type est représentée figure 1.

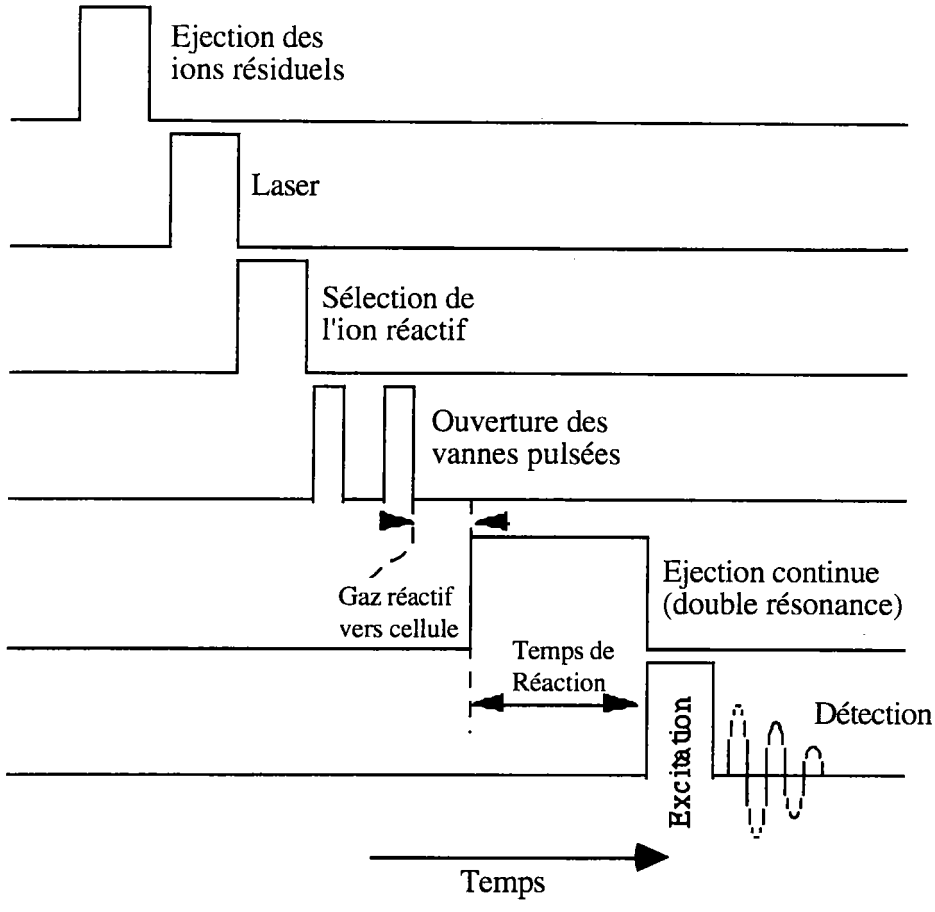

Figure 1 : Séquence expérimentale type utilisée au cours de l'étude.
Réactions en mode d'ions positifs

L'acétophénone

Etant donné que les études des réactions ion/molécule sont un thème nouveau au LSMCL, nous avons commencé notre étude avec une molécule modèle dont le comportement vis à vis de différents cations était en partie déjà connu. Comme ce composé devait être suffisament volatil pour être introduit facilement dans l'instrument, nous avons choisi l'acétophénone. Sa structure est représentée figure 2

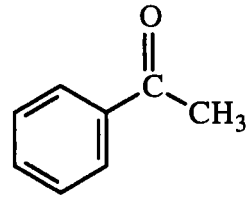

Figure 2 : Acétophénone.

Mécanismes de complexation et/ou réaction en phase gazeuse entre l'acétophénone et divers ions positifs

Des ions produits par laser (M^+ = Na^+, Mg^+, Ca^+, Ba^+, Ti^+, V^+, Mn^+, Cr^+, Fe^+, Ni^+, Co^+, Cu^+, Zn^+, Al^+, In^+ and Si^+) ont été piégés dans la cellule FTMS et l'acétophénone (L) a été introduite au moyen des vannes pulsées. Des essais de thermalisation des ions primaires à l'aide d'argon n'ont pas donné lieu à des différences notables en ce qui concerne les produits formés ou les vitesses de réaction. Néanmoins, on ne peut pas totalement exclure l'existence de certains ions excités participant aux réactions. Les produits de réactions primaires, secondaires et d'ordres plus élevés ont été détectés en fonction du temps de réaction. Suivant les ions primaires utilisés, plusieurs comportements réactionnels ont été mis en évidence :

i) formation de complexes ML_n^+ ,

$$M^+ + L \longrightarrow ML^+ \xrightarrow{L_{n-1}} ML_n^+$$

n=2 : M = Na, Cr, Fe, Ni, Co, Cu, Zn, In
n=2-3 : M = Ba, Al
n=2-4 : M = Mg, Ca, Mn

ii) décarbonylation du complexe métal-ligand $[ML_n - CO]^+$, avec M = Fe, Co, Ni

$$\begin{array}{ccccc} M^+ + L & \longrightarrow & ML^+ & \xrightarrow{L} & ML_2^+ \\ & & \downarrow -CO & & \\ & & [ML - CO]^+ & \xrightarrow{L} & [ML_2 - CO]^+ \end{array}$$

iii) déshydrogénation, déshydratation, $[M(O)L_n\text{-}X]^+$, X=H_2, H_2O, avec M=Ti, V

$$MO^+ + nL \rightarrow MOL_n^+ \rightarrow \left[MOL_n - xH_2O\right]^+ + xH_2O$$

n = 1-5; x = 1-3.

$$M^+ + nL \rightarrow \left[ML_n - H_2\right]^+ \rightarrow \left[ML_n - H_2 - xH_2O\right]^+$$

n = 1-5; x = 1-4.

iv) tranfert de charge et/ou ionisation électronique,

$$L + M^+ \rightarrow L^{+\cdot} + M \rightarrow [L - X]^+ + X^\bullet$$

X = CH_3, $COCH_3$

$$L^{+\bullet} + L \rightarrow [L + H]^+ + [L - H]^\bullet$$

v) abstraction d'oxygène essentiellement par le silicium,

$$Si^+ + L \rightarrow [SiL - H]^+ + H$$
$$\rightarrow [L - O]^+ + SiO$$
$$\rightarrow [L - OH]^+ + SiOH$$
$$\rightarrow [L - COCH_2]^+ + SiOC_2H_2$$

vi) réactions impliquant des molécules d'eau

$$Ca^+ + H_2O \rightarrow \left[Ca^+ \cdots H_2O\right] \rightarrow \left[Ca^{2+}OH^-\right]^+ + H$$
$$\downarrow nL$$
$$\left[L_nCa^{2+}OH^-\right]^+$$

Les comportements observés pour Fe^+, Ni^+ et Al^+ sont en accord avec ceux publiés précédement. De nombreux autres chemins réactionnels ont été mis en évidence au cours de cette étude.

La première génération de produits est principalement composée de complexes ML^+ , de leurs produits de décarbonylation, ainsi que de produits issus de tranferts de charge suivis de fragmentation de la molécule. Les produits de seconde géneration sont des adduits, des adduits décarbonylés ainsi que le dimère protoné de l'ion moléculaire de l'acétophénone. Les réactions d'ordres plus élevés donnent lieu à des complexes de plus haut rang. Les déshydrogénation et déshydratation n'ont été observées que pour le titane et le vanadium. Les produits impliquant la réaction de molécules d'eau sont des sous-produits de réaction de Ca^+, Ba^+ et Al^+

Une fois notre procédure expérimentale établie et les principaux processus étant compris, nous avons pu appliquer cette méthode d'ionisation à d'autres composés ; des molécules polyhalogénées ; avec comme objectif principal la comparaison des réactions ion/molécule en mode positif et en mode négatif.

La perfluorotributylamine

La perfluorotributylamine (PFTBA) est une molécule bien connue en spectrométrie de masse puisqu'elle sert courament à l'étalonnage des appareils travaillant en ionisation électronique (EI). Sa structure est représentée figure 3 :

Au cours de cette étude, 21 ions élémentaires monochargés (les élements étudiés sont regroupés dans le tableau 1) ont été produits par ablation laser d'échantillons solides (Irradiance 10^9-10^{10} W cm^{-2}). Ces ions ont été isolés et mis en présence de molécules neutres de PFTBA (L). La PFTBA a été introduite dans le spectromètre au moyen des vannes pulsées ou directement à partir du vase d'expansion. Il n'existe pas de différences notables en ce qui concerne les ions obtenus, quel que soit le mode d'introduction utilisé.

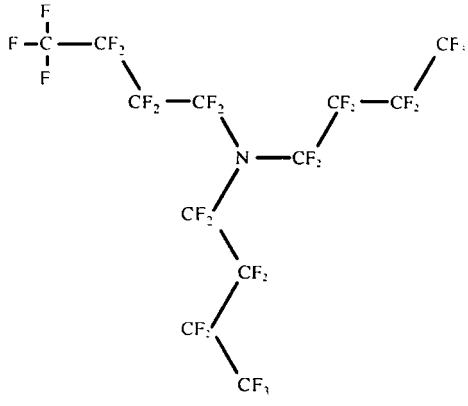

Figure 3 : PFTBA

Tableau 1 : Elements ayant servi à l'étude de la réactivité de la PFTBA.

IA																	0
	IIA											IIIB	IVB	VB	VIB	VIIB	
Li												B					
Na	Mg	IIIA	IVA	VA	VIA	VIIA	-----	VIII	-----		IB	IIB	Al	Si				
K	Ca		Ti	V	Cr	Mn	Fe	Co	Ni		Cu	Zn						
			Zr		Mo								In	Sn				

Contrairement à ce qui a été observé pour l'acétophénone, le temps de réaction a peu d'influence sur les spectres obtenus pour la PFTBA. Un temps de réaction plus long n'a pas pour conséquence l'apparition de nouveaux produits, tous les ions observés étant produits durant les quelques premières millisecondes.

Divers produits de réaction ont été observés suivant l'ion projectile utilisé. Le pic moléculaire de la PFTBA n'a cependant jamais été détecté quel que soit l 'ion projectile, la fluence ou la longueur d'onde du laser utilisé. L'absence de cet ion n'est pas surprenante. En effet, l'ionisation de la PFTBA par transfert de charge nécessiterait une énergie supérieure à 11.3 eV. Aucun des ions primaires étudiés n'a une énergie de recombinaison aussi élevée.

Ionisation et dissociation de la PFTBA par des ions positifs

Dans presque tous les cas étudiés, des ions fragments de la PFTBA ont été observés. Parallèlement, de nombreux ions contenant des métaux sont également formés. Aucune tendance très singnificative liée à la nature des éléments de la classification périodique ne s'est clairement manifestée dans les résultats obtenus. Nous avons donc pris le parti de grouper les résultats en fonction des ions préférentiellement formés :

i) fragmentations de la PFTBA ;

Presque tous les ions étudiés ont donné lieu à des ions fragments de la PFTBA. Ceci a été observé de façon particulièrement marquée dans le cas du bore, du silicium, du titane et du vanadium, et dans une moindre mesure pour l'indium, le zirconium et le molybdène. Seuls le magnésium, le calcium, le chrome et l'étain se sont distingués par une faible tendance à fragmenter la PFTBA

ii) formation de complexes LM^+;

La PFTBA peut être cationisée par le lithium, le chrome, le cobalt, le nickel, le cuivre, le sodium et le zinc. L'élimination de F_2 à partir du complexe formé est fréquement observée sauf dans le cas du lithium.

iii) abstraction de fluorure par le métal;

C'est la principale réaction observée dans le cas de l'aluminium, du fer et du zinc, elle donne lieu à l'ion $[L\text{-}F]^+$. Tous les autres ions donnent ce fragment en moindre abondance, sauf le magnésium, le calcium, le chrome et l'étain qui ne conduisent pas à la formation de cet ion.

iv) formation de $[L - F_2]^+$;

Seuls le magnésium, l'étain, le titane, le vanadium et le manganèse ont donné lieu à ce type de réactions.

v) formation de complexes LMF^+;

L'abstraction de fluor par le calcium conduit à l'ion CaF^+ qui lui-même réagit avec une molécule neutre pour former LMF^+.

vi) formation de $[LM - F]^+$;

Ceci n'a été observé que dans le cas du calcium

vii) formation de $[L\text{-}C_4F_9+M]^+$

Observé seulement pour le calcium et le cobalt.

Conséquences

L'encadrement de l'énergie d'ionisation de $[(C_4F_9)_2N{=}CFC_3F_7]$ a pu être réalisé connaissant les énergies d'ionisation des ions MF^+ détectés et non détectés. Cette énergie se situe dans la gamme 7.69 à 8.0 eV.

Une tentative de comparaison de ces mécanismes réactionnels avec ceux de la tributylamine (TBA) ne nous ont pas permis de dégager de conclusions probantes. Si la fonction amine joue une certain rôle dans les réactions observées, le remplacement des atomes de fluor par l'hydrogène entraîne une plus grande disponibilité des électrons de la paire libre de l'azote et donc une réactivité très différente .

Contrôle de la fragmentation de la PFTBA

L'excitation du mouvement cyclotron des ions primaires induit une augmentation du taux de fragmentation de la PFTBA. Dans certains cas, des fragments n'apparaissent que si l'excitation est appliquée.

Le contrôle des paramètres expérimentaux permet donc de contrôler le taux de fragmentation de la PFTBA. Ceci implique la possibilité d'obtenir des séries d'ions de masses bien connues pouvant servir à la calibration de l'instrument. Des spectres contenant des adduits, des ions métalliques élémentaires, ainsi que toute la série des pics de la PFTBA permettent ainsi d'avoir une gamme de calibration encore plus large qu'en ionisation électronique (de m/z 20 à 740 contre m/z 69 à 502 ; voir Chapitre III 7).

Application de la méthode à d'autres molécules polyhalogénées.

L'étude s'est poursuivie par l'étude de trois composés halogénés très différents quant à leurs structures, leurs utilisations et leurs propriétés physico-chimiques (voir tableau 2). Il s'agit du dichlorodifluorométhane (gazeux), un représentant de la classe des fréons, de l'halothane (liquide), un anesthésique courament utilisé et de l'endosulfane (solide), un insecticide et acaricide non systématique. Les formules développées de ces trois molécules sont représentées figure 4.

Tableau 2 : Quelques caractéristiques des composés étudiées. (IE : énergie d'ionisation)

	Dichlorodifluoro -methane Cl_2CF_2	Halothane $BrCHClCF_3$	Endosulfane $C_9H_6Cl_6O_3S$
M / u	120	199	404
Etat (à 25°C)	gazeux	liquide	solide
Pression de vapeur / kPa	651.0 (25°C)	39.9 (25°C)	0.0012 (80°C)
IE/eV	11.75±0.04	11.0	-
ΔH_f(ion) /kJmol-1	656	363 (361)	-

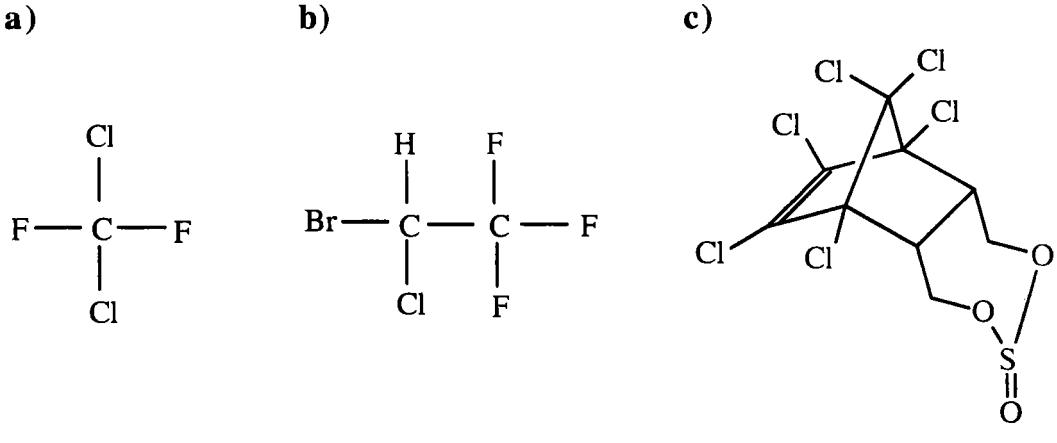

Figure 4. a) dichlorodifluorométhane, b) halothane, c) endosulfane.

Les trois molécules ont été ionisées par des ions positifs produits par laser. Les ions moléculaires ou des produits résultant de l'abstraction d'un halogène ont été principalement détectés comme le montre le tableau 3.

La PFTBA a été utilisée avec succès dans une procédure d'étalonnage des spectres obtenus pour l'endosulfane. Cette expérience ouvre la possibilité d'autres applications de cette méthode d'étalonnage pour divers composés polyhalogénés.

Tableau 3 : principaux ions correspondant à l'ion moléculaire ou à la perte d'halogène détectés lors de l'analyse des molécules polyhalogénées. La TBA est incluse pour comparaison.

Molécule	**Ions positifs détectés**			
PFTBA $(C_4F_9)_3N$	ML^+			$[L-F]^+$
TBA $(C_4H_9)_3N$	ML_n^+	$[L+H]^+$	L^+	
Dichlorodifluoromethane				$[L-F]^+$
Cl_2CF_2				$[L-Cl]^+$
Halothane			L^+	$[L-Br]^+$
$BrCHClCF_3$				
Endosulfane	ML^+	$[L+H]^+$	L^+	
$C_9H_6SO_3Cl_6$				

Réactions en mode d'ions négatifs

L'ablation/désorption laser de métaux et de sels de métaux a été utilisée pour induire la formation d'électrons ou d'ions négatifs. Ces espèces négatives ont ensuite servi de projectile pour l'ionisation de diverses molécules polyhalogénes. La procédure appliquée est représentée figure 5.

Suivant la nature du projectile ionisant, trois méthode d'ionisation peuvent être distinguées :

i) l'ionisation chimique par capture d'électron (ECCI)

ii) l'ionisation chimique par des ions négatifs (NICI)

iii) l'auto-ionisation chimique négative (Self-NICI)

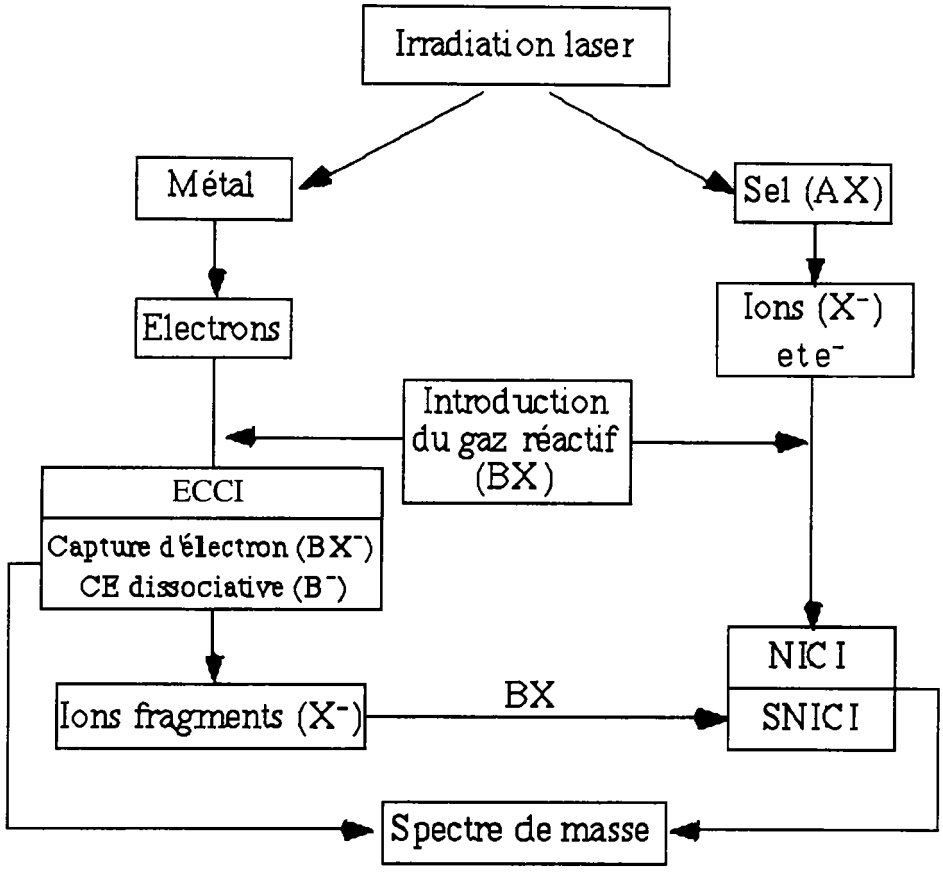

Figure 5 : Méthodes d'ionisation chimique négatives utilisée au cours de la présente étude

La capture électronique se produit grâce aux électrons émis par le métal subissant l'impact laser. Les molécules sont ionisées par interaction électron-molécule. Les deux principaux mécanismes sont la capture électronique résonante et la capture électronique dissociative (voir figure 6a)

Dans les expériences d'ionisation chimique par des ions négatifs (NICI), les ions halogènes (X^-) formés par des halogénures de métaux ont été utilisés comme projectiles ionisant (voir figure 6b). Dans certains cas, des ions fragments X^- , produits à partir de la molécule étudiée par capture électronique dissociative, ont été utilisés comme projectiles. La molécule substrat était donc dans ce cas ionisée par ses propres fragments. On parle d'auto-ionisation chimique négative (Self-NICI, voir figure 6c).

Au cours de cette étude, différents métaux et sels ont été utilisés pour produire les espèces projectiles par irradiation laser. La PFTBA, le dichlorodifluoro-méthane, l'halothane et l'endosulfane ont été étudiés en mode négatif. Le tableau 4 résume les résultats obtenus pour les quatre composés étudiés dans les différents modes d'ionisation possibles.

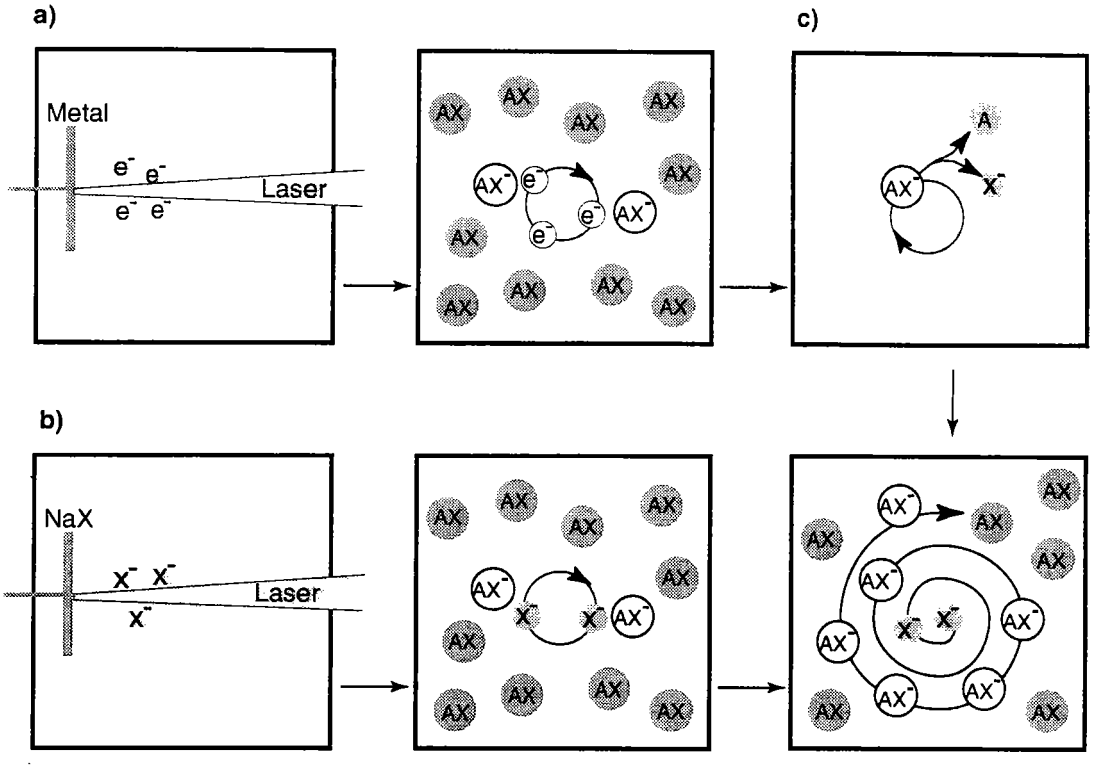

Figure 6 : Représentation de l'ionisation des molécules neutres en mode négatif.a) ECCI, b) NICI, c) Self-NICI.

Quatre longueurs d'ondes ont été utilisées pour la PFTBA et principalement 355 nm pour les autres composés. Les molécules ont été introduites dans la cellule FTMS et ionisées par le projectile approprié. Pour les expériences en ECCI, c'est l'aluminium qui a été choisi comme cible car il avait été étudié de façon particulièrement approfondie en mode positif et offrait donc la possibilité d'une conversion rapide entre le mode négatif et le mode positif sans avoir à changer de nombreux paramètres expérimentaux.

Tableau 4 : Principaux ions observés suivant le mode d'ionisation chimique négative utilisé (L = molécule intacte).

Molécule	**ECCI (Dissociative)**	**NICI**	**Self-NICI**
Cl_2CF_2	Cl^-	L^-, $[L+Cl]^-$	$[L+Cl]^-$
$BrCHClCF_3$	Br^-, $[L-H]^-$	Br^-, $[L-H]^-$, $[L+F]^-$	
$C_9H_6SO_3Cl_6$	L^-, Cl^-		$[L-H]^-$, $[L+Cl]^-$
PFTBA	$[L-2F]^-$	$[L-2F+X]^-$	

Ces méthodes d'ionisation sont bien adaptées à l'ionisation de molécules polyhalogénées car celles-ci ont des affinités électroniques positives. Les ions moléculaires ou quasi-moléculaires ainsi que des fragments ont été observées pour toutes les molécules. Non seulement ces trois méthodes d'ionisation sont complémentaires entre elles, mais elles sont également complémentaires de l'ionisation chimique positive car les comportements observés peuvent être différents.

Pour définir sans ambiguité les ions formées, une méthode d'étalonnage avec la PFTBA comme étalon interne a également été utilisée en mode négatif.

Comparaison des produits de réaction de la PFTBA par ionisation chimique positive et négative

Tous les ions fragments de la PFTBA obtenus par ionisation chimique sont regroupés dans les tableaux 5 et 6 pour le mode négatif et positif respectivement. On note qu'il existe des filliations communes dans les deux modes d'ionisation (en grisé dans les tableaux). Cependant, nous ne pouvons certifier que leur structures sont similaires. Les ions marqués d'une astérisque sont les principaux produits détectés dans le cas des réactions avec le magnésium et l'étain mais sont observés avec une faible abondance dans le cas du fer, du manganèse, du titane et du vanadium.

Tableau 5. Fragments de la PFTBA en ionisation chimique négative par capture d'électron.

	x=0	x=1	x=2	x=3	x=4	x=5	x=6	x=7	x=8	x=9	x=10
$NC_{12}F_{27-x}$	-	-	**633**	-	**595**	-	557	-	-	-	-
$NC_{11}F_{25-x}$	-	-	583	564	545	526	-	-	-	-	-
$NC_{10}F_{23-x}$	-	-	533	**514**	-	476	-	-	-	-	-
NC_9F_{21-x}	-	-	-	464	-	-	-	-	-	-	312
NC_8F_{19-x}	-	**452**	433	414	-	-	-	-	-	-	-
NC_7F_{17-x}	-	402	383	364	-	-	-	-	-	-	-
NC_6F_{15-x}	-	352	333	314	295	276	-	-	-	-	-
NC_5F_{13-x}	-	302	283	264	-	226	-	-	-	-	-
NC_4F_{11-x}	-	-	-	214	-	-	-	-	-	-	-
NC_3F_{9-x}	-	-	-	164	-	-	-	-	-	-	-
NC_2F_{7-x}	-	-	-	114	-	-	-	-	-	-	-

Tableau 6. Fragments de la PFTBA en ionisation chimique positive.

	x=0	x=1	x=2	x=3	x=4	x=5	x=6	x=7	x=8	x=9	x=10
$NC_{12}F_{27-x}$	-	**652**	633 *	**614**	595 *	576	557	-	-	-	-
$NC_{11}F_{25-x}$	-	602	-	-	545	526	-	-	469	-	-
$NC_{10}F_{23-x}$	-	552	533	-	-	476	-	-	-	-	-
NC_9F_{21-x}	-	**502**	-	464	-	426	-	-	-	-	-
NC_8F_{19-x}	-	-	-	**414**	395	376	-	-	-	-	-
NC_7F_{17-x}	-	402	-	364	-	326	-	-	-	-	-
NC_6F_{15-x}	-	352	-	314	295	-	-	-	-	-	-
NC_5F_{13-x}	-	-	-	264	-	226	-	-	-	-	-
NC_4F_{11-x}	-	-	-	214	-	176	-	-	-	-	-
NC_3F_{9-x}	-	-	-	164	-	-	-	-	-	-	-
NC_2F_{7-x}	-	-	-	114	-	-	-	-	-	-	-

Conclusion et perspectives

L'ionisation induite par des espèces produites par plasma laser a été utilisée avec succès pour l'analyse de molécules polyhalogénées. Les modes d'ionisation positifs et négatifs ont été étudiés par spectrométrie de masse à transformée de Fourier.

Tableau 7 : Principaux ions détectés pour les 5 composés étudiés en mode d'ionisation chimique positive ou négative. (M = métal; L^+ or L^- = ions moléculaire)

Molécule	**Ions positifs**				**Ions négatifs**		
Acétophénone $C_6H_5COCH_3$	ML_n^+	$[L+H]^+$	L^+				$[L-H]^-$
PFTBA $(C_4F_9)_3N$	ML^+			$[L-F]^+$	$[L-F_2+X]^-$, $[L-F_2]^-$		
TBA $(C_4H_9)_3N$	ML_n^+	$[L+H]^+$	L^+		non détecté		
Dichlorodifluorométhane Cl_2CF_2				$[L-F]^+$ $[L-Cl]^+$	$[L+Cl]^-$	L^-	
Halothane $BrCHClCF_3$			L^+	$[L-Br]^+$	$[L+F]^-$		$[L-H]^-$
Endosulfane $C_9H_6SO_3Cl_6$	ML^+	$[L+H]^+$	L^+		$[L+Cl]^-$	L^-	$[L-H]^-$

Nous pouvons en conclure que les méthodes d'ionisation chimique appliquées au cours de cette étude sont complémentaires et donnent des informations pertinentes sur les composés étudiés. Les ions détectés, et plus particulièrement les ions moléculaires (ou apparentés) ainsi que les adduits, pour tous les composés étudiés sont regroupés dans le tableau 7.

L'ionisation chimique en mode positif se produit via des réactions ion/molécule. Pour établir le protocole expérimental et définir les paramètres influants, la première série d'expériences a été menée sur un composé modèle dont la réactivité était connue à priori. L'acétophénone a été choisie dans ce but et les résultats obtenus sont en accord avec la bibliographie. De nombreux autres chemins réactionnels ont également été déterminés pour ce composé.

La méthode a ensuite été appliquée au cas des composés polyhalogénés. Dans un premier temps, 21 ions élémentaires ont été mis en présence de la PFTBA et les produits de réactions recensés. De nombreux comportements réactionnels ont pu être dégagés. L'ion moléculaire de la PFTBA n'a pas été détecté. La réactivité des cations des métaux de transition est reliée à leur configuration électronique mais de nombreuses réactions observées nécessitent encore une étude des mécanismes plus approfondie.

La réactivité de la PFTBA a été comparée à celle de son analogue hydrogéné (la TBA). Les mécanismes de réactions des deux composés sont fondamentalement différents. En dehors de la caractéristique d'être une amine, la perhalogénation joue, comme on pouvait s'y attendre, un grand rôle dans le comportement de la molécule. La PFTBA a une affinité électronique élevée alors que la TBA possède une très forte affinité protonique. La paire libre de l'azote doit être plus disponible dans la TBA que dans la PFTBA, où le fluor retient les électrons.

La méthode d'ionisation a ensuite été appliquée avec succès dans le cas de trois molécules polyhalogénées de structures très différentes. Les ions moléculaires ainsi que des produits résultant de l'abstraction d'halogène ont été observés.

Le contrôle de la fragmentation de la PFTBA par l'excitation du mouvement cyclotron des ions primaires a permis de mettre au point une méthode d'étalonnage qui a été appliquée avec succès dans le cadre de l'étude de l'endosulfane.

Pour compléter l'étude de la réactivité des composés polyhalogénés, l'ionisation chimique négative a été réalisée. Ces molécules ont en effet une grande affinité électronique et peuvent donc former facilement des ions négatifs. Le PFTBA et les trois autres composés polyhalogénés étudiés en mode positif ont été nos principaux sujets d'étude.

Trois méthodes d'ionisation ont été utilisées suivant que les projectiles ionisant aient été des électrons produits par un métal irradié, des ions négatifs produits par un sel irradié ou encore des ions négatifs générés par capture électonique dissociative des molécules étudiées.

Nous avons pu montrer que ces méthodes sont bien adaptées pour l'ionisation des composés polyhalogénés. L'ion moléculaire ou pseudo-moléculaire et des fragments caractéristiques ont été détectés pour tous les composés. Aucune des trois méthodes d'ionisation ne peut cependant être considérée comme universelle, elles

sont complémentaires. De plus, elles complètent avantageusement les données obtenues par ionisation chimique positive.

La PFTBA a pu être utilisée comme étalon interne en mode négatif également. Nous avons même pu montrer que la gamme de masse accessible, que ce soit en mode positif ou négatif, est considérablement plus large que celle obtenue classiquement en ionisation électronique.

Brièvement, du point de vue analytique, nous avons pu montrer la validité l'ionisation chimique induite par des espèces formées au sein d'un plasma laser. Cette méthode pourra être employée dans d'autres techniques de spectrométrie de masse. La PFTBA peut ainsi être utilisée en tant qu'étalon sur une gamme plus large qu'en ionisation électronique.

Les mécanismes de réactions déjà connus par ailleurs ont été confirmés et nombre d'autres ont été révélés. Néanmoins, il reste encore du travail pour comprendre de façon précise certaines des réactions observées.

Un meilleur contrôle des conditions expérimentales pour la production de photoélectrons devrait permettre d'avoir une vue plus approfondie sur les réactions de capture d'électron.

Biography and List of Publications

Biography

I was born in 1966 in Raša near Labin, Croatia. I finished primary and secondary school in Labin. At the Faculty of Natural Sciences and Mathematics at the University of Zagreb, I studied chemistry. In 1991 I got B. Sc. My diploma work was dealing with the superconductors. During the student days I went for two traineeships: in 1988, ASTRA Pharmaceutical Production AB, Sodertalje, Sweden, at dr. M. Hjalmasson group, dealing with organic synthesis, GLC and HPLC analysis of products; and in 1989, F.Hoffman-La Roche & Co, Basel, Switzerland at Prof. Dr. K. Bernauer, dealing with organic synthesis as well.

In 1991 I started after graduate studies, also at the University of Zagreb. At the same time I started to work in the Laboratory for chemical kinetics and atmospheric chemistry, Physical Chemistry Department at "Ruđer Bošković" Institute, in the group of Prof. Leo Klasinc. There, I started to work with Fourier transform mass spectrometers. My M. Sc. work was entitled: "Some applications in laser desorption FTMS" and it was supervised by Dr. Dunja Srzić. It was finished in 1994.

My Ph. D. Thesis was co-supervised between the University of Zagreb, Croatia and University of Metz, France. Apart of "Ruđer Bošković" Institute, the work was performed in the Laboratory for Laser Chemistry and Mass Spectrometry, directed by Prof. Jean François Muller where I was working from October 1995 until June 1997 with some breaks.

Up to now, my research work resulted with eleven published papers in the international scientific journals and a few that are in preparation. I took an active part in about ten scientific conferences and schools.

List of Publications

1. R. Freund, S. Martinović, and K. Bernauer, "23. Diastereoselective Spirocyclization of Imines of 2-Substituted 1*H*-Indole-3-ethylamines (=Tryptamines): Variation of the Electrophile and the Substituent at C(2) and Its Influence on the Steric Outcome"
   Helv. Chim. Acta , 75 (1992) 282-287.

2. Z. Božičević, V. Butković, T. Cvitaš, J. Jeftic, L. Klasinc, B. Kovač, I. Lisac, J. Lovrić, R.Marčec, A.Marki, S. Martinović, M. Orhanović, Lj. Paša Tolić, D. Srzić, N. Šinik, D. Tiljak, and A. Vrančić, "Tropospheric Ozone Measurements in Zagreb" in "Photo-Oxidants: Precursors and Products", Ed. P. Borrell,
   SPB Academic Publishing, The Hague, 1992.

3. D. Srzić, S. Martinović, P. Vujanić and Z. Meić, "Randomization in the Fragmentation of Benzophenone"
   *Rapid Comm. Mass Spectrom.*7 (1993) 163-166.

4. D. Srzić, Lj. Paša Tolić, S. Martinović, D. Plavšić and L.Klasinc, "Laser Desorption Fourier Transform Mass Spectrometry of $[Ta_6X_{12}]X_2 \cdot 8H_2O$, X = Cl, Br"
   Rapid Comm. Mass Spectrom. 8 (1994) 56-58.

5. D. Srzić, S. Martinović, Lj. Paša Tolić, D. Šepacand V. Šunjić, "LD FTMS Investigation of Rh(I) Complexes with Chiral 1,5-Bisnitrogen Ligands"
   Croat. Chem. Acta 67 (1994) 149-153.

6. H. Zorc, Lj. Paša Tolić, S.Martinović, and D. Srzić, "Synthesis and Laser Desorption Fourier Transform Mass Spectrometry of Massive Fullerenes"
   Full. Sci. Tech. 2, (1994) 471-480.

7. D. Srzić, S. Martinović, Lj. Paša Tolić, N.Kezele, S.M. Shevchenko, and L. Klasinc, "Laser Desorption FTMS of Lignins"
   Rapid Comm. Mass Spectrom. 9, (1995) 245-249.

8. S. Martinović, Lj. Paša Tolić, D. Srzić, N. Kezele, D. Plavšić, and L.Klasinc "Laser Desorption/Ionization Fourier Transform Ion Cyclotron Resonance Mass Spectrometry of $[Nb_6X_{12}]X_2 \cdot 8H_2O$, X=Cl or Br"
   *Rapid Comm. Mass Spectrom.*10 (1996) 51-53.

9. D. Srzić, Lj. Paša Tolić, S. Martinović, N.Kezele, Lj. Senković, S.M. Shevchenko and L. Klasinc, "Laser Desorption FTMS of Biopolymers"
   Rapid Comm. Mass Spectrom. 10 (1996) 580-582.

10. L. Klasinc, D. Srzić, Lj. Paša Tolić and S. Martinović, "Gas Phase Properties of $ONOO^-$ Anion and $ONOO^{-\cdot}$ Radical"
    Croat. Chem. Acta. 69(3) (1996) 1007-1011.

11. C. Joblin, C. Masselon, P. Boissel, P. de Parceval, S. Martinović, and J-F.Muller "Simulation of Interstellar Aromatic Hydrocarbons using Ion Cyclotron Resonance: Preliminary Results:"
    Acepted for publication in *Rapid Comm. Mass Spectrom.*

12. S. Martinović, C. Masselon and J.F. Muller, "Gas Phase Reactions of Metal and Silicon Cations with Acetophenone"
    Submitted to *J. Mass Spectrom.*

13. S. Martinović, C. Masselon and J.F. Muller, "Laser-induced Positive-Ion and Negative-Electron Ionization of PFTBA Molecule in a FT-ICR Mass Spectrometer. "
    in preparation

14. S. Martinović and J.F. Muller, "Laser-induced Negative Chemical Ionization of Halogenated Compounds in FT-ICR Mass Spectrometer."
    in preparation

Appendices

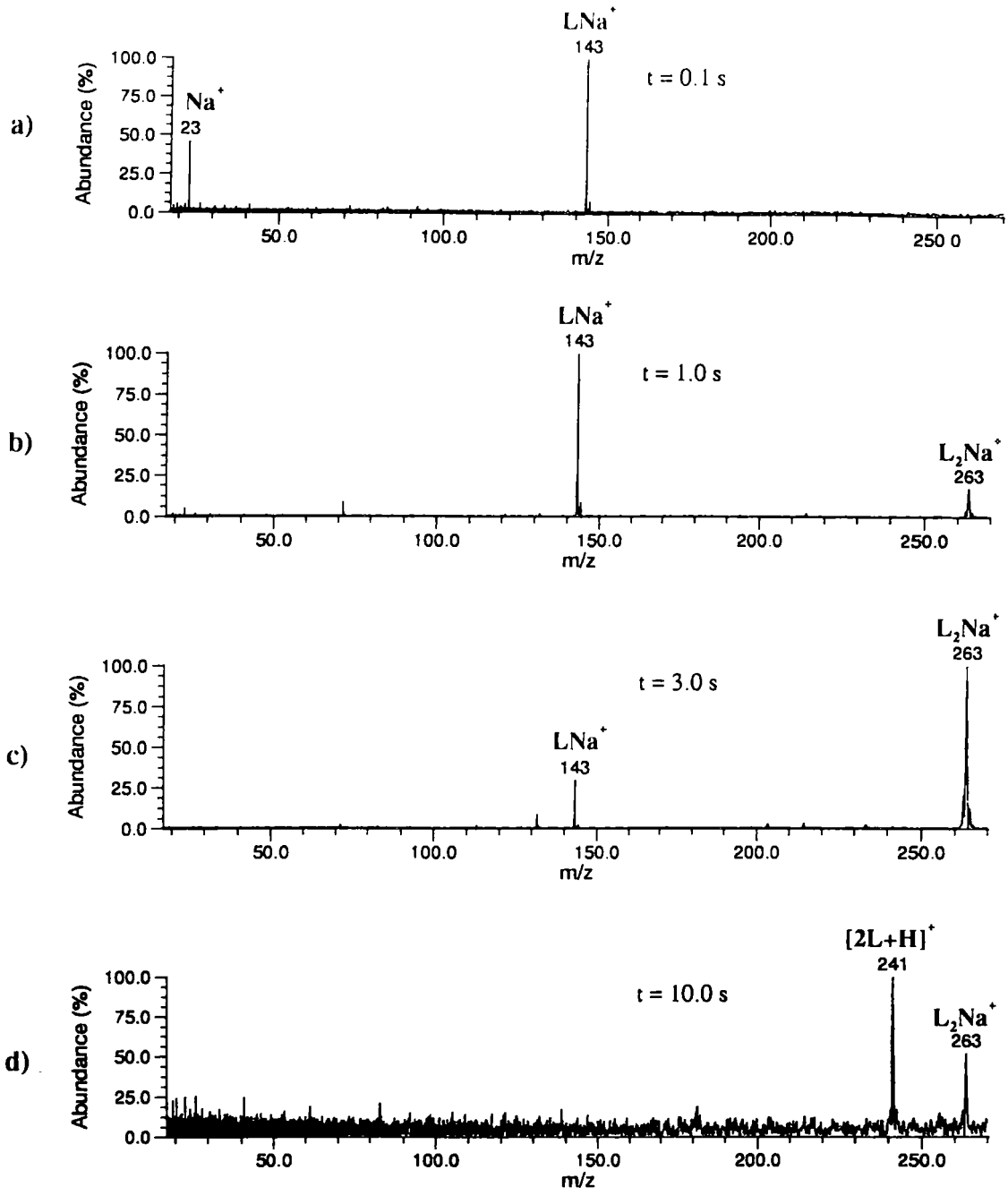

Figure A1: Positive ion FT-ICR mass spectra of the ionic products of the reaction of Na^+ with acetophenone (L) at the different reaction times.

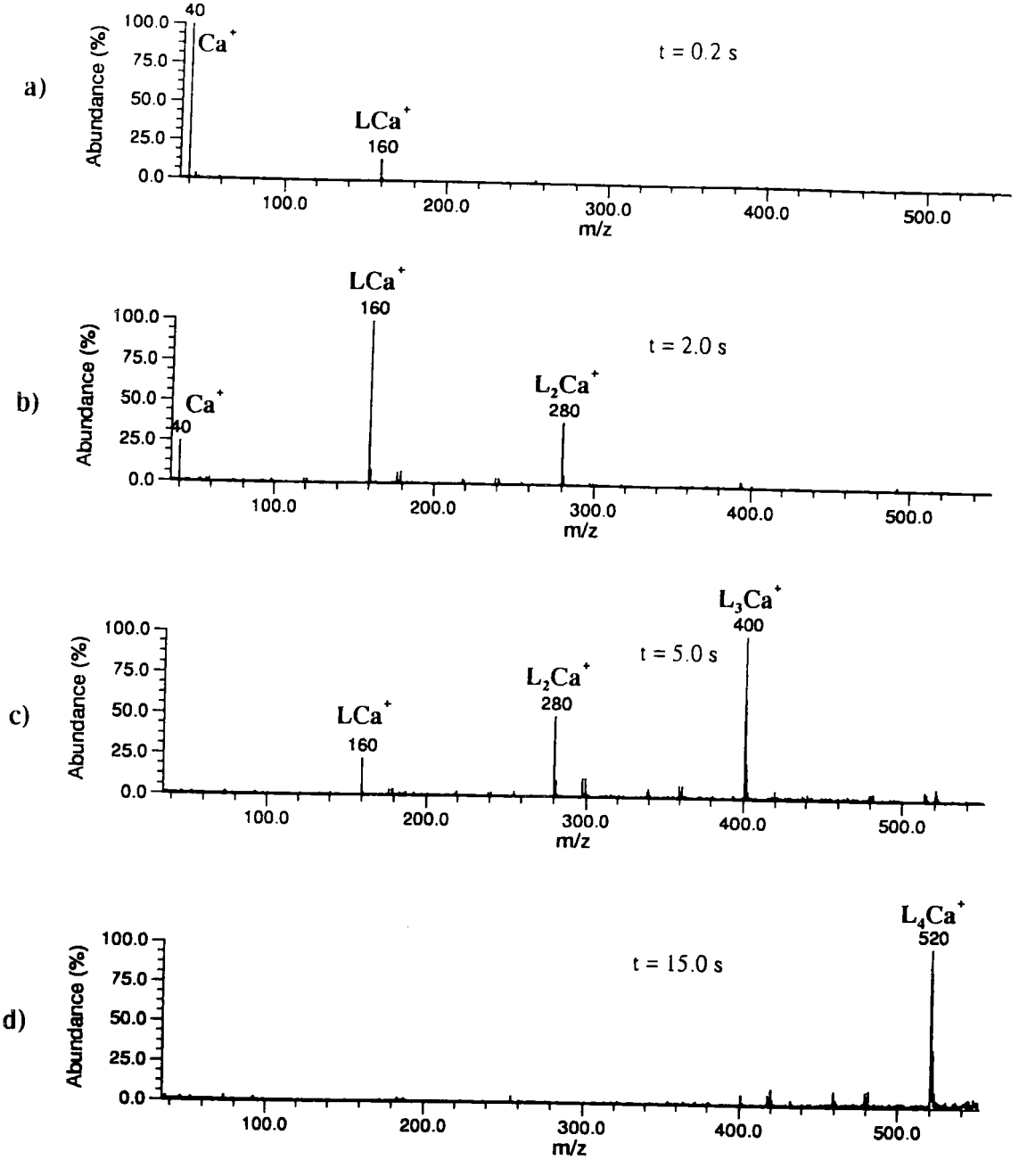

Figure A2: Positive ion FT-ICR mass spectra of the ionic products of the reaction of Ca^+ with acetophenone (L) at the different reaction times.

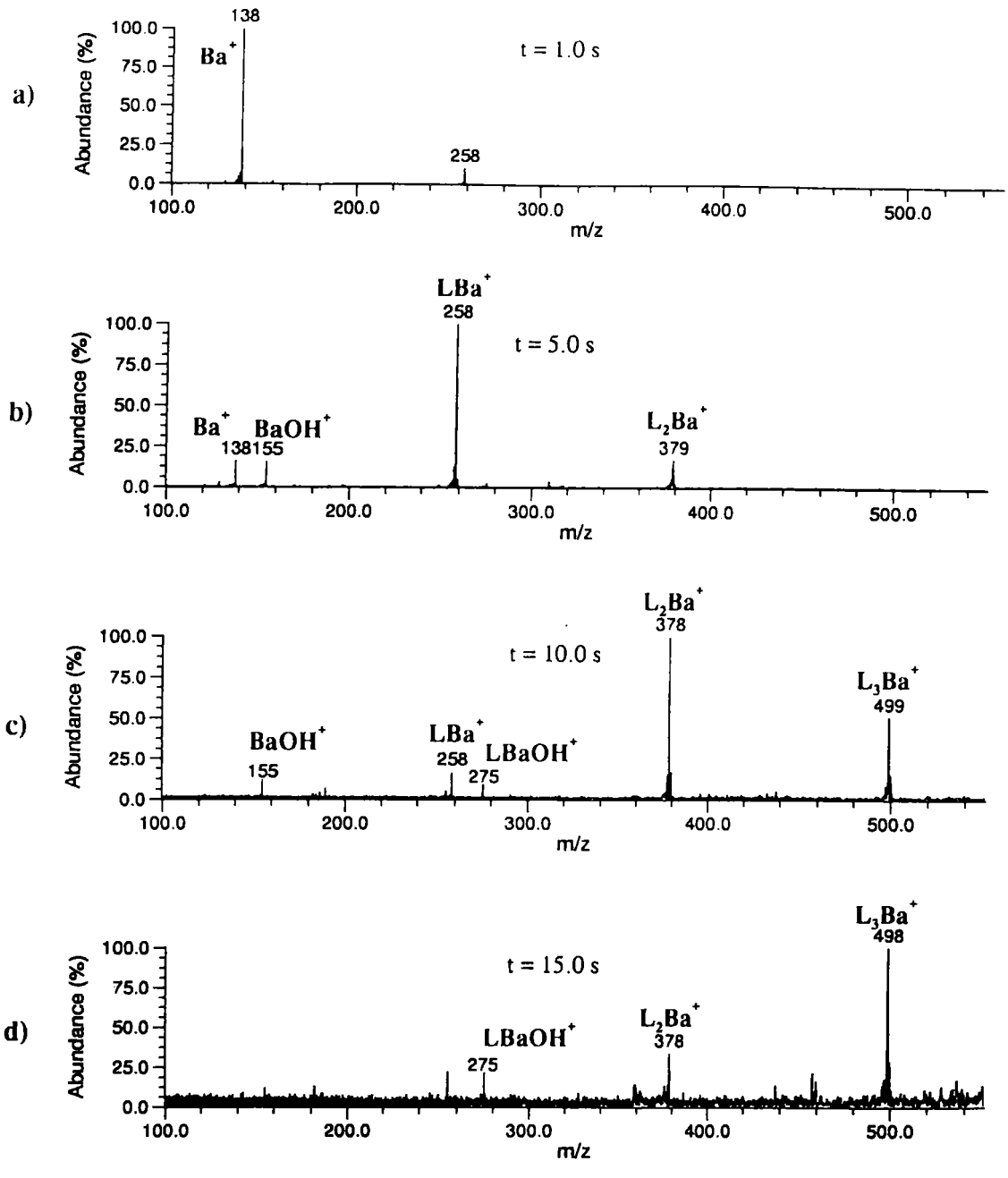

Figure A3: Positive ion FT-ICR mass spectra of the ionic products of the reaction of Ba^+ with acetophenone (L) at the different reaction times.

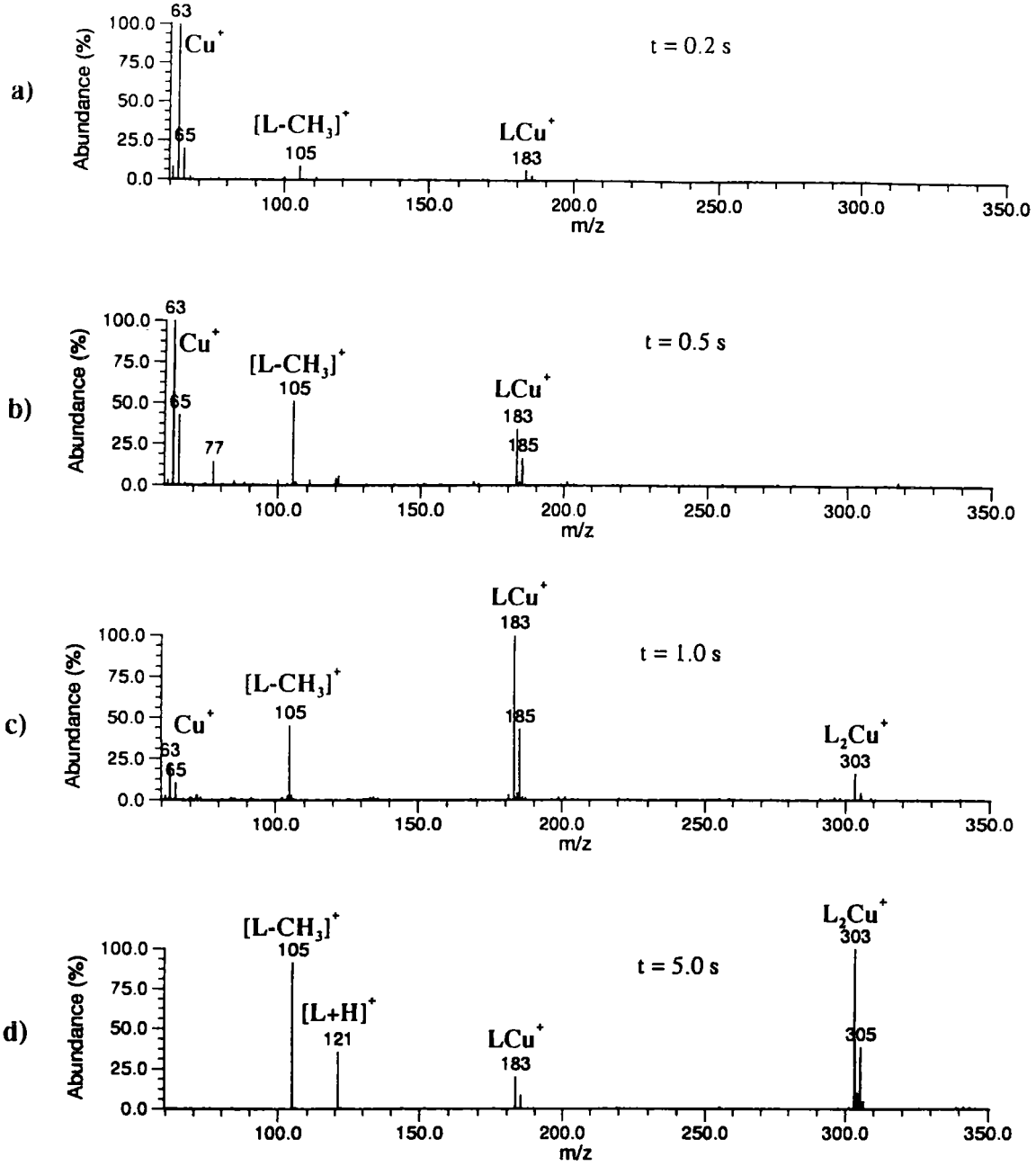

Figure A4: Positive ion FT-ICR mass spectra of the ionic products of the reaction of Cu^+ with acetophenone (L) at the different reaction times.

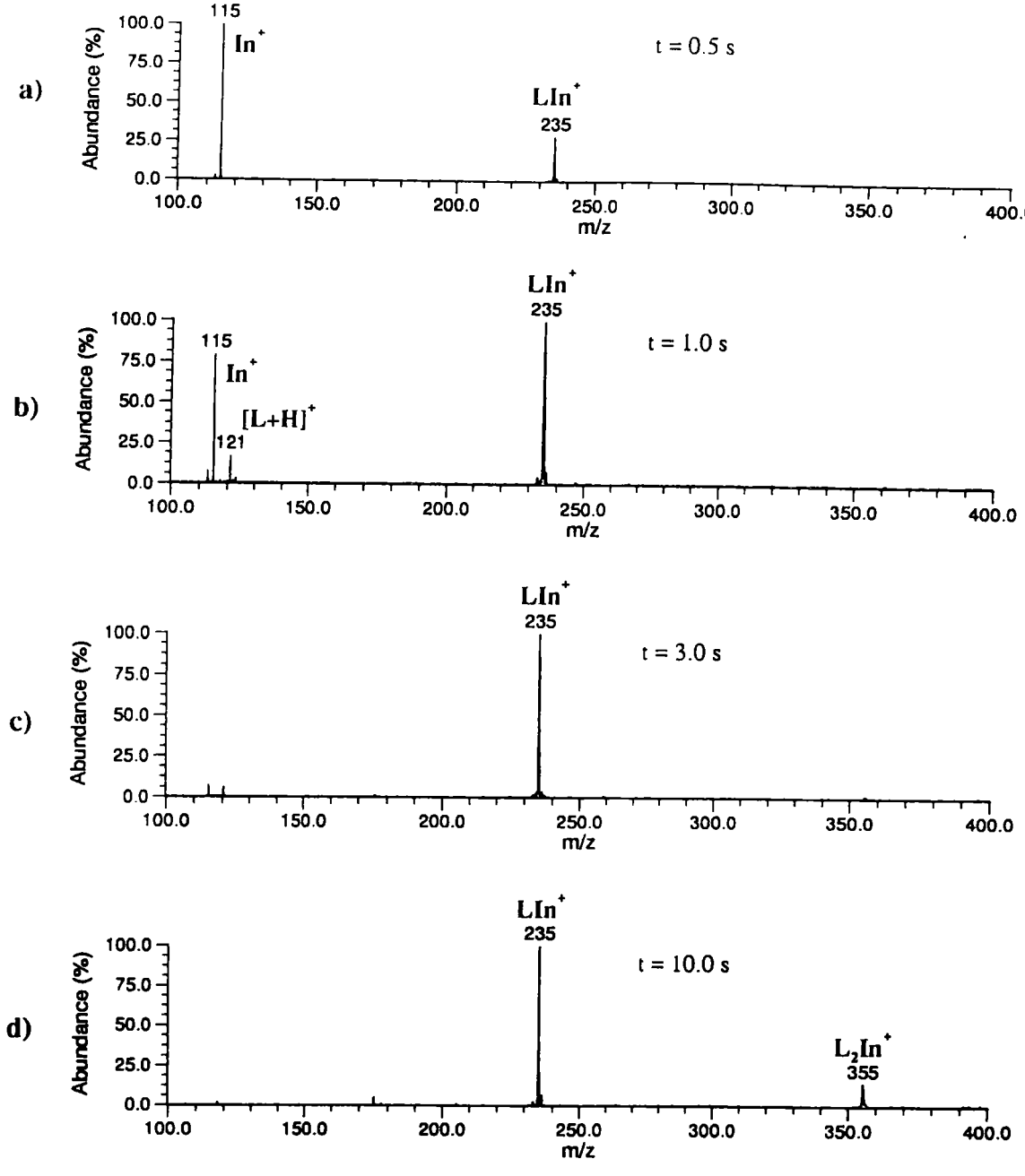

Figure A5: Positive ion FT-ICR mass spectra of the ionic products of the reaction of In^+ with acetophenone (L) at the different reaction times.

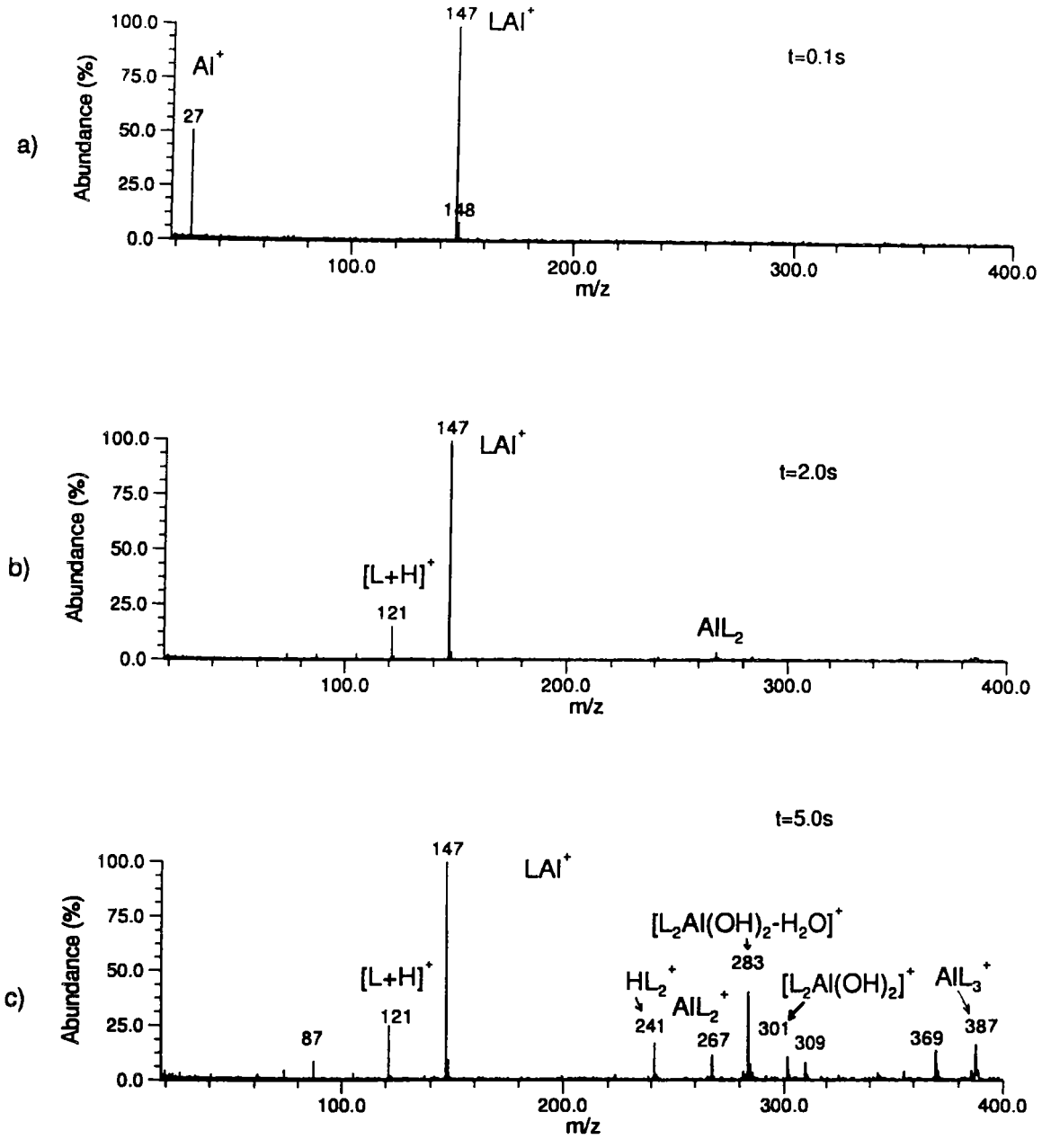

Figure A6: Positive ion FT-ICR mass spectra of the ionic products of the reaction of Al^+ with acetophenone (L) at the different reaction times.

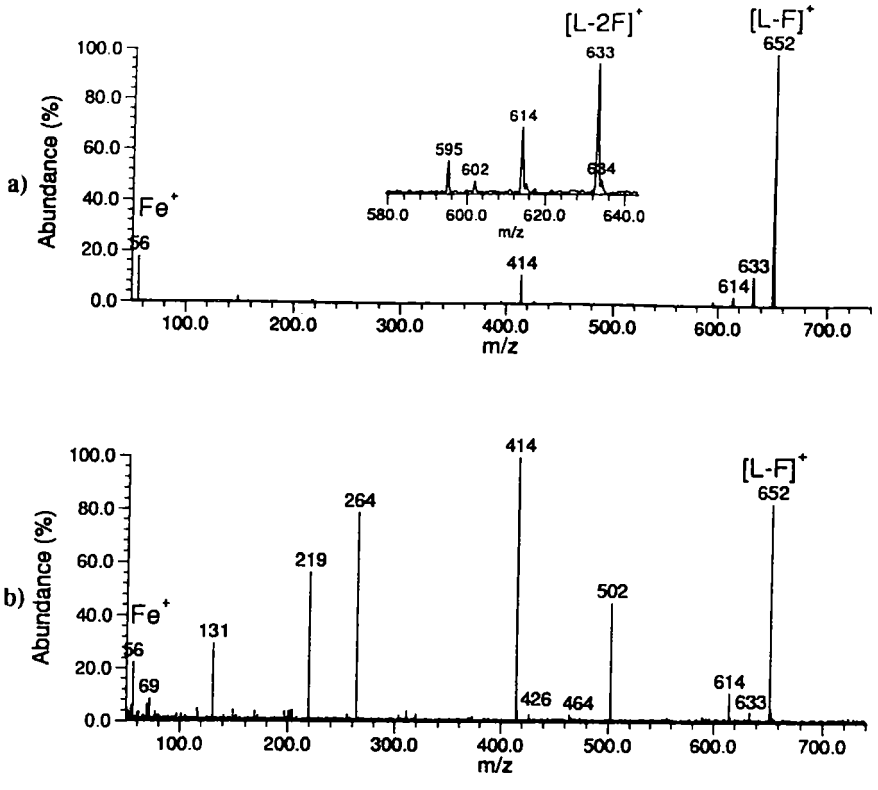

Figure B1: Positive ion FT-ICR mass spectra of the products of the Fe^+ reaction with PFTBA: a) without prior Fe^+ excitation; b) with the excitation of the cyclotron motion of Fe^+ ions. 1.0 s delay before broadband excitation in both cases.

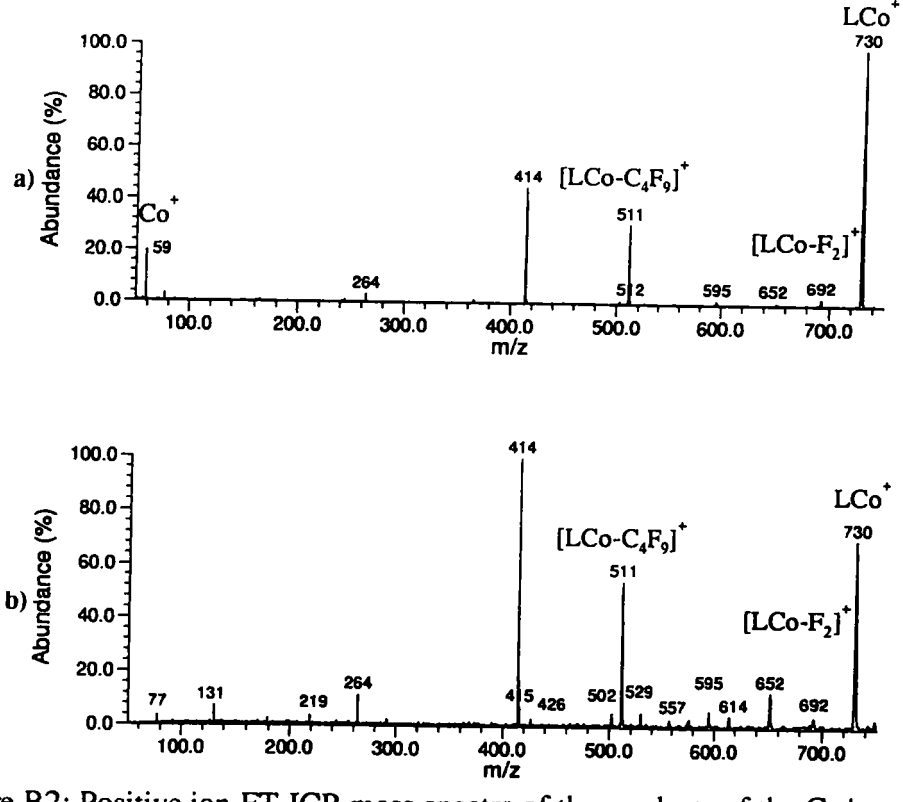

Figure B2: Positive ion FT-ICR mass spectra of the products of the Co^+ reaction with PFTBA: a) without prior Co^+ excitation; b) with the excitation of the cyclotron motion of Co^+ ions. 1.0 s delay before broadband excitation in both cases.

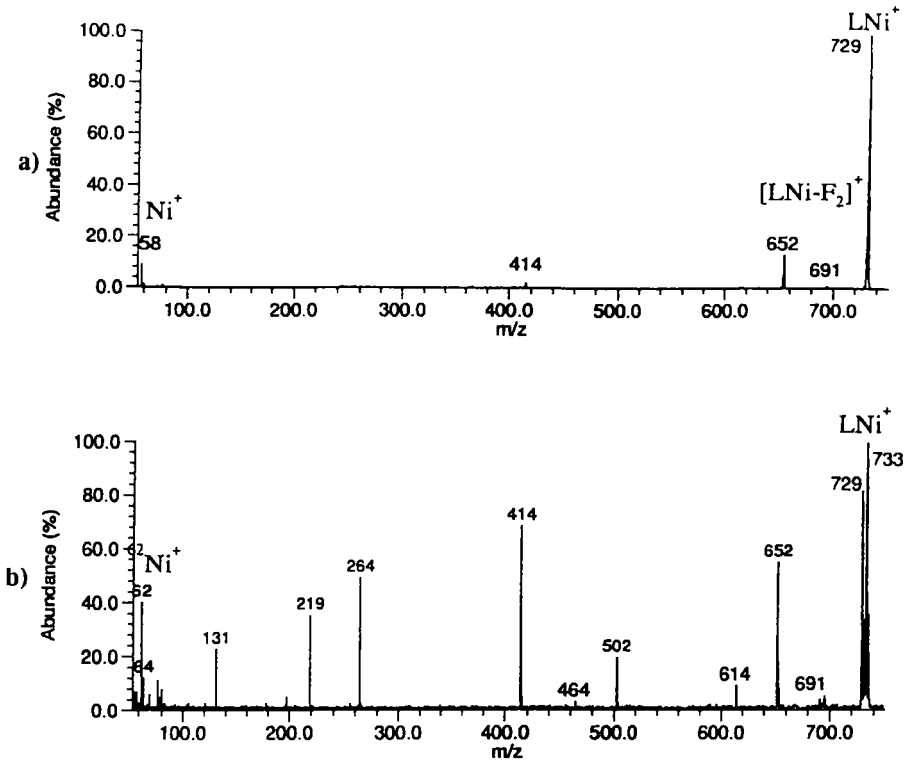

Figure B3: Positive ion FT-ICR mass spectra of the products of the Ni^+ reaction with PFTBA: a) without prior Ni^+ excitation; b) with the excitation of the cyclotron motion of Ni^+ ions. 1.0 s delay before broadband excitation in both cases.

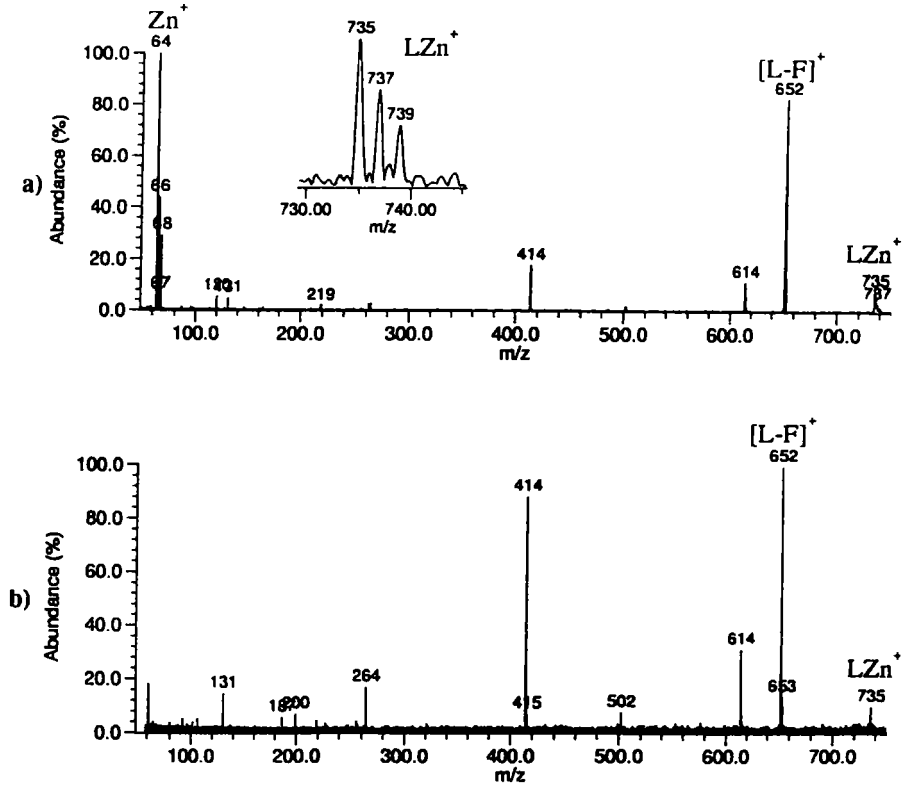

Figure B6: Positive ion FT-ICR mass spectra of the products of the Zn^+ reaction with PFTBA: a) without prior Zn^+ excitation; b) with the excitation of the cyclotron motion of Zn^+ ions. 1.0 s delay before broadband excitation in both cases.

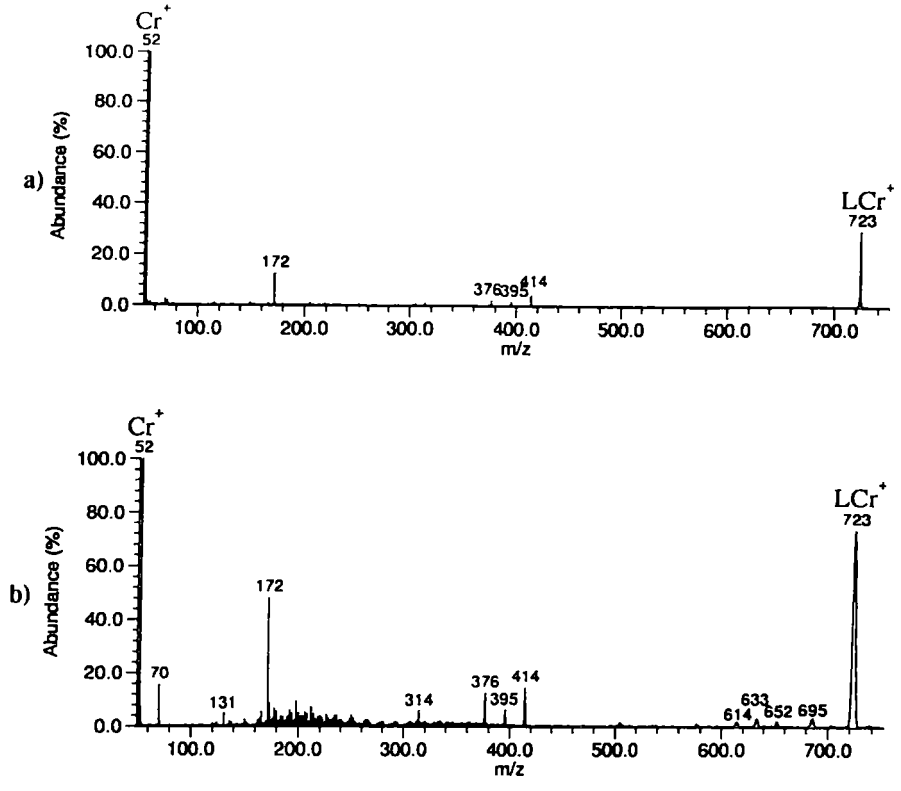

Figure B5: Positive ion FT-ICR mass spectra of the products of the Cr^+ reaction with PFTBA: a) without prior Cr^+ excitation; b) with the excitation of the cyclotron motion of Cr^+ ions. 1.0 s delay before broadband excitation in both cases.

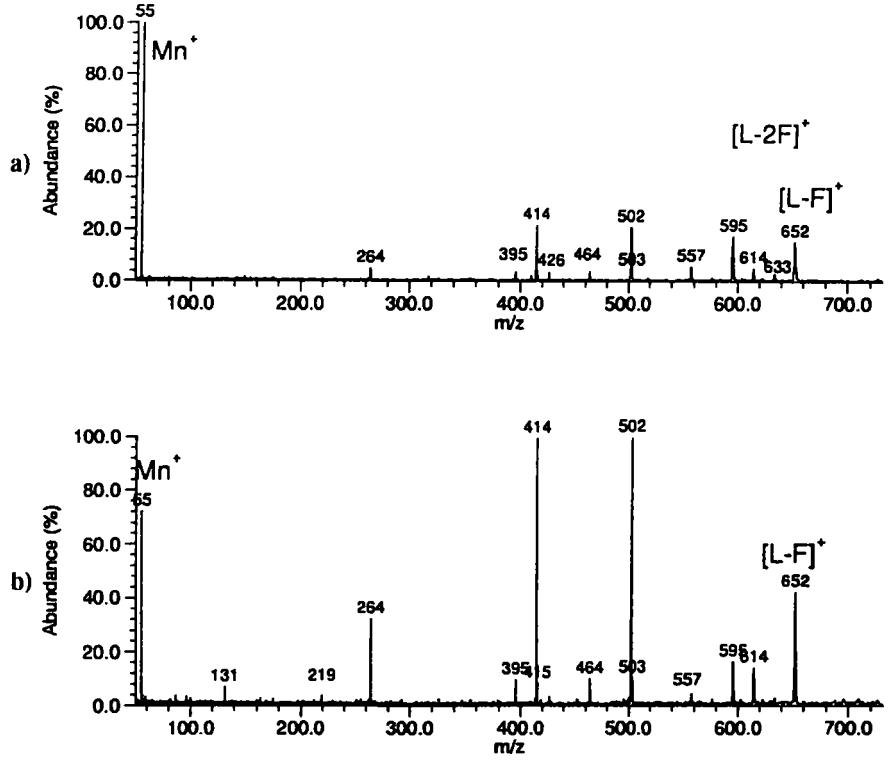

Figure B6: Positive ion FT-ICR mass spectra of the products of the Mn^+ reaction with PFTBA: a) without prior Mn^+ excitation; b) with the excitation of the cyclotron motion of Mn^+ ions. 1.0 s delay before broadband excitation in both cases.

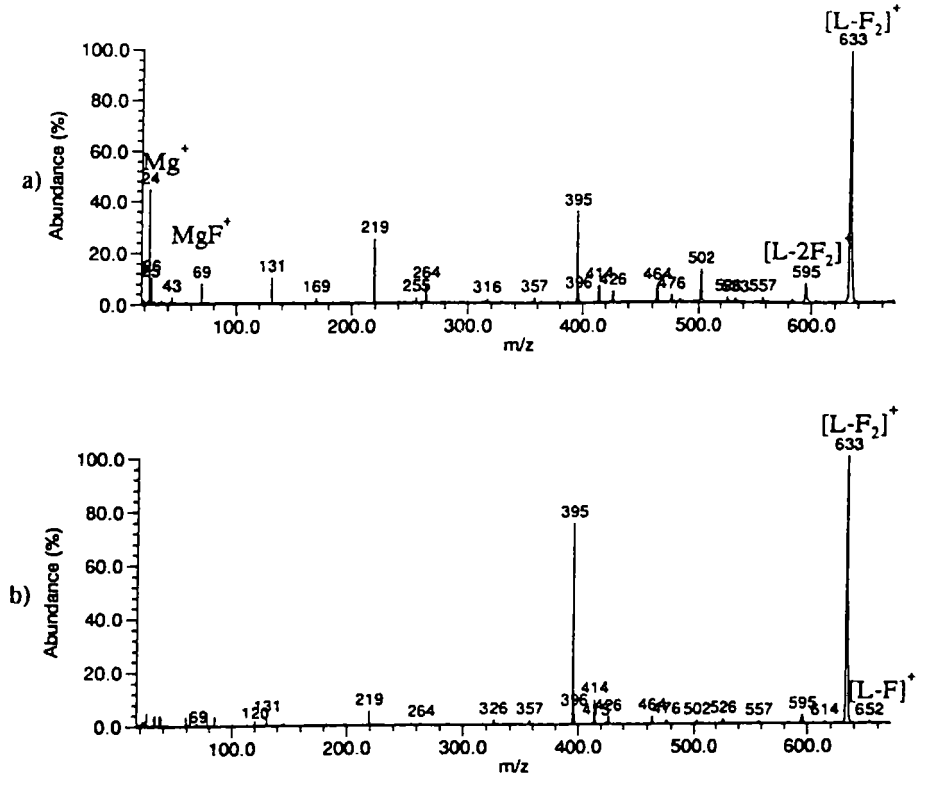

Figure B3: Positive ion FT-ICR mass spectra of the products of the Mg^+ reaction with PFTBA: a) without prior Mg^+ excitation; b) with the excitation of the cyclotron motion of Mg^+ ions. 1.0 s delay before broadband excitation in both cases.

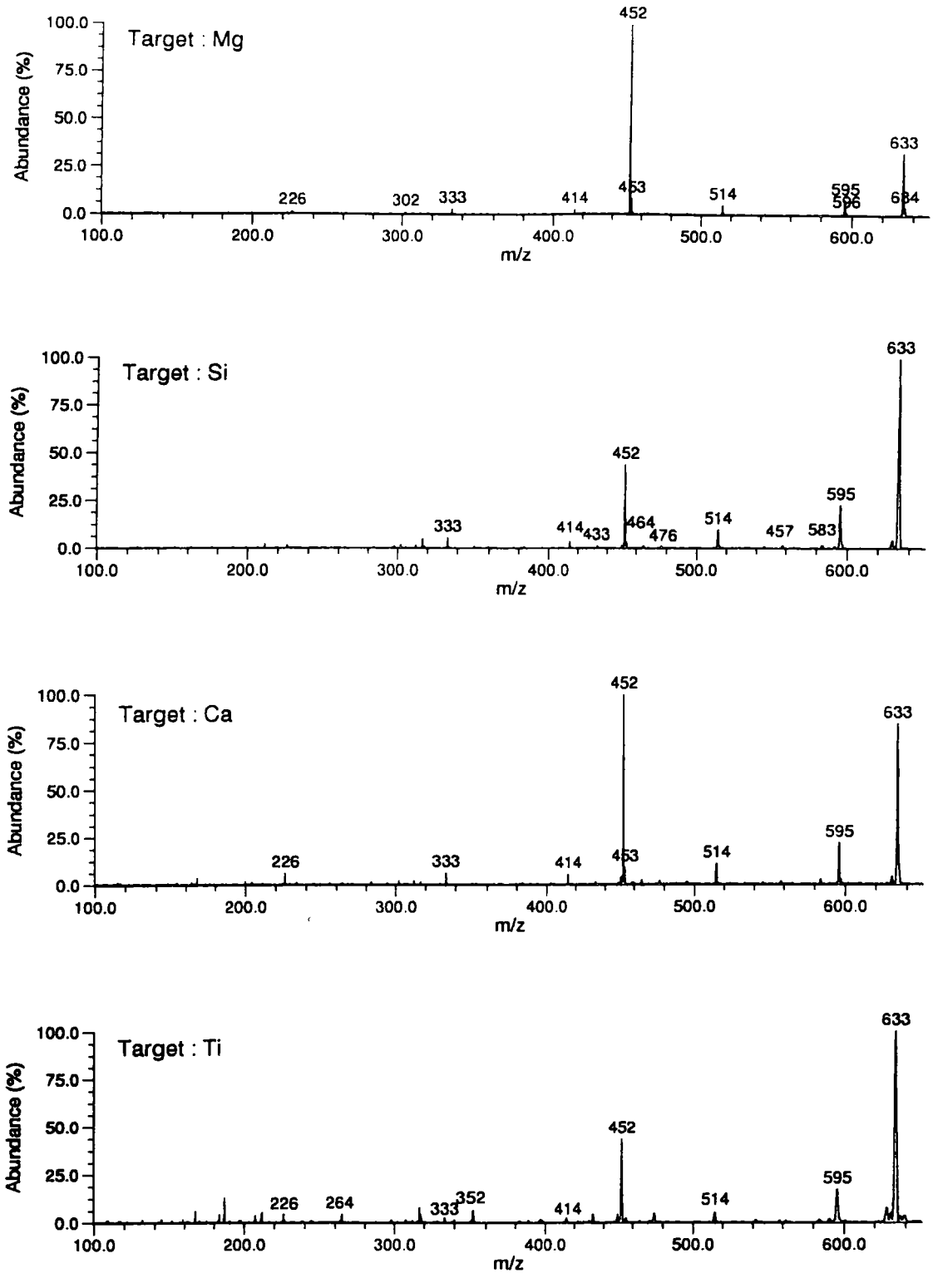

Figure C1 : FT ICR-negative ion mass spectra of PFTBA ionized by electrons produced by laser ablation of different solid target: Mg, Si, Ca and Ti, respectively.

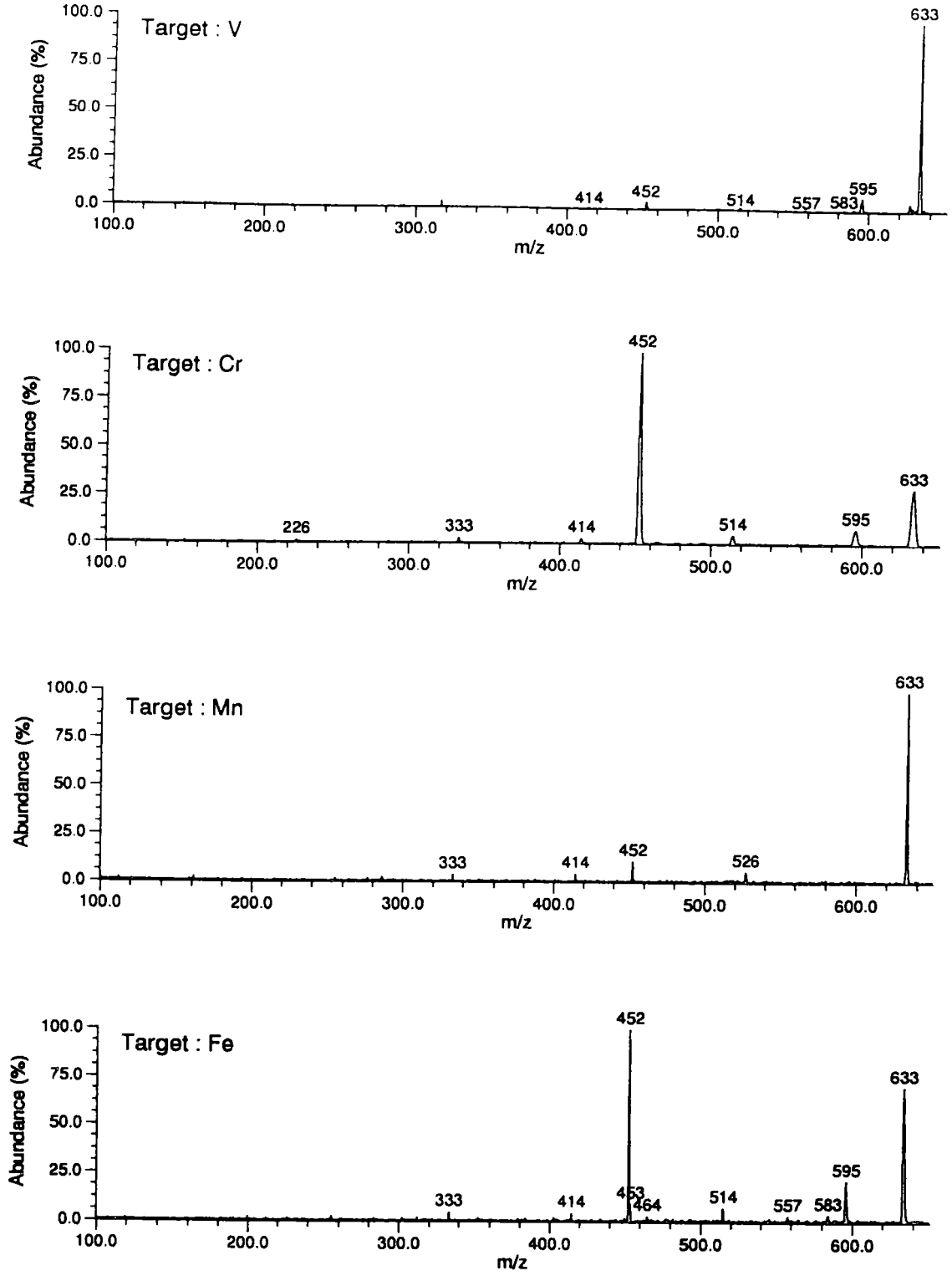

Figure C2: Negative ion FT-ICR mass spectra of PFTBA ionized by electrons produced by laser ablation of different solid targets: a) V, Cr, Mn and Fe respectively.

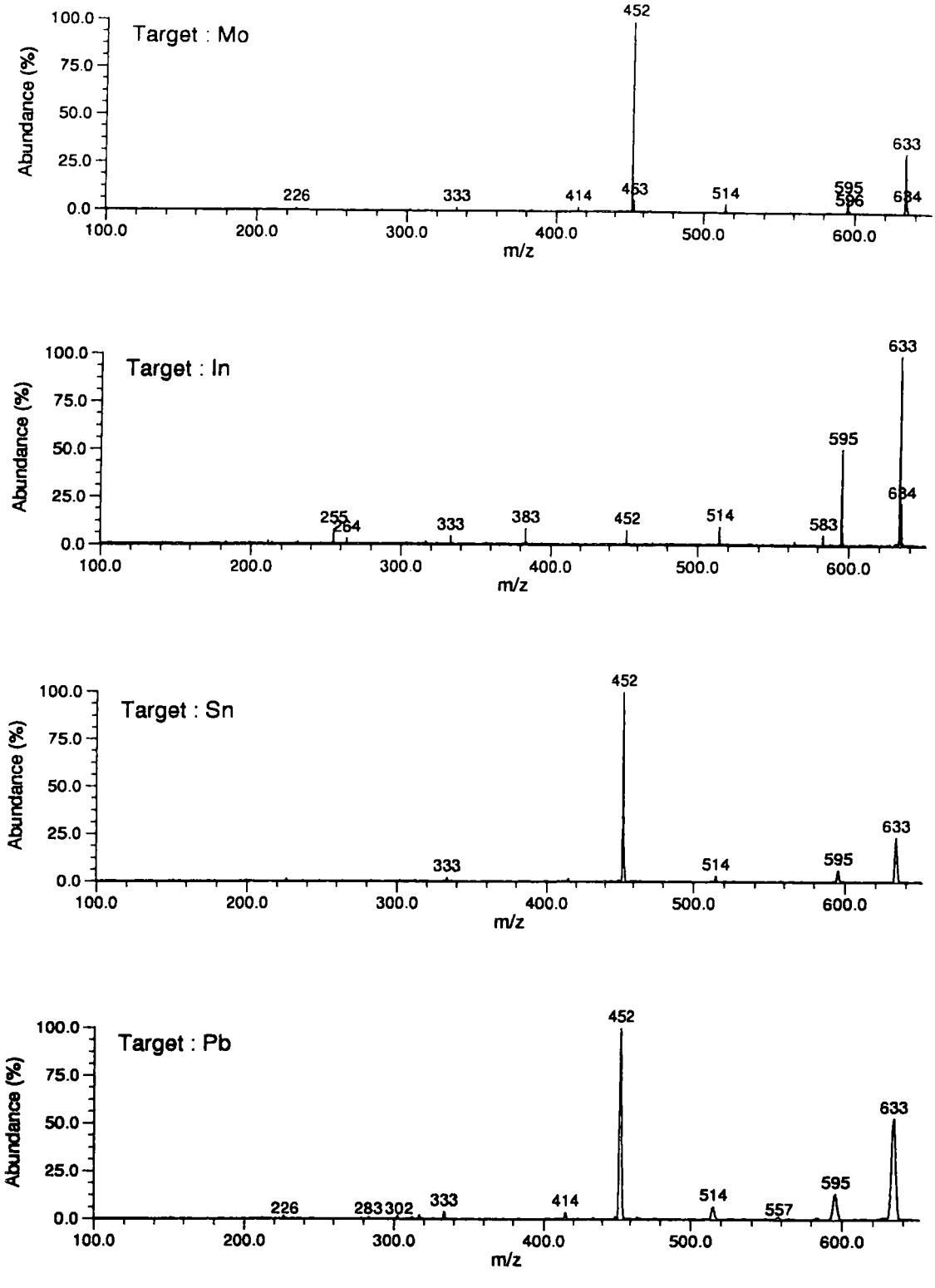

Figure C3 : FT ICR-negative ion mass spectra of PFTBA ionized by electrons produced by laser ablation of different solid target: Mo, In, Sn and Pb, respectively.

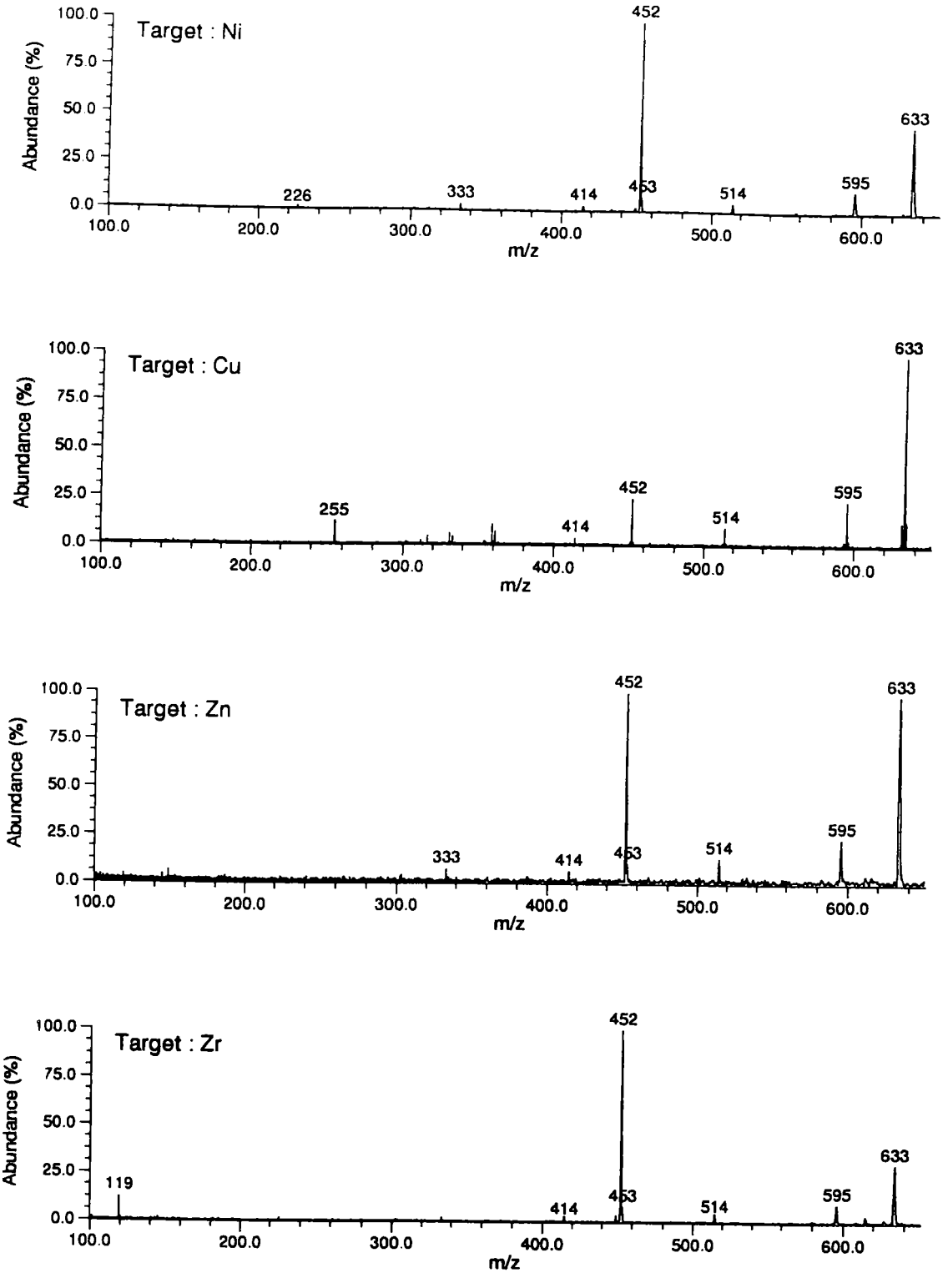

Figure C4: Negative ion FT-ICR mass spectra of PFTBA ionized by electrons produced by laser ablation of different solid targets: a) Ni, Cu, Zn and Zr respectively.

Résumé

Les réactions ion/molecule en phase gazeuse entre des ions positifs ou négatifs produits par laser et des molécules organiques ont été étudiées par spectrométrie de masse de résonance cyclotronique à transformée de Fourier. Des cibles de métal pur, de sels halogènes ou encore de silicium ont été irradiées par un faisceau laser, ce qui a conduit à la formation d'ions positifs et négatifs mais également à des électrons. La réactivité de ces espèces vis à vis de molécules organiques volatiles a été étudiée et les mécanismes de réactions établis.

La molécule d'acétophénone a été testée en tant que composé modèle pour les réactions avec des cations de l'élément métallique ou semiconducteur (Si). Des relations entre la réactivité des 18 différents cations sélectionnés ont été établies avec leur configuration électronique et leur énergie de promotion. Les paramètres expérimentaux optimaux ayant été ainsi définis, la procédure a été appliquée à l'ionisation et aux réactions ion/molécule de divers composés polyhalogénés. Ainsi la perfluorotributylamine a été mise en présence de 21 cations élémentaires différents. Les produits et les mécanismes des réactions observées ont été caractérisés. D'autres composés polyhalogénés rencontrés en chimie de l'environnement (dichlorodifluorométhane, halothane et endosulfane) ont été ionisés et détectés suivant la même méthodologie.

L'ionisation en mode négatif (par réaction ion/molecule) a également été étudiée en tant que méthode complémentaire. Dans ce cas, les projectiles servant à l'ionisation ont été soit des électrons formés lors de l'interaction laser-matière à haute irradiance, soit des anions halogénés produits par laser ou encore ces mêmes anions résultant de la fragmentation de la molécule cible en phase gazeuse. Les mécanismes d'attachement d'électrons entrent en compétition avec l'ionisation par réactions ion/molecule.

Mots clés : ***Spectrométrie de masse de résonance cyclotronique à transformée de Fourier, plasma laser, réactions ions/molecules, ionisation chimique positive et négative, ions métalliques.***

Titre : ***Ionisation induite par plasma laser de molecules organiques volatiles. Etude des processus et des reactions ion/molecule consecutives par spectrometrie de masse de résonance cyclotronique à transformee de Fourier***

Abstract

Gas phase ion/molecule reactions between laser-produced positive or negative ions and organic molecules were studied by Fourier transform ion cyclotron resonance mass spectrometry. Pure metal, metal halide salt and silicon wafer targets were irradiated by laser pulse, and positive and negative ions as well as electrons were formed. Their reactivity towards volatile organic molecules was studied and reaction mechanisms established.

Acetophenone was tested as a model compound for reactions with metal and silicon cations. Reactivities of different cations were correlated to their electronic configuration and promotion energy. Established experimental procedures were applied for ionization and ion-molecule reactions of polyhalogenated molecules. Perfluorotributylamine was allowed to react with 21 different elemental cations and reaction products and mechanisms were defined. Some other environmental polyhalogenated derivatives (dichlorodifluoromethane, halothane and endosulfane) were analyzed by the same method.

As a complementary ionization method, negative mode ionization (reactions) were studied. Three different ionizing projectiles: laser-produced electrons and halide ions as well as fragment halide ions were used to ionize (react with) the above mentioned molecules. Electron attachment mechanisms are concurrent to negative ion/molecule reactions.

Key words : *Fourier Transform Ion Cyclotron Resonance Mass Spectrometry, laser plasma, ion-molecule reactions, (negative and positive) chemical ionization, metal ions.*